



Universitat de Girona

ANALYSIS OF CHEMICAL BONDING AND AROMATICITY FROM ELECTRONIC DELOCALIZATION DESCRIPTORS

Ferran FEIXAS GERONÈS

Dipòsit legal: GI-1023-2011

<http://hdl.handle.net/10803/37471>

ADVERTIMENT. La consulta d'aquesta tesi queda condicionada a l'acceptació de les següents condicions d'ús: La difusió d'aquesta tesi per mitjà del servei [TDX](#) ha estat autoritzada pels titulars dels drets de propietat intel·lectual únicament per a usos privats emmarcats en activitats d'investigació i docència. No s'autoritza la seva reproducció amb finalitats de lucre ni la seva difusió i posada a disposició des d'un lloc aliè al servei TDX. No s'autoritza la presentació del seu contingut en una finestra o marc aliè a TDX (framing). Aquesta reserva de drets afecta tant al resum de presentació de la tesi com als seus continguts. En la utilització o cita de parts de la tesi és obligat indicar el nom de la persona autora.

ADVERTENCIA. La consulta de esta tesis queda condicionada a la aceptación de las siguientes condiciones de uso: La difusión de esta tesis por medio del servicio [TDR](#) ha sido autorizada por los titulares de los derechos de propiedad intelectual únicamente para usos privados enmarcados en actividades de investigación y docencia. No se autoriza su reproducción con finalidades de lucro ni su difusión y puesta a disposición desde un sitio ajeno al servicio TDR. No se autoriza la presentación de su contenido en una ventana o marco ajeno a TDR (framing). Esta reserva de derechos afecta tanto al resumen de presentación de la tesis como a sus contenidos. En la utilización o cita de partes de la tesis es obligado indicar el nombre de la persona autora.

WARNING. On having consulted this thesis you're accepting the following use conditions: Spreading this thesis by the [TDX](#) service has been authorized by the titular of the intellectual property rights only for private uses placed in investigation and teaching activities. Reproduction with lucrative aims is not authorized neither its spreading and availability from a site foreign to the TDX service. Introducing its content in a window or frame foreign to the TDX service is not authorized (framing). This rights affect to the presentation summary of the thesis as well as to its contents. In the using or citation of parts of the thesis it's obliged to indicate the name of the author.



PhD thesis:

Analysis of Chemical Bonding and Aromaticity from Electronic
Delocalization Descriptors

Ferran Feixas Geronès
2010

Doctorat Interuniversitari en Química Teòrica i Computacional

PhD supervisors:
Prof. Miquel Solà i Puig
Dr. Jordi Poater i Teixidor
Dr. Eduard Matito i Gras

Memòria presentada per a optar al títol de Doctor per la Universitat de Girona



Universitat de Girona

El professor Miquel Solà i Puig, catedràtic d'Universitat a l'àrea de Química Física de la Universitat de Girona, el doctor Jordi Poater i Teixidor, investigador Ramón y Cajal a l'Institut de Química Computacional de la Universitat de Girona, i el doctor Eduard Matito i Gras, investigador postdoctoral Marie-Curie de l'Institut de Física de la University of Szczecin.

CERTIFIQUEM:

Que aquest treball titulat "Analysis of Chemical Bonding and Aromaticity from Electronic Delocalization Descriptors", que presenta en Ferran Feixas Geronès per a l'obtenció del títol de Doctor, ha estat realitzat sota la nostra direcció i que compleix els requeriments per a poder optar a Menció Europea.

Signatura

Prof. Miquel Solà Puig

Dr. Jordi Poater i Teixidor

Dr. Eduard Matito i Gras

Girona, 1 de desembre de 2010

*"I quan penses dur a terme el teu somni?
-va demanar el mestre al deixeble.
Quan tingui la oportunitat
-va respondre.
El Mestre li contestà
-L'oportunitat mai no arriba. L'oportunitat és aquí."
Anthony de Mello*

A tots vosaltres

Preface

Since the advent of quantum mechanics, theoretical and computational chemistry have played a pivotal role in chemistry. From the very beginning, theoretical chemists have been primarily focused on the development of new methodologies that may provide an explanation for most of the chemical phenomena. However, progress in the applicability of theoretical and computational chemistry depends on the advances in computational power. This fact limited the interaction between experimental and theoretical chemists for a long time. Notwithstanding, at the end of the first decade of the 21st century, we have arrived at a position where theory and experiment play a complementary role in exploring chemical questions. Theoretical chemistry is now commonly used to address complex problems in chemistry, biochemistry, or materials science, from the study of small molecules in the gas phase to the simulation of protein folding in complex environments.¹

Interactions between electrons determine the structure and properties of matter from molecules to solids. Therefore, the understanding of the electronic structure of molecules will enable us to extract relevant chemical information. Since the work of Lewis,² the concept of electron pair has been placed at the epicenter of the discussion about the properties of chemical bonding. Hence, the pair density, that accounts for the correlated motion of a couple of electrons, has been very important in the interpretation of electronic structure. The pair density and its related quantities, such as the concept of Fermi Hole, are discussed in detail in Chapter 1. Interestingly, these quantities have been widely used to elucidate the nature of chemical bonding in a plethora of systems. In chemistry, global molecular properties are as important as the properties of a given atom or region of the molecular space. The partition of molecular space into different regions helps us to unravel how the electrons are localized in a specific region or which is the number of electrons shared among two or more regions of the space. In Chapter 2 we will see how we can more clearly understand the nature of chemical bonding from the concept of electron delocalization.

From the discovery of benzene in 1825³ to the present day, the concept of aromaticity has experienced several revolutions that have fueled the interest of both theoretical and experimental chemists. The discovery of new aromatic compounds is not about to slow down. Undoubtedly, the major breakthrough of the last decade in the field of aromaticity took place in 2001, when the first all-metal cluster, MAl_4^- (M = Li, Na, or Cu), was characterized.⁴ This finding gave rise to one of the most

striking features of all-metal aromatic clusters, the so-called multifold aromaticity, that is, the presence of σ -, π -, δ -, or even ϕ -aromaticity. As the number of new aromatic molecules grows, the quest for the quantification of aromaticity has become one of the challenges of theoretical chemists. Thus, the concept of aromaticity is one of the cornerstones of past and current chemistry. However, at the same time, it is also considered a *chemical unicorn*⁵ due to the fact that aromaticity is not a directly measurable property, and it cannot be defined unambiguously. In Chapter 3, the main advances in the field and the most widely used descriptors of aromaticity will be reviewed.

On the other hand, Chapters 5, 6, and 7 are devoted to the applications of the above presented theory and correspond to the works of the present thesis, that contains twelve accepted publications. First, we focus our attention on the analysis of chemical bonding by means of the Electron Localization Function (ELF)⁶ and the Domain-Averaged Fermi Hole analysis (DAFH).^{7,8} The four projects collected in Chapter 5 are a consequence of the research stays at the Université Pierre et Marie-Curie with Prof. Bernard Silvi, and at the Czech Academy of Science with Prof. Robert Ponec. In the first section, the ELF is approximated in terms of natural orbitals in order to bridge the gap between the (expensive) correlated expression and the (sometimes inaccurate) monodeterminantal definition. The next sections are dedicated to DAFH analysis. First, this analysis is generalized to open-shell systems; second, the open-shell definition is used to analyze the bonding patterns of some triplet dications; and, third, the peculiarities of the ultrashort Cr-Cr bond are analyzed from the point of view of DAFH.

In recent years, many methods to quantify aromaticity based on different physico-chemical properties have been proposed. In Chapter 6 we assess the performance of these indicators by analyzing their advantages and drawbacks. Throughout this chapter, we propose a series of tests based on well-known aromaticity trends that can be applied to evaluate the aromaticity of current and future indicators of aromaticity in both organic and inorganic species. Since the aromaticity is tightly connected with the concept of electron delocalization, in Chapter 7 we investigate the nature of electron delocalization in both aromatic and antiaromatic systems in the light of Hückel's $(4n + 2)$ rule. Finally, from the conclusions gathered in Chapter 6, we analyze the phenomenon of multiple aromaticity in all-metal clusters that present σ , π , and/or δ aromaticity.

Resum de la tesi

Des del sorgiment de la mecànica quàntica, la química teòrica i computacional ha jugat un paper fonamental en el món de la química. Des de bon principi, els químics teòrics s'han centrat en el desenvolupament de noves metodologies que poden proporcionar una explicació per a la majoria de fenòmens químics. No obstant, els avenços en l'aplicació de la química computacional han estat molt lligats als avenços en el camp de la computació. Aquest fet ha limitat la interacció entre els químics experimentals i teòrics durant gran part del segle XX. Tot i això, al final de la primera dècada del segle XXI, hem arribat a una posició on la teoria i l'experiment juguen un paper complementari en l'exploració de tot tipus de problemes químics. La química teòrica s'ha convertit en una eina d'ús comú per fer front a problemes complexos que abarquen camps com la química o la bioquímica, des de l'estudi de molècules petites en fase gasosa a la simulació del plegament de proteïnes.¹

Les interaccions entre electrons determinen l'estructura i propietats de la matèria. Per tant, la comprensió de l'estructura electrònica de les molècules ens permetrà extreure informació química rellevant. Des del treball de Lewis,² el concepte de parell d'electrons es troba a l'epicentre de la discussió sobre les propietats de l'enllaç químic. Per tant, la densitat de parells, que representa el moviment correlacionat d'un parell d'electrons, ha jugat un paper clau en la interpretació de l'estructura electrònica. Les propietats de la densitat de parells i les seves quantitats associades, com ara el forat de Fermi, es discutiran en detall al Capítol 1. Aquestes quantitats s'han utilitzat àmpliament per desentrallar la naturalesa de l'enllaç químic en una gran quantitat de sistemes. En química, tan importants com les propietats globals de la molècula ho són les propietats d'un àtom o una regió de l'espai molecular. La partició de l'espai en diferents regions pot ajudar-nos a esbrinar com es localitzen els electrons dins una regió específica o quin és el nombre d'electrons compartits entre dues o més regions de l'espai. En el Capítol 2 veurem com podem analitzar la naturalesa de l'enllaç químic a partir del concepte de deslocalització electrònica.

Des del descobriment de la molècula de benzè l'any 1825³ fins a l'actualitat, el concepte d'aromaticitat ha experimentat diverses revolucions que han provocat l'interès dels químics teòrics i experimentals. El descobriment de nous compostos aromàtics no para d'augmentar exponencialment. Sens dubte, el gran avanç de l'última dècada en el camp de l'aromaticitat es va dur a terme l'any 2001, quan el primer compost totalment metàl·lic amb propietats aromàtiques va ser caracteritzat, MAI_4^- (M = Li, Na, o Cu).⁴ Aquesta troballa va donar lloc a una de les característiques més

sorprenents del anells aromàtics formats per només metalls: l'anomenada aromaticitat múltiple, és a dir, la presència d'aromaticitat de tipus σ , π , δ , o fins i tot ϕ . Com que el nombre de noves molècules aromàtiques no para de créixer, la recerca per la quantificació de l'aromaticitat s'ha convertit en un dels reptes dels químics teòrics. Així doncs, el concepte d'aromaticitat és una de les pedres angulars de la química actual, però al mateix temps, també és considerat un *unicorn químic*,⁵ degut a que l'aromaticitat no és una propietat directament mesurable, i per tant no es pot definir sense ambigüitat. Al Capítol 3 revisarem els principals avenços en el camp de l'aromaticitat i els seus descriptors més utilitzats.

D'altra banda, els Capítols 5, 6, i 7 estan dedicats a les aplicacions d'aquesta tesi, que conté un total de dotze publicacions acceptades. En primer lloc, centrem la nostra atenció en l'anàlisi de l'enllaç químic per mitjà de la funció de localització electrònica (ELF)⁶ i l'anàlisi dels anomenats *domain averaged Fermi holes* (DAFH).^{7,8} Els quatre projectes recollits en el Capítol 5 són conseqüència de les estades de recerca realitzades a la Université Pierre et Marie Curie amb el Prof. Bernard Silvi, i a l'Acadèmia Txeca de les Ciències amb el Prof. Robert Ponec. A la primera secció, proposem una aproximació de la ELF en termes d'orbitals naturals per tal de reduir la distància entre l'expressió a nivell correlacionat que porta associat un elevat cost computacional i la definició (moltes vegades inexacta) basada en funcions d'ona monodeterminants. Les següents seccions estan dedicades a l'anàlisi dels DAFH. En primer lloc, aquest anàlisi s'ha generalitzat a sistemes de capa oberta, en segon lloc, la definició dels DAFH a capa oberta s'utilitza per analitzar els patrons d'enllaç d'algunes dicacions en estat triplet, i, en tercer lloc, les peculiaritats dels enllaços extremadament curts de Cr-Cr s'analitzen des del punt vista dels DAFH.

En els últims anys, s'han proposat molts mètodes per quantificar l'aromaticitat basats en diferents propietats fisicoquímiques. En el Capítol 6 s'avalua el comportament d'aquests indicadors analitzant els seus avantatges i inconvenients. Al llarg d'aquest capítol, es proposen una sèrie de tests basats en tendències d'aromaticitat conegudes que es poden aplicar per avaluar el comportament dels indicadors actuals en espècies tan orgàniques com inorgàniques. Com que l'aromaticitat està estretament vinculada amb el concepte de deslocalització electrònica, en el Capítol 7 s'investiga la naturalesa de la deslocalització d'electrons en sistemes aromàtics i antiaromàtics que segueixen la regla $4n + 2$ que proposà Hückel. Finalment, a partir de les conclusions reunides al Capítol 6, analitzarem el fenomen de l'aromaticitat múltiple en sistemes metàl·lics que presenten aromaticitat de tipus σ , π , i δ .

Agraïments

*"Caminante, no hay camino
se hace camino al andar"*
Antonio Machado

Sempre he pensat que el doctorat és com fer el Camí de Santiago, cada matí agafes les bici, vas fent etapes, coneixes gent, nous llocs, i tot i saber quin és l'objectiu final saps que el que és veritablement important és viure el dia a dia, l'avui, l'aquí i l'ara. Ara que comença l'últim tram de l'última etapa, la il·lusió per arribar al final queda enterbolida per una barreja de sentiments, per una banda l'alegria per tots els moments viscuts, per tot el que he après, i per l'altra la tristesa de saber que s'acaba una etapa genial. Si que és cert que al llarg del camí hi ha algun Cebreiro o Creu de Ferro amb pendent del 20% que t'obliga a baixar pinyons i a apretar fort les dents, però un cop has coronat el cim valores tot l'esforç i rius recordant tots els entrebancs de la pujada. Però si alguna cosa he après al llarg d'aquests anys de doctorat és que molt més important que els resultats obtinguts són les persones que t'acompanyen i que et vas trobant al llarg de la caminada. Les persones que t'ajuden, amb els qui rius, que t'animen, en definitiva, els qui et fan fàcil el camí, o dit d'una altra manera, les persones que fan que cada moment, que cada dia, sigui especial i diferent. Que sapiguen que de tots vosaltres n'estic constantment aprenent. En aquestes línies no podré agrair-vos la meitat del que voldria ni la meitat del que us mereixeu. Abans de res, moltes gràcies a tots!

En primer lloc, vull donar les gràcies als tres responsables que això hagi tirat endavant, els directors de la tesi, Miquel, Jordi i Edu. No veig la tesi com un premi individual sinó com un el premi a un treball d'equip. Us vull agrair el vostre recolzament en tot moment, el vostre entusiasme, els infinits consells, per dirigir-me sempre cap a la direcció correcta i perquè he pogut aprendre constantment de tots vosaltres. Particularment, a en Miquel voldria donar-li les gràcies perquè sense ell possiblement no hauria escrit aquesta tesi ni estaria fent actualment el doctorat, ja que va ser a partir de tenir-lo de professor, que en gran part s'em va despertar un interès real per seguir amb la química teòrica. A en Jordi, codirector de la tesi, vull agrair-li especialment haver-me donat la oportunitat d'entrar dins el món de la biomedicina. Si he pogut demanar els projectes de les beques per anar de postdoc ha estat gràcies a en Jordi, ja sigui tan per ajudar-me a definir el projecte com per totes les correccions

i comentaris posteriors. A l'Edu, codirector de la tesi, però per sobre de tot un amic, agrair-li en primer lloc totes les hores, que espero que no siguin perdudes, que ha dedicat a explicar-me tot tipus de conceptes al llarg d'aquests cinc anys. També pels infinits consells, xerrades de tots tipus, sopars a base de feta cheese al millor bar d'Atenes, congressos, converses futboleres... Gràcies a tots tres per la vostra paciència, per aguantar els meus despistes i per ajudar-me en tot moment. A tots tres moltes gràcies, he estat aprenent constantment de vosaltres i ho continuaré fent.

No em voldria oblidar de l'Annapaola i en Lluís, ja que m'han ofert la possibilitat d'endisar-me en el fascinant món de la fotoquímica, dels mecanismes de reacció impossibles i de les conicals interseccions entre estats ultraexcitats, i també per la oportunitat d'anar a Jena d'estada, gràcies per totes les hores dedicades! També a en Marcel per tota la seva ajuda amb el tema LUCTA, que per un neòfit de l'ADF i del món MM com jo va ser difícil. A la resta del sector IQCcià, als séniors, Josep Maria, Sílvia, Emili, Miquel Duran, Ramon, Sergei, Alexander, especial menció a la Carme, per contrarrestar tot lo despistats que podem ser en el tema papeleo i per fer-nos riure sempre que baixem al bar. Després d'haver voltat molt per Europa t'adones de que veritablement no hi ha enlloc com a casa i això és gràcies a vosaltres, l'IQC és com una família i sempre pensaré que és el millor grup on he pogut estar.

Voldria agrair a en Bernard, en Robert i la Leticia perquè m'han tractat com a casa en les estades que he fet. A Bernard quiero agradecerle la estancia de cuatro meses a Paris, por todo lo que pude aprender acerca de ELF y ToPMoD, por los increíbles cous-cous que comíamos cerca del laboratorio, y porque coincidimos en que la Bretanya francesa es de los mejores sitios del mundo. I want to thank Robert for his hospitality throughout the two months that I spent in Prague, for all that I learned about DAFH, for his guided tours (every tuesday after lunch) to the most incredible places of one of the best cities in Europe, for the delicious lunch with his family at his place, for the three apples that I found every morning on the table, and finally, for give me the opportunity to carry out a research stay in the research center with the best cantine of the world, long live dumplings! Finalmente, agradecer a Leticia y a todo su grupo por la estancia en Jena, llegar el día 10 de enero a -25 grados no fue fácil, pero en seguida me sentí como en casa, también quiero agradecer particularmente a Vero y a Suso por toda su ayuda y paciencia en el tema de les dinámicas. Especial menció als erasmus de Paris i a la colla de l'Spanish Stammtisch de Jena per tots els bons moments, sopars, etc Merci beaucoup! Vielen danke!

Be, arribat a aquest punt toca centrar-me amb tota la colla de freaks (o amics) amb qui hem compartit infinitat de bons moments i aventures de tot tipus. Tot va començar al 177 (l'origen de tot nou Iqcià), amb el treball experimental. Tot estava tan col·apsat que en Dani (l'immortal del 177) ocupava mitja taula i jo l'altre meitat. Després, un grup d'irreductibles iqcians vam emprendre un llarg viatge cap a la conquesta de noves terres, a l'altra banda de la muntanya, on hem viscut grans moments. No em vull deixar ningú, tots vosaltres també sou part de la tesi (sense vosaltres potser l'hauria acabat abans ;) (esto es roja no??) però no m'ho hauria passat tan bé): a la Sílvia (la meva germana gran a l'IQC), en Pata (el meu germà fotoquímic), Dani (com es pot ser tan freak), Juanma (gestor de l'Univers i explotador de becaris de 1r any (algú ho havia de dir)), Lluís (Ramb... no he dit! Independència o no?), Cristina (freak multidimensional), Dachs (gadgetocàmera sempre a punt), Diaz (màxima potència sobre la bici), Mireia (la mama del despatx), Eloy (Chygramos-Córdoba), Pedro (Peeetraaaaa!), Oscar (compadre y místico que s'està gelant a Suècia), Samat (more wine? wine not), Yevhen (els seus - què significa...?-originen discussions interminables al despatx), David (de les Xungues), Quansong (Quantum Li, com va això?), Albert (la Roca, el mestre dels blocks), Torrentxu (sempre a l'avantguarda de la música), Quim (algun xiste més?) i també a tota la nova generació d'iqcians Carles, Majid, Sergi, Laia, Mickael, Luz i Marc, estar a l'IQC trastoca, oju! Només de recordar tots els bons moments se'm posa la pell de gallina: els kebabs ultrapicants i les partides interminables de pocha de manchester-liverpool, el cuba bar i la secta herbalife de Colonia, les migdiades als parcs i les llargues estones al centre comercial (mallrats!) de Goteborg, l'atac de les gavines assassines de Helsinki, els dominis propis d'Amsterdam, el feta cheese d'Atenes, l'espicha d'Oviedo. Però també els freaks de la bici (que casi no ho expliquen), els freaks de can Miá (ja toca no?), els freaks del 177 (Se ha matao Paco!), els freaks del jocs de taula (com el junglespeed cap), els freaks del japó (Arigatou!), els freaks del futbol (Inda forever!), els freaks de l'apm (ho haveu vist?), hi ha algú normal? Ens ho hem passat i ens ho seguirem passant molt bé! Afegir només que per fi he trobat gent més despistat i impuntual que jo! Si alguna cosa he après és que un no arriba mai tard, sinó que arriba quan s'ho proposa. I com no, no vull oblidar-me de tota la tribu experimental, que tot i que els matxaquem a les jodete son molt bones persones (Mira si es buena persona), pels sopars al basc, els estiu a carpes, etc. Venga pues, arreando que es tarde!

Especial menció a la Summerschool de Dinamarca amb la Sílvia i en Pata, la veritat

és que va ser genial, Saatana Perkele!, encuentros en la tercera fase amb en Hussein (quin crack!!!), socialitzant fins a altes hores, en Pisuke (sanhilali), la locomotora Vargas, les hores de problemes amb en Philip Callaghan (how is it going?), les partides al rotten, l'esmorzar, el dinar, els pastissos de berenar, els sopar, la peixera, la sauna, en Hellboy, el caçador de cocodrils (impagable l'escena del projector), en pepe olsen, el tigre de helgaker, en collina, els partits de futbol de 3 hores, el freak que feia problemes fins a les 12 de la nit (quin matat!),... i com no el paper fonamental que va tenir en el viatge el regalís (nunca mais). Que consti en acte!

No em puc oblidar de la Penya de l'Espardenya! Annes D, Santi, Alba, Naiara, Mònica F, Mònica B, Maira, Marta, Carla, Xevi, Ferram, Pilar, Olga, Quim. Sense vosaltres la carrera no hagués estat el mateix, festes, sopar de gala, viatge a Tunísia, a la biblio fins a les mil de la nit, sopars al suca-mulla, el brie amb pebrots, la peli Vaig Fort, carpes de Girona, els partits de basket de l'es Tio Conco Team. Però sobretot perquè seguim organitzant tot tipus d'events per anar-nos trobant, amics invisibles, sopars de barrakes, KUAK!!!

Kasikeno Productions presenta... a la colla de Banyoles, Albert, Anna L., Anna P., Chak, David, Edu, Enric, Ester, Fina, Joan, Jordi, Maria L., Maria M., Maria V., Mariona, Miki, Sílvia, que us puc dir que no us hagi dit en 18 hores de cotxe seguides per anar a Berlin? Suecia, Frankfurt, Cannes, Madrid, Londres, Berlin, Euskadi, Bretanya, Aquitània, Noruega... Gràcies per totes les hores que hem passat i seguirem passant junts, festes de tot tipus, converses paranoiques a l'Ateneu, tot tipus de concerts, fins i tot un concert insonor!, Marie-Claire, la Trini Sánchez Mata (Trini la que mata), carnavals, ens ho partim?, i com no els grans èxits de la Kasikeno Street Band: fred del nord ja som aquí, corren rumors rhapsody, que bé que vius, no acabaria mai! Perdoneu-me per arribar sempre tard, però quan marxi de postdoc segur que trobeu a faltar els sms "faig 20 minuts tard".

Last but no least, els més importants, ja que sense ells res seria possible i mai els hi podré agrair prou tot el que han fet per mi. La meva família, la mare, el pare, en Guillem (des de Porto amb la cesi, la nair i la isis), i als que per mi també són germans, en Milla (i per extensió la Pharbin i en Subó) i la Tabita, a tots vull donar-vos les gràcies per tots els valors que m'heu transmès, per tot el que m'heu permès veure i viure i per ser sempre allà on calia. Moltes vegades no t'adones del valor que tenen les coses fins al cap d'un temps. Les rutes per pràcticament tot Europa amb el volskwagen jetta i tenda, les classes amb els ganduls, els dinars a la

casa, les converses sobre el Barça amb en Milla, mirar Amelie i Diarios de Motocicleta repetidament amb en Guillem, el viatge que va fer a Bangladesh per buscar els pares de'n Milla, els consells però sobretot per deixar-me completa llibertat. No m'agradaria oblidar-me dels avis ni de la resta de la família. Als avis de Banyoles pel seu suport constant, per preocupar-se per mi, per preguntar-me sempre què es el que estic investigant i escoltar-me, ara podré venir més sovint a dinar :). L'àvia de Palafrugell per ser una avia diferent, es la persona que més optimisme i dinamisme m'ha transmès, no havia vist mai ningú amb tantes inquietuds i estic molt orgullós que sigui la meva àvia. Us estimo molt a tots!!

Full List of Publications

The thesis is based on the following publications:

Chapter 5

1. Feixas, F.; Matito, E.; Duran, M.; Solà, M.; Silvi, B.; The Electron Localization Function at the Correlated Level: A Natural Orbital Formulation. *J. Chem. Theory Comput.* 6, 2736-2742, **2010**
2. Ponec, R.; Feixas, F.; Domain Averaged Fermi Hole Analysis for Open-shell systems. *J. Phys. Chem. A* 113, 5773-5779, **2009**
3. Feixas, F.; Ponec, R.; Fiser, J.; Schröder, D.; Roithová, J.; Price, S.D.; Bonding analysis of the $[C_2O_4]^{2+}$ intermediate formed in the reaction of CO_2^{2+} with neutral CO_2 . *J. Phys. Chem. A* 113, 6681-6688, **2010**
4. Ponec, R.; Feixas, F.; Peculiarities of Multiple Cr-Cr Bonding. Insights from the analysis of Domain- Averaged Fermi Holes. *J. Phys. Chem. A* 113, 8394-8400, **2009**

Chapter 6

5. Matito, E.; Feixas, F.; Solà, M.; Electron Delocalization and Aromaticity Measures within the Hückel Molecular Orbital Method. *J. Mol. Struct. (THEOCHEM)* 811, 3-11, **2007**
6. Feixas, F.; Matito, E.; Poater, J.; Solà, M.; Aromaticity of Distorted Benzene Rings. Exploring the Validity of Different Indicators of Aromaticity. *J. Phys. Chem. A* 111, 4513-4521, **2007**
7. Feixas, F.; Jiménez-Halla, J.O.C.; Matito, E.; Poater, J.; Solà, M.; Is the aromaticity of the benzene ring in the $(\eta^6 - C_6H_6)Cr(CO)_3$ complex larger than that of the isolated benzene molecule?. *Pol J. Chem.* 81, 783- 797, **2007**
8. Feixas, F.; Matito, E.; Poater, J.; Solà, M.; On the Performance of Some Aromaticity Indices: A Critical Assessment Using a Test Set. *J. Comput. Chem.* 29, 1543-1554, **2008**
9. Feixas, F.; Jiménez-Halla, J.O.C.; Matito, E.; Poater, J.; Solà M.; A Test to Evaluate the Performance of Aromaticity Descriptors in All-Metal and Semimetal Clusters. An Appraisal of Electronic and Magnetic Indicators of Aromaticity. *J. Chem. Theory Comput.* 6, 1118-1130, **2010**

Chapter 7

10. Feixas, F.; Matito, E.; Solà, M.; Poater, J.; Analysis of Hückel's $[4n+2]$ Rule Through Electronic delocalization measures. *J. Phys. Chem. A* 112 13231-13238, **2008** special issue: Sason Shaik Festschrift.
11. Feixas, F.; Matito, E.; Solà, M.; Poater, J.; Patterns of π -electron delocalization in aromatic and antiaromatic organic compounds in the light of the Hückel's $[4n+2]$ Rule. *Phys. Chem. Chem. Phys.* 12, 7126-7137, **2010**
12. Feixas, F.; Matito, E.; Duran, M.; Poater, J.; Solà, M.; Aromaticity and electronic delocalization in all-metal clusters with single, double, and triple aromatic character. *Theor. Chem. Acc.* Accepted for publication, **2010**, in the Special Issue devoted to Theoretical Chemistry in Spain.

Publications not included in this thesis:

13. Leyva, V.; Corral, I.; Schmierer, T.; Heinz, B.; Feixas, F.; Migani, A.; Blancafort, Ll.; Gilch, P.; González, L.; Electronic States of o-Nitrobenzaldehyde: A Combined Experimental and Theoretical Study. *J. Phys. Chem. A* 112, 5046, **2008**
14. Feixas, F.; Solà, M.; Swart, M.; Chemical bonding and aromaticity in metalloporphyrins. *Can. J. Chem.* 87, 1063-1073, **2009** in the Special Issue dedicated to Professor T. Ziegler
15. Solà, M.; Feixas, F.; Jiménez-Halla, J.O.C.; Matito, E.; Poater, J.; A Critical Assessment of the Performance of Magnetic and Electronic Indices of Aromaticity. *Symmetry* 2, 1156-1179, **2010**
16. Feixas, F.; Matito, E.; Swart, M.; Poater, J.; Solà, M.; Electron Delocalization in Organometallic Compounds: From Agostic Bond to Aromaticity *AIP Conference Proceedings of the International Conference on Computational Methods in Science and Engineering, ICCMSE 2009, AIP*, Accepted for publication, **2010**
17. Migani, A.; Leyva, V.; Feixas, F.; Schmierer, T.; Gilch, P.; Corral, I.; González, L.; Blancafort, Ll.; Excited State Hydrogen Transfer in ortho-nitrobenzaldehyde: A correlated diagram translated to a conical intersection triangle and cascade, Submitted for publication, **2010**

List of Acronyms

Abbreviation	Description
1-RDM	First-order Reduced Density Matrix
2-PD	Two-Particle Density
2-RDM	Second-order Reduced Density Matrix
AIM	Atom In a Molecule
AOM	Atomic Overlap Matrix
ASE	Aromatic Stabilization Energy
BB	Buijse and Baerends approach
BCP	Bond Critical Point
BLA	Bond Length Alternation
BLE	Bond Length Elongation
CASSCF	Complete Active Space Self Consistent Field
CBO	Coulson Bond Order
CCP	Cage Critical Point
CCSD	Coupled Cluster Singles and Doubles
CISD	Configuration Interaction Singles and Doubles
CP	Conditional Probability
DAFH	Domain-Averaged Fermi Hole
DI	Delocalization Index
DFT	Density Functional Theory
ELF	Electron Localization Function
ESI	Electron Sharing Index
FBO	Fuzzy-atom Bond Order
FLU	Aromatic Fluctuation index
HEG	Homogenous Electron Gas
HF	Hartree-Fock
HF-XCD	Hartree-Fock Exchange-Correlation Density
HOMA	Harmonic Oscillator Model of Aromaticity
HMO	Hückel Molecular Orbital
LI	Localization Index
MBO	Mayer-Bond Order
MCI	Multicenter Index
MO	Molecular Orbital
MP2	Second-order Moller-Plesset Perturbation Theory

Abbreviation	Description
NCP	Nuclear Critical Point
NICS	Nucleus-independent chemical shifts
NNA	Non-Nuclear Attractor
PDI	Para-Delocalization Index
QTAIM	Quantum Theory of Atoms in Molecules
RCP	Ring Critical Point
RDM	Reduced Density Matrix
XCD	Exchange-Correlation Density

Contents

Preface	vii
Resum de la tesi	ix
Agraïments	xi
Full List of Publications	xvii
List of Acronyms	xxi
1 Introduction	1
1.1 From Quantum Mechanics to Quantum Chemistry	1
1.2 A brief overview of Quantum Chemistry	3
1.3 Physical Interpretation of the Wave Function	5
1.4 Density Functions	6
1.5 Density Matrices	8
1.6 Two-electron Densities and Holes	10
1.6.1 Pair Density and Exchange Correlation Density	11
1.6.2 Conditional Probability and Pair Correlation Function	14
1.6.3 Fermi and Coulomb Holes	15
2 Methodology	21
2.1 The Atom in a Molecule	22
2.1.1 Quantum Theory of Atoms in Molecules	23
2.1.2 Fuzzy Atom Schemes	29
2.2 Electron Sharing Indices	30
2.2.1 Definition	31
2.2.2 Example: $Cr(CO)_6$	38
2.3 Domain-Averaged Fermi Hole Analysis	41
2.3.1 DAFH definition	41
2.3.2 Example: $Cr(CO)_6$	44
2.4 Electron Localization Function	50
2.4.1 Becke's Definition	50

2.4.2	Example: $Cr(CO)_6$	53
3	Aromaticity	59
3.1	Key Advances	60
3.2	Descriptors of Aromaticity	66
4	Objectives	75
5	Applications I: The Nature of the Chemical Bond from Electron Localization Function and Domain-Averaged Fermi Holes	77
5.1	Electron Localization Function at the Correlated Level: A Natural Orbital Formulation	79
5.2	Domain Averaged Fermi Hole Analysis for open-shell systems	87
5.3	Bonding Analysis of the $[C_2O_4]^{2+}$ Intermediate Formed in the Reaction of CO_2^{2+} with Neutral CO_2	95
5.4	Peculiarities of Multiple Cr-Cr bonding. Insights from the Analysis of Domain-Averaged Fermi Holes	105
6	Applications II: Critical assessment on the performance of a set of aromaticity indexes	113
6.1	Electron Delocalization and Aromaticity Measures within the Hückel Molecular Orbital Method	115
6.2	Aromaticity of Distorted Benzene Rings: Exploring the Validity of Different Indicators of Aromaticity	125
6.3	Is the Aromaticity of the Benzene Ring in the $(\eta^6 - C_6H_6)Cr(CO)_3$ Complex Larger than that of the Isolated Benzene Molecule?	135
6.4	On the Performance of Some Aromaticity Indices: A Critical Assessment Using a Test Set	151
6.5	A Test to Evaluate the Performance of Aromaticity Descriptors in All-Metal and Semimetal Clusters. An Appraisal of Electronic and Magnetic Indicators of Aromaticity	177
7	Applications III: Study of electron delocalization in organic/inorganic compounds	193
7.1	Analysis of Hückel's $[4n + 2]$ Rule through Electronic Delocalization Measures	195
7.2	Patterns of π -electron Delocalization in Aromatic and Antiaromatic Organic Compounds in the Light of Hückel's $[4n + 2]$	205

7.3	Aromaticity and electronic delocalization in all-metal clusters with single, double, and triple aromatic character	219
8	Results and Discussion	233
8.1	Applications I	233
8.1.1	Electron Localization Function	233
8.1.2	Domain-Averaged Fermi Holes	236
8.2	Applications II	247
8.2.1	Electronic Aromaticity indices at HMO level	248
8.2.2	A Critical Assessment on the Performance of Aromaticity Criteria in Organic Systems	250
8.2.3	A Critical Assessment on the Performance of Aromaticity Criteria in All-Metal Clusters	256
8.3	Applications III	259
8.3.1	Electron Delocalization in Organic Systems	260
8.3.2	Electron Delocalization in All-Metal Clusters	267
9	Conclusions	271

Chapter 1

Introduction: Quantum Mechanics, Density Matrices and Density Functions

1.1 From Quantum Mechanics to Quantum Chemistry

Toward the end of the 19th century, many scientists considered physics as a complete discipline that gave a successful explanation for different natural phenomena and allowed to interpret the results of most of the experiments. The contributions of Galileo and Newton to classical mechanics, or the works of Faraday and Maxwell in the field of electricity and magnetism, signified extremely important advancements in the comprehension of the physical reality, from the large objects of the universe to the quotidian things around us.

Quantum Mechanics is at the heart of many areas of physics. This theory plays a critical role in understanding the laws of nature that govern the domain of the small, that is, particles such as electrons, or bigger entities like atoms and molecules. The quantum theory was a rupture with regard to the intuitive way of conceiving the physical world. Do electrons behave like waves or like particles? Or more interestingly, could an electron behave like a particle and a wave at the same time? The works of Max Planck, Erwin Schrödinger, or Werner Heisenberg among many others, firmly established the basis of quantum theory and supposed one of the major breakthroughs of the 20th century. In the realm of quantum mechanics, mathemat-

ics plays a key role. Thus, the Hilbert space, the abstract algebra, or the theory of probabilities allow to predict the results of many experiments with surprisingly accurate precision. In quantum theory, the scientific predictions of the results are statistical in nature, and are treated in terms of probabilities. Consequently, concepts such as uncertainty, fuzziness, and probability are deeply linked to quantum theory. The determinism that characterized classical mechanics gave way to the indeterminism associated with quantum mechanics. Quantum mechanics has been very successful in accounting for many experimental results in particle physics and in the properties of atoms and molecules.

However, the first steps of quantum mechanics were followed by a lengthily discussion about the validity of this theory to describe physical reality. During this period, some authors claimed that quantum mechanics was barely a statistical theory that could not provide a complete description of the physical world and, thus, some variables that would improve the comprehension of the theory must remain occult. For instance, the entanglement phenomena has been at the epicenter of the debate about the incompleteness of the quantum theory. Notwithstanding, the theory was accepted by most of the physical community and played a key role from the very beginning. The discovery of quantum theory found potential applications in other fields of science such as chemistry, giving birth to the area called Quantum Chemistry. The main objectives of this thesis will be addressed from the quantum chemical point of view.

At the end of 19th century, great advances in the field of chemistry had been made up to that time. For instance, the initially controversial concept of molecule was finally widely accepted; the impressing work of Mendeleev gave rise to the periodic table of the elements; and Kekulé finally unraveled the structure of benzene. However, the mechanism of how a chemical reaction occurs, or concepts such as the nature of chemical bonding or the aromaticity of a given molecule remained unexplainable. Hence, a heated debate over atoms, molecules, or the early concepts of chemical bonding occupied a central position in the most important conferences before the 20th century. One of the most striking advances was published in 1916 by G. N. Lewis.² In that paper, Lewis proposed a model to study the chemical bonding based on the concept of lone and sharing electron pairs. The first steps towards the concepts of electron localization and delocalization were established. Although the Lewis model presents some pitfalls, it has been widely used from the very beginning by most of the chemical community to account for the electronic distribution of a

given molecule.

Like physics, chemistry experimented a step forward with the advent of quantum mechanics. Nevertheless, the mathematical complexity associated with quantum chemical calculations distanced experimental chemists from theoretical chemists. This gap was reduced with the fast advances in computational power giving rise to the so-called computational chemistry. Thus, from computational chemistry, it is possible to explore the potential energy surface of complex reactions and describe their reaction mechanism. In addition, the magnetic properties of a large group of molecules could be accurately predicted or the dynamical behavior of biological systems could be analyzed through molecular simulations. Quantum chemistry opened a completely new way to analyze the electronic structure or physical and chemical molecular properties. In the last decades, a large number of new methods has been proposed to improve the conception of chemistry. However, chemists still use some old chemical conceptions such as bonding strength, atomic charges or aromaticity to provide an explanation for different chemical phenomena. Consequently, one of the main aims of several theoretical research groups has been to reconcile these old concepts with quantum mechanics. But how can we use quantum mechanics to evaluate the nature of chemical bonding or the aromaticity of a conflicting system? Will this information help us to predict the stability or reactivity of organic and inorganic molecules, and offer explanations for different chemical phenomena? In the next chapters of this thesis, we will give an overview of the most widely used methods to analyze the chemical bonding and aromaticity.

1.2 A brief overview of Quantum Chemistry

We will briefly summarize the basic concepts of quantum chemistry that are needed to understand the next sections and chapters. The ultimate goal of quantum chemistry is to find the (approximate) solution of time-independent, non-relativistic Schrödinger equation that gives the description of the statistical behavior of particles:

$$\hat{H}\Psi_i(\vec{x}_1, \vec{x}_2, \dots, \vec{x}_N, \vec{R}_1, \vec{R}_2, \dots, \vec{R}_M) = \varepsilon_i\Psi_i(\vec{x}_1, \vec{x}_2, \dots, \vec{x}_N, \vec{R}_1, \vec{R}_2, \dots, \vec{R}_M) \quad (1.1)$$

where \hat{H} is the Hamiltonian operator for a molecular system composed by M nuclei

and N electrons. The \hat{H} contains the kinetic operators, \hat{T}_e and \hat{T}_N , which describe the kinetic energy of the electrons and nuclei respectively, and three potential operator terms, \hat{V}_{ee} , \hat{V}_{Ne} , and \hat{V}_{NN} , that account for both attractive and repulsive potential energies. Each state i is associated with a wave function. Therefore, Ψ_i is the wave function of the state i of the system which depends on the $3N$ spatial electronic coordinates (\vec{r}_N) and the N electronic spin coordinates (\vec{s}_N) that are collectively named as \vec{x}_N , and the $3M$ spatial nuclear coordinates (\vec{R}_M). ε_i are the numerical values of the energy of state i .

Consequently, the main aim of quantum chemistry is to solve the Schrödinger equation in order to find the eigenfunctions, i.e. the wave functions Ψ_i , and the corresponding eigenvalues ε_i of \hat{H} . The wave function, Ψ_i , contains all the information that can be known about a quantum system. Once the wave function is determined, all properties of interest can be acquired by applying the appropriate operators to the wave function. However, the exact solution of the Schrödinger equation is unaffordable and, thus, there is a need to find different strategies to solve approximately this eigenfunction-eigenvalue problem.

The first basic approach, that can be easily applied in most of the cases, is the so-called Born-Oppenheimer approximation. Since the nuclei are much heavier than the electrons and, thus, much slower, it is a good approximation to take the extreme point and consider the electrons as moving in the field of fixed nuclei, as two separated motions. Then, the Born-Oppenheimer approximation evaluates the motions of nuclei and electrons separately, which extremely simplifies the problem. In this way, the \hat{H} may be divided into electronic and nuclear terms, \hat{H}_{elec} and \hat{H}_{nuc} , and the solutions of the Schrödinger equation with \hat{H}_{elec} are the electronic wave function $\Psi_{elec}(\vec{x}_1, \vec{x}_2, \dots, \vec{x}_N)$ and the electronic energy E_{elec} . Now, the Ψ_{elec} explicitly depends on the \vec{x}_N coordinates and parametrically on \vec{R}_M . Finally, the total energy E_{tot} is the sum of E_{elec} and the constant nuclear energy E_{nuc} , which is the nuclear repulsion term of the \hat{H} :

$$\hat{H}_{elec}\Psi_{elec}(\vec{x}_N; \vec{R}_M) = E_{elec}\Psi_{elec}(\vec{x}_N; \vec{R}_M) \quad (1.2)$$

$$E_{tot} = E_{elec} + E_{nuc} \quad (1.3)$$

From now on we will only consider the electronic wave function and we will refer to

it as Ψ .

1.3 Physical Interpretation of the Wave Function

In Quantum Mechanics, concepts such as bond order, atomic charge or aromaticity are not *observables*, that is, they cannot be directly measured by means of any operator, and therefore, they have no physical direct interpretation. Moreover, the wave function itself is not an observable. Hence, how can we translate the information of quantum theory to shed some light on the nature of these widely used chemical concepts? In 1926, Max Born proposed the physical interpretation of the square of the wave function, $|\Psi|^2$, in terms of probabilities. This statistical analysis provides the probability to find N particles in a given region:

$$|\Psi(\vec{x}_1, \vec{x}_2, \dots, \vec{x}_N)|^2 d\vec{x}_1 d\vec{x}_2 \dots d\vec{x}_N \quad (1.4)$$

This equation informs us about the probability of finding simultaneously electrons $1, 2, \dots, N$ in volume elements $d\vec{x}_1, d\vec{x}_2, \dots, d\vec{x}_N$. Due to the fact that electrons are indistinguishable, the exchange of two electron coordinates must not change this probability:

$$|\Psi(\vec{x}_1, \vec{x}_2, \dots, \vec{x}_i, \vec{x}_j, \dots, \vec{x}_N)|^2 = |\Psi(\vec{x}_1, \vec{x}_2, \dots, \vec{x}_j, \vec{x}_i, \dots, \vec{x}_N)|^2 \quad (1.5)$$

Consequently, there are only two possibilities that when interchanging their coordinates the probability remains unaltered, first, the wave functions are identical or, second, the interchange of two coordinates leads to a sign change. This requirement is fulfilled by two groups of particles. The bosons, which have integer spin and their wave function is symmetric with respect to the interchange of coordinates, and the fermions that have half-integer spin and their switch leads to an antisymmetric wave function. For fermions we have:

$$\Psi(\vec{x}_1, \vec{x}_2, \dots, \vec{x}_i, \vec{x}_j, \dots, \vec{x}_N) = -\Psi(\vec{x}_1, \vec{x}_2, \dots, \vec{x}_j, \vec{x}_i, \dots, \vec{x}_N) \quad (1.6)$$

Since the electrons are fermions with spin $1/2$, we will deal with antisymmetric wave functions. The antisymmetry principle is the quantum-mechanical generalization of Pauli exclusion principle, two electrons with the same spin cannot occupy the same state. Hence, the electrons are constrained by the Pauli exclusion principle. The consequences of this principle have a crucial importance on the localization and

delocalization of electrons, the main topic of this thesis. As the integral of Eq. 1.4 over the full space equals one, the probability of finding N electrons anywhere in the space must be exactly the unity:

$$\int \dots \int |\Psi(\vec{x}_1, \vec{x}_2, \dots, \vec{x}_N)|^2 d\vec{x}_1 d\vec{x}_2 \dots d\vec{x}_N = 1 \quad (1.7)$$

To sum up the information presented up to now, in classical physics we can, in principle, measure, determine and predict, for instance, the position and the velocity of a moving object with full precision. On the other hand, in quantum mechanics the predictions are statistical in nature, and, for instance, we can study the probability of finding a portion of particles like electrons in a given region. This portion of electrons can be associated with the concept of electronic charge and, thus, with the so-called electron density. Consequently, the square of the wave function leads to both the electron density and the pair density, which are one-particle and two-particle electron distributions, respectively. The information given by the density and the pair density can be translated to acquire the electronic structure of a given molecule and, hence, one can study properties such as the chemical bonding or the aromaticity of a plethora of systems.

1.4 Density Functions

In this section, the concepts of electron density and pair density are defined. We have a system with N electrons which is described by a wave function, $\Psi(\vec{x}_1, \vec{x}_2, \dots, \vec{x}_N)$. As previously mentioned, the product of $\Psi(\vec{x}_1, \vec{x}_2, \dots, \vec{x}_N)$ with its complex conjugate $\Psi^*(\vec{x}_1, \vec{x}_2, \dots, \vec{x}_N)$ gives the probability of finding electron 1 between \vec{x}_1 and $\vec{x}_1 + d\vec{x}_1$, while electron 2 is between \vec{x}_2 and $\vec{x}_2 + d\vec{x}_2$, ..., and electron N is between \vec{x}_N and $\vec{x}_N + d\vec{x}_N$. It is particularly interesting to study the probability of finding electron one regardless of the position of the remaining $N - 1$:

$$d\vec{x}_1 \int \Psi(\vec{x}_1, \vec{x}_2, \dots, \vec{x}_N) \Psi^*(\vec{x}_1, \vec{x}_2, \dots, \vec{x}_N) d\vec{x}_2 \dots d\vec{x}_N \quad (1.8)$$

since the electrons are indistinguishable the probability of finding one electron is

$$\rho(\vec{x}_1) = N d\vec{x}_1 \int \Psi(\vec{x}_1, \vec{x}_2, \dots, \vec{x}_N) \Psi^*(\vec{x}_1, \vec{x}_2, \dots, \vec{x}_N) d\vec{x}_2 \dots d\vec{x}_N \quad (1.9)$$

where $\rho(\vec{x})$ is the so-called density function. The integration of Eq. 1.9 with respect

to the spin coordinates leads us to the probability density, which is known as the electron density, $\rho(\vec{r})$:

$$\begin{aligned}\rho(\vec{r}_1) &= \int \rho(\vec{x}_1) ds_1 \\ &= N d\vec{x}_1 \int \Psi(\vec{x}_1, \vec{x}_2, \dots, \vec{x}_N) \Psi^*(\vec{x}_1, \vec{x}_2, \dots, \vec{x}_N) d\vec{s}_1 d\vec{x}_2 \dots d\vec{x}_N\end{aligned}\quad (1.10)$$

The electron density is the angular stone of density functional theory (DFT) due to the fact that it contains all the information needed to describe the energy of the ground state of a given molecule. As opposed to the wave function, the electron density is an observable and can be measured experimentally by means of X-ray diffraction. Since Ψ is normalized, and the electrons are indistinguishable, the integration over the whole space is N , that is, the total number of electrons:

$$\int \rho(\vec{r}_1) d\vec{r}_1 = N \quad (1.11)$$

For the sake of clarity, the electron density can also be represented as

$$\rho(\vec{x}_1) = \gamma^{(1)}(\vec{x}_1) \quad (1.12)$$

The definition of the pair density is also interesting. The concept of electron pair is the cornerstone of Lewis' model and will play a crucial role in methodologies devoted to the analysis of chemical bonding. The probability of finding electrons 1 and 2 in the volume elements \vec{x}_1 and \vec{x}_2 is given by

$$d\vec{x}_1 d\vec{x}_2 \int \Psi(\vec{x}_1, \vec{x}_2, \dots, \vec{x}_N) \Psi^*(\vec{x}_1, \vec{x}_2, \dots, \vec{x}_N) d\vec{x}_3 \dots d\vec{x}_N \quad (1.13)$$

$$\gamma^{(2)}(\vec{x}_1, \vec{x}_2) = N(N-1) \int \Psi(\vec{x}_1, \vec{x}_2, \dots, \vec{x}_N) \Psi^*(\vec{x}_1, \vec{x}_2, \dots, \vec{x}_N) d\vec{x}_3 \dots d\vec{x}_N \quad (1.14)$$

The pair density is a two-particle electron distribution which informs us about the probability density of finding a certain couple of electrons, e.g. 1 and 2, irrespective of the position of the remaining $N-2$ electrons. The interpretation is analogous to the one given by the electron density of finding one electron in a particular region. One can also define a spinless pair density:

$$\gamma^{(2)}(\vec{r}_1, \vec{r}_2) = \int \gamma^{(2)}(\vec{x}_1, \vec{x}_2) ds_1 ds_2 \quad (1.15)$$

1.5 Density Matrices

As previously mentioned, the N -electron wave function obtained by solving the Schrödinger equation for a many-particle system contains all the possible information about the quantum state. This wave function, that it is very difficult to obtain, includes a large amount of information that will not be employed at all. Thus, from this wave function is usually too complicated to provide a simple physical picture of the system. Notwithstanding, it is possible to use alternative mathematical structures called reduced density matrices. These density matrices are simpler than the wave function itself and have a more direct physical meaning. For instance, the two-electron reduced density matrix (2-RDM) comprises all the physically and chemically important information. In principle, the 2-RDM can be used to compute the energy and the atomic and molecular properties without the need of the many-particle wave function.⁹ However, there are some conditions, such as the N -representability, which has to be fulfilled to ensure that the 2-RDM derives from the N -electron wave function. This field has potential applications in many areas of physics and chemistry, e.g., it could represent a bridge between the density functional theory and the *ab initio* wave function methods.¹⁰

From the N -electron wave function, $\Psi(\vec{x}_1, \dots, \vec{x}_N)$, one can define the N -order density matrix (DM) as

$$\gamma^{(n)}(\vec{x}_1' \dots \vec{x}_N' | \vec{x}_1 \dots \vec{x}_N) = \Psi^*(\vec{x}_1', \dots, \vec{x}_N') \Psi(\vec{x}_1, \dots, \vec{x}_N) \quad (1.16)$$

where N is the number of electrons in our system. This matrix depends upon $2N$ variables which is beyond feasible computations with current computers. The number of variables is reduced to construct the m -order reduced density matrices, by integration of $N - m$ of its coordinates:

$$\gamma^{(m)}(\vec{x}_1' \dots \vec{x}_m' | \vec{x}_1 \dots \vec{x}_m) = \binom{n}{m} m! \int \gamma^{(n)}(\vec{x}_1' \dots \vec{x}_m', \vec{x}_{m+1} \dots \vec{x}_N | \vec{x}_1 \dots \vec{x}_N) \Delta_{m+1}^N d\vec{x}_{m+1} \dots \vec{x}_N \quad (1.17)$$

where Δ_{m+1}^N is the generalized Dirac delta

$$\Delta_{m+1}^N = \prod_{i=m+1}^N \delta(\vec{x}_i' - \vec{x}_i) \quad (1.18)$$

The first-order (1-RDM) reduced density matrices are particularly interesting:

$$\gamma^{(1)}(\vec{x}_1' | \vec{x}_1) = N \int \Psi^*(\vec{x}_1' \dots \vec{x}_m', \vec{x}_{m+1} \dots \vec{x}_N) \Psi(\vec{x}_1, \dots, \vec{x}_N) \Delta_2^N d\vec{x}_2 \dots \vec{x}_N \quad (1.19)$$

and also the second-order reduced density matrices:

$$\gamma^{(2)}(\vec{x}_1' \vec{x}_2' | \vec{x}_1 \vec{x}_2) = N(N-1) \int \Psi^*(\vec{x}_1' \dots \vec{x}_m', \vec{x}_{m+1} \dots \vec{x}_N) \Psi(\vec{x}_1, \dots, \vec{x}_N) \Delta_3^N d\vec{x}_3 \dots \vec{x}_N \quad (1.20)$$

Let us now show how we can use the m -RDM in order to compute the density functions described in the above section. The wave function can be expanded in terms of Slater determinants:

$$\Psi = \sum_K c_K \psi_K \quad (1.21)$$

where ψ_K are the Slater determinants constructed from a set of orthonormalized spin orbitals:

$$\psi_K = \frac{1}{\sqrt{N!}} |\chi_1(\vec{x}_1), \chi_2(\vec{x}_2), \dots, \chi_N(\vec{x}_N)| \quad (1.22)$$

In this case, Eq. 1.17 can be further simplified to obtain

$$\gamma^{(m)}(\vec{x}_1' \dots \vec{x}_m' | \vec{x}_1 \dots \vec{x}_m) = \sum_{\substack{i_1 i_2 \dots i_m \\ j_1 j_2 \dots j_m}} \Gamma_{i_1 i_2 \dots i_m}^{j_1 j_2 \dots j_m} \chi_{i_1}^*(\vec{x}_1'), \dots, \chi_{i_m}^*(\vec{x}_m') \chi_{j_1}(\vec{x}_1), \dots, \chi_{j_m}(\vec{x}_m) \quad (1.23)$$

Thus, the m -RDM is calculated as an expansion of our basis set. The $\Gamma_{i_1 i_2 \dots i_m}^{j_1 j_2 \dots j_m}$ is computed from the coefficients c_K given in Eq. 1.21. For our purposes, it is particularly interesting to further simplify Eq. 1.23 by only taking into account the diagonal terms of the m -RDM, i.e., $x_i = x_i'$. Then, we get the m -order density

functions

$$\gamma^{(m)}(\vec{x}_1 \dots \vec{x}_m) = \sum_{\substack{i_1 i_2 \dots i_m \\ j_1 j_2 \dots j_m}} \Gamma_{i_1 i_2 \dots i_m}^{j_1 j_2 \dots j_m} \chi_{i_1}^*(\vec{x}_1), \dots, \chi_{i_m}^*(\vec{x}_m) \chi_{j_1}(\vec{x}_1), \dots, \chi_{j_m}(\vec{x}_m) \quad (1.24)$$

Consequently, we can express the one-electron density as

$$\gamma^{(1)}(\vec{x}_1) = \sum_{i,j} \chi_i^*(\vec{x}_1) \Gamma_i^j \chi_j(\vec{x}_1) \quad (1.25)$$

And the two-electron density, which is used to study the electron correlation, is represented in the following manner

$$\gamma^{(2)}(\vec{x}_1, \vec{x}_2) = \sum_{\substack{i,j \\ k,l}} \chi_i^*(\vec{x}_1) \chi_j^*(\vec{x}_2) \Gamma_{ij}^{kl} \chi_k(\vec{x}_1) \chi_l(\vec{x}_2) \quad (1.26)$$

It is worth noticing that the algorithm needed to obtain $\Gamma_{i_1 i_2 \dots i_m}^{j_1 j_2 \dots j_m}$ was designed in our laboratory by Dr. Eduard Matito in order to calculate the Configuration Interaction Singles and Doubles (CISD) first and second order density matrices. This program has been extended in this thesis to generate the m -order density matrices from the Complete Active Space Self Consistent Field (CASSCF) (see Chapter 5.1 for further applications).

In the case of monodeterminantal wave functions, the density matrices must be diagonal regardless of the order of the matrix. In particular, we can express the p-RDM in terms of 1-RDM:

$$\gamma^{(m)}(\vec{x}_1' \dots \vec{x}_m' | \vec{x}_1 \dots \vec{x}_m) = \begin{vmatrix} \gamma^{(1)}(\vec{x}_1' | \vec{x}_1) & \dots & \gamma^{(1)}(\vec{x}_1' | \vec{x}_p) \\ \vdots & \ddots & \vdots \\ \gamma^{(1)}(\vec{x}_p' | \vec{x}_1) & \dots & \gamma^{(1)}(\vec{x}_p' | \vec{x}_p) \end{vmatrix} \quad (1.27)$$

1.6 Two-electron Densities and Holes

The pair density contains all the information referring to the correlated motion of two electrons. The correlation between same spin electrons is called exchange while the correlation due to different spin electrons is called Coulomb correlation. The exchange correlation arises from the antisymmetry of the wave function. At the Hartree-Fock level, the exchange correlation is the only one taken into account,

while the Coulomb correlation is neglected. The effect of the Coulomb correlation can be accounted for by means of second-order perturbation theory, configuration interaction (CI), or Coupled Cluster (CC) methods among others. The DFT also introduces these correlation effects but in a different manner. The same information regarding the correlation of electrons is found in other quantities derived from the pair density, such as the exchange correlation density and in the conditional probability.

1.6.1 Pair Density and Exchange Correlation Density

The pair density can be decomposed in terms of an uncorrelated density and another part that accounts for the electron correlation (both exchange and Coulomb correlations):

$$\gamma^{(2)}(\vec{x}_1, \vec{x}_2) = \gamma^{(1)}(\vec{x}_1)\gamma^{(1)}(\vec{x}_2) + \gamma_{XC}(\vec{x}_1, \vec{x}_2) \quad (1.28)$$

where the first term corresponds to a fictitious pair density constructed as a product of two independent electron distributions, and the second is the so-called exchange correlation density (XCD), $\gamma_{XC}(\vec{x}_1, \vec{x}_2)$.¹¹ The XCD represents the difference between the probability density of finding two electrons, one at x_1 and the other at x_2 , in a correlated and uncorrelated fashion. As $\gamma^{(1)}(\vec{x}_1)$ integrates to N and $\gamma^{(2)}(\vec{x}_1, \vec{x}_2)$ to $N(N - 1)$, the integration of this quantity over the whole space gives the total number of electrons $-N$:¹

$$\int \int \gamma_{XC}(\vec{x}_1, \vec{x}_2) d\vec{x}_1, d\vec{x}_2 = -N \quad (1.31)$$

¹The XCD could also be defined as the difference between the uncorrelated and correlated motions of two electrons:

$$\gamma^{(2)}(\vec{x}_1, \vec{x}_2) = \gamma^{(1)}(\vec{x}_1)\gamma^{(1)}(\vec{x}_2) - \gamma_{XC}(\vec{x}_1, \vec{x}_2) \quad (1.29)$$

and then, the integration of this quantity gives:

$$\int \int \gamma_{XC}(\vec{x}_1, \vec{x}_2) d\vec{x}_1, d\vec{x}_2 = N \quad (1.30)$$

This definition has been used in most of the publications of Chapters 5, 6, and 7 to introduce the domain averaged fermi holes and the electron sharing indices.

In the next chapter, we will see the role played by the XCD to assess the electron localization and delocalization between two given atoms, or regions, of the molecular space. Before entering to the world of molecular partition and electron sharing indices, we will see how Eq. 1.29 can be manipulated for monodeterminantal wave functions. In the literature most of the calculations are closed-shell and with monodeterminantal wave functions, using both HF or DFT within the Kohn and Sham formalism, the pair density of Eq. 1.29 can be further simplified in terms of the 1-RDM using Eq. 1.27:

$$\gamma^{(2)}(\vec{x}_1' \dots \vec{x}_2) = \begin{vmatrix} \gamma^{(1)}(\vec{x}_1|\vec{x}_1) & \gamma^{(1)}(\vec{x}_1|\vec{x}_2) \\ \gamma^{(1)}(\vec{x}_2|\vec{x}_1) & \gamma^{(1)}(\vec{x}_2|\vec{x}_2) \end{vmatrix} \quad (1.32)$$

Let us now split Eq. 1.32 in terms of its spins cases:

$$\begin{aligned} & \gamma^{(2)\alpha\alpha}(\vec{r}_1, \vec{r}_2) + \gamma^{(2)\alpha\beta}(\vec{r}_1, \vec{r}_2) + \gamma^{(2)\beta\alpha}(\vec{r}_1, \vec{r}_2) + \gamma^{(2)\beta\beta}(\vec{r}_1, \vec{r}_2) \\ &= (\gamma^{(1)\alpha}(\vec{r}_1) + \gamma^{(1)\beta}(\vec{r}_1))(\gamma^{(1)\alpha}(\vec{r}_2) + \gamma^{(1)\beta}(\vec{r}_2)) \\ &+ (\gamma^{(1)\alpha}(\vec{r}_1|\vec{r}_2) + \gamma^{(1)\beta}(\vec{r}_1|\vec{r}_2))(\gamma^{(1)\alpha}(\vec{r}_2|\vec{r}_1) + \gamma^{(1)\beta}(\vec{r}_2|\vec{r}_1)) \\ &= \gamma^{(1)\alpha}(\vec{r}_1)\gamma^{(1)\alpha}(\vec{r}_2) + \gamma^{(1)\alpha}(\vec{r}_1)\gamma^{(1)\beta}(\vec{r}_2) \\ &+ \gamma^{(1)\beta}(\vec{r}_1)\gamma^{(1)\alpha}(\vec{r}_2) + \gamma^{(1)\beta}(\vec{r}_1)\gamma^{(1)\beta}(\vec{r}_2) \\ &+ \gamma^{(1)\alpha}(\vec{r}_1|\vec{r}_2)\gamma^{(1)\alpha}(\vec{r}_2|\vec{r}_1) + \gamma^{(1)\beta}(\vec{r}_1|\vec{r}_2)\gamma^{(1)\beta}(\vec{r}_2|\vec{r}_1) \end{aligned} \quad (1.33)$$

where, after the integration over one coordinate, the cross-spin out-of-diagonal terms of the 1-RDM, $\gamma^{(1)\alpha}(\vec{r}_1|\vec{r}_2)\gamma^{(1)\beta}(\vec{r}_2|\vec{r}_1) = 0$ due to the orthonormality of the spin functions. Interestingly, in the case of monodeterminantal wave functions, the cross-spins contributions, which are responsible for the Coulomb correlation, come only from the fictitious product of one-electron densities and, thus, the electrons with antiparallel spin move in a completely uncorrelated fashion. This fact has important consequences in the calculation of both the electron localization function and electron

sharing indices as we will see in the next chapters.

In a large number of cases, the HF approximation dramatically fails, for instance in some strong covalent interactions. Thus, the inclusion of Coulomb correlation is crucial to describe the electronic structure of the system. As previously mentioned, the calculation of the *exact* pair density is usually unaffordable. Fortunately, the pair density can be successfully approximated in terms of natural orbitals for correlated wave functions. Some of the most popular approximations have been summarized in the introduction of Chapter 5.1.

After bringing together the terms corresponding to the density and pair density, Eq. 1.33 can be simplified as:

$$\gamma^{(2)}(\vec{r}_1, \vec{r}_2) = \gamma^{(1)}(\vec{r}_1)\gamma^{(1)}(\vec{r}_2) + \gamma^{(1)\alpha}(\vec{r}_1|\vec{r}_2)\gamma^{(1)\alpha}(\vec{r}_2|\vec{r}_1) + \gamma^{(1)\beta}(\vec{r}_1|\vec{r}_2)\gamma^{(1)\beta}(\vec{r}_2|\vec{r}_1) \quad (1.34)$$

Only in the case of closed-shell monodeterminantal wave functions, the α and β contributions that come from the out-of-diagonal terms of the 1-RDM can be collected together. Thus, the second order density matrix can be obtained from the 1-RDM one:

$$\gamma^{(2)}(\vec{r}_1, \vec{r}_2) = \gamma^{(1)}(\vec{r}_1)\gamma^{(1)}(\vec{r}_2) + \frac{1}{2}\gamma^{(1)}(\vec{r}_1|\vec{r}_2)\gamma^{(1)}(\vec{r}_2|\vec{r}_1) \quad (1.35)$$

Therefore, the spinless version of the XCD within a monodeterminantal wave function is

$$\gamma_{XC}(\vec{r}_1, \vec{r}_2) = \frac{1}{2} \left| \gamma^{(1)}(\vec{r}_1|\vec{r}_2) \right|^2 \quad (1.36)$$

This is the expression of the XCD which is used in most of this thesis to calculate the values of the electron sharing indices (see Chapters 6 and 7), where the calculations have been essentially performed at the DFT level within the Kohn-Sham approach with both closed and open-shell monodeterminantal wave functions. From Eq. 1.36, one can generalize the expression of the *exact* pair density as

$$\gamma^{(2)}(\vec{r}_1, \vec{r}_2) = \gamma^{(1)}(\vec{r}_1)\gamma^{(1)}(\vec{r}_2) + \frac{1}{2}\gamma^{(1)}(\vec{r}_1|\vec{r}_2)\gamma^{(1)}(\vec{r}_2|\vec{r}_1) + \lambda^{(2)}(\vec{r}_1, \vec{r}_2) \quad (1.37)$$

where $\lambda^{(2)}(\vec{r}_2, \vec{r}_1)$ is the so-called cumulant matrix.¹² This term was proposed by Kutzelnigg and Mukherjee and accounts for the exact correlation contribution. In Chapter 5.1 this formula has been approximated by means of a natural orbital approach. Thus, at the correlated level, the formula for the XCD can be rewritten as:

$$\gamma_{XC}(\vec{r}_1, \vec{r}_2) = \frac{1}{2}\gamma^{(1)}(\vec{r}_1|\vec{r}_2)\gamma^{(1)}(\vec{r}_2|\vec{r}_1) + \lambda^{(2)}(\vec{r}_1, \vec{r}_2) \quad (1.38)$$

Obviously, within the framework of HF approximation one has $\lambda^{(2)}(\vec{r}_1, \vec{r}_2) = 0$.

1.6.2 Conditional Probability and Pair Correlation Function

As we have seen, the XCD, as the pair density, contains all the information concerning the correlated motion of two electrons. We can go one step further and define the so-called conditional probability (CP). The CP describes the probability of finding electron 2 at position \vec{r}_2 when electron 1 is fixed at the position \vec{r}_1 .

$$P(\vec{r}_2; \vec{r}_1) = \frac{\gamma^{(2)}(\vec{r}_1, \vec{r}_2)}{\gamma^{(1)}(\vec{r}_1)} \quad (1.39)$$

Taking advantage of the definition of the pair density one can obtain

$$P(\vec{r}_2; \vec{r}_1) = \gamma^{(1)}(\vec{r}_2) + \frac{\gamma_{XC}(\vec{r}_1, \vec{r}_2)}{\gamma^{(1)}(\vec{r}_1)} \quad (1.40)$$

Hence, the CP integrates to $N - 1$ electrons, that is, all electrons except the reference electron 1 which is located at \vec{r}_1 :

$$\int P(\vec{r}_2; \vec{r}_1) d\vec{r}_2 = N - 1 \quad (1.41)$$

On the other hand, we can further manipulate the expression of the XCD, Eq. 1.29, with the purpose of obtaining the *pair correlation function*, $f(\vec{r}_1; \vec{r}_2)$. This function, which is defined positive and dimensionless, informs us about the kind of correlation that our system presents. In the case of independent electrons, the value of the $f(\vec{r}_1; \vec{r}_2)$ is 0. First, the spinless formula of the XCD can be written as

$$\gamma_{XC}(\vec{r}_1, \vec{r}_2) = \gamma^{(2)}(\vec{r}_1, \vec{r}_2) - \gamma^{(1)}(\vec{r}_1)\gamma^{(1)}(\vec{r}_2) \quad (1.42)$$

Then, one may divide the terms of Eq. 1.42 by $\gamma^{(1)}(\vec{r}_1)\gamma^{(1)}(\vec{r}_2)$, so that we get the dimensionless expression of the function $f(\vec{r}_1; \vec{r}_2)$:

$$f(\vec{r}_1; \vec{r}_2) = \frac{\gamma_{XC}(\vec{r}_1, \vec{r}_2)}{\gamma^{(1)}(\vec{r}_1)\gamma^{(1)}(\vec{r}_2)} = \frac{\gamma^{(2)}(\vec{r}_1, \vec{r}_2)}{\gamma^{(1)}(\vec{r}_1)\gamma^{(1)}(\vec{r}_2)} - 1 \quad (1.43)$$

Thus, the formula of the pair density can be reformulated in terms of the pair correlation function as proposed by McWeeny:¹³

$$\gamma^{(2)}(\vec{r}_1, \vec{r}_2) = \gamma^{(1)}(\vec{r}_1)\gamma^{(1)}(\vec{r}_2)[1 + f(\vec{r}_1; \vec{r}_2)] \quad (1.44)$$

The pair correlation function will help us to interpret the concepts of Fermi and Coulomb holes which are described in the next section.

Finally, a clear link can be established between the conditional probability, $P(\vec{r}_2; \vec{r}_1)$, and the pair correlation function, $f(\vec{r}_1; \vec{r}_2)$:

$$P(\vec{r}_2; \vec{r}_1) = \gamma^{(1)}(\vec{r}_2)[1 + f(\vec{r}_1; \vec{r}_2)] \quad (1.45)$$

1.6.3 Fermi and Coulomb Holes

From the difference between the $P(\vec{r}_2; \vec{r}_1)$ and the probability of finding an electron at \vec{r}_2 , one could define the so-called *exchange-correlation hole*. The same result is obtained by multiplying the $f(\vec{r}_1; \vec{r}_2)$ function by the uncorrelated $\gamma^{(1)}(\vec{r}_2)$:

$$\begin{aligned}
h_{XC}(\vec{r}_1; \vec{r}_2) &= P(\vec{r}_2; \vec{r}_1) - \gamma^{(1)}(\vec{r}_2) \\
&= f(\vec{r}_1; \vec{r}_2)\gamma^{(1)}(\vec{r}_2)
\end{aligned} \tag{1.46}$$

or in terms of XCD can be expressed as

$$h_{XC}(\vec{r}_1; \vec{r}_2) = \frac{\gamma_{XC}(\vec{r}_1, \vec{r}_2)}{\gamma^{(1)}(\vec{r}_2)} \tag{1.47}$$

Since the inclusion of electron correlation usually leads to a depletion of charge at \vec{r}_2 when compared to $\gamma^{(1)}(\vec{r}_2)$, it can be seen that $h_{XC}(\vec{r}_1; \vec{r}_2)$ is defined nonpositive. That is, the electron correlation leads to a decrease of the electron density at the vicinity of \vec{r}_2 in comparison to the independent particle situation. Due to the Pauli exclusion principle, electrons with the same spin will have strong difficulties coexisting in the same region of the space. Usually, the Coulomb interaction between same spin electrons will play a less critical role in the exchange-correlation hole. This depletion of electronic charge is the main reason to give the name *hole* to this quantity. Therefore, the $h_{XC}(\vec{r}_1; \vec{r}_2)$ is a region of the space that surrounds the electron where the presence of the other electrons is diminished. Interestingly, due to the fact that XCD integrates to $-N$ and $\gamma^{(1)}(\vec{r}_2)$ to N , the integration of $h_{XC}(\vec{r}_1; \vec{r}_2)$ over the whole space gives rise to the charge of one electron:

$$\int h_{XC}(\vec{r}_1; \vec{r}_2) = -1 \tag{1.48}$$

The $h_{XC}(\vec{r}_1; \vec{r}_2)$ plays a key role in density functional theory. We are interested in its decomposition in Fermi and Coulomb counterparts. As previously done for the XCD, one can split the conditional probability or the pair correlation factor in terms of their spin contributions:

$$P^{\alpha\alpha}(\vec{r}_2; \vec{r}_1) = \frac{\gamma^{(2)\alpha\alpha}(\vec{r}_1, \vec{r}_2)}{\gamma^{(1)\alpha}(\vec{r}_1)} \tag{1.49}$$

$$f^{\alpha\alpha}(\vec{r}_1; \vec{r}_2) = \frac{\gamma^{(2)\alpha\alpha}(\vec{r}_1, \vec{r}_2)}{\gamma^{(1)\alpha}(\vec{r}_1)\gamma^{(1)\alpha}(\vec{r}_2)} - 1 \tag{1.50}$$

$$P^{\alpha\beta}(\vec{r}_2; \vec{r}_1) = \frac{\gamma^{(2)\alpha\beta}(\vec{r}_1, \vec{r}_2)}{\gamma^{(1)\alpha}(\vec{r}_1)} \quad (1.51)$$

$$f^{\alpha\beta}(\vec{r}_1; \vec{r}_2) = \frac{\gamma^{(2)\alpha\beta}(\vec{r}_1, \vec{r}_2)}{\gamma^{(1)\alpha}(\vec{r}_1)\gamma^{(1)\beta}(\vec{r}_2)} - 1 \quad (1.52)$$

Eq. 1.49 gives us the probability of finding one electron with spin α in the position \vec{r}_2 when there is an electron with the same spin at \vec{r}_1 , while Eq. 1.51 gives us the probability when the other electron of the pair has spin β . Thus, Eq. 1.49 accounts for the Fermi correlation due to the Pauli exclusion principle whereas Eq. 1.51 is related to the Coulomb repulsion. The expressions 1.50 and 1.52 represent the ratio of the correlated pair density, $\gamma^{(2)\alpha\alpha}(\vec{r}_1, \vec{r}_2)$ and $\gamma^{(2)\alpha\beta}(\vec{r}_1, \vec{r}_2)$, and the uncorrelated fictitious densities, that is, $\gamma^{(1)\alpha}(\vec{r}_1)\gamma^{(1)\alpha}(\vec{r}_2)$ and $\gamma^{(1)\alpha}(\vec{r}_1)\gamma^{(1)\beta}(\vec{r}_2)$. Therefore, we can obtain the hole functions by multiplying the expressions 1.50 and 1.52 by the corresponding one-electron density:

$$h^{\alpha\alpha}(\vec{r}_1; \vec{r}_2) = f^{\alpha\alpha}(\vec{r}_1; \vec{r}_2)\gamma^{(1)\alpha}(\vec{r}_2) \quad (1.53)$$

$$h^{\alpha\beta}(\vec{r}_1; \vec{r}_2) = f^{\alpha\beta}(\vec{r}_1; \vec{r}_2)\gamma^{(1)\beta}(\vec{r}_2) \quad (1.54)$$

Analogously, the hole function may be written in terms of CP by subtracting this quantity to the one-electron density:

$$h^{\alpha\alpha}(\vec{r}_1; \vec{r}_2) = P^{\alpha\alpha}(\vec{r}_2; \vec{r}_1) - \gamma^{(1)\alpha}(\vec{r}_2) \quad (1.55)$$

$$h^{\alpha\beta}(\vec{r}_1; \vec{r}_2) = P^{\alpha\beta}(\vec{r}_2; \vec{r}_1) - \gamma^{(1)\beta}(\vec{r}_2) \quad (1.56)$$

Hence, the $h_{XC}(\vec{r}_1; \vec{r}_2)$ is partitioned into different contributions:

$$h_{XC}(\vec{r}_1; \vec{r}_2) = h^{\alpha\alpha}(\vec{r}_1; \vec{r}_2) + h^{\alpha\beta}(\vec{r}_1; \vec{r}_2) + h^{\beta\alpha}(\vec{r}_1; \vec{r}_2) + h^{\beta\beta}(\vec{r}_1; \vec{r}_2) \quad (1.57)$$

By gathering, on the one hand, the same spin terms and, on the other, the cross

spin terms we get:

$$h_{XC}(\vec{r}_1; \vec{r}_2) = h_X(\vec{r}_1; \vec{r}_2) + h_C(\vec{r}_1; \vec{r}_2) \quad (1.58)$$

where $h_X(\vec{r}_1; \vec{r}_2)$ is the so-called Fermi hole due to the same spin interaction and related to the antisymmetry requirement of the wave function, while $h_C(\vec{r}_1; \vec{r}_2)$ is the Coulomb hole resulting from the electrostatic interaction. At the HF level, the Coulomb hole is neglected. As previously said, the Fermi hole usually dominates by far over the Coulomb hole, and as the $h_{XC}(\vec{r}_1; \vec{r}_2)$ the Fermi hole integrates to -1 :

$$\int h_X(\vec{r}_1; \vec{r}_2) d\vec{r}_2 = -1 \quad (1.59)$$

This is a direct consequence of the Pauli exclusion principle which ensures that two electrons of same spin cannot be at the same position. The shape of the hole depends on the system, but is usually deeper in the vicinity of the reference electron and tends to zero when we move away from this position because the presence of the reference electrons is less notorious. When the position of electron 2 tends to the position of the reference electron, the Fermi hole has to be equal to minus the density of electrons with the same spin at the position of the reference electron:

$$\lim_{\vec{r}_2 \rightarrow \vec{r}_1} h_X(\vec{r}_1; \vec{r}_2) = -\gamma^{(1)}(\vec{r}_1) \quad (1.60)$$

Thus, from Eqs. 1.48 and 1.60 it is clear that the Coulomb hole must integrate to zero:

$$\int h_C(\vec{r}_1; \vec{r}_2) d\vec{r}_2 = 0 \quad (1.61)$$

This means that there is a nonzero probability of finding two electrons with different spin at the same position of the space. The concept of the Fermi hole will be of capital importance in the next chapter when the electron localization function, the electron sharing indices, and the domain-averaged Fermi holes will be defined.

Alternatively, the exchange and Coulomb holes could be defined in terms of XCD as

$$\gamma_{XC}(\vec{r}_1, \vec{r}_2) = \gamma_X(\vec{r}_1, \vec{r}_2) + \gamma_C(\vec{r}_1, \vec{r}_2) \quad (1.62)$$

$$\begin{aligned} h_{XC}(\vec{r}_1; \vec{r}_2) &= \frac{\gamma_{XC}(\vec{r}_1, \vec{r}_2)}{\gamma^{(1)}(\vec{r}_2)} = \frac{\gamma_X(\vec{r}_1, \vec{r}_2)}{\gamma^{(1)}(\vec{r}_2)} + \frac{\gamma_C(\vec{r}_1, \vec{r}_2)}{\gamma^{(1)}(\vec{r}_2)} \\ &= h_X(\vec{r}_1; \vec{r}_2) + h_C(\vec{r}_1; \vec{r}_2) \end{aligned} \quad (1.63)$$

Chapter 2

Methodology: Molecular Space Partitions, Electron Localization and Electron Delocalization

In the following chapter we will see how the information provided by the concepts introduced in the previous sections can be translated to shed some light on the electronic distribution of the molecule. The wave function contains more information than what is really needed; therefore, the one- and two-electron quantities may play a critical role on the description of the system. As we have seen, the two-electron quantities (i.e. the pair density, the exchange correlation density, the conditional probability and the hole functions) inform us about the correlated motion of electrons and, thus, one knows how the electrons are distributed throughout the net of nuclei that form the molecule. In addition, we have seen where the electrons with the same and different spin can and cannot coexist. The forces that govern these restrictions are the Pauli's exclusion principle, represented by the Fermi hole, and the electrostatic interaction, expressed in terms of the Coulomb hole.

In the previous chapter, the general expressions for these two-electron quantities have been presented. However, it is somewhat difficult to extract relevant chemical information when these quantities are integrated over the whole space; in part, due to the fact that integration returns the total number of electrons, or pairs of electrons, of the system. For instance, in the Cope's rearrangement reaction, where there is no need for other reactants and it only needs heat to take place, the total number of electrons of the diene is not altered along the mechanism but the electronic structure dramatically changes. Consequently, the bonding nature varies,

some bonds are broken, other are formed, and some others change their nature. In chemistry, the properties of a given atom or region of the molecular space are as important as global molecular properties. Thus, the partition of the molecular space into different regions helps to unravel how the electrons are localized in a specific region or which is the number of electrons shared between two or more regions. However, there is no unique way to define an atom in a molecule. Hence, first of all we will describe the most used partitions by discussing their applicability, and the strong and weak points of each method. All this information will help us to study the nature of particular chemical bonds or the aromaticity of a given ring in the following chapters of this thesis.

Atomic properties like the atomic charge, the concepts of bond order or bonding strength, the characteristics of a specific functional group, or the aromaticity of a particular ring, have been widely used to rationalize the structure or reactivity of a given system. As mentioned in the beginning of this thesis, none of the chemical concepts listed above is an observable. Thus, the main aim of this chapter will be to connect these chemical concepts with quantum-mechanics via the above mentioned two-electron densities. This chapter is organized as follows. First, a brief summary of the Quantum Theory of Atoms and Molecules (QTAIM) will be presented. Second, we will outline the most used partitions of the molecular space. Finally, we will introduce the concepts of Electron Sharing indices (ESI), Domain Averaged Fermi Holes (DAFH), and Electron Localization Function (ELF).

2.1 The Atom in a Molecule

In the last years, several research groups have been involved in a lengthy discussion about the best way to define the atom within a molecule and to calculate the atomic contributions to global quantities. Basically, these definitions can be split into two different schemes of atomic partition.

First, we have the methods that partition the Hilbert space of basis functions into its atomic contributions, where the atom can be identified with the nucleus and the subspace of basis functions centered at this nucleus. The most popular Hilbert-space based definition is the Mulliken population analysis¹⁴ that can be performed from any *ab initio* calculation. However, this easy and intuitive method presents some drawbacks, for instance, strong basis set dependence, or some problems in describing the overlap population between a pair of atoms that show differences of electroneg-

ativity.

Second, we have the definitions based on the partition of the real 3D molecular space. These definitions can be divided into two groups according to how the boundaries of the regions are defined. On the one hand, the ones that present sharp boundaries, such as the Voronoi cells,¹⁵ the Daudel loges,¹⁶ or the Electron Localization Function⁶ that will be introduced at the end of this chapter. Among them, the QTAIM,¹⁷ that will be described in the following section, is the most popular. Nevertheless, several pitfalls have been found for QTAIM, e.g., the presence of non-nuclear attractors or the expensive and time-consuming integrations of the sharp atomic boundaries. On the other hand, the concept of *fuzzy atom*¹⁸ has gained increasing popularity in the last decade. In contrast to the non-overlapping QTAIM atomic regions, the atomic domains obtained from the fuzzy schemes do not have boundaries and exhibit a continuous transition from one region to another. These characteristics enable us to reduce the computational cost associated with the integration of non-overlapping regions. In general, the fuzzy atom based methods present a good agreement with the QTAIM results.

2.1.1 Quantum Theory of Atoms in Molecules

The Quantum Theory of Atoms in Molecules, introduced by Richard F. W. Bader,¹⁷ aims to link the experimental observations of chemistry to the electron density, or more specifically, to the topology of the electron density distribution. Originally, the QTAIM was called the Atoms in Molecules (AIM) theory. However, in the last years, Bader has preferred to call it QTAIM, because the theory is based on quantum mechanics. More specifically, the theory is related to the generalized action principle which establishes that the matter, which is a closed system, is composed of interacting open systems. These systems, which are bounded regions, can be obtained from the topological division of the electronic distribution and can be identified as atoms in a molecule. Thus, the molecular properties expressed in terms of electron density can be partitioned into atomic contributions by integrating the electron density over the region assigned by the topology of the charge distribution. The main advantage of QTAIM is that this can relate the classic picture of atoms connected by bonds to the quantum-mechanical description of molecules, where the concept of bond is meaningless.

To sum up, one may relate concepts such as chemical structure, chemical bond-

ing, or chemical reactivity to the topological partition of the electron density, or in Bader words "*AIM theory enables one to link the language of chemistry with that of physics*". Next, we will briefly summarize the fundamental aspects of the topology of the electron density.

Topology of the electron density

The topology of the electron density is based on the concept of the critical point, i.e., a maximum, minimum, or saddle point. The critical point is defined as the spatial point where the first derivative of the function, in our case the electron density, vanishes.

$$\vec{\nabla}\rho(\vec{r}) = \vec{i} \frac{\partial\rho(\vec{r})}{\partial x} + \vec{j} \frac{\partial\rho(\vec{r})}{\partial y} + \vec{k} \frac{\partial\rho(\vec{r})}{\partial z} = \vec{0} \quad (2.1)$$

The $\vec{0}$ signifies that each individual component of the gradient must be equal to zero (this condition is fulfilled at the critical point and at ∞). In order to classify the critical points we have to analyze the second derivatives, that is, the so-called Hessian matrix \mathbf{H} at the position of the critical points r_c :

$$\mathbf{H} = \begin{pmatrix} \frac{\partial^2\rho(\vec{r})}{\partial x^2} & \frac{\partial^2\rho(\vec{r})}{\partial x\partial y} & \frac{\partial^2\rho(\vec{r})}{\partial x\partial z} \\ \frac{\partial^2\rho(\vec{r})}{\partial y\partial x} & \frac{\partial^2\rho(\vec{r})}{\partial y^2} & \frac{\partial^2\rho(\vec{r})}{\partial y\partial z} \\ \frac{\partial^2\rho(\vec{r})}{\partial z\partial x} & \frac{\partial^2\rho(\vec{r})}{\partial z\partial y} & \frac{\partial^2\rho(\vec{r})}{\partial z^2} \end{pmatrix} \quad (2.2)$$

The Hessian Matrix can be diagonalized, since it is real and symmetric. The diagonalization is equivalent to a rotation of the coordinate system $\vec{r}(x, y, z) \rightarrow \vec{r}'(x', y', z')$ that has been done through a unitary transformation $\vec{r}' = \vec{r}\mathbf{U}$, where \mathbf{U} is the unitary matrix. Thus, one can transform the \mathbf{H} into its diagonal representation via $\mathbf{U}^{-1}\mathbf{H}\mathbf{U} = \Lambda$. The expression is

$$\mathbf{\Lambda} = \begin{pmatrix} \frac{\partial^2 \rho(\vec{r})}{\partial x'^2} & 0 & 0 \\ 0 & \frac{\partial^2 \rho(\vec{r})}{\partial y'^2} & 0 \\ 0 & 0 & \frac{\partial^2 \rho(\vec{r})}{\partial z'^2} \end{pmatrix} = \begin{pmatrix} \lambda_1 & 0 & 0 \\ 0 & \lambda_2 & 0 \\ 0 & 0 & \lambda_3 \end{pmatrix} \quad (2.3)$$

where eigenvalues λ_1 , λ_2 , and λ_3 are the curvatures of the density according to the three principal axes, x' , y' , and z' , respectively. Interestingly, the trace of the Hessian matrix is invariant with respect to the rotation of the coordinate system and is known as the Laplacian of the electron density, $\nabla^2 \rho(\vec{r})$:

$$\vec{\nabla}^2 \rho(\vec{r}) = \vec{\nabla} \cdot \vec{\nabla} \rho(\vec{r}) = \frac{\partial^2 \rho(\vec{r})}{\partial x^2} + \frac{\partial^2 \rho(\vec{r})}{\partial y^2} + \frac{\partial^2 \rho(\vec{r})}{\partial z^2} \quad (2.4)$$

Classification of critical points

The critical points are classified with respect to their rank ω which is the number of non-zero curvatures of the Hessian, and the signature σ , that is the algebraic sum of the signs of the curvatures, i.e., each curvature contributes +1 or -1. The critical points are symbolized as (ω, σ) :

(3,-3) Nuclear Critical Point (NCP), Attractor or Atomic Critical Point:

All the curvatures of the Hessian are negative, $\lambda_1, \lambda_2, \lambda_3 < 0$ (local maximum). Every single atomic region is defined by one, and only one, (3,-3) attractor.

(3,-1) Bond Critical Point (BCP): Two curvatures of the Hessian are negative, $\lambda_1, \lambda_2 < 0$, while one is positive, $\lambda_3 > 0$, i.e., it is a saddle point of order 1, which is maximum in the plane defined by the negative eigenvectors and minimum in the perpendicular direction. The bond critical point is found between two NCP and, in general, indicates the presence of a chemical bond. The values of electron density and other properties calculated at the BCP provide valuable information about the nature of the interaction between the two atoms.

(3,+1) Ring Critical Point (RCP): Two curvatures of the Hessian are positive, $\lambda_2, \lambda_3 > 0$, while one is negative, $\lambda_1 < 0$, that is, a saddle point of order 2, which is maximum in the plane defined by the positive eigenvectors and

minimum in the perpendicular direction. This RCP can be found on the vicinity of the center of chemical rings.

(3,+3) Cage Critical Point (CCP): All the curvatures of the Hessian are positive, $\lambda_1, \lambda_2, \lambda_3 > 0$, that is, a local minimum; e.g. the center of cubane molecule or C_{60} .

The number and type of critical points that one can find in a molecule has to fulfill the Poincaré-Hopf relationship

$$n_{NCP} - n_{BCP} + n_{RCP} - n_{CCP} = 1 \quad (2.5)$$

From the Topology of the Electron Density to the Definition of an Atom in a Molecule

From the topological analysis described above, one can define the atom in a molecule. The nuclei represent local maxima in the real space and exert an attractive force that determines the electronic distribution around the field of nuclei (see Figures a-2.1, c-2.1, and d-2.1). This accumulation of charge in the vicinity of the nuclear critical point allows a natural partitioning of the molecular space into mononuclear regions, i.e., $\Omega = A, B, \dots$. The gradient vector field of the electron density, $\vec{\nabla}\rho(\vec{r})$, describes trajectories, also called gradient paths, that originate and terminate at a critical point (see Figure c-2.1), i.e. where $\vec{\nabla}\rho(\vec{r}) = \vec{0}$. The boundaries of these atomic regions are determined by the zero flux in the gradient vector field of the electron density:

$$\vec{\nabla}\rho(\vec{r}) \cdot \vec{n}(\vec{r}) = \vec{0} \quad \forall \vec{r} \in S(\Omega) \quad (2.6)$$

where $n(\vec{r})$ is the unit vector normal to the surface $S(\Omega)$. From this boundary condition, also called the "zero-flux" surface condition, the molecular space is partitioned into non-overlapping regions that own one $(3, -3)$ attractor. Thus, the gradient vector lines associated with each atomic region converge to the NCP, which "attract" the gradient vector lines to its position, and define the atom in a molecule. The atomic contributions to a global quantity can be obtained by integrating this quantity over the whole space. For instance, the integration of the electron density over the region A gives the amount of charge located in this atomic domain.

$$N_A = \int_A \rho(\vec{r}) d\vec{r} \quad (2.7)$$

The sum of all atomic populations, i.e. $N_A + N_B + \dots$, must give the total number of electrons, N , of the molecular system. From the electron population one may define the atomic charge as:

$$q_A = Z_A - N_A \quad (2.8)$$

where Z_A is the atomic number. In some cases, one can find a local maximum, $(3, -3)$ attractor, in a position that does not correspond to those of the atomic nuclei. This non-nuclear local maximum, which is surrounded by its own region and has its gradient vector lines, is the so-called *non-nuclear attractor* (NNA).¹⁹⁻²¹ This phenomenon, which mostly occurs when the molecule presents metal nuclei, represents one of the main disadvantages of the QTAIM theory because it increases the complexity of the integration of the atomic regions. The presence of NNA in all-metal aromatic and antiaromatic rings is discussed in Chapter 7.3.

On the other hand, for each BCP $(3, -1)$ there is a pair of trajectories that originates at the BCP and terminates at the neighboring NCP. This gradient line that connects the pair of atomic regions is called the *bond path* (see Figure a-2.1).²² The BCP is the lowest value of the electron density along the bond path. Despite the controversy generated by this concept, the bond path is widely used as an indicator of all kinds of chemical bonding.²³⁻³⁰

Finally, the Laplacian of the electron density (see Figure e-2.1) tells us where the electronic charge is accumulated (negative sign) and where a deficiency exists. The $\nabla^2 \rho(\vec{r})$ has been widely calculated at the BCP with the aim of defining the nature of the atomic interaction.¹⁷ Negative values imply an accumulation of charge in the bonding region and, thus, the interaction is covalent. On the other hand, positive values are characteristic of ionic or Van der Waals interactions. In addition, the Laplacian has been used to define the atomic shell structure.

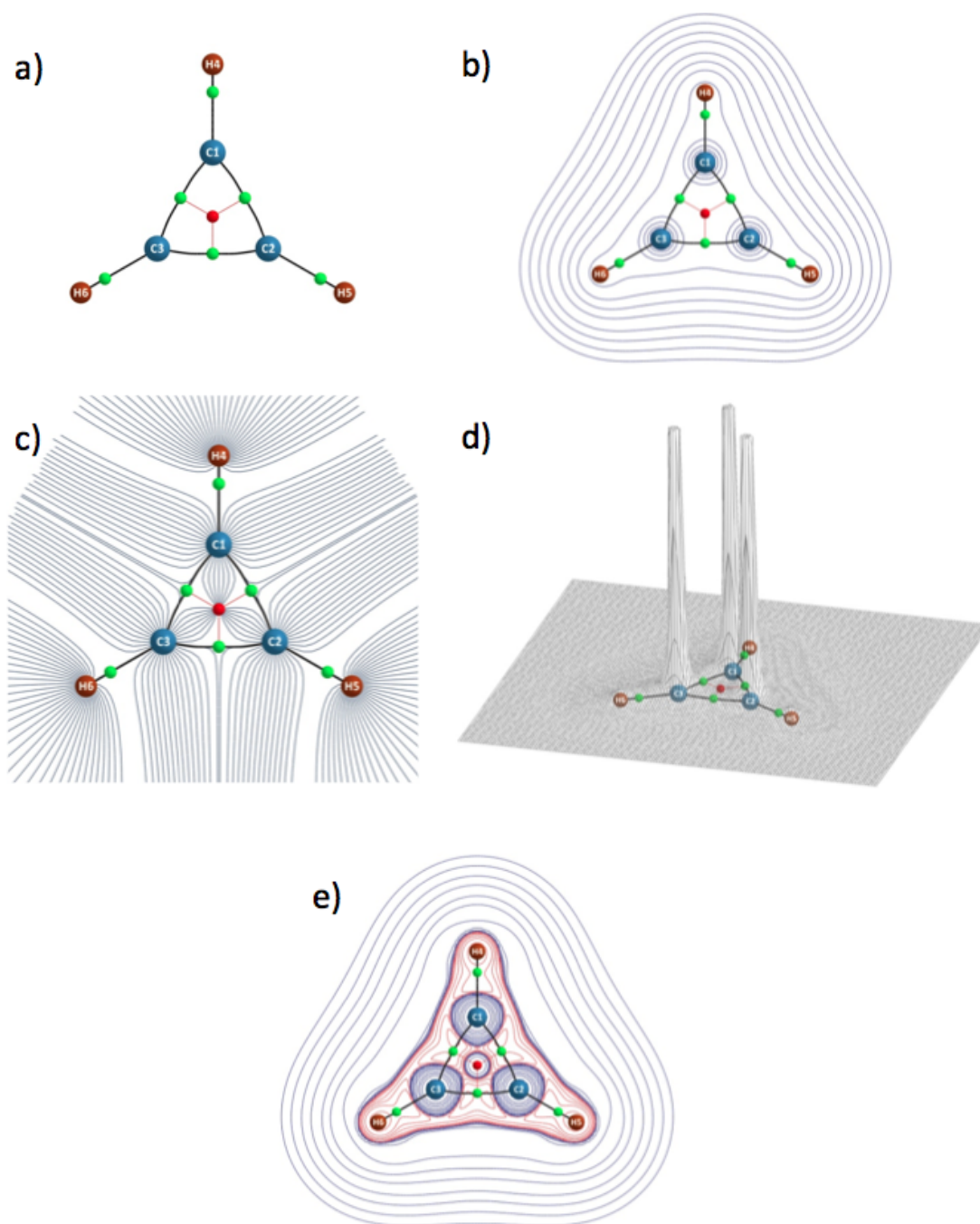


Figure 2.1: QTAIM analysis of $C_3H_3^+$. a) Topology of the electron density and critical points of $C_3H_3^+$: bond critical points in green, ring critical points in red, and bond paths in black; b) contour map of the electron density; c) trajectories of $\nabla\rho(\vec{r})$; d) relief map of electron density; e) contour map of the laplacian of the electron density (positive values in blue and negative values in red).

2.1.2 Fuzzy Atom Schemes

The concept of fuzzy atom is based on the division of the molecular space into atomic domains which do not have sharp boundaries but where there is a continuous transition from one region to another. Hence, part of the physical space is assumed to be shared to some extent by two or more atoms. This transition is expressed in terms of weight functions $w_A(\vec{r})$ which are defined for each atom A . The weight functions are obtained by assigning a weight factor to every point of the space, \vec{r} . The continuous non-negative function, $w_A(\vec{r})$, has to fulfill the following condition when summing over all the atoms of the system:

$$\sum_A w_A(\vec{r}) = 1 \quad (2.9)$$

The weight function is close to one in the vicinity of the nucleus and tends to zero as the distance to the nucleus increases. There are different strategies to define the $w_A(\vec{r})$. Fuzzy atoms were firstly related to the Hirshfeld's original idea of promolecular densities:³¹

$$w_A(\vec{r}) = \frac{\rho_A^0(\vec{r})}{\sum_A \rho_A^0(\vec{r})} \quad (2.10)$$

where the weight factor is the ratio of the isolated atomic density ρ_A^0 and the promolecular density $\sum_A \rho_A^0(\vec{r})$. Thus, one can calculate the atomic population as

$$N_A = \int \rho_A(\vec{r}) d\vec{r} = \int w_A(\vec{r}) \rho(\vec{r}) d\vec{r} \quad (2.11)$$

The main criticism to the classical Hirshfeld method is that the choice of the electronic state of the isolated atoms can seriously influence the resulting atomic population. This drawback has recently been overcome by Bultinck et al. with the so-called Iterative Hirshfeld approach or Hirshfeld-I.^{32,33} In this thesis, we have used Becke's method for multicentric integration:³⁴

$$w_A(\vec{r}) = \frac{P_A(\vec{r})}{\sum_B P_B(\vec{r})} \quad (2.12)$$

The weight factors are obtained through an algebraic function $P_A(\vec{r})$ for each atom

which is close to one in the vicinity of the nucleus and progressively tends to zero when the distance from the nucleus increases. This function depends on a set of atomic radii, such as those from Koga³⁵ or Slater,³⁶ that controls the size of the Voronoi cells, and upon a stiffness parameter k that controls the shape of the atom. Previous studies have proven the reasonable performance of Becke's scheme.^{18,37–39} Good agreement with QTAIM is found for covalent unpolarized bonds while for ionic systems or bonds involving B, Be, or Al, the deviation is more important, in part because the atomic regions obtained with QTAIM relatively differ from those obtained from the fuzzy atom approach.³⁷ Despite the fact that the atomic populations are sensibly affected by the definition of the atom in a molecule,⁴⁰ the electron sharing indices³⁷ and the electronic aromaticity indices^{38,39,41} are almost unaffected by the partition of the molecular space. In addition, the fuzzy approach is far less expensive than QTAIM. In the next section, we will analyze the dissociation of LiH by means of electron sharing indices with the aim of comparing the performance of QTAIM and fuzzy partitions.

2.2 Electron Sharing Indices

The analysis of the electronic distribution in molecules has occupied a central position from the seminal work of Lewis.² In the picture proposed by Lewis, the electrons are gathered in pairs around the molecule. These electron pairs can be classified as lone pairs (electrons which are localized in one atom) and bonding pairs (electrons that are shared between two atoms). However, this intuitive picture of electron distribution does not take into account the quantum nature of electrons. The advent of quantum mechanics triggered the interest in quantifying the electron sharing between two or more regions of the molecule. From the very beginning, the concept of electron sharing between two atoms has been associated with the concept of *bond order*. In 1938, Coulson was the first who used quantum mechanics to calculate the extent of electron sharing between two regions of the molecule.⁴² He called this measure "bonds of fractional order" and, interestingly, he applied these bond orders to study some polyenes and aromatic molecules. Therefore, the concepts of aromaticity and bond order has been tightly connected from the very beginning. From then on, the concept of bond order followed its evolution, gaining popularity among the electron structure descriptors used to characterize the chemical bonding of molecular systems. The term bond order does not comprise all the indices that account for the electron sharing of a pair of atoms. For this reason, in order to avoid controversy, we prefer to use the term electron sharing indices (ESI) proposed by Fulton.⁴³

Since the work of Coulson, several ESI have been described in the literature that can be classified according to the way they define an atom in a molecule. Mulliken's population analysis¹⁴ and Mayer's extension to bond orders and valences, e.g. the Mayer Bond Order (MBO),⁴⁴⁻⁴⁷ have taken a prominent role due to their simplicity and low computational cost. However, as previously mentioned, this definition of an atom within a molecule in the framework of Hilbert space presents some drawbacks that constrain its use. In the first chapter, we have shown the role played by the two-electron quantities on the description of the correlated motion of electrons. Thus, concepts such as pair density, exchange-correlation density, or conditional probability, describe how the electrons are localized and delocalized throughout the molecule. It was from the work of Wiberg⁴⁸ that the ESI based on the exchange-correlation density has become a primary concern. Among them, the most popular are those derived from QTAIM, such as the so-called delocalization index (DI),⁴⁹ Fuzzy-Atom, such as the fuzzy atom bond order (FBO),¹⁸ and Hirshfeld atomic partitions of the molecular space.

The ESI are not limited to analyzing the electron sharing between a couple of bonded atoms. They have been widely used to study the interaction between non-bonded regions, as the para delocalization index (PDI), which measures the number of electrons delocalized between the atoms in para position of six-membered rings and informs us about the aromaticity of the ring.⁵⁰ In addition, ESI are also employed to investigate to what extent the electrons are shared between more than two atoms or regions, the so-called multicenter indices.^{51,52} To sum up, although there is no unique definition of ESI, many of them have a common pattern: they measure the extent the electrons are shared by two or more entities, usually atoms.

2.2.1 Definition

In this thesis we will focus on the ESI based on the XCD which has been the most accepted approach for the calculation of these descriptors. As previously shown in Eq. 1.42, the XCD is the difference between the pair density $\gamma^{(2)}(\vec{r}_1, \vec{r}_2)$ and a fictitious pair density, which is the product of two independent one-electron distributions:

$$\gamma_{XC}(\vec{r}_1, \vec{r}_2) = \gamma^{(2)}(\vec{r}_1, \vec{r}_2) - \gamma^{(1)}(\vec{r}_1)\gamma^{(1)}(\vec{r}_2) \quad (2.13)$$

This function informs us about the motion of a pair of electrons contained in the

pair density by avoiding the individual electron distribution of the one-particle density. Thus, it is expected to be close to zero for two points distant in space and integrates to $-N$ when it is analyzed over the whole molecular space. In 1975, Bader and Stephens studied how the XCD can be used as a measure of electron pair distribution.⁵³ First, they analyzed the correlation contained in an atomic region of the molecule by integrating the XCD over the atomic domain A :

$$\int_A \int_A \gamma_{XC}(\vec{r}_1, \vec{r}_2) d\vec{r}_1 d\vec{r}_2 = \int_A \int_A \gamma^{(2)}(\vec{r}_1, \vec{r}_2) d\vec{r}_1 d\vec{r}_2 - \int_A \gamma^{(1)}(\vec{r}_1) d\vec{r}_1 \int_A \gamma^{(1)}(\vec{r}_2) d\vec{r}_2 \quad (2.14)$$

which at the same time measures to what extent the electrons are localized within a region of the space. However, it is more interesting to evaluate the partition of the XCD between two different regions A and B of the space which can be related with the correlative interaction between these two domains. To this end, Bader et al. proposed the integration of the XCD over two different atomic regions:

$$\int_A \int_B \gamma_{XC}(\vec{r}_1, \vec{r}_2) d\vec{r}_1 d\vec{r}_2 = \int_A \int_B \gamma^{(2)}(\vec{r}_1, \vec{r}_2) d\vec{r}_1 d\vec{r}_2 - \int_A \gamma^{(1)}(\vec{r}_1) d\vec{r}_1 \int_B \gamma^{(1)}(\vec{r}_2) d\vec{r}_2 \quad (2.15)$$

which also quantifies the delocalization or sharing of electrons over these regions. However, these quantities were not used as ESI until the beginning of the nineties.

ESI based on the HF-XCD and XCD

In 1991, Cioslowski and Mixon proposed the first ESI based on the QTAIM atomic partition and they called it *covalent bond order*.⁵⁴

$$\delta^C(A, B) = 2 \sum_i \lambda_i^2 S_{ii}(A) S_{ii}(B) \quad (2.16)$$

where λ_i are the occupations of the localized natural orbitals obtained after the isopycnic transformation procedure.^{55,56} The terms S_{ii} represent the diagonal elements of the atomic overlap matrix (AOM) of the localized spin orbitals integrated over the domain of atom A . It is worth mentioning that S_{ii} can be expressed as $S_{ii} = \int_A \chi_i^*(\vec{r}_1) \chi_i(\vec{r}_1) d\vec{r}_1$.

In 1993, Fulton introduced another ESI within the QTAIM.⁴³ He used the XCD expressed in terms of the 1-RDM and integrated over two different regions of the space. From Eq. 1.36, the ESI can be written as

$$\begin{aligned}\delta^F(A, B) &= \int_A \int_B \gamma^{(1)}(\vec{r}_1|\vec{r}_2)^{[1/2]} \gamma^{(1)}(\vec{r}_2|\vec{r}_1)^{[1/2]} d\vec{r}_1 d\vec{r}_2 \\ &+ \int_B \int_A \gamma^{(1)}(\vec{r}_1|\vec{r}_2)^{[1/2]} \gamma^{(1)}(\vec{r}_2|\vec{r}_1)^{[1/2]} d\vec{r}_1 d\vec{r}_2 \\ &= 2 \int_A \int_B \gamma^{(1)}(\vec{r}_1|\vec{r}_2)^{[1/2]} \gamma^{(1)}(\vec{r}_2|\vec{r}_1)^{[1/2]} d\vec{r}_1 d\vec{r}_2\end{aligned}\quad (2.17)$$

where $\gamma^{(1)}(\vec{r}_1|\vec{r}_2)^{[1/2]}$ 1-RDM is calculated as

$$\gamma^{(1)}(\vec{r}_1|\vec{r}_2)^{[1/2]} = \sum_k \lambda_k^{1/2} \eta_k^*(\vec{r}_1) \eta_k(\vec{r}_2) \quad (2.18)$$

and λ_k are the natural occupancies of the η_k natural spin orbitals. In terms of AOM, Eq. 2.17 is rewritten as

$$\delta^F(A, B) = 2 \sum_{ij} \lambda_i^{1/2} \lambda_j^{1/2} S_{ij}(A) S_{ij}(B) \quad (2.19)$$

where the $S_{ij}(A)$ are the elements of the AOM of the natural spin orbitals integrated over the region of atom A.

In 1994, Angyán and coworkers proposed another ESI based on the HF-XCD within the QTAIM formalism:⁵⁷

$$\delta^A(A, B) = \int_A \int_B \gamma^{(1)}(\vec{r}_1|\vec{r}_2) \gamma^{(1)}(\vec{r}_2|\vec{r}_1) d\vec{r}_1 d\vec{r}_2 = 2 \sum_{ij} \lambda_i \lambda_j S_{ij}(A) S_{ij}(B) \quad (2.20)$$

In 1997, Ponec and Uhlik proposed a general expression that allows to incorporate the concept of bond order within the QTAIM and makes possible a generalization beyond the monodeterminantal case.⁵⁸ Finally, in 1999, Fradera et al. recovered Bader's original expressions of the XCD and they used it for the first time as an ESI.⁴⁹ This quantity is better known as the delocalization index (DI):

$$\begin{aligned}
\delta(A, B) &= 2 \int_B \int_A \gamma_{XC}(\vec{r}_1, \vec{r}_2) d\vec{r}_1 d\vec{r}_2 \\
&= 2 \int_B \int_A \gamma^{(2)}(\vec{r}_1, \vec{r}_2) d\vec{r}_1 d\vec{r}_2 - 2 \int_A \gamma^{(1)}(\vec{r}_1) d\vec{r}_1 \int_B \gamma^{(2)}(\vec{r}_2) d\vec{r}_2 \quad (2.21)
\end{aligned}$$

When the wave function is expressed in terms of single determinants, as in most of this thesis, the DI can be written in terms of 1-RDM, such as Eq. 1.36:

$$\delta(A, B) = -2 \int_B \int_A \gamma_{xc}(\vec{r}_1, \vec{r}_2) d\vec{r}_1 d\vec{r}_2 \quad (2.22)$$

$$= \int_B \int_A |\gamma^{(1)}(\vec{r}_1, \vec{r}_2)|^2 d\vec{r}_1 d\vec{r}_2 \quad (2.23)$$

For monodeterminantal wave functions, $\delta(A, B)$ can be expressed in terms of AOM as

$$\delta(A, B) = 2 \sum_{ij} S_{ij}(A) S_{ij}(B) \quad (2.24)$$

This measure will be used in the second half of this thesis to quantify the aromaticity by means of electron delocalization measures. It can be easily proved that the definitions of Fulton, Angyán, and Fradera are equivalent for monodeterminantal wavefunctions. In addition, all those ESIs have been computed within the QTAIM framework. In principle, any other partition of the molecular physical space, e.g. fuzzy atom approach, could be applied (see Chapter 7.3).

Statistical interpretation of ESI

Another interesting property that can be extracted from the XCD is the so-called localization index (LI) which informs us about the number of electrons which are localized in one atomic domain:

$$\lambda(A) = \int_A \int_A \gamma_{xc}(\vec{r}_1, \vec{r}_2) d\vec{r}_1 d\vec{r}_2 = \sum_{ij} S_{ij}(A)^2 d\vec{r}_2 \quad (2.25)$$

Thus, from Eqs. 2.21 and 2.25 one can relate the LI with the same-atom contribution of the DI:

$$\lambda(A) = \frac{\delta(A, A)}{2} \quad (2.26)$$

The expected number of electrons in the basin of atom A, i.e. the population of A, is calculated as

$$\langle N(A) \rangle = \int_A \gamma^{(1)}(\vec{r}_1) d\vec{r}_1 \quad (2.27)$$

and its variance is

$$\begin{aligned} \sigma^2[N(A)] &= \langle N^2(A) \rangle - \langle N(A) \rangle^2 \\ &= \int_A \gamma^{(1)}(\vec{r}_1) d\vec{r}_1 - \int_A \gamma_{xc}(\vec{r}_1, \vec{r}_2) d\vec{r}_1 d\vec{r}_2 \\ &= N(A) - \lambda(A) = \sum_{B \neq A} \delta(A, B) = \delta(A) \end{aligned} \quad (2.28)$$

Thus, the variance corresponds to the number of electrons which are not localized in region A, that is, the number of electrons of region A which are delocalized to the other regions of the molecular space $\delta(A)$. In addition, one can define the relative fluctuation which measures the ratio of electrons delocalized in a given basin with respect to the population of that basin

$$\lambda_F(A) = \frac{\sigma^2[N(A)]}{N(A)} = \frac{N(A) - \lambda(A)}{N(A)}.100 \quad (2.29)$$

From Eq. 2.28, the LI is the expected number of electrons minus its uncertainty (variance) in its atomic basin. On the other hand, the electronic populations of two different regions of the space are not independent variables. This means that we can analyze the covariance of different atomic populations:

$$\begin{aligned} cov(A, B) &= V[N(A), N(B)] = \langle N(A)N(B) \rangle - \langle N(A) \rangle \langle N(B) \rangle = \\ &= - \int_B \int_A \gamma_{xc}(\vec{r}_1, \vec{r}_2) d\vec{r}_1 d\vec{r}_2 = - \frac{\delta(A, B)}{2} \end{aligned} \quad (2.30)$$

Therefore, the ESI between two atoms A and B is proportional to the covariance of

their electron populations. In order to estimate the importance of a given interaction between a pair of regions with respect to the number of electrons delocalized in that region, one can calculate the contribution analysis which is expressed as:

$$CA(A, B) = \frac{V[N(A), N(B)]}{\sum_{A \neq B} V[N(A), N(B)]} = -\frac{V[N(A), N(B)]}{\sigma^2[N(A)]}.100 \quad (2.31)$$

The sum of all ESI values involving a given atom reads as

$$\sum_{A \neq B} \delta(A, B) = -2 \sum_{A \neq B} V[N(A), N(B)] = \delta(A) \quad (2.32)$$

which may be viewed as the number of electrons of the atom A shared with the other regions, that is, the valence of the atom in a closed shell system.⁴⁴ Then, the total number of electrons, N , can be recovered from the expressions of all DI and LI:

$$\sum_i \left(\sum_{j \neq i} \left(\frac{1}{2} \delta(A_i, A_j) \right) + \lambda(A_i) \right) = \sum_i \langle N(A_i) \rangle = N \quad (2.33)$$

It is worth mentioning that all the ESI defined above are non-negative quantities (the negative sharing between two atoms could be considered rather unphysical). In the case of single determinant wave functions, it is clear that from Eqs. 1.36 and 2.21 the ESI cannot be negative. For correlated wave functions the two-center ESI defined in Eq. 2.21 must be non-negative because when the population of one region, $\langle N(A) \rangle$, increases, the population of the other region, $\langle N(B) \rangle$ must decrease. The covariance of both quantities is negative as Eq. 2.30 shows. It is worth noticing that only two-center ESI are defined non-negative while three-, four-, five- or six-center ESI could take negative values.^{51,59-62} In order to illustrate this fact, the general formula of the multicenter bond indices can be expressed in terms of n -order central moment of the electron population used in probability theory:⁶²

$$\delta(A_i, \dots, A_n) = \frac{(-2)^{n-1}}{n-1} \left\langle \prod_{i=1}^n \left(\hat{N}(A_i) - \langle N(A_i) \rangle \right) \right\rangle \quad (2.34)$$

where \hat{N} is the electron number operator. Therefore, when the order of the expres-

sion is two, it is clear from Eq. 2.34 that $-2(\hat{N}(A) - \langle N(A) \rangle)(\hat{N}(B) - \langle N(B) \rangle)$ must be positive because if $\langle N(A) \rangle$ is greater than $\hat{N}(A)$, $\langle N(B) \rangle$ must be smaller than $\hat{N}(B)$. On the other hand, when the order of the multicenter bond is higher than two, for instance three i.e. $2(\hat{N}(A) - \langle N(A) \rangle)(\hat{N}(B) - \langle N(B) \rangle)(\hat{N}(C) - \langle N(C) \rangle)$, different options can occur, e.g. $\langle N(A) \rangle$ could be greater while $\langle N(B) \rangle$ and $\langle N(C) \rangle$ smaller than their respective electron number operators, or $\langle N(A) \rangle$ and $\langle N(B) \rangle$ greater whereas $\langle N(C) \rangle$ smaller, etc. Thus, three and higher order multicenter indices could take either positive or negative values depending on the electron distribution of the molecule.

Finally, when the ESI is defined from the 1-RDM it can be decomposed into its α and β counterparts. These spin contributions only differ in the case of open-shell calculations. Interestingly, in this section we have seen how a link between quantum chemistry and old chemical concepts, such as atomic charge, valence, or bond order, has been established.

Multicenter Bond indices

The Lewis theory² is based on the concept of 2-center 2-electron (2c-2e) bonds. These kinds of bonds are able to describe the structure of most of the molecules. However, there are some systems that present more complex bonding patterns. For instance, the structure of electron deficient boranes, e.g. diborane, is characterized by a 3-center 2-electron bond (3c-2e). However, the topological analysis of the electron density can only define bonds between pairs of atoms and, thus, $\rho(\vec{r})$ cannot be used to characterize three-center interactions. In contrast to $\rho(\vec{r})$, the definition of ESI can be generalized to study the electron delocalization between three or more atoms, the so-called multicenter bond indices.⁵⁹ Bochicchio et al. provided the generalization of multicenter indices in the framework of QTAIM. For example, the 3-center ESI depend on the expensive third-order density, $\gamma^{(3)}(\vec{r}_1, \vec{r}_2, \vec{r}_3)$.⁵² Thus, the calculation of multicenter bond indices at the correlated level implies the obtention of high-order densities. Nevertheless, at the HF level, the general expression of these indices can be made more comprehensible when it is written in terms of AOM:

$$\delta(A, B, C) = 8 \sum_{ijk} S_{ij}(A) S_{jk}(B) S_{ki}(C) \quad (2.35)$$

Interestingly, positive $\delta(A, B, C)$ values represent 3c-2e bonds, while negative values are characteristic of 3c-4e bonds. This particular characteristic of 3-c ESI has

been recently used to study the nature of metal-hydrogen interactions, in particular, agostic interactions.^{63,64} As we will see in the next sections, one of the main applications of multicenter indices is the quantification of aromaticity.^{60,61} The main applications of ESI have been extensively reviewed in the literature.^{65,66}

Desirable properties of an ESI: the case of LiH dissociation

There is a certain set of properties that must be fulfilled by an ESI. As previously mentioned, a desired property of a two-center ESI is being always non-negative. This requirement is fulfilled by ESI obtained from QTAIM and Fuzzy-Atom partitions while the Wiberg-Mayer Bond Orders, which are based on Mulliken's partition, could show negative values. For instance, another desirable property is the asymptotic tendency to zero when the distance between the two atoms increases to infinity, that is, for a no electron sharing situation.

In 2005, Ponec and coworkers put forward another example that could be used to assess the performance of an ESI, which is the dissociation of diatomic ionic molecules into their neutral species.⁶⁷ In the equilibrium geometry, there is a small amount of electrons shared. When increasing the internuclear distance one electron should be transferred from the negative charged atom to the positive one. Thus, at a certain distance one should observe a maximum of electron sharing which represents the transition from a rather electrostatic interaction to a more covalent situation. In the case of LiH, Ponec and coworkers showed that this maximum was only reproduced by QTAIM-ESI, while the Mulliken-ESI clearly fails to predict it. Two years later, Matito et al. extended this study to Fuzzy-Atom partitions (see Figure 2.2) showing that the Fuzzy-Becke-ESI also fails to reproduce this maximum.³⁹ However, the performance of Fuzzy-Atom-ESI could be improved by dynamically tuning the atomic radii according to the position of the bond critical point, this is the so-called Fuzzy-rho method.³⁹ It is worth noticing that Bultinck and coworkers have found a small maximum of electron sharing according to QTAIM-ESI when two covalent molecules, CO and NO^+ , are dissociated into their neutral species.⁶⁸ Matito and coworkers attributed this maximum of electron sharing to the sudden change on the relative atomic size at the vicinity of the equilibrium geometry.⁶⁹

2.2.2 Example: $Cr(CO)_6$

In order to illustrate the concepts that are being introduced in this section, we will analyze the bonding patterns of $Cr(CO)_6$ from different perspectives.

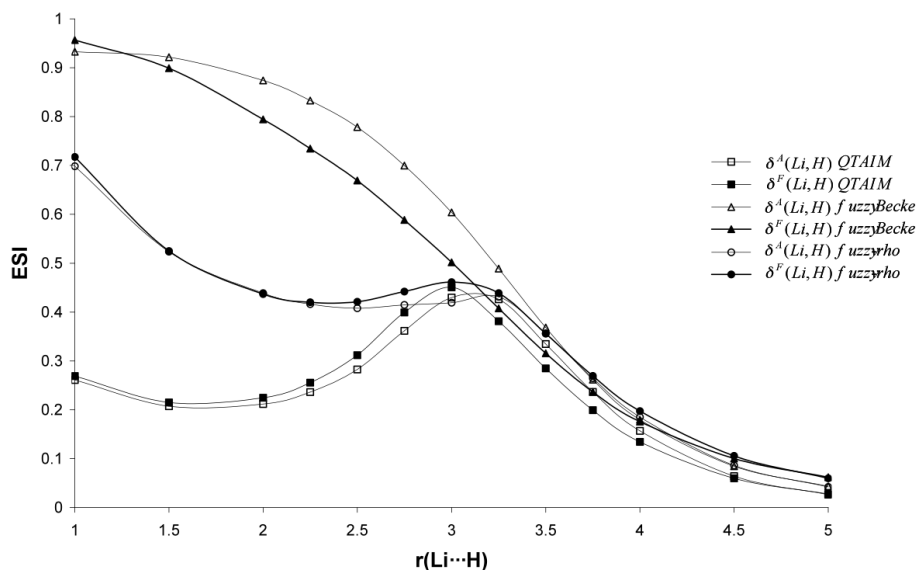


Figure 2.2: LiH dissociation into neutral species; Ángyan and Fulton ESI for QTAIM, Becke’s Fuzzy-Atom and Fuzzy-rho partitions. Distances are in ÅAdapted from reference³⁹

Table 2.1 comprises the above-mentioned integrated quantities for $Cr(CO)_6$, that is, the atomic population (N), the atomic charge (q), and the localization (λ) and delocalization indices (δ) obtained within the framework of the QTAIM. These values are compared to the ones obtained for the free carbon monoxide CO . First, we can see how the atomic charge of the carbon atom of the $Cr(CO)_6$ decreases about 0.2 e in comparison to the C located in the CO molecule, whereas the atomic charge of the O remains practically constant. Thus, the C atom present a depletion of charge when it is complexed to the Cr atom. On the other hand, the value of the 2c-ESI corresponding to the number of electrons shared between C and O atom is moderately smaller than CO , 1.544 e and 1.726 e respectively. However, this decrease on the number of electrons shared between C and O does not correspond to an increase in the number of electrons localized on the C atom, $\lambda(C)$, in fact, $\lambda(C)$ also decreases when going from CO to $Cr(CO)_6$ (3.914 e CO and 3.553 e for $Cr(CO)_6$). Therefore, the electrons are delocalized toward the Cr basin, as points out the significant electron delocalization between Cr and C, $\delta(Cr, C) = 0.817e$. These results are in line with the Dewar-Chatt-Duncanson^{70,71} scheme, that describes a σ -donation from the CO π -orbital to an unoccupied d orbital of the Cr

Table 2.1: B3LYP calculation for $Cr(CO)_6$ and CO (6-31G(d,p) basis set for C and O and Roos augmented Double Zeta ANO for Cr). QTAIM basin (N), electronic charge (q), localization index ($\lambda(A)$), and electron sharing indices ($\delta(A, B)$).

Molecule	Atom	N	q	λ	Pair	$\delta(A, B)$
$Cr(CO)_6$	Cr	22.803	1.197	19.911	Cr,C	0.817
	C	4.995	1.005	3.553	C,O	1.544
	O	9.204	-1.204	8.300		
CO	C	4.778	1.222	3.914	C,O	1.726
	O	9.222	-1.222	8.358		

while exists a backdonation from an occupied d orbital of the Cr to an unoccupied π^* of CO.

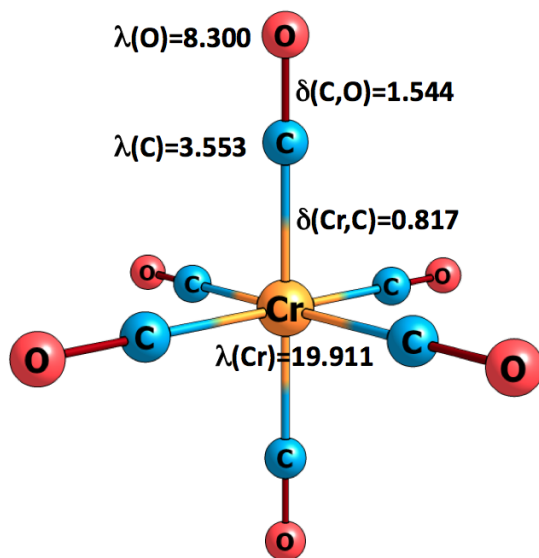


Figure 2.3: Localization (λ) and delocalization indices (δ) of $Cr(CO)_6$ obtained within the framework of the QTAIM

2.3 Domain-Averaged Fermi Hole Analysis

In the last decades, several research groups have put considerable effort into trying to reconcile the picture of bonding proposed by G. N. Lewis and the one provided by the pair density within quantum mechanics. The concept of electron pair has been at the epicenter of the discussion for a long time, however, its role in chemical bonding is not completely clarified yet. In the previous section, we have described the idea of electron sharing index as a numerical measure of electron localization and delocalization. In this section, we will focus on the so-called Domain Averaged Fermi Hole (DAFH) analysis which could help us to study the electron pair distribution in a more visual fashion.^{68,72–80} In contrast to the ESI based on the XCD, the concept of DAFH was introduced in terms of the conditional probability and the Fermi Hole function. Nevertheless, it is possible to find an alternative definition of the DAFH based on the XCD. Thus, the DAFH represents an interesting quantity that provides a rich source of structural information whose analysis can contribute to the visualization and the understanding of the electronic structure of molecules.

2.3.1 DAFH definition

The original definition of the DAFH was proposed by Robert Ponec in 1997.^{7,8} The expression of the DAFH derives from the idea of the conditional probability (CP) mentioned above in Eq. 1.39, which represents the probability of finding one electron of the pair when the position of the second electron, the reference electron, is fixed at some point or region of the molecular space. Prior to the definition of the DAFH, the conditional probability was widely used in other contexts to study the nature of the chemical bond, for instance, the CP is the cornerstone of the electron localization function.⁶ Another quantity that is fundamental to the definition of the DAFH is the Fermi Hole function whose formula has been pointed out in Eq. 1.53. The concept of Fermi Hole was introduced by Wigner in the field of solid state physics⁸¹ but during the past years its use in chemistry has been extensively discussed.

As previously mentioned in Eq. 2.38, the Fermi hole function is obtained by subtracting the conditional probability from the one-electron density in order to reflect the *net* effect of electron pairing. Usually, the second electron is predominantly distributed in the vicinity of the reference electron showing the electron pairing of electrons. Its main disadvantage is that the form of the Fermi hole depends on the precise location of the reference electron which is rather incompatible with the uncertainty of quantum mechanics. When the reference electron is fixed at different

points of the space, we obtain different Fermi holes. Hence, it is more convenient and realistic to introduce the so-called domain-averaged Fermi-hole in which the reference electron is not fixed at a point but is allowed to be found anywhere in some region of space, A . Interestingly, one can assign this region to an atomic domain, a functional group, or a couple of bonded atoms. For instance, the region could be defined in terms of QTAIM atomic domains, although other molecular partitions are equally useful. Next, we develop the formulation of this method:

First, the conditional probability can be integrated over the region A :

$$P_A(\vec{r}_2; \vec{r}_1) = \frac{\int_A \gamma^{(2)}(\vec{r}_1, \vec{r}_2) d\vec{r}_1}{\int_A \gamma^{(1)}(\vec{r}_1) d\vec{r}_1} \quad (2.36)$$

From the definition of the CP one can straightforwardly obtain the expression of the averaged Fermi Hole:

$$h_A(\vec{r}_1) = P_A(\vec{r}_2; \vec{r}_1) - \gamma^{(1)}(\vec{r}_1) \quad (2.37)$$

This averaged Fermi hole satisfies the normalization of Eq. 1.59 independently of the form of the region A :

$$\int_A h_A(\vec{r}_1) d\vec{r}_1 = -1 \quad (2.38)$$

Further manipulation of Eq. 2.37 is needed to obtain relevant chemical information. Thus, $h_A(\vec{r}_1)$ expression has to be multiplied by the atomic populations N_A with the aim of achieving the definition of the DAFH:

$$g_A(\vec{r}_1) = N_A h_A(\vec{r}_1) \quad (2.39)$$

where $N_A = \int_A \gamma^{(1)}(\vec{r}_1) d\vec{r}_1$. This term is introduced because the Fermi hole is derived from the CP and describes the distribution of one electron of the pair. The localization of a single electron in region A is an artificial act that does not reflect the fact that in the real molecule the region is populated by N_A electrons rather than by one. In terms of spin orbitals, the DAFH definition can be read as

$$g_A(\vec{r}_1) = \sum_{ij} \chi_i(\vec{r}_1) G_i^j \chi_j(\vec{r}_1) \quad (2.40)$$

where G_i^j is the hole matrix which represents the hole in an appropriate basis.

The DAFH analysis provides useful information not only about the core and lone electron pairs associated with the atomic domain A but also about the free and broken valences created by the formal splitting of the bonds that are not included in the region of interest. The procedure consists of several steps. First, the diagonalization of the G_i^j matrix in an appropriate basis. Second, the resulting eigenvectors, and the corresponding eigenvalues, are localized through an isopycnic transformation. In this step, the usually delocalized eigenvectors are transformed into more localized functions that could be associated with what chemists traditionally call the electron structure of molecules, i.e. chemical bonds, lone pairs, and valences. The eigenvectors localized in the atomic region have eigenvalues close to two, this means that the electron pair is localized in region A , i.e., core electrons and lone pairs. On the other hand, broken valences of nonpolar bonds have eigenvalues close to one. Finally, the formal splitting of polar bonds results in free valences whose eigenvalues are deviated from unity in function of the polarity of the bond. The sum of all the eigenvalues η_i obtained after the diagonalization of the hole matrix satisfies the relation

$$\sum_i \eta_i = N_A \quad (2.41)$$

Although the original definition was based on the conditional probability, the DAFH can be alternatively formulated in terms of XCD. Thus, from Eq. 1.29, the DAFH is written as

$$\begin{aligned} g_A(\vec{r}_1) &= \int_A \gamma_{XC}(\vec{r}_1, \vec{r}_2) d\vec{r}_2 = \int_A \gamma^{(2)}(\vec{r}_1, \vec{r}_2) d\vec{r}_2 - \gamma^{(1)}(\vec{r}_1) \int_A \gamma^{(1)}(\vec{r}_2) d\vec{r}_2 \\ &= \int_A \gamma^{(2)}(\vec{r}_1, \vec{r}_2) d\vec{r}_2 - \gamma^{(1)}(\vec{r}_1) N_A \end{aligned} \quad (2.42)$$

For monodeterminantal wave functions the DAFH can be expressed in terms of AOM:

$$g_A(\vec{r}_1) = \sum_{ij} S_{ij}(A) \chi_i(\vec{r}_1) \chi_j(\vec{r}_1) \quad (2.43)$$

Recently, the correlated expression of the DAFH in terms of 2-RDM⁷⁶ and the one-electron approximation have been formulated.⁷⁹ In addition, this technique has been studied by means of simple analytic models⁸² and a close connection between the DAFH and the full electron number distribution function (EDF) has been presented.⁸³

Connection with ESI

Further integration of Eq. 2.42 over the region B leads to the definition of $\delta(A, B)$:

$$\delta(A, B) = \int_B g_A(\vec{r}_1) d\vec{r}_1 \quad (2.44)$$

2.3.2 Example: $Cr(CO)_6$

Next, we will see how the DAFH analysis can help us to study the bonding patterns of $Cr(CO)_6$. To this end, the DAFH analysis has been performed using the QTAIM partition for three different fragments: the Cr, C, and O atoms (see Figures 2.4, 2.5, and 2.6). The most relevant information provided by this analysis concerns the detection of electron pairs that remain intact within the fragment as well as the broken valences formed by the formal splitting of Cr-C or C-O bonds required to isolate the fragment from the rest of the molecule. For the Cr fragment we have found 18 non-zero eigenvalues. A closer inspection of the graphical form of the associated eigenvectors shows that 5 of them have eigenvalues equal to 2.000 and correspond to electron pairs of completely filled 1s, 2s, and 2p inner shells. Then, there is a group of 4 eigenvalues ranging from 1.992 to 1.981 (Figures a-2.4, b-2.4, c-2.4, and d-2.4) which are associated with the electron pairs of completely filled 3s and 3p valence shells of Cr which are completely localized within the Cr basin. These electron pairs have no relevance for the analysis of metal-ligand bonding. The remaining eigenvectors, which present eigenvalues between two and zero, correspond to the broken valences arising from the formal splitting of the Cr-C bonds and, thus, are relevant to explain the nature of the chemical bond. First, we have 6 eigenvectors with eigenvalues equal to 0.262 (Figure f-2.4) that are associated with the σ -donation from the CO π -orbital to an unoccupied d orbital of Cr.

The high deviations of these eigenvalues from unity indicate high polarity of Cr-C ligand σ bonds, and the degree of polarity can approximately be estimated by the actual value 0.262, which can be regarded as the contribution of the Cr atom to an unevenly shared electron pair of the above formally broken bond. Finally, there are 3 eigenfunctions with eigenvalues equal to 1.091 (Figure e-2.4) which correspond to the backdonation from an occupied d orbital of the Cr to an unoccupied π^* of CO.

Then, we analyze the C (Figure 2.5) and O (Figure 2.6) fragments by comparing the values obtained with the ones of the free carbon monoxide (Figure 2.7). First, both C and O fragments present 5 (essentially) non-zero eigenvalues. The Figures a-2.5 and a-2.6 correspond to the $1s^2$ core electrons of C and O respectively. The Figure a-2.5 eigenfunction with eigenvalue equal to 1.601 is associated with the broken valence of the partially populated σ Cr-C bond, and could be related to the Figure f-2.4 eigenvector, thus, 1.6 electrons of this electron pair are localized within the C fragment while 0.3 are located in the Cr fragment. On the other hand, the oxygen lone-pair (Figure f-2.4) is completely localized in the O fragment as its eigenvalue equal to 1.998 shows. In the case of free carbon monoxide, both the carbon and oxygen lone-pairs are completely localized in their respective fragments (Figures b-2.7 and g-2.7). Finally, we will focus on the C-O bond. Each fragment has 3 eigenvalues that could be associated with the broken valences of the formal splitting of C-O bond, one σ - (Figures c-2.5 and c-2.6) and two π -components (Figures d-2.5/e-2.5 and d-2.6 /e-2.7). The eigenvalues of these 3 eigenvectors show that the bond is strongly polarized towards the oxygen atom. In comparison with the free CO, the eigenvalues and eigenvectors of the oxygen fragment of $Cr(CO)_6$ remains almost unaltered whereas the ones corresponding to the C fragment are slightly more affected although the changes are not significant (see Figures 2.5, 2.6, and 2.7). Thus, the low alteration of the complexed CO fragment with respect to the free CO could be related with a weak interaction between the CO ligand and the Cr metal atom.

Finally, we have also computed the DAFH using the Mulliken partition of the molecular space. Whereas the shape of the eigenfunctions remains more or less unchanged with respect to QTAIM, the eigenvalues present significant variations. As Figures 2.4, 2.5, 2.6, and 2.7 show, the Mulliken partition leads to a less polarized description of the Cr-C and C-O bonds where the eigenvalues of the broken valences are more close to 1 than in the case of QTAIM.

Fragment: Cr

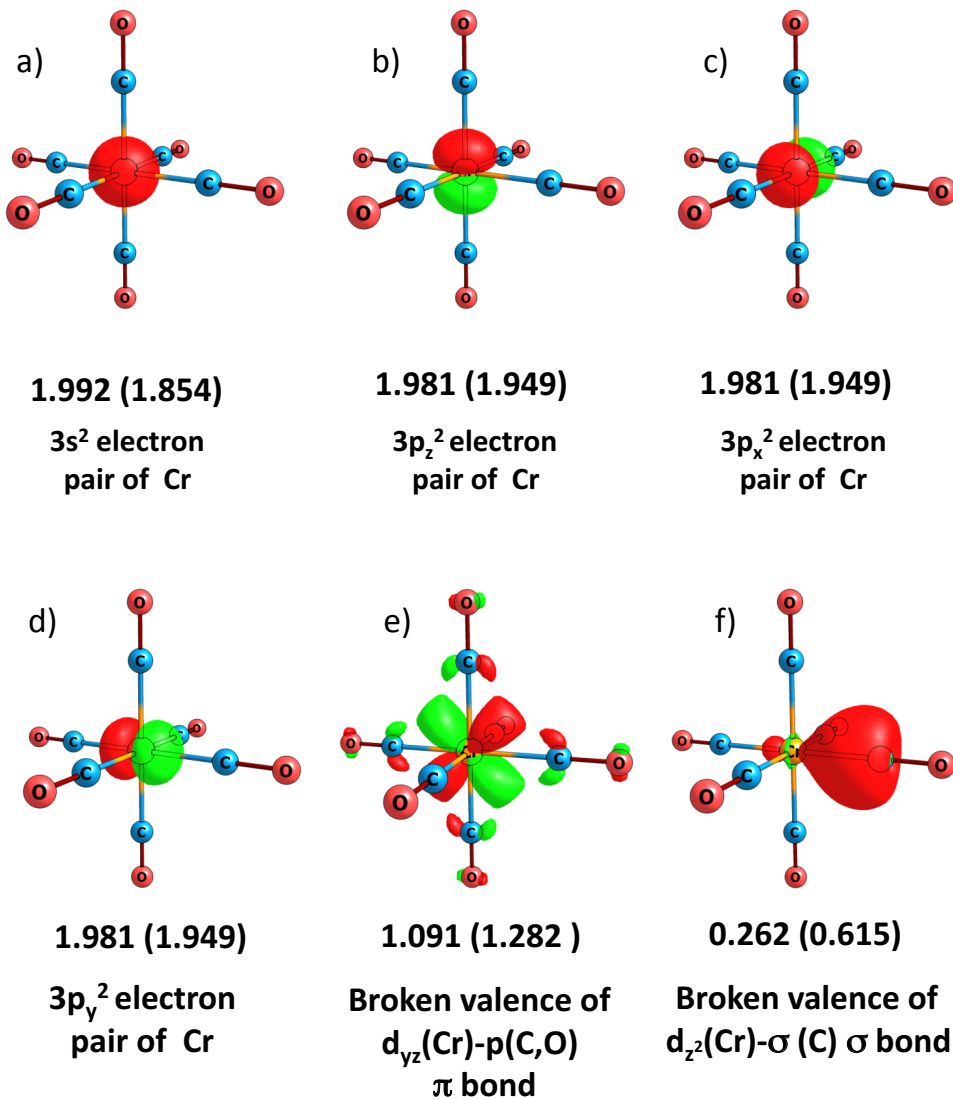


Figure 2.4: Results of the DAFH analysis for the $Cr(CO)_6$ complex. Selected eigenvectors of the Fermi holes corresponding to electron pairs and broken valences of the holes averaged over the Cr fragment. The numbers indicate the eigenvalues of the corresponding hole for the "exact" QTAIM form of the analysis, and the values in parentheses correspond to the "approximate" Mulliken-like approach.

Fragment: C

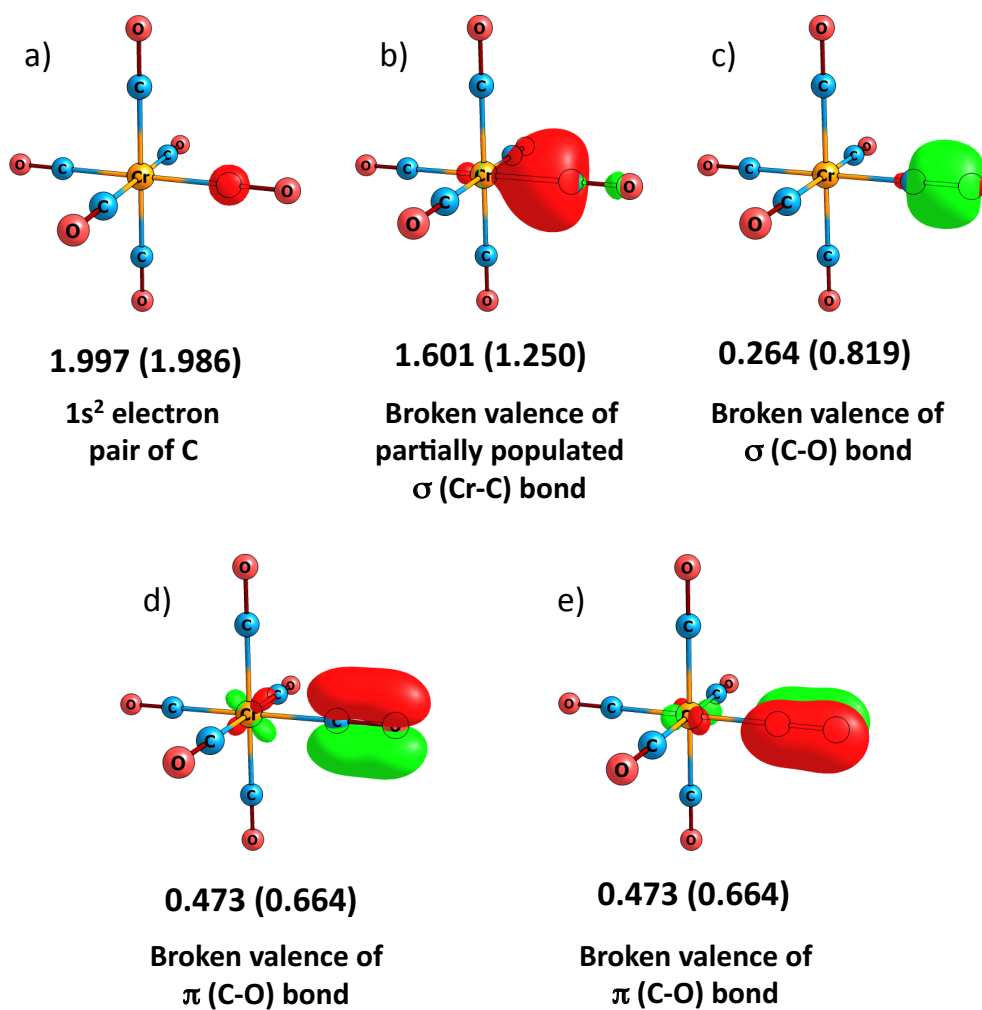


Figure 2.5: Results of the DAFH analysis for the $Cr(CO)_6$ complex. Selected eigenvectors of the Fermi holes corresponding to electron pairs and broken valences of the holes averaged over the C fragment. The numbers indicate the eigenvalues of the corresponding hole for the "exact" QTAIM form of the analysis, and the values in parentheses correspond to the "approximate" Mulliken-like approach.

Fragment: O

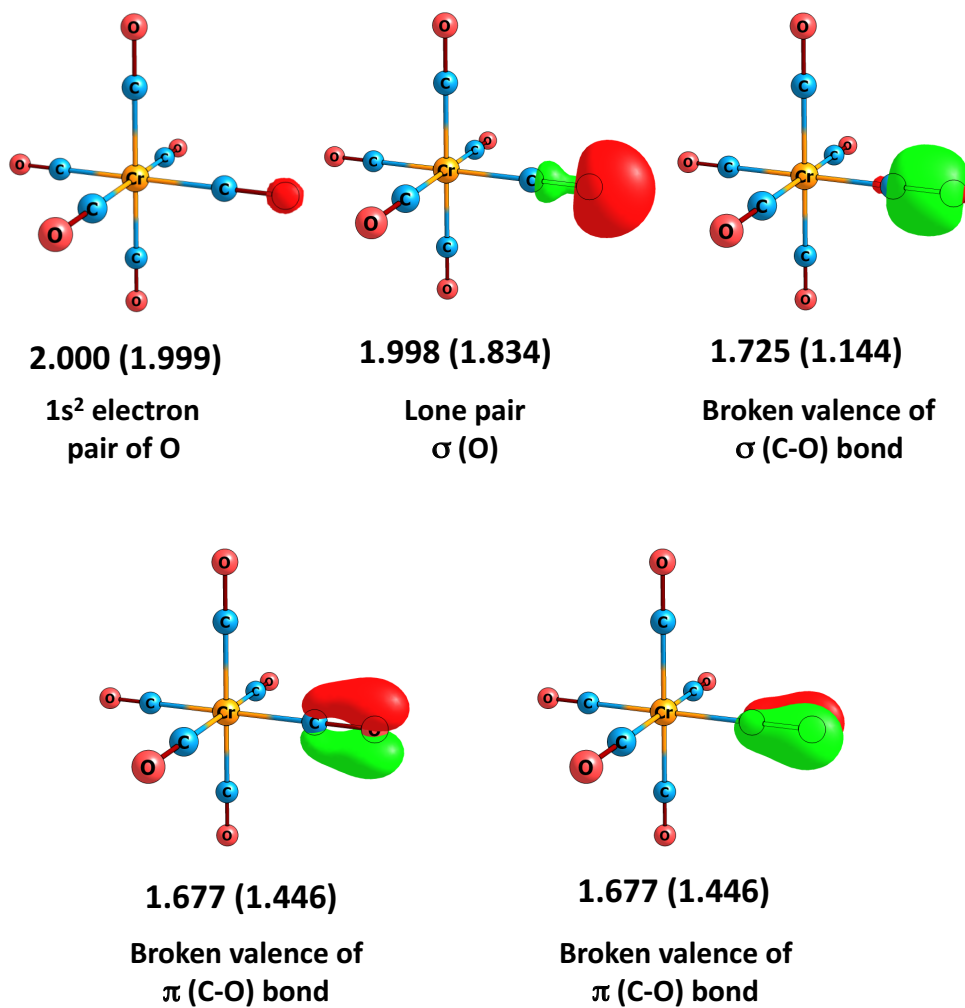
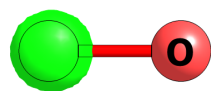
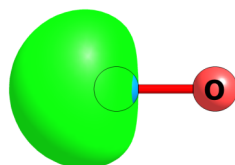


Figure 2.6: Results of the DAFH analysis for the $Cr(CO)_6$ complex. Selected eigenvectors of the Fermi holes corresponding to electron pairs and broken valences of the holes averaged over the O fragment. The numbers indicate the eigenvalues of the corresponding hole for the "exact" QTAIM form of the analysis, and the values in parentheses correspond to the "approximate" Mulliken-like approach.

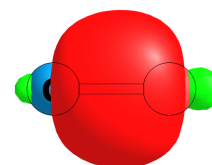
a) Fragment: C



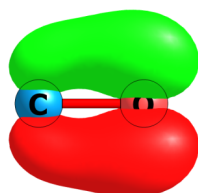
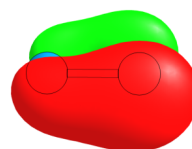
1.996 (1.995)

1s² electron
pair of C

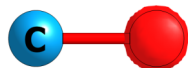
1.891 (1.922)

Lone pair
 σ (C)

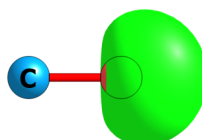
0.239 (0.809)

Broken valence of
 σ (C-O) bond0.326 (0.582)
Broken valence of
 π (C-O) bond0.326 (0.582)
Broken valence of
 π (C-O) bond

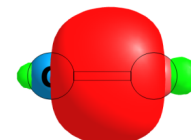
a) Fragment: O



2.000 (1.999)

1s² electron
pair of O

1.999 (1.903)

Lone pair
 σ (O)

1.761 (1.191)

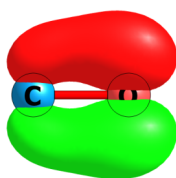
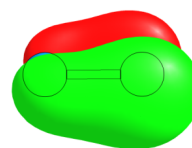
Broken valence of
 σ (C-O) bond1.674 (1.418)
Broken valence of
 π (C-O) bond1.674 (1.418)
Broken valence of
 π (C-O) bond

Figure 2.7: Results of the DAFH analysis for the free carbon monoxide. Selected eigenvectors of the Fermi holes corresponding to electron pairs and broken valences of the holes averaged over the C and O fragments. The numbers indicate the eigenvalues of the corresponding hole for the "exact" QTAIM form of the analysis, and the values in parentheses correspond to the "approximate" Mulliken-like approach.

2.4 Electron Localization Function

In this chapter, we have seen how the division of the molecular space into QTAIM regions provides relevant information about the localization and delocalization of electrons. Moreover, we have shown the differences between QTAIM partition of the electron density, which is based on sharp boundaries, and the so-called fuzzy-atom partitions of the same quantity that exhibit a continuous transition from one region to the other. In the present section, we will study another partition of the molecular space with non-overlapping boundaries. In this case, the molecular space is not divided according to the topology of the electron density but to the topology of the Electron Localization Function (ELF) which is based on the same spin conditional probability (see Eq. 1.49). The ELF was introduced in 1990 by Becke and Edgecombe who used this function to generate interesting pictures of the atomic shell structure, and the core, lone pairs and binding regions.⁶ One year later, Savin and coworkers reformulated the ELF in terms of the density functional theory, associating the ELF with the excess of kinetic energy density due to the Pauli repulsion.⁸⁴ In the regions where the Pauli repulsion is strong, ELF is close to one, representing well-localized electrons which may be identified with chemical bond and lone pairs. On the other hand, when ELF is close to zero, the probability of finding the same spin electrons close together is high. In the last decade, several definitions of quantities that resemble the ELF have been proposed.⁸⁵⁻⁸⁷

2.4.1 Becke's Definition

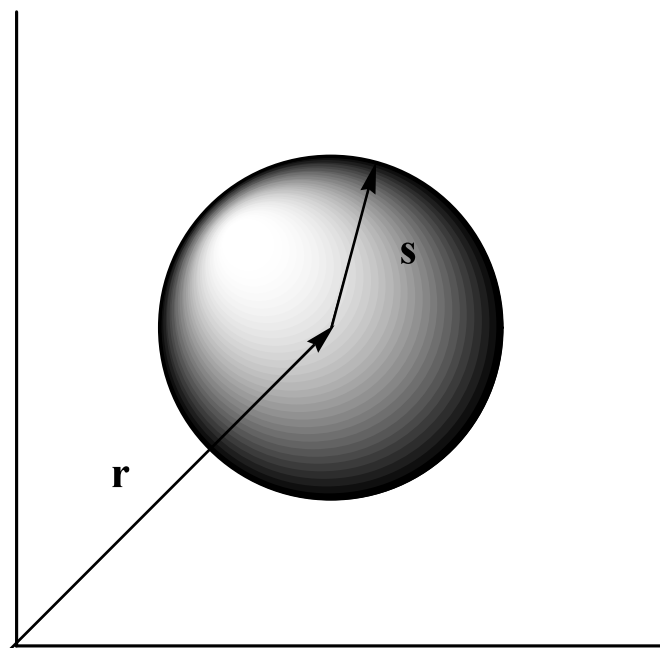
Becke and Edgecombe proposed to use the spherical average of the Fermi contribution of the conditional probability (see Figure 2.8) Eq. 1.49 as a measure of electron localizability:

$$P(\vec{r}, \vec{s}) = \left\langle e^{\vec{s} \cdot \vec{\nabla}} P^{\sigma\sigma}(\vec{r}, \vec{r} + \vec{s}) \right\rangle = \frac{\sinh(\vec{s} \cdot \vec{\nabla})}{\vec{s} \cdot \vec{\nabla}} P^{\sigma\sigma}(\vec{r}, \vec{r} + \vec{s}) \Big|_{\vec{s}=\vec{0}} \quad (2.45)$$

where $\sigma = \alpha$ or β . Eq. 2.45 can be expanded around the reference electron, i.e. when $s = 0$, in terms of series of Taylor:

$$P(\vec{r}, \vec{s}) = \left\langle e^{\vec{s} \cdot \vec{\nabla}} P^{\sigma\sigma}(\vec{r}, \vec{r} + \vec{s}) \right\rangle = \left(1 + \frac{1}{6} \vec{s}^2 \vec{\nabla}_s^2 + \dots \right) P^{\sigma\sigma}(\vec{r}, \vec{r} + \vec{s}) \Big|_{\vec{s}=\vec{0}} \quad (2.46)$$

Since the leading term of the Taylor expansion is $\frac{1}{6} \vec{s}^2 \vec{\nabla}_s^2 P^{\sigma\sigma}(\vec{r}, \vec{r} + \vec{s})$, we can approx-

Figure 2.8: Spherical region centered at \vec{r} with radius \vec{s}

imate the spherical average of the Fermi contributions to the conditional probability as

$$P(\vec{r}, \vec{s}) = \langle e^{\vec{s} \cdot \vec{\nabla}} P^{\sigma\sigma}(\vec{r}, \vec{r} + \vec{s}) \rangle \approx \left(\frac{1}{6} \vec{s}^2 \vec{\nabla}_s^2 + \dots \right) P^{\sigma\sigma}(\vec{r}, \vec{r} + \vec{s})|_{\vec{s}=\vec{0}} \quad (2.47)$$

which is directly linked with the curvature of the Fermi hole at the HF level.⁸⁸ Becke and Edgecombe used the relative ratio of Eq. 2.47 with respect to the same quantity for the homogenous electron gas (HEG)⁸⁹ assuming a monodeterminantal wave function:

$$D_\sigma^0 = \frac{3}{5} (6\pi^2)^{2/3} (\rho^\sigma)^{5/3} = \frac{3}{10} (3\pi^2)^{2/3} (\rho^\sigma)^{5/3} = c_F (\rho^\sigma)^{5/3} \quad (2.48)$$

where c_F is the Fermi constant. Thus, taking advantage of the definition of the CP in terms of pair density and one-electron density, the relative ratio is given by:

$$\chi(\vec{r}) = \frac{D_\sigma}{D_\sigma^0} = \frac{\vec{\nabla}_s^2 \gamma^{(2)\sigma\sigma}(\vec{r}, \vec{r} + \vec{s})|_{\vec{s}=\vec{0}}}{c_F (2\rho^\sigma)^{8/3}} \quad (2.49)$$

Although the relative ratio can recover the chemical structure, Becke and Edgecombe preferred to scale the previous function as

$$ELF = \eta(\vec{r}) = \frac{1}{1 + \left(\frac{D_\sigma}{D_\sigma^0}\right)^2} = \frac{1}{1 + \chi(\vec{r})^2} \quad (2.50)$$

The probability of finding one electron with spin α when there is another electron with the same spin nearby is lower when the former electron is localized. Thus, the ELF value is larger for localized systems. It can be easily proved that the ELF function ranges in the interval $[0, 1]$. In contrast to the electron density, the ELF is practically zero in the region of the space between the first and the second atomic shells, while the density at this point is significantly larger. On the other hand, in the valence region, the ELF function takes values close to 1 while the electron density is much lower. If ELF values are equal to one then the electrons are fully localized, whereas if $ELF = 1/2$, i.e. $D_\sigma = D_\sigma^0$, then the electrons are delocalized as in the HEG, the *ideal* delocalized system. Thus, the ELF basins are regions of the molecular space which are surrounded by a zero flux surface but, in contrast to the QTAIM, the ELF basins are not obtained from the topology of the electron density but from the topology of the ELF function. Thus, ELF partition leads to a molecular space partition that is more connected to Lewis concepts, such as bonding regions, lone pairs or core basins.^{90,91}

Finally, from the average population and the pair population one may analyze the variance and the covariance basin populations in the same ways as we have shown for the ESI in the previous sections. Thus, from Eqs. 2.28 and 2.30, it is possible to obtain the values of the variance and the covariance of the ELF basins.

ELF at Correlated Level

The definition of the ELF using the HEG as a reference has given rise to several criticisms.^{86,87} Interestingly, in 2003, Bernard Silvi proposed a new method to account for the electron localization which is identical to the ELF but without the

use of HEG.⁸⁵ Kohout and coworkers followed a similar process to achieve identical results.^{86,87} Matito et. proved the equivalence of both definitions at the correlated level for closed- and open-shell species.⁹²

$$ELF = \left[1 + \left(\frac{\vec{\nabla}_s^2 \gamma^{(2)\beta\beta}(\vec{r}, \vec{r} + \vec{s})|_{\vec{s}=\vec{0}} + \vec{\nabla}_s^2 \gamma^{(2)\alpha\alpha}(\vec{r}, \vec{r} + \vec{s})|_{\vec{s}=\vec{0}}}{2c_F(\rho^\sigma(\vec{r}))^{8/3}} \right)^2 \right]^{-1} \quad (2.51)$$

In order to compute the ELF from Eqs. 2.50 and 2.51, the curvature of the pair density must be calculated, which in terms of molecular orbitals is given by:

$$\begin{aligned} \vec{\nabla}_1^2 \gamma^{(2)\sigma\sigma}(\vec{r}, \vec{r}_1)|_{\vec{r}_1=\vec{r}} &= \sum_{ijkl} \Gamma_{ij}^{kl} \chi_i^*(\vec{r}) \chi_k(\vec{r}) \left[\chi_l(\vec{r}) \vec{\nabla}^2 \chi_j^*(\vec{r}) \right. \\ &\quad \left. + \chi_j^*(\vec{r}) \vec{\nabla}^2 \chi_l(\vec{r}) + 2\vec{\nabla} \chi_j^*(\vec{r}) \vec{\nabla} \chi_l(\vec{r}) \right] \end{aligned} \quad (2.52)$$

where Γ_{ij}^{kl} is the second order density matrix. Up to now, the correlated analysis was only possible with CISD wave functions, nevertheless, throughout this thesis the calculation of the ELF has been extended to CASSCF wave functions. However, the numerical complexity of the exact approach limits the use of the calculations of the ELF at correlated level to small systems. The first objective of this thesis is to propose a natural orbital approach of the ELF with the aim of extending this correlated analysis to larger systems.

2.4.2 Example: $Cr(CO)_6$

Finally, we analyze the picture of the chemical bonding in $Cr(CO)_6$ from the point of view of the ELF.

Topology of the ELF

As DAFH, the ELF provides a graphical representation of the electronic structure that can be used to rationalize the chemical bonding in a more visual fashion. In contrast to QTAIM, the local maxima of the ELF lead to the so-called localization domains which do not correspond to atomic domains of the QTAIM but to chemically relevant regions. Thus, from the ELF partition of the molecular space three different domains are obtained: bonding and non-bonding domains, and core basins, which inform us about how the electrons are localized. The organization of the spatial

domains will help us to classify the chemical bonds. Figure 2.9 represents the basins obtained from the topology of the ELF for the $Cr(CO)_6$. As it can be seen, the valence basins $V(O)$, $V(C,O)$, and $V(Cr,C)$ are depicted in red, blue, and green respectively, while the core basin, $C(C)$ and $C(Cr)$ in light grey. Thus, $V(O)$ is associated with the oxygen lone pair, $V(C,O)$ with the carbon and oxygen bonding basins, while $V(Cr,C)$ seems to suggest that there is an interaction between C and Cr atoms, however, the $V(Cr,C)$ is not centered between $C(C)$ and $C(Cr)$ which could indicate a closed-shell interaction.

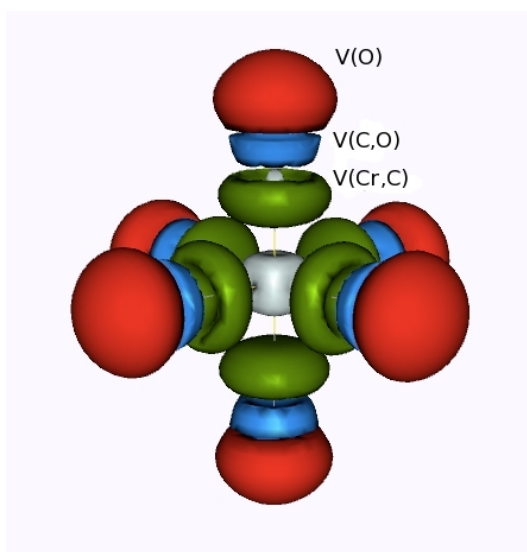


Figure 2.9: ELF=0.60 isosurface for $Cr(CO)_6$ (6-31G(d,p) basis set for C and O and Roos augmented Double Zeta ANO for Cr). The valence basins for oxygen, carbon, and chromium are indicated.

Bifurcation analysis

The hierarchy of the localization basins is analyzed by means of the bifurcation analysis. A localization domain is a volume limited by one or more isosurfaces and containing at least one attractor. We say irreducible domain when it contains only one attractor, otherwise we have a reducible domain. In order to obtain the irreducible domains one has to increase the value of the ELF isosurface, then the reducible domains reduce to smaller reducible or to irreducible domains. Thus, the localization domains may be ordered by increasing value of ELF isosurface as represented in the bifurcation diagram of Figure 2.10. This information help us to

elucidate the nature of the interaction. In the case of $Cr(CO)_6$, when $ELF=0.23$ the different Cr-CO fragments separate from each other, because each CO fragment hardly interact with the others. Then, at $ELF=0.58$ $V(Cr,C)$ separates from the CO, this fact points out the closed shell character of this fragment. In contrast to $V(Cr,C)$, the covalent C-O bond separates when $ELF=0.80$.

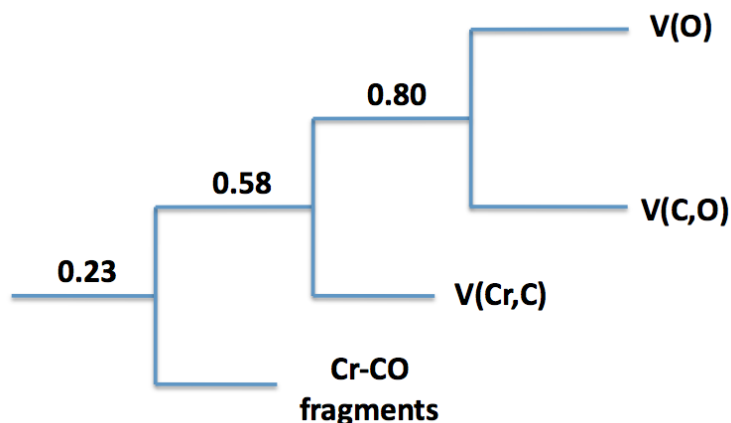


Figure 2.10: ELF bifurcation diagram for $Cr(CO)_6$

Statistical interpretation of the ELF domains

Table 2.2 collects the values of the basin populations ($N(\Omega_i)$), standard deviations ($\sigma^2(\Omega_i)$), relative fluctuation ($\lambda_F(\Omega_i)$), and contributions of the basins to the variance $\sigma^2(\Omega_i)$. First, the core basins of C and O contain the highly localized $1s^2$ core electrons as the standard deviation shows. On the contrary, the core electrons of Cr atoms are more spread and correlated with valence basins such as $V(Cr,C)$. With respect to the valence basins, the basin population of $V(O)$ is 4.34 e because it contains the lone pair of oxygen, in addition, $V(O)$ highly correlates with $V(C,O)$ (CA=63%). In the case of $V(C,O)$, the basin population is 3.12 e and, thus, we have a triple bond which is highly polarized towards oxygen as the contribution analysis shows ($V(O)=63\%$). Finally, despite the average population of $V(Cr,C)$ basin is 2.76 e, these electrons are highly polarized towards the O, i.e. $V(C,O)=23\%$ and $V(O)=16\%$, as well as the Cr, $C(Cr)=25\%$. Therefore, the topology and the bifurcation analyses of the ELF suggest a closed shell interaction between Cr and C. The closed shell nature of the Cr-C interaction is also predicted by the analysis of the

Table 2.2: B3LYP calculation for $Cr(CO)_6$ and CO (6-31G(d,p) basis set for C and O and Roos augmented Double Zeta ANO for Cr). Basin populations ($N(\Omega_i)$), standard deviations ($\sigma^2(\Omega_i)$), relative fluctuations ($\lambda_F(\Omega_i)$), and contributions of the other basins (%) to $\sigma^2(\Omega_i)$, obtained for the $Cr(CO)_6$.

Ω	$N(\Omega_i)$	$\sigma^2(\Omega_i)$	$\lambda_F(\Omega_i)$	Contribution analysis (>10%)
$C(C)$	2.08	0.24	11.54%	38% V(Cr,C), 38% V(C,O), 13% V(O)
$C(O)$	2.14	0.34	15.89%	32% V(C,O), 61% V(O)
$C(Cr)$	21.30	2.47	11.60%	13% V(Cr,C)
$V(O)$	4.34	1.42	32.72%	15% V(Cr,C), 63% V(C,O), 14% C(C)
$V(C, O)$	3.12	1.45	46.47%	21% V(Cr,C), 61% V(O)
$V(Cr, C)$	2.76	1.30	47.10%	23% V(C,O), 25% C(Cr), 16% V(O)

$\rho(r_{bcp})$ and the $\nabla^2(r_{bcp})$ of the electron density at the bond critical point.⁶⁶ In addition, this interaction shows some correlation between C(Cr) and V(Cr,C) according to the contribution analysis.

Recently, Tiana and coworkers have analyzed the chemical bonding in classical and nonclassical transition metal carbonyls by means of the interacting quantum atoms approach (IQC) within the framework of the QTAIM.⁹³

To sum up, in this section we have seen how the ESI, DAFH, and ELF analyses give similar electron delocalization pictures for the $Cr(CO)_6$, showing how each of these quantum-mechanical tools could complement the others. In addition, we have pointed out the importance of the partition of the molecular space, whereas the ESI and DAFH take advantage of atomic domains generated by the topology of the electron density, the ELF is based on the localization domains obtained from the partition of the conditional probability of the same spin pairs. Despite the interpretation of the chemical interaction usually coincides, in some cases different pictures of the chemical bond are obtained from the QTAIM and ELF based methods.⁹⁴ Thus, one should step carefully when interpreting the results arisen from these methods.

Finally, it is worth noticing that similar efforts regarding the study of electron localization and delocalization have been done in the field of solid-state and condensed matter physics. Although this field is beyond the scope of this thesis we briefly

enumerate some widely used methods. First, the representation of the wave function in terms of the maximally localized Wannier⁹⁵ functions has been used from the thirties to obtain atomic contributions to the band structure in solid materials. Then, the crystal orbital overlap populations can be related to the concept of bond order for a solid⁹⁶ (the crystal orbitals are a linear combination of Bloch orbitals). QTAIM theory has been explored from the solid-state perspective by many authors, from which is worth mentioning Prof. Gatti.⁹⁷ Interestingly, the ESI, DAFH, and ELF methodologies have also been extended to study the electron localization and delocalization when periodic boundary conditions are adopted in the field of solid state. The ELF community have been traditionally most active in this aspect,^{90,98,99} especially, after the publication of a doctoral thesis about chemical bonding in crystalline solids.¹⁰⁰ In addition, the delocalization indices have recently broaden the scope to solid state DFT calculations.^{101,102} The extension of DAFH analysis to periodic boundary conditions is currently on the way in the laboratory of Prof. Ponc.

Chapter 3

Aromaticity and its Quantification

Originally, the concept of aromaticity was introduced to rationalize the structure, stability, and reactivity of benzene and related organic compounds. However, in the last decades, the boundaries of aromaticity have been extended to new areas of chemistry and to a large list of highly diverse species, which were unimaginable some decades ago.^{103,104} The proliferation of new aromatic compounds compelled to reconsider the traditional definition based on the Hückel's $(4n + 2)\pi$ electrons rule. Thus, species considered as Möbius aromatic^{105,106} disobeyed the $(4n + 2)\pi$ electrons rule while spherical aromatic compounds such as certain fullerenes added a third dimension to aromaticity.^{107,108} Both descriptions broke down the well-established relation between aromaticity and planarity. Moreover, metalloaromaticity¹⁰⁹ opened the way to organometallic and inorganic aromatic species and the discovery of σ -aromaticity^{110,111} demonstrating that, in some cases, the contribution of the σ -orbitals is crucial to explaining high electron delocalization. Consequently, the definition and limits of aromaticity have been constantly updated in order to take into account the whole spectrum of new aromatic compounds. Nowadays, the concept of aromaticity can be used to explain structure, stability, and reactivity not only of classical organic compounds but also of many organometallic and inorganic species, in particular, all-metal and semimetal clusters.

Parallel with the evolution of aromaticity, the aromaticity descriptors have been involved in a constant progress with the aim of predicting the aromatic character of a large list of uncountable and differing compounds. Probably, the nose was the first aromaticity descriptor because it was used to classify the organic substances with a characteristic smell as "aromatic" from the very beginning. However, the emergence of theoretical calculations produced a renewed impulse that allowed chemists

to widen the boundaries of aromaticity towards a large variety of new compounds. Erich Hückel and his theory of molecular orbitals (HMO),^{112,113} together with the famous $4n + 2$ π -electrons rule, pioneered the research of new rules and indices that could allow us to differentiate the aromatic molecules from the rest. In 1938, Coulson was the first to apply the concept of *bond order* to explain the electronic structure of aromatic molecules in the framework of HMO.⁴² Nowadays, a large list of complex aromaticity indices based on several concepts of quantum mechanics have been described to elucidate the aromaticity and antiaromaticity of a plethora of molecules.

3.1 History and Key Advances: From Benzene to All-metal Aromatic Clusters

In 1825, the English chemist Michael Faraday synthesized, for the first time, the benzene molecule.³ This discovery was described in the book called *A Manual of Chemistry* published by Lewis C. Beck in 1831 as follows¹¹⁴

NEW CARBURATES OF HYDROGEN, DISCOVERED BY MR.
FARADAY

Bicarburet of hydrogen. 6 Carb. 36 + 3 Hyd. 3 = 39

”When oil gas is subjected, in proper vessels, to a pressure high of thirty atmospheres, a fluid deposited in the proportion of nearly a gallon from 1000 cubic feet, which may be drowned off and preserved in glass bottles of ordinary strength. By repeated distillations, and by exposing the distilled liquid to a temperature of zero, Mr. Faraday obtained a substance to which has applied to above name.

The bicarburet of hydrogen, at common temperature, is a colorless transparent liquid, which smells like oil gas, and has also a slight odor of almonds.”

As can be seen, benzene was initially named bicarburet of hydrogen and formulated as C_6H_3 . Nine years after Faraday’s discovery, the German scientist Eilhard Mitscherlich obtained the same compound via distillation of benzoic acid and lime,¹¹⁵ using the German name *benzin* to designate it. In 1865, Kékulé proposed that the structure of benzene was a regular hexagon with a hydrogen at each corner.¹¹⁶ Later, he modified his theory to treat benzene as a mixture of cyclohexa-

trienes in rapid equilibrium:

”My mental eye, rendered more acute by the repeated visions of the kind, could now distinguish larger structures of manifold conformation; long rows sometimes more closely fitted together all twining and twisting in snake-like motion. But look! What was that? One of the snakes had seized hold of its own tail, and the form whirled mockingly before my eyes.”

Thus, benzene became the first of a large set of compounds with a more or less pleasant smell. The term aromaticity was named after the Greek term *aroma* which means ”pleasant odor”. Aromaticity is one of the most used chemical concepts in the literature, from research papers to organic text books. Actually, the whole discipline of chemistry is strongly influenced by aromatic compounds because two out of three molecules have aromatic character. For instance, the proper prediction of the aromaticity of a given compound is crucial to assessing the failure or success of a chemical reaction. In this way, Erlenmeyer established the basis for the reactivity of aromatic compounds finding that the substitution is more favorable than the addition.¹¹⁷ From the very beginning, many chemists have attempted to explain the stability and chemical behavior of aromatic molecules in terms of the chemical structure and the nature of chemical bond.

Since the isolation of benzene, the number of aromatic compounds has exponentially increased (see Table 3.1 for a summary of the main advances in the field of aromaticity). Before the end of the 19th century, the list was enlarged with benzene related monocyclic six-membered rings (6-MR). Then, the concept of aromaticity was extended to polycyclic rings such as naphthalene, anthracene, or phenanthrene, and to rings with heteroatoms such as thiophene and pyrrole, and to annulenes and their ions, e.g. tropylium cation. The work of Hückel helped to find a rule to discern between aromatic and non-aromatic compounds. With the concept of metalloaromaticity, aromaticity broke the confinements of organic chemistry. On the other hand, Heilbronner defined Möbius aromaticity, which follows exactly the opposite behavior of $4n + 2$ rule. By means of theoretical calculations, Baird described a rule for triplet aromaticity which was experimentally validated by Wörner et al. in 2006.¹³⁶ In 1978, Aihara introduced the three-dimensional aromaticity in boron clusters. Hirsh’s rule allows to predict the spherical aromaticity of recently discovered

Table 3.1: List of the key advances of the concept of aromaticity listed in chronological order. Adapted from.¹¹⁸

Year	Main contributor(s)	Contributions
1825	Michael Faraday ³	Isolation of benzene
1865	August Kékulé ¹¹⁶	Cyclohexatriene benzene formula
1866	Ernlenmeyer ¹¹⁷	Reactivity basis for aromaticity
1922	Crocker ¹¹⁹	Aromaticity sextet
1931	Hückel ^{112,113}	$(4n + 2)\pi$ electron rule
1938	Evans, Warhurst ¹²⁰	Transition state stabilization by aromaticity
1945	Calvin, Wilson ¹²¹	Metalloaromaticity
1959	Winstein ¹²²	Generalization of homoaromaticity
1964	Heilbronner ¹⁰⁵	Möbius aromaticity
1965	Breslow ¹²³	Recognition of aromaticity
1970	Osawa ¹²⁴	Superaromaticity
1972	Clar ¹²⁵	Clar aromatic sextet
1972	Baird ¹²⁶	Triplet aromaticity
1978	Aihara ¹²⁷	Three-dimensional aromaticity
1979	Dewar ^{110,111}	σ -aromaticity
1979	Schleyer ¹²⁸	Double and in-plane aromaticity
1985	Shaik and Hiberty ¹²⁹	π -electron distortivity
1985	Kroto and Smalley ¹³⁰	Discovery of fullerenes
1991	Iijima ¹³¹	Discovery of nanotube
2001	Boldyrev and Wang ⁴	All-metal aromaticity
2005	Schleyer and Tsipis ^{132,133}	d-orbital aromaticity
2007	Boldyrev and Wang ¹³⁴	δ -aromaticity
2008	Tsipis and Tsipis ¹³⁵	ϕ -aromaticity

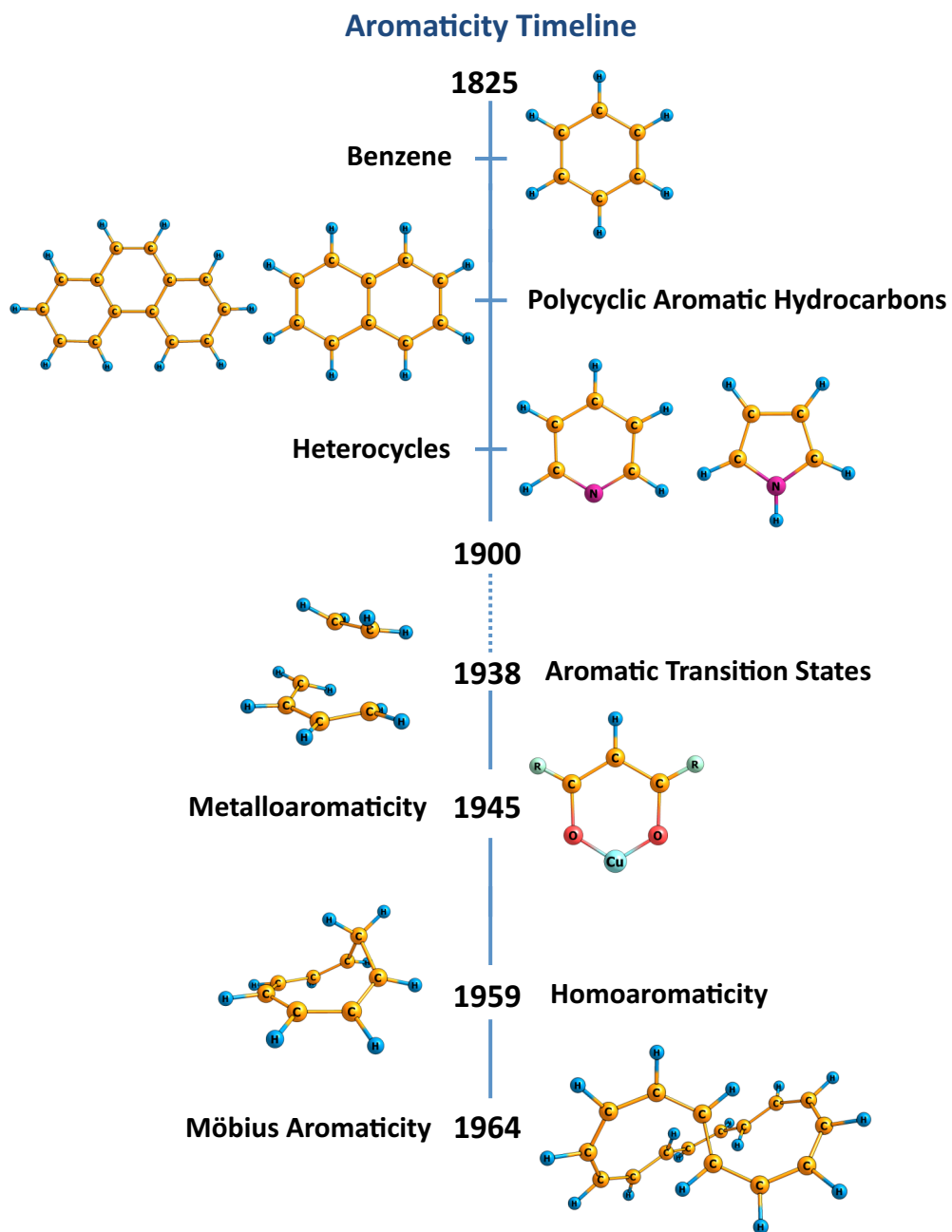


Figure 3.1: Most relevant advances of the concept of Aromaticity from 1825 to 1970

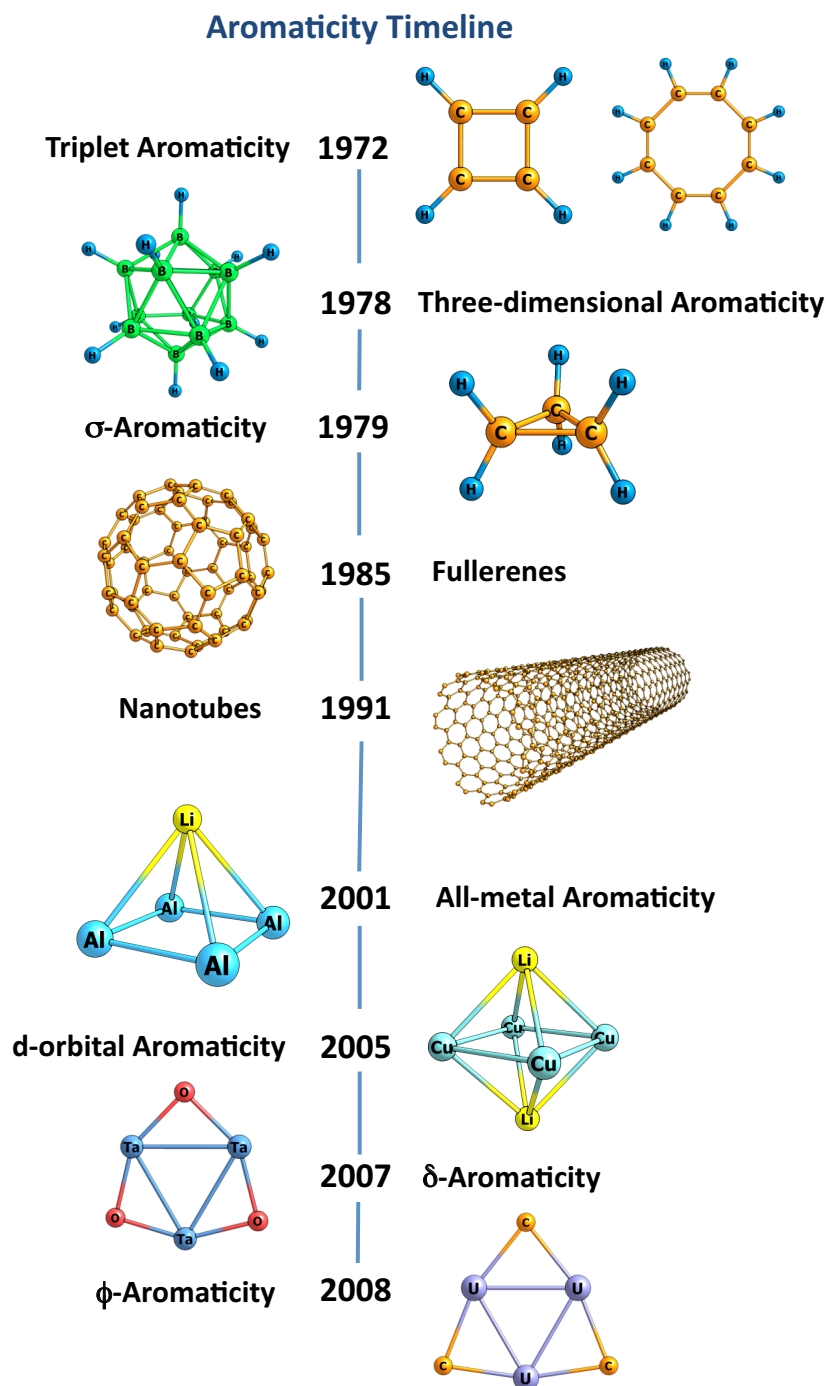


Figure 3.2: Most relevant advances of the concept of Aromaticity from 1970 to 2010

fullerenes and nanotubes.¹³⁷ Finally, the most important recent breakthrough in the field of aromaticity took place in 2001, when Boldyrev, Wang et al., characterized the first all-metal aromatic cluster Al_4^{2-} . The properties of such molecules make them potentially useful for technical applications such as specific and very efficient catalysts, drugs, and other novel materials with as yet unimagined features. At variance with the classical aromatic organic molecules that possess only π -electron delocalization, these compounds present σ -, π -, and δ - (involving d orbitals) or even ϕ - (involving f orbitals) electron delocalization, exhibiting characteristics of what has been called multifold aromaticity.

The unstoppable evolution of aromaticity has led to a situation where two molecules with completely different origins could share some properties. For instance, what does the aromatic paradigm, i.e. benzene, have in common with the first all-metal aromatic cluster Al_4^{2-} ? Although at first glance they look rather different, these two compounds share a large list of properties: structurally, both present bond length equalization and are planar; energetically, both show enhanced stability in comparison to similar molecules; with respect to reactivity, both exhibit low reactivity but present electrophilic aromatic substitution; magnetically, both sustain a ring current and magnetic susceptibility exaltation; and electronically, both present highly delocalized electrons. On the other hand, due to the metallic nature of aluminum, Al_4^{2-} shows other interesting properties such as: σ electron delocalization and ring current, i.e., it is doubly aromatic $\sigma + \pi$, and has exalted linear and nonlinear optical properties, such as higher polarizability or higher second hyperpolarizability.¹³⁸

Definition of Aromaticity

As previously mentioned, the advent of quantum mechanics supposed to renounce to a large list of classical concepts. Aromaticity is not an observable property and, thus, its rigorous definition does not have a place in the framework of quantum mechanics. However, the concept of aromaticity, that has been widely used for both experimentalist and computational chemists, has persisted as a tool to explain several chemical phenomena despite lacking a clear and unambiguous definition. The definition and limits of aromaticity have been constantly reformulated with the aim of taking into account the whole spectrum of new aromatic compounds. In this way, Schleyer and coworkers proposed the following definition:¹¹⁸

”Aromaticity is a manifestation of electron delocalization in closed cir-

cuits, either in two or in three dimensions. This results in energy lowering, often quite substantial, and a variety of unusual chemical properties. These include a tendency toward bond length equalization, unusual reactivity, and characteristic spectroscopic features. Since aromaticity is related to induced ring currents, magnetic properties are particularly important for its detection and evaluation.”

Since it is not an observable property, aromaticity is measured from its multiple manifestations. The most common aromaticity descriptors are those based on structural parameters, energetic criteria, magnetic properties, reactivity indices, or electron delocalization measures. Thus, the quantification of aromaticity is a rather cumbersome process. In addition, it is worth mentioning that some authors suggest abandoning the term aromaticity and using another nomenclature such as energetic-aromaticity, structural-aromaticity, or magnetic aromaticity.^{139,140}

3.2 Descriptors of Aromaticity

As previously said, the most common aromaticity descriptors are those based on structural parameters, energetic criteria, magnetic properties, reactivity indices, or electron delocalization measures. Despite its multiple manifestations, one may think that all the aromaticity indices lead to the same conclusions. However, Katritzky et al. demonstrated by means of a statistical analysis that the magnetic-aromaticity is orthogonal to other measures, such as the energetic-aromaticity or geometrical-aromaticity.¹⁴¹ Nowadays, the aromaticity is considered a multidimensional property, and many authors suggest using several indicators of aromaticity before assessing the actual aromaticity of the system. The main indicators of aromaticity used in this thesis will be extensively discussed in Chapters 6.1-6.5 where their performance is evaluated using a test set.

The most important advances in the field of aromaticity indices are summarized in Tables 3.2 and 3.3, where they are classified in function of the measured property, i.e. energetic, magnetic, structural, reactivity, or electronic. Next, we outline the aromaticity indices that have been used in this thesis.

Table 3.2: List of the main advances on the quantification and classification of aromatic compounds. Adapted from.¹¹⁸

Year	Main contributor(s)	Contribution	Type
1931	Hückel ^{112,113}	$(4n + 2)\pi$ electron rule	
1933	Pauling ¹⁴²	Valence bond and resonance	Energetic
1953	Meyer ¹⁴³	The difference in the proton magnetic shielding between benzene and noncyclic olefins observed	Magnetic
1956	Pople ¹⁴⁴	Induced ring current effects on NMR chemical shifts: deshielding of benzene protons	Magnetic
1965	Dewar ¹⁴⁵	Dewar resonance energy	Energetic
1968	Dauben ¹⁴⁶	Diamagnetic susceptibility exaltation	Magnetic
1972	Krygowski ¹⁴⁷	Harmonic oscillator model of aromaticity (HOMA)	Structural
1981	Lazzeretti and Zanasi ¹⁴⁸	<i>Ab initio</i> current density plots	Magnetic
1983	Jug ¹⁴⁹	Jug structural index	Structural
1985	Bird ¹⁵⁰	Bird structural index	Structural
1988	Zhou, Parr, Garst ¹⁵¹	Hardness	Reactivity
1990	Schleyer ¹⁵²	Extensively using Li^+ NMR to study aromaticity	Magnetic
1996	Schleyer ¹⁵³	Nucleus-independent chemical shifts (NICS)	Magnetic
1996	Fowler and Steiner ¹⁵⁴	Extensive application of current density plots to study aromaticity	Magnetic
1997	Schleyer ¹⁵⁵	Dissected NICS, localized molecular orbital (LMO)	Magnetic
1998	Geerlings and De Proft ¹⁵⁶	Derivatives of molecular valence	
1999	Sundholm ¹⁵⁷	Aromatic ring-current shielding (ARCS)	Magnetic
1999	Mo ¹⁵⁷	Block-localized wave function	Energetic
2001	Fowler and Steiner ¹⁵⁴	Ipsocentric partition of total $(\sigma + \pi)$ current density into orbital contributions	Magnetic
2003	Corminboeuf and Schleyer ¹⁵⁸	Dissected NICS, GIAO-CMO	Magnetic
2004	Merino and Heine ¹⁵⁹	Induced magnetic field	Magnetic
2004	Sundholm ¹⁶⁰	Integrated induced currents (GIMIC)	Magnetic
2006	Stanger, ¹⁶¹ Solà ¹⁶²	NICS-scan	Magnetic

Energetic Aromaticity - ASE

In 1933, Pauling and Wheland analyzed the differences between the actual π -electron energy of benzene and the π -electron energy of analogous hypothetical species with localized π -electrons. This study led to the introduction of the concept of resonance energy (RE) in terms of valence bond theory.¹⁴² Therefore, the energetic-based indicators of aromaticity make use of the fact that conjugated cyclic π -electron compounds are more stable than their chain analogues which has no cyclic π -electron delocalization. The most common used energetic measure of aromaticity is the aromatic stabilization energy (ASE), calculated as the reaction energy of a homodesmotic reaction.¹⁶³ The main disadvantage of these methods is the difficulty to isolate the aromatic stabilization from other important effects that stabilize or destabilize a molecule.

Structural Aromaticity - HOMA

The structural aromaticity descriptors are based on the idea that the tendency toward bond length equalization and the symmetry of the ring are important manifestations of aromaticity. Among the most common structural-based measures, the harmonic oscillator model of aromaticity (HOMA)¹⁴⁷ index defined by Kruszewski and Krygowski has proven to be one of the most effective structural indicators of aromaticity:

$$HOMA = 1 - \frac{\alpha}{n} \sum_{i=1}^n (R_{opt} - R_i)^2 \quad (3.1)$$

where n is the number of bonds considered and α is an empirical constant (for C-C, C-N, C-O, and N-N bonds $\alpha=257.7, 93.5, 157.4,$ and $130.3,$ respectively) fixed to give HOMA= 0 for a model nonaromatic system and HOMA=1 for a system with all bonds equal to an optimal value R_{opt} , assumed to be achieved for fully aromatic systems. R_i stands for the running bond length. The HOMA value can be decomposed into the energetic (EN) and geometric (GEO) contributions according to the next relation:¹⁶⁴

$$HOMA = 1 - EN - GEO = 1 - \alpha(R_{opt} - \bar{R})^2 - \frac{\alpha}{n} \sum_i (\bar{R} - R_i)^2 \quad (3.2)$$

The GEO contribution measures the decrease or increase in bond length alteration

while the EN term takes into account the lengthening/shortening of the mean bond lengths of the ring.

Magnetic Aromaticity - NICS

Magnetic indices of aromaticity are based on the π -electron ring current that is induced when the system is exposed to external magnetic fields. Originally, the magnetic susceptibility exaltation and anisotropy of magnetic susceptibility received substantial support but, undoubtedly, nowadays the most widely used magnetic-based indicator of aromaticity is the nucleus independent chemical shift (NICS), proposed by Schleyer and co-workers.^{118,153} NICS is defined as the negative value of the absolute shielding computed at a ring center or at some other interesting point of the system, for instance 1 Å above the ring center. Rings with large negative NICS values are considered aromatic. The more negative the NICS values, the more aromatic the rings are.

NICS has many advantages among other indicators of aromaticity. First, it is a very accessible and easy to compute descriptor despite its elevated computational cost; second, it can be used to discuss both the local and the global aromaticity of molecules, and, third, it does not use reference values, so it can be easily applied to any molecule. However, it is not free from criticism. Lazzeretti^{140,165} and Aihara¹⁶⁶ have pointed out in several works that NICS's validity to indicate diamagnetic ring currents is limited by the potential spurious contributions from the in-plane tensor components that, at least in classical organic aromatic compounds, are not related to aromaticity. This effect is partially avoided by using NICS(1),¹⁶⁷ that is considered to better reflect the π -electron effects, or with its corresponding out-of-plane tensor component (NICS(1)_{zz}) or even better with the π contribution to this component computed at the ring center or at 1 Å above (NICS(0) _{π zz} and NICS(1) _{π zz}, respectively). In 1997, the first dissected NICS were introduced by Schleyer et al.¹⁵⁵ and were applied to study the aromaticity of some inorganic rings. NICS _{π} values can be calculated through the decomposition of NICS indices into their canonical molecular orbital (CMO) components¹⁶⁸ using the NBO 5.0 program.¹⁶⁹ NICS(1) _{π} and NICS(0) _{π zz} were reported to be the best measures of aromaticity among the different NICS-related definitions in organic molecules.^{170,171} Other problems that can be found are related to ring size dependence of NICS values¹⁷² or, recently, Castro and coworkers have shown that NICS values strongly depend on the inclusion of relativistic effects in molecules containing heavy elements.¹⁷³

Table 3.3: List of the main advances on the quantification and classification of aromatic compounds by means of electronic properties. Adapted from¹¹⁸

Year	Main contributor(s)	Contribution	Type
2000	Giambiagi ⁶⁰	Multicenter bond indices (I_{ring})	Electronic
2000	Chesnut, ¹⁷⁸ Silvi ¹⁷⁹	Electron localization function to measure aromaticity	Electronic
2003	Poater, Fradera, and Solà ⁵⁰	Para-delocalization index (PDI)	Electronic
2004	Fuentealba ¹⁸⁰	Bifurcation of the Electron localization function	Electronic
2005	Matito and Solà ¹⁸¹	Aromatic fluctuation index (FLU)	Electronic
2005	Bultinck ⁶¹	Multicenter index (MCI)	Electronic

Every aromaticity index introduced up to now presents its advantages and drawbacks. Some descriptors, such as HOMA, are computationally inexpensive but, for instance, may fail on predicting the aromatic character of the Diels-Alder reaction transition state.¹⁷⁴ Other descriptors, such as NICS, have been widely used to predict the aromaticity of a large series of systems. As previously mentioned, some drawbacks have been also reported.^{175–177} Therefore, some aromaticity descriptors fail on giving the expected answer from most elementary chemical problems. For this reason, the performance of aromaticity indices and their adequacy for each chemical situation must be a prime aim for aromaticity researchers. In Chapter 6, we propose a set of fifteen aromaticity tests using a number of examples for which most chemists would agree about the expected aromaticity trends in a given series of compounds. The tests had been chosen to fulfill two requirements. First, the size of the systems involved must be relatively small to facilitate a fast application and, second, controversial cases must be avoided. Then, we analyze the advantages and drawbacks of a group of widely used aromaticity descriptors. Thus, we will conclude showing which descriptors are more adequate for each situation and, in addition, we will propose an alternative methodology for testing future aromaticity indices.

Aromaticity from ESI

In Chapter 7, we will focus on the analysis of aromaticity by means of electron delocalization measures (see Table 3.3 for a complete list of electron-based aromaticity descriptors). Our group has a great deal of experience in the field of

electron structure characterization by means of electron localization and delocalization measures.^{38,39,50,174,181–189} In 2003, this knowledge was channeled to propose a new measure of aromaticity based on the delocalization indices described in the previous chapter. This work was carried out by Poater et al., who defined the para-delocalization index (PDI) which measures the electron sharing between the *para* positions of a given 6-MR.⁵⁰ The idea of PDI derives from the work of Fulton and Bader who found a higher electron delocalization between *para* carbons than between *meta* despite the longer distance between the carbon atoms of the former. Before introducing PDI, let us consider that the ring structure consists of n atoms, represented by the following string $\mathcal{A}=\{A_1,A_2,\dots,A_n\}$, whose elements are ordered according to the connectivity of the atoms in the ring. Thus, PDI is defined as the average of para delocalization indices:

$$PDI(\mathcal{A}) = \frac{\delta(A_1, A_4) + \delta(A_2, A_5) + \delta(A_3, A_6)}{3} \quad (3.3)$$

The main shortcoming of PDI is that it is limited to 6-MR. Two years later, with the aim of extending the applicability to any given size of a ring, Matito et al. constructed a new measure called aromatic fluctuation index (FLU) based on comparing the electron sharing between bonded pairs of atoms in a ring:¹⁸¹

$$FLU(\mathcal{A}) = \frac{1}{n} \sum_{i=1}^n \left[\left(\frac{V(A_i)}{V(A_{i-1})} \right)^\alpha \left(\frac{\delta(A_i, A_{i-1}) - \delta_{ref}(A_i, A_{i-1})}{\delta_{ref}(A_i, A_{i-1})} \right) \right]^2 \quad (3.4)$$

where $A_0 \equiv A_n$ and $V(A)$ is the atomic valence as described in Eq. 2.32. $\delta_{ref}(A_i, A_{i-1})$ is taken from an aromatic molecule, for instance, for C-C bonds the molecule chosen as a reference is benzene. Finally, α is a simple function to ensure the first term in Eq. 3.4 is always greater or equal to 1,

$$\alpha = \begin{cases} 1 & V(B) \leq V(A) \\ -1 & V(B) < V(A) \end{cases} \quad (3.5)$$

FLU is close to zero in aromatic species, and greater than zero for non-aromatic or antiaromatic species. However, FLU strongly depends on reference values that prevent its use to study the aromaticity of inorganic systems.

From the work of Giambiagi,^{60,190} the interest in multicenter indices as aromaticity

descriptors has grown exponentially. The I_{ring} index was defined by Giambiagi as

$$I_{ring}(\mathcal{A}) = \sum_{i_1, i_2, \dots, i_n}^{occ} S_{i_1 i_2}(A_1) S_{i_2 i_3}(A_2) \dots S_{i_n i_1}(A_n) \quad (3.6)$$

where S_{ij} is the overlap of molecular orbitals i and j in the atom A . I_{ring} will provide large values for aromatic molecules. It is worth noticing here that the normalized version of I_{ring} has recently been defined by Cioslowski, Matito and Solà.¹⁹¹

$$I_{NG}(\mathcal{A}) = \frac{\pi^2}{4NN_\pi} I_{ring}(\mathcal{A})^{1/N} \quad (3.7)$$

where N is the total number of atoms in the ring and N_π the total number of π electrons. In 2005, Bultinck and coworkers proposed an extension of the I_{ring} index of Giambiagi.⁶¹ This index, which is called multicenter index of aromaticity (MCI), has been successfully applied to a broad number of situations, from simple organic compounds to complex all-metal clusters with multiple aromaticity.^{32,192–198}

$$MCI(\mathcal{A}) = \sum_{\mathcal{P}(\mathcal{A})} I_{ring}(\mathcal{A}) = \quad (3.8)$$

$$= \sum_{\mathcal{P}(\mathcal{A})} \sum_{i_1, i_2, \dots, i_n}^{occ} S_{i_1 i_2}(A_1) S_{i_2 i_3}(A_2) \dots S_{i_n i_1}(A_n) \quad (3.9)$$

where $\mathcal{P}(\mathcal{A})$ stands for $n!$ permutations of elements in the string $\mathcal{P}(\mathcal{A})$. However, this index has been associated with a remarkable computational cost that limits its use to rings up to nine members. This drawback has been partially solved with the so-called pseudo- π method, although the results obtained are less accurate.¹⁹⁹ For planar species, $S_{\sigma\pi}(A) = 0$ and MCI can be exactly split into the σ - and π -contributions in order to obtain MCI_σ and MCI_π . This feature is especially interesting to evaluate multifold aromaticity in all-metal clusters. Finally, there is a normalized version of the MCI index, the so-called I_{NB} , given by:¹⁹¹

$$I_{NB}(\mathcal{A}) = \frac{C}{4NN_\pi} [2N \cdot MCI(\mathcal{A})]^{1/N} \quad (3.10)$$

where $C \approx 1.5155$.

Following this, in Chapter 7 will study in detail the electron delocalization of aromatic compounds. To this end, a series of organic and inorganic aromatic and antiaromatic compounds have been selected. The main aim of the last part of this thesis is to find electron delocalization patterns that could represent a step forward towards a better comprehension of the electronic delocalization behavior of aromatic or antiaromatic systems. In the future, this research will lead to the development of new aromaticity indices based on electron delocalization measures with lower computational cost that could be applied to a wide set of compounds without any restrictions.

Chapter 4

Objectives

The main goal of the present thesis is the analysis of chemical bonding and aromaticity by means of electron delocalization measures. In the previous chapters, we have underlined the potential of electron delocalization to account for the electronic structure of molecules. Likewise, we have seen how electron sharing indices (ESI), domain-averaged Fermi holes (DAFH), and electron localization function (ELF) can be successfully used as tools to shed light on the nature of the chemical bond. Moreover, we have outlined the key role that aromaticity plays in several fields of chemistry and summarized the plethora of descriptors used for its quantification.

This thesis is divided into three different blocks. The first is devoted to the analysis of chemical bonding, while the second and the third deal with the concept of aromaticity.

The ELF was defined in the framework of monodeterminantal wave functions. Later on, due to the limitations of the HF approximation, the definition of the ELF was extended to take into account correlation effects. However, the high computational cost associated with the *exact* two-particle density (2-PD) limits the use of correlated ELF to small systems. To bridge the gap between the expensive 2-PD and the (sometimes) inaccurate expression at the HF level, *the first aim of this thesis is to propose an approximation of the ELF in terms of natural orbitals*. On the other hand, the DAFH analysis performs remarkably well to discern the picture of bonding in nontrivial molecules. Up to now, this analysis has been limited to closed-shell systems. To overcome this limitation, *the second goal of the this thesis is to generalize the expression of the DAFH to study both closed- and open-shell systems*. From the previous generalization, we will study the bonding patterns of some open

shell systems and the peculiarities of the ultrashort Cr-Cr bond.

Aromaticity is a key property that accounts for the molecular and electronic structure, stability, and reactivity of a large list of compounds. Since aromaticity is not a measurable property, it cannot be defined unambiguously. Therefore, several methods can be used to quantify the aromaticity of a given compound. These indices are based on structural, magnetic, energetic, or electronic properties. In many cases, results obtained from different indicators of aromaticity may reveal contradictory trends. Hence, *the third objective is to study the ability of some of the most widely used aromaticity indices to give the expected answer from a series of tests that share widely accepted and well-understood aromatic trends.* In contrast to organic species, only few descriptors can provide reliable measures of aromaticity for all-metal clusters. In the spirit of the previous objective, *the fourth aim is to propose a test to evaluate the performance of current aromaticity indices in the realm of all-metal clusters.* From the information gathered in this section, we will be able to establish the advantages and drawbacks of aromaticity indices and, thus, recommend which descriptor must be used in each situation.

The ESIs have been proven to be a powerful tool to quantify the aromaticity of a given ring. In our research group, two widely used aromaticity indicators based on electron delocalization have recently been proposed. The para delocalization index (PDI) and the aromatic fluctuation indicator (FLU) have been successfully applied to rationalize the electronic structure, stability, and reactivity of a large list of aromatic compounds. However, they present some restrictions: PDI descriptor can be only applied to 6-MR while FLU index depends on reference values which prevent its use for inorganic species. On the other hand, electronic multicenter indices perform remarkably well but have been associated with a high computational cost and relative dependence on the level of calculation. To overcome these constraints, *the fifth goal of this thesis is to study in detail the electron delocalization of aromatic and antiaromatic compounds of both organic and inorganic species in order to define, in the near future, a powerful aromaticity descriptor.* To this end, the patterns of π -electron delocalization will be analyzed for typical organic compounds, while in the last part of the thesis, σ -, π -, and δ aromaticity will be assessed for a series of all-metal clusters. In the near future, all the information collected in Chapters 6 and 7 will be used to define a new index of aromaticity based on electron delocalization measures that could be applied without any restrictions.

Chapter 5

Applications I: The Nature of the Chemical Bond from Electron Localization Function and Domain-Averaged Fermi Holes

5.1 Electron Localization Function at the Correlated Level: A Natural Orbital Formulation

Feixas, F.; Matito, E.; Duran, M.; Solà, M.; Silvi, B.; *J. Chem. Theory Comput.* 6, 2736-2742, **2010**

Ferran Feixas, Eduard Matito, Miquel Duran, Miquel Solà, and Bernard Silvi. “Electron Localization Function at the Correlated Level: A Natural Orbital Formulation”. *Journal of chemical theory and computation*. Vol. 6, issue 9 (Septiembre 14, 2010) : p. 2736-2742

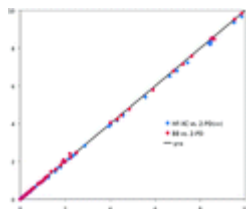
<http://pubs.acs.org/doi/full/10.1021/ct1003548>

<http://dx.doi.org.10.1021/ct1003548>

Publication Date (Web): August 23, 2010 (Article)

ABSTRACT

In this work we present a 2-fold approximation for the calculation of the electron localization function (ELF) which avoids the use of the two-particle density (2-PD). The first approximation is used for the calculation of the ELF itself and the second one is used to approximate pair populations integrated in the ELF basins. Both approximations only need the natural orbitals and their occupancies, which are available for most methods used in electronic structure calculations. In this way, methods such as CCSD and MP2 can be used for the calculation of the ELF despite the lack of a pertinent definition of the 2-PD. By avoiding the calculation of the 2-PD, the present formulation provides the means for routine calculations of the ELF in medium-size molecules with correlated methods. The performance of this approximation is shown in a number of examples.



5.2 Domain Averaged Fermi Hole Analysis for open-shell systems

Ponec, R.; Feixas, F.; *J. Phys. Chem. A* 113, 5773-5779, **2009**

Ponec, R., Feixas, F. “Domain averaged Fermi hole analysis for open-shell Systems”. *Journal of physical chemistry A*. Vol. 113, issue 19 (May 14, 2009) : p. 5773-5779

<http://pubs.acs.org/doi/full/10.1021/jp9015245>

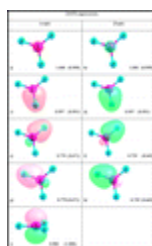
<http://dx.doi.org.10.1021/jp9015245>

DOI: 10.1021/jp9015245

Publication Date (Web): April 22, 2009

ABSTRACT

The Article reports the extension of the new original methodology for the analysis and visualization of the bonding interactions, known as the analysis of domain averaged Fermi holes (DAFH), to open-shell systems. The proposed generalization is based on straightforward reformulation of the original approach within the framework of unrestricted Hartree–Fock (UHF) and/or Kohn–Sham (UKS) levels of the theory. The application of the new methodology is demonstrated on the detailed analysis of the picture of the bonding in several simple systems involving the doublet state of radical cation $\text{NH}_3^{(+)}$ and the triplet ground state of the O_2 molecule.



5.3 Bonding Analysis of the $[C_2O_4]^{2+}$ Intermediate Formed in the Reaction of CO_2^{2+} with Neutral CO_2

Feixas, F.; Ponec, R.; Fiser, J.; Schröder, D.; Roithová, J.; Price, S.D.; *J. Phys. Chem. A* 113, 6681-6688, 2010

Ferran Feixas, Robert Ponec, Jiri Fisure, Jana Roithová, Detlef Schröder and Stephen D. Price. “Bonding Analysis of the $[\text{C}_2\text{O}_4]^{2+}$ Intermediate Formed in the Reaction of CO_2^{2+} with Neutral CO_2 “. *Journal of physical chemistry, A*. Vol. 114, issue 24 (June 24, 2010) : p. 6681-6688

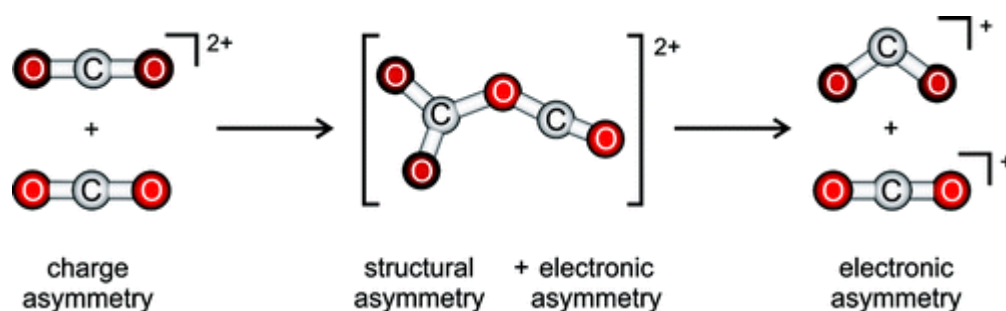
<http://pubs.acs.org/doi/abs/10.1021/jp1020559>

<http://dx.doi.org.10.1021/jp1020559>

Publication Date (Web): May 28, 2010 (Article)

DOI: 10.1021/jp1020559

ABSTRACT



The bonding patterns of the $[\text{C}_2\text{O}_4]^{2+}$ dication formed upon interaction of CO_2^{2+} with neutral CO_2 are investigated using the analysis of domain-averaged Fermi holes (DAFHs). The DAFH approach provides an explanation for the previously observed “asymmetry” of the energy deposition in the pair of CO_2^+ monocations formed in the thermal reaction $\text{CO}_2^{2+} + \text{CO}_2 \rightarrow [\text{C}_2\text{O}_4]^{2+} \rightarrow 2 \text{CO}_2^+$, specifically that the CO_2^+ monocation formed from the dication dissociates far more readily than the CO_2^+ monocation formed from the neutral molecule. The bonding pattern is consistent with a description of intermediate $[\text{C}_2\text{O}_4]^{2+}$ as a complex between the triplet ground state of CO_2^{2+} with the singlet ground state of neutral CO_2 , which can, among other pathways, smoothly proceed to a nondegenerate pair of ${}^4\text{CO}_2^+ + {}^2\text{CO}_2^+$ where the former stems from the dication and the latter stems from the neutral reactant. Hence the “electronic history” of the components is retained in the $[\text{C}_2\text{O}_4]^{2+}$ intermediate. In addition, dissociation of ${}^4\text{CO}_2^+$ is discussed based on CCSD and CASSCF calculations. Equilibrium geometries for the ground electronic states of $\text{CO}_2^{0/+ / 2+}$ and some other relevant structures of CO_2^+ are determined using the MRCI method.

5.4 Peculiarities of Multiple Cr-Cr bonding. Insights from the Analysis of Domain-Averaged Fermi Holes

Ponec, R.; Feixas, F.; *J. Phys. Chem. A* 113, 8394-8400, **2009**

R. Ponec, Ferran Feixas. "Peculiarities of multiple Cr–Cr bonding. Insights from the analysis of domain-averaged fermi holes". *Journal of physical Chemistry A*. Vol. 113, issue 29 (23 July 2009) : p. 8394-8400

<http://pubs.acs.org/doi/abs/10.1021/jp903144q>

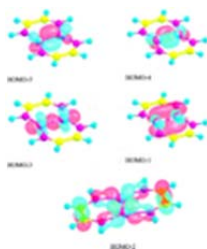
<http://dx.doi.org/10.1021/jp903144q>

DOI: 10.1021/jp903144q

Publication Date (Web): July 1, 2009

Abstract

The recently proposed methodology known as the analysis of domain-averaged Fermi holes was *applied to reveal the nature and peculiarity of metal–metal bonding interactions in two recently reported complexes with an ultrashort, presumably quintuple Cr–Cr bond. The results of the analysis straightforwardly confirm the considerable reduction of the Cr–Cr bond order resulting from depletion of the electron density from one of the electron pairs involved in the metal–metal bonding. Because of this depletion, the Cr–Cr bond can be best classified as the effective quadruple bond, with the contribution of another weak component corresponding to the antiferromagnetic coupling of electrons in one of the available δ -electron pairs.*



Chapter 6

Applications II: Critical assessment on the performance of a set of aromaticity indexes

6.1 Electron Delocalization and Aromaticity Measures within the Hückel Molecular Orbital Method

Matito, E.; Feixas, F.; Solà, M.; *J. Mol. Struct. (THEOCHEM)* 811, 3-11, **2007**

Eduart Matito, Ferran Feixas, Miquel Solà. "Electron delocalization and aromaticity measures within the Hückel molecular orbital method". *Journal of molecular structure: THEOCHEM*. Vol. 811, issues 1-3 (June 2007) : p. 3-11

<http://dx.doi.org/10.1016/j.theochem.2007.01.015>

<http://www.sciencedirect.com/science/article/pii/S0166128007000589>

Received 12 December 2006; Accepted 10 January 2007. Available online 28 January 2007.

Abstract

In this paper, we review the electronic aromaticity measures from the perspective of the Hückel molecular orbital (HMO) theory. The analysis of FLU, PDI, I_{ring} and SCI in the framework of the HMO theory provides an interesting scenario for the interpretation of these indices. Within the Hückel theory the formulas for the Coulson bond orders are easily obtained in a closed form for annulenes, which enables the production of analytical expressions for some of the aromaticity measures. These analytical functions are used to study the ring size dependence of current aromaticity indices. Besides, HMO calculations of polycyclic benzenoids complete the analysis of the electronic aromaticity indices reviewed in this paper, by showing how HMO theory explains the changes in aromaticity due to annulation. All these results help grasping the meaning and the behavior of the electronic aromaticity indices.

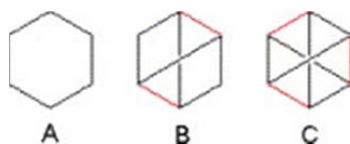


Fig. 3.

All possible patterns of connectivity for benzene according to HMO calculations.

6.2 Aromaticity of Distorted Benzene Rings: Exploring the Validity of Different Indicators of Aromaticity

Feixas, F.; Matito, E.; Poater, J.; Solà, M.; *J. Phys. Chem. A* 111, 4513-4521, **2007**

Ferran Feixas, Eduard Matito, Jordi Poater and Miquel Solà. "Aromaticity of distorted benzene rings: explorin the validity of diferent indicators of aromaticity". Journal of physical Chemistry A. Vol. 24, issue 20 (24 May 2007) : p. 4513-4521

<http://pubs.acs.org/doi/abs/10.1021/jp0703206>

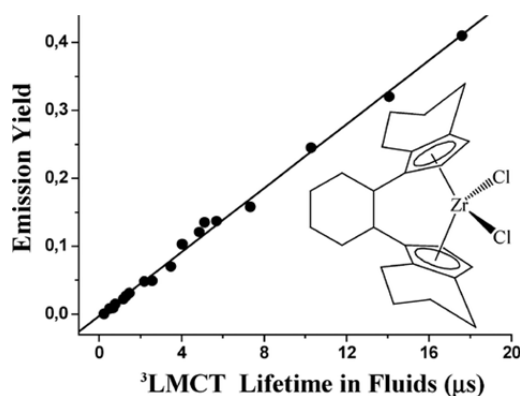
<http://dx.doi.org/10.1021/jp0703206>

Publication Date (Web): April 21, 2007 (Article)

DOI: 10.1021/jp0703206

Abstract

The effect of three in-plane (bond length alternation, bond length elongation, and clamping) and three out-of-plane deformations (boatlike, chairlike, and pyramidalization) on the aromaticity of the benzene molecule has been analyzed employing seven widely used indicators of aromaticity. It is shown that only the aromatic fluctuation index (FLU) is able to indicate the expected loss of aromaticity because of distortion from the equilibrium geometry in all deformations analyzed. As FLU has been shown previously to fail in other particular situations, we conclude that there is not yet a single indicator of aromaticity that works properly for all cases. Therefore, to reach safer conclusions, aromaticity analyses should be carried out employing a set of aromaticity descriptors on the basis of different physical manifestations of aromaticity.



6.3 Is the Aromaticity of the Benzene Ring in the $(\eta^6 - C_6H_6)Cr(CO)_3$ Complex Larger than that of the Isolated Benzene Molecule?

Feixas, F.; Jiménez-Halla, J.O.C.; Matito, E.; Poater, J.; Solà, M.; *Pol J. Chem.* 81, 783- 797, **2007**

Is the Aromaticity of the Benzene Ring in the $(\eta^6\text{-C}_6\text{H}_6)\text{Cr}(\text{CO})_3$ Complex Larger than that of the Isolated Benzene Molecule?*

by F. Feixas¹, J.O.C. Jiménez-Halla¹, E. Matito^{1,2}, J. Poater³ and M. Solà^{1**}

¹*Institut de Química Computacional and Departament de Química, Universitat de Girona, 17071 Girona, Catalonia, Spain
e-mail: miquel.sola@udg.es*

²*Institute of Physics, Szczecin University, 70-451 Szczecin, Poland*

³*Afdeling Theoretische Chemie, Scheikundig Laboratorium der Vrije Universiteit, De Boelelaan 1083, NL-1081 HV Amsterdam, The Netherlands*

(Received October 27th, 2006)

The aromaticity of the benzene ring in the $(\eta^6\text{-C}_6\text{H}_6)\text{Cr}(\text{CO})_3$ complex is analyzed using several indicators of aromaticity based on different physical manifestations of this property. All indices used except NICS show that there is a clear reduction of the aromaticity of benzene upon coordination to the $\text{Cr}(\text{CO})_3$ complex. The particular behavior of the NICS index has been analyzed in detail and we have concluded that the reduction of the NICS value in the benzene ring of the $(\eta^6\text{-C}_6\text{H}_6)\text{Cr}(\text{CO})_3$ complex is not a manifestation of an increased aromaticity but is due to the ring currents generated by the electron pairs that take part in the benzene– $\text{Cr}(\text{CO})_3$ bonding.

Key words: aromaticity, benzene, $(\eta^6\text{-C}_6\text{H}_6)\text{Cr}(\text{CO})_3$ complex, Nucleus-Independent Chemical Shift (NICS), *Para*-Delocalization Index (PDI), Harmonic Oscillator Model of Aromaticity (HOMA), Aromatic Fluctuation Index (FLU), Six Center Index (SCI), Atoms in Molecules (AIM) Theory

$(\eta^6\text{-Arene})$ tricarbonylchromium complexes are among the most extensively studied half-sandwich complexes [1–6]. In the quest for new molecular switches, special attention has been focused on the reaction mechanisms of thermally induced inter-ring haptotropic rearrangements that occur in $(\eta^6\text{-arene})$ tricarbonylchromium complexes, in particular in those taking place in chromium tricarbonyl complexes of substituted naphthalenes [6–11], but also in larger polycyclic aromatic hydrocarbons (PAHs) [11–17]. The barrier to tripodal rotation of the $\text{Cr}(\text{CO})_3$ fragment about the arene ring–Cr axis has also been the subject of many experimental and theoretical investigations [18–21].

Coordination of the chromium tricarbonyl complex to a given PAH takes place usually to the ring with the highest electron density [22,23], which is in many cases the most aromatic [24]. It is widely accepted that the structure, reactivity, and aroma-

* Dedicated to Professor T.M. Krygowski on the occasion of his 70th birthday.

**To whom correspondence should be addressed. E-mail: miquel.sola@udg.es
Phone: +34-972-418912. Fax: +34-972-418356.

ticity of the PAH are altered significantly upon complexation with the chromium tricarbonyl complex. Thus, after coordination the ring expands, loses its planarity, and shows an increased difference between alternated short and long C–C bonds [22,25]. Moreover, the reactivity of the coordinated ring dramatically changes due to complexation. The strong electron withdrawing character of the chromium tricarbonyl complex makes the coordinated PAH more susceptible to nucleophilic addition rather than electrophilic substitution and also increases the acidity of the aryl and benzylic hydrogens [25–27]. On the other hand, the effect of chromium tricarbonyl complexation on aromaticity is more controversial. According to Mitchell and co-workers [28–31], the benzene ring in tricarbonylchromium-complexed benzene is about 30–40% more aromatic than benzene itself. Their conclusion was based on chemical shift data and coupling constants which suggest that the benzene ring in certain annulene systems coordinated to the chromium tricarbonyl complex resists bond fixation better than the same ring in the uncomplexed annulene species does. Schleyer *et al.* [32] using nucleus-independent chemical shifts (NICS) and ^1H NMR chemical shifts data, concluded that the aromaticity of the benzene ring in $(\eta^6\text{-C}_6\text{H}_6)\text{Cr}(\text{CO})_3$ is similar to that of the free benzene molecule. The authors found that NICS value computed in the centre of the benzene ring supports an increased aromatic character of the ring upon complexation, whereas the upfield ^1H NMR chemical shifts (and also ^{13}C NMR chemical shifts [9]) of the H atoms attached to the benzene ring by *ca.* 2 ppm and the positive value of the diamagnetic susceptibility exaltation point out the opposite conclusion [32]. In fact, Simion and Sorensen [33] ten years before concluded from diamagnetic susceptibility exaltation data that the benzene ring coordinated to the chromium tricarbonyl complex is antiaromatic. A similar opinion is held by Hubig *et al.* [25] who consider that the charge transfer from the arene to the transition metal in metal-arene coordination leads to a complete loss of the aromaticity of the π -system.

In this context, the aim of the present paper is to shed light on the controversial aromaticity of the benzene ring coordinated to the chromium tricarbonyl complex, a question that has been debated for about 40 years [34]. The evaluation of aromaticity is usually performed by analyzing its manifestations and this leads to the classical structural, magnetic, energetic, and reactivity-based measures of aromaticity [35,36]. At this point, we must note the important contribution by Katritzky-Krygowski and co-workers who found, by means of principal component analyses, that aromaticity is a multidimensional property and, as a consequence, aromatic compounds are better characterized using a set of indexes based on different physical properties [36–40]. Most aromaticity studies of PAHs coordinated to $\text{Cr}(\text{CO})_3$ have employed a single magnetic descriptor of aromaticity or a set of magnetic-based indices. Here we propose to use a set of indices that take into account structural, electronic, and magnetic manifestations of aromaticity.

Descriptors of aromaticity. As a structure-based measure, we have made use of the harmonic oscillator model of aromaticity (HOMA) index, defined in a landmark study by Kruszewski and Krygowski [41,42] as:

$$HOMA = 1 - \frac{\alpha}{n} \sum_{i=1}^n (R_{opt} - R_i)^2 \quad (1)$$

where n is the number of bonds considered, and α is an empirical constant (for C–C bonds $\alpha = 257.7$) fixed to give $HOMA = 0$ for a model nonaromatic system, and $HOMA = 1$ for a system with all bonds equal to an optimal value R_{opt} (1.388 Å for C–C bonds), assumed to be achieved for fully aromatic systems. R_i stands for a running bond length. This index has been found to be one of the most effective structural indicators of aromaticity [39,43].

Magnetic indices of aromaticity are based on the π -electron ring current that is induced when the system is exposed to external magnetic fields. In this work, we have used the NICS, proposed by Schleyer and co-workers [44–46], as a magnetic descriptor of aromaticity. It is defined as the negative value of the absolute shielding computed at a ring centre or at some other interesting point of the system. Rings with large negative NICS values are considered aromatic.

Three aromaticity criteria based on electron delocalization have been employed [47]. These indexes try to measure the cyclic electron delocalization of mobile electrons in aromatic rings. First, the *para*-delocalization index (PDI) [48,49], which is obtained using the delocalization index (DI) [50,51] as defined in the framework of the Atoms in Molecules (AIM) theory of Bader [52–54]. The PDI is an average of all DI of *para*-related carbon atoms in a given six-membered ring. The DI value between atoms A and B, $\delta(A,B)$, is obtained by double integration of the exchange-correlation density $\Gamma_{XC}(\vec{r}_1, \vec{r}_2)$ over the basins of atoms A and B, which are defined from the condition of zero-flux gradient in the one-electron density, $\rho(\mathbf{r})$ [52–54]:

$$\delta(A,B) = -2 \int_A \int_B \Gamma_{XC}(\vec{r}_1, \vec{r}_2) d\vec{r}_1 d\vec{r}_2 \quad (2)$$

For closed-shell monodeterminantal wavefunctions one obtains:

$$\delta(A,B) = 4 \sum_{i,j}^{N/2} S_{ij}(A) S_{ij}(B) \quad (3)$$

The summations in Eq. (3) run over all the $N/2$ occupied molecular orbitals. $S_{ij}(A)$ is the overlap of the molecular orbitals i and j within the basin of atom A. $\delta(A,B)$ provides a quantitative idea of the number of electron pairs delocalized or shared between atoms A and B. Previous works [48,49,55,56] have shown that for a series of planar and curved polycyclic aromatic hydrocarbons there is a satisfactory correlation between NICS, HOMA, and PDI.

As the second index based on electronic delocalization, we have used the aromatic fluctuation index (FLU) [57], which describes the fluctuation of electronic

charge between adjacent atoms in a given ring. The FLU index is based on the fact that aromaticity is related to the cyclic delocalized circulation of π electrons, and it is constructed by considering the amount of electron sharing between contiguous atoms, which should be substantial in aromatic molecules, and also by taking into account the similarity of electron sharing between adjacent atoms. It is defined as:

$$FLU = \frac{1}{n} \sum_{A-B}^{RING} \left[\left(\frac{V(B)}{V(A)} \right)^\alpha \left(\frac{\delta(A,B) - \delta_{ref}(A,B)}{\delta_{ref}(A,B)} \right) \right]^2 \quad (4)$$

with the sum running over all adjacent pairs of atoms around the ring, n being equal to the number of members in the ring, $\delta_{ref}(C,C) = 1.4$ (the $\delta(C,C)$ value in benzene at the HF/6-31G(d) level [57]), and $V(A)$ is the global delocalization of atom A given by:

$$V(A) = \sum_{B \neq A} \delta(A,B) \quad (5)$$

Finally, α is a simple function to make sure that the first term in Eq. (4) is always greater or equal to 1, so it takes the values:

$$\alpha = \begin{cases} 1 & V(B) > V(A) \\ -1 & V(B) \leq V(A) \end{cases} \quad (6)$$

Third, the Six Center Index (SCI), which is a class of multicenter index that provides another good measure of aromaticity [58,59]. For closed-shell monodeterminantal wavefunctions it reads:

$$SCI = \frac{16}{3} \sum_{\alpha} \sum_{i,j,k,l,m,n}^{N/2} \Gamma_{\alpha} [S_{ij}(A)S_{jk}(B)S_{kl}(C)S_{lm}(D)S_{mn}(E)S_{ni}(F)] \quad (7)$$

where Γ_{α} stands for a permutation operator which interchanges the atomic labels A, B, ..., F to generate up to 6! combinations. For the indexes used, we have that the more negative the NICS, the lower the FLU index, and the higher the HOMA, PDI, and SCI values, the more aromatic the rings are.

Computational details. All calculations have been performed with the Gaussian 03 [60] and AIMPAC [61] packages of programs, at the B3LYP level of theory [62–64] with the 6-31G(d,p) basis set [65–67]. All aromaticity criteria have also been evaluated at the same B3LYP/6-31G(d,p) level of theory.

The GIAO method [68] has been used to perform calculations of NICS at ring centres (NICS(0)) determined by the non-weighted mean of the heavy atoms coordinates and at several distances above and below the centre of the ring taken into analysis.

Calculation of atomic overlap matrices and computation of DI and SCI were performed with the AIMPAC [61] and ESI-3D [69] collection of programs. Calculation of these DIs with the density functional theory (DFT) cannot be performed exactly because the electron-pair density is not available at this level of theory [70]. As an approximation, we have used the Kohn-Sham orbitals obtained from a DFT calculation to compute Hartree-Fock-like DIs through Eq. (3), which does not account for electron correlation effects. In practice the values of the DIs obtained using this approximation are generally closer to the Hartree-Fock values than correlated DIs obtained with a configuration interaction method [70,71]. The numerical accuracy of the AIM calculations has been assessed using two criteria: i) The integration of the Laplacian of the electron density ($\nabla^2\rho(r)$) within an atomic basin must be close to zero; ii) The number of electrons in a molecule must be equal to the sum of all the electron populations of the molecule, and also equal to the sum of all the localization indices and half of the delocalization indices in the molecule. For all atomic calculations, integrated absolute values of $\nabla^2\rho(r)$ were always less than 0.001 a.u. For all molecules, errors in the calculated number of electrons were always less than 0.01 a.u.

RESULTS AND DISCUSSION

The B3LYP/6-31G(d,p) optimization of benzene leads to a C–C bond length of 1.397 Å not far from the experimental [72] and CCSD/TZ2P [73] results of 1.390 and 1.392 Å, respectively. The B3LYP/6-31G(d,p) optimized structure of ($\eta^6\text{-C}_6\text{H}_6$)Cr(CO)₃ in Figure 1 is also very close to that obtained experimentally by X-ray and neutron diffraction [74,75] and to that reported by previous theoretical calculations [19,32,76]. In the experimental and theoretical molecular structure, the Cr(CO)₃ group is placed staggered with respect to the C–H bonds of benzene to reduce steric repulsions. The average C–C bond length in benzene when coordinated to Cr(CO)₃ is 1.415 Å. Therefore, after coordination there is an expansion of the benzene ring corresponding to an average increase of the C–C bond length of 0.018 Å. Coordination also induces a bond length alternation (BLA) between short and long C–C bonds of 0.019 Å. The B3LYP/6-31G(d,p) distance from the Cr atom to the center of the ring is 1.720 Å (exp.: 1.724–1.726 Å) [74,75]. Interestingly, there is a significant pyramidalization of the C atoms measured from the $\angle\text{CCCH}$ dihedral angle of about 178° that leads to a benzyl hydrogen atoms slightly bent towards the Cr(CO)₃ fragment [19]. In particular, the H atoms are 0.033 Å (exp.: 0.03 Å [75]) displaced from the plane defined by the C atoms of the benzene ring. The calculated B3LYP/6-31G(d,p) binding energy of benzene in ($\eta^6\text{-C}_6\text{H}_6$)Cr(CO)₃ is 67.0 kcal·mol⁻¹, a value significantly larger than the experimental result of 53 kcal·mol⁻¹ [77]. We attribute the difference, in part, to the lack of basis set superposition error correction in our calculations, which is expected to reduce the computed binding energy by at least 7 kcal·mol⁻¹ as inferred from the calculations of Furet and Weber [76] using a similar basis set.

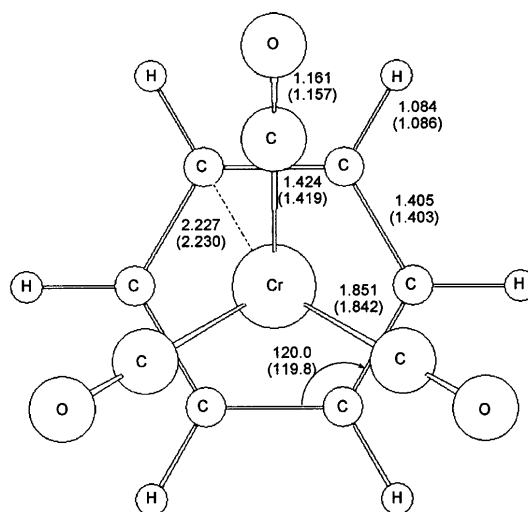


Figure 1. Most relevant optimized B3LYP/6-31G(d,p) and experimental [75] (in parentheses) bond lengths and angles of the $(\eta^6\text{-C}_6\text{H}_6)\text{Cr}(\text{CO})_3$ complex. Distances in Å and angles in degrees.

The nature of the bond between the arene and the metal in $(\eta^6\text{-arene})\text{tricarboxylchromium}$ complexes was discussed by Albright, Hoffmann, and coworkers some years ago [78]. These authors found that the interaction of the degenerate $2e$ LUMO and $2a_1$ LUMO+1 orbitals with the highest occupied π -orbitals of the arene with the appropriated symmetry is the dominant bonding mechanism [22]. Charge transfer from the highest occupied π -orbitals of the arene to the lowest unoccupied $2e$ and $2a_1$ orbitals of $\text{Cr}(\text{CO})_3$ partially breaks the C–C bonds, thus explaining the observed expansion of the aromatic ring and the increase in BLA in $(\eta^6\text{-C}_6\text{H}_6)\text{Cr}(\text{CO})_3$. The pyramidalization of the C atoms in the ring moves somewhat the π -electron density to the center of the benzene ring, thus favoring the interaction between the highest occupied π -orbitals of benzene and the unoccupied $2e$ and $2a_1$ orbitals of $\text{Cr}(\text{CO})_3$. The bonding mechanism in $(\eta^6\text{-arene})\text{tricarboxylchromium}$ complexes indicates that donation is larger than backdonation (as in carbenes [79]) and, as a consequence, the electron-rich arene is transformed into an electron-poor acceptor and a target for nucleophilic attacks [22]. The charge transfer from the benzene ring to the $\text{Cr}(\text{CO})_3$ fragment in the optimized $(\eta^6\text{-C}_6\text{H}_6)\text{Cr}(\text{CO})_3$ complex is 0.866 e (see Table 1) according to the generalized atomic polar tensor (GAPT) charges defined by Cioslowski [80].

Because of the loss of π electron density in the ring, one should expect a partially disruption of aromaticity in the benzene ring of $(\eta^6\text{-C}_6\text{H}_6)\text{Cr}(\text{CO})_3$ in comparison to free benzene, as discussed by Hubig *et al.* [25]. This is also something expected from the BLA and bond length elongation that the benzene ring experiences upon coordination [81,82]. Indeed, this is what most indicators of aromaticity used in the present work show. The HOMA of the benzene ring changes from 0.981 to 0.796 when going

from free to coordinated benzene. PDI and SCI also decrease in the same direction from 0.103 to 0.036 e and from 0.075 to 0.019 e, respectively. Finally, the FLU index slightly increases from 0.000 in isolated benzene to 0.009 in the benzene ring of the $(\eta^6\text{-C}_6\text{H}_6)\text{Cr}(\text{CO})_3$ complex. Thus, HOMA, PDI, FLU, and SCI indexes indicate the expected reduction of the aromaticity of the benzene ring upon complexation. Moreover, PDI, FLU, and SCI values in Table 1 show a steady reduction of aromaticity when the distance between the Cr atom and the benzene ring is reduced.

Table 1. PDI (electrons), FLU, SCI (electrons), and GAPT charge on the benzene ring (electrons) for the complex at different Cr–C₆H₆ distances (in Å)^{a,b}.

R(Cr–C ₆ H ₆) ^c	PDI	FLU	SCI	GAPT charge
1.22	0.019	0.019	0.009	1.035
1.42	0.022	0.014	0.012	0.997
1.62	0.031	0.010	0.017	0.917
1.72	0.036	0.009	0.019	0.866
1.82	0.044	0.007	0.024	0.812
2.02	0.059	0.005	0.033	0.699
2.22	0.073	0.003	0.042	0.579
2.42	0.085	0.002	0.051	0.451
2.62	0.093	0.001	0.059	0.321
2.82	0.097	0.001	0.064	0.207
3.02	0.101	0.001	0.067	0.124
3.22	0.102	0.001	0.070	0.073
3.42	0.103	0.000	0.071	0.040
3.62	0.103	0.000	0.073	0.025
3.82	0.103	0.000	0.073	0.017
4.02	0.103	0.000	0.074	0.012
4.22	0.103	0.000	0.074	0.011
4.42	0.103	0.000	0.074	0.011
4.62	0.103	0.000	0.075	0.009

^aFor comparison, the PDI, FLU, and SCI values for the free benzene are 0.103 e, 0.000, and 0.075 e at the B3LYP/6-31G(d,p) level of theory.

^bOnly the R(Cr–C₆H₆) is changed at each point. The rest of structural parameters are frozen to the values that they have in the B3LYP/6-31G(d,p) optimized structure of the $(\eta^6\text{-C}_6\text{H}_6)\text{Cr}(\text{CO})_3$ complex.

^cThe B3LYP/6-31G(d,p) optimized structure (see Figure 1) corresponds to R(Cr–C₆H₆) = 1.72 Å.

As reported by Schleyer and coworkers [46], we find that the magnetic-based NICS(0) index of benzene complexed to Cr(CO)₃ is much larger in absolute value than the NICS(0) of free benzene (–26.7 vs. –9.9 ppm), thus indicating an increase of

aromaticity when benzene is coordinated to $\text{Cr}(\text{CO})_3$, as claimed by Mitchell and co-workers [28–31]. Using NICS(1) similar results are obtained. We have also analyzed the out-of-plane component of the NICS(0), the $\text{NICS}(0)_{zz}$, which is considered to be a better NICS-based indicator of aromaticity [83,84]. In this case, we recover the expected result of a clear reduction of aromaticity when going from benzene ($\text{NICS}(0)_{zz} = -14.3$ ppm) to the $(\eta^6\text{-C}_6\text{H}_6)\text{Cr}(\text{CO})_3$ complex ($\text{NICS}(0)_{zz} = -7.4$ ppm). Thus, all analyzed indexes (including NICS_{zz} and NICS_π [46]) except NICS denote neither an increase of aromaticity [28–31] nor a constant aromaticity [32] but a clear decrease of the aromaticity of the benzene ring upon coordination. This result is not surprising if one takes into account the bonding mechanism of benzene to the $\text{Cr}(\text{CO})_3$ complex discussed above.

At this stage the reason for the breakdown of NICS in this particular species is unclear. In previous works [85,86], some of us showed that the failure of NICS to measure local aromaticity in π -stacked species is due to the coupling between magnetic fields coming from aromatic rings located above or below the analyzed ring. With this in mind, a possible hypothesis that may explain the breakdown of NICS to show a reduction of aromaticity of the benzene ring upon complexation is that the observed NICS reduction in the $(\eta^6\text{-C}_6\text{H}_6)\text{Cr}(\text{CO})_3$ complex does not correspond to a real aromaticity increase of the benzene ring but to the couplings between the induced magnetic fields of the $\text{Cr}(\text{CO})_3$ and benzene fragments. To check this hypothesis, we have summed the NICS profiles of the ground state of the optimized and isolated $\text{Cr}(\text{CO})_3$ and benzene species (see Figure 2) placing the benzene and $\text{Cr}(\text{CO})_3$ complex at the same ring–metal distance as that of the optimized $(\eta^6\text{-C}_6\text{H}_6)\text{Cr}(\text{CO})_3$ complex without further reoptimization of the two fragments. The NICS profile obtained together with that of the $(\eta^6\text{-C}_6\text{H}_6)\text{Cr}(\text{CO})_3$ complex are shown in Figure 3a. As can be seen, the $\text{NICS}(0)$ of the optimized $(\eta^6\text{-C}_6\text{H}_6)\text{Cr}(\text{CO})_3$ complex is much more negative than that corresponding to the sum of the C_6H_6 and $\text{Cr}(\text{CO})_3$ profiles. The latter sum of profiles simulates the NICS profile that results from the direct coupling of the induced magnetic fields generated by the unperturbed densities of the isolated C_6H_6 and $\text{Cr}(\text{CO})_3$ fragments brought together at the $R(\text{Cr}\text{--}\text{C}_6\text{H}_6) = 1.720$ Å distance. This means that there is a remarkable change of the NICS profile upon complexation that must be attributed to the formation of the chemical bond between benzene and $\text{Cr}(\text{CO})_3$ in the $(\eta^6\text{-C}_6\text{H}_6)\text{Cr}(\text{CO})_3$ complex. So, the observed change in NICS profile has to be mainly produced by the magnetic field generated by the electron pairs that participate most in the formation of the chemical bond between C_6H_6 and the metal. These electron pairs become more delocalized after bond formation and can contribute more to the total ring current and the induced magnetic field at a given point. This hypothesis is confirmed by the profiles that are obtained by increasing the $R(\text{Cr}\text{--}\text{C}_6\text{H}_6)$ with increments of 0.5 Å without reoptimization of the complex and the fragments. As can be seen in Figure 3, for a $R(\text{Cr}\text{--}\text{C}_6\text{H}_6) = 3.220$ Å (and also for larger distances) the NICS profile of the $(\eta^6\text{-C}_6\text{H}_6)\text{Cr}(\text{CO})_3$ complex and that corresponding to the sum of the isolated C_6H_6 and $\text{Cr}(\text{CO})_3$ fragments are almost the same. This is so, because at this distance the chemical bond is not formed. Indeed, the charge

transfer according to GAPT charges is only 0.07 e, so the interaction between the two fragments is residual. The small differences found in the two profiles at $R(\text{Cr}-\text{C}_6\text{H}_6) = 3.220 \text{ \AA}$ are basically due to the different geometries of the C_6H_6 system. For the NICS profile of the $(\eta^6\text{-C}_6\text{H}_6)\text{Cr}(\text{CO})_3$ complex, we took the geometry of the C_6H_6 in the complex which differs from the equilibrium geometry because, as said before, the ring expands and undergoes BLA upon complexation. Because of the geometry differences, the NICS profile of the deformed benzene differs from that of the isolated benzene molecule, the former showing as expected a somewhat smaller aromatic character.

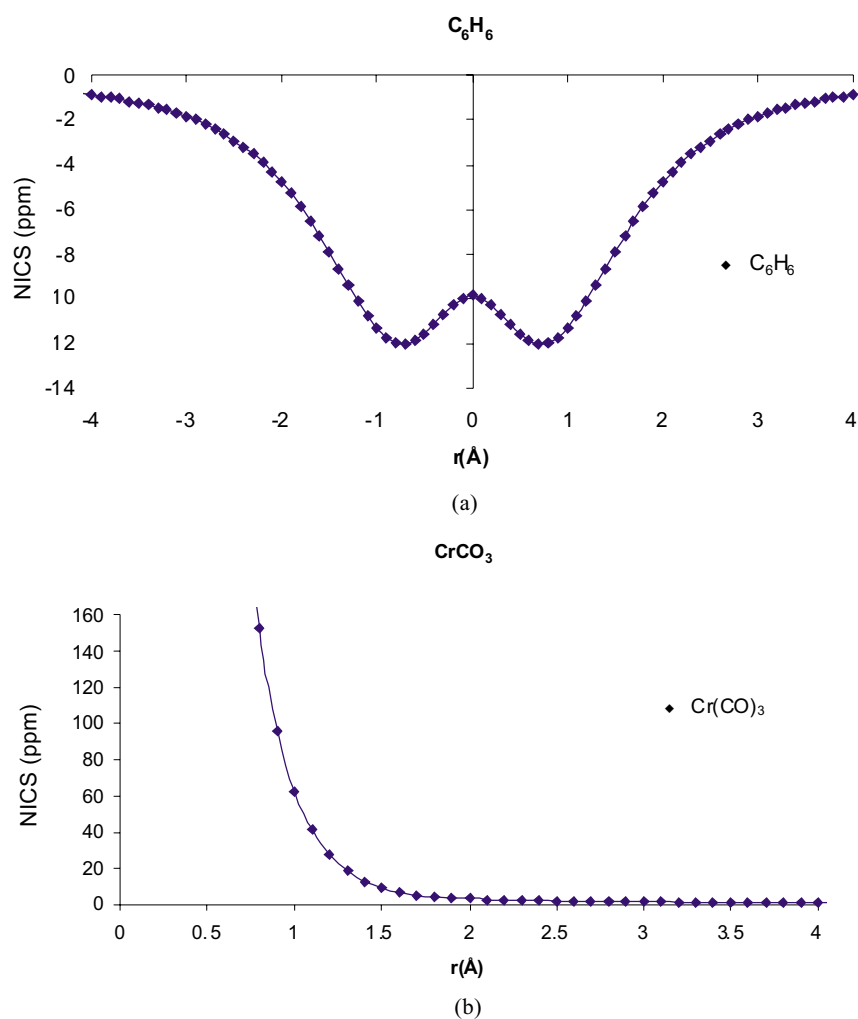


Figure 2. B3LYP/6-31G(d,p) NICS profiles (in ppm) of the isolated and optimized (a) benzene and (b) $\text{Cr}(\text{CO})_3$ complex. The benzene profile starts at the ring centre and moves in the direction perpendicular to the plane defined by the ring. The $\text{Cr}(\text{CO})_3$ profile starts at the Cr atom and moves in the direction away from the $\text{Cr}(\text{CO})_3$ complex along the C_3 axis.

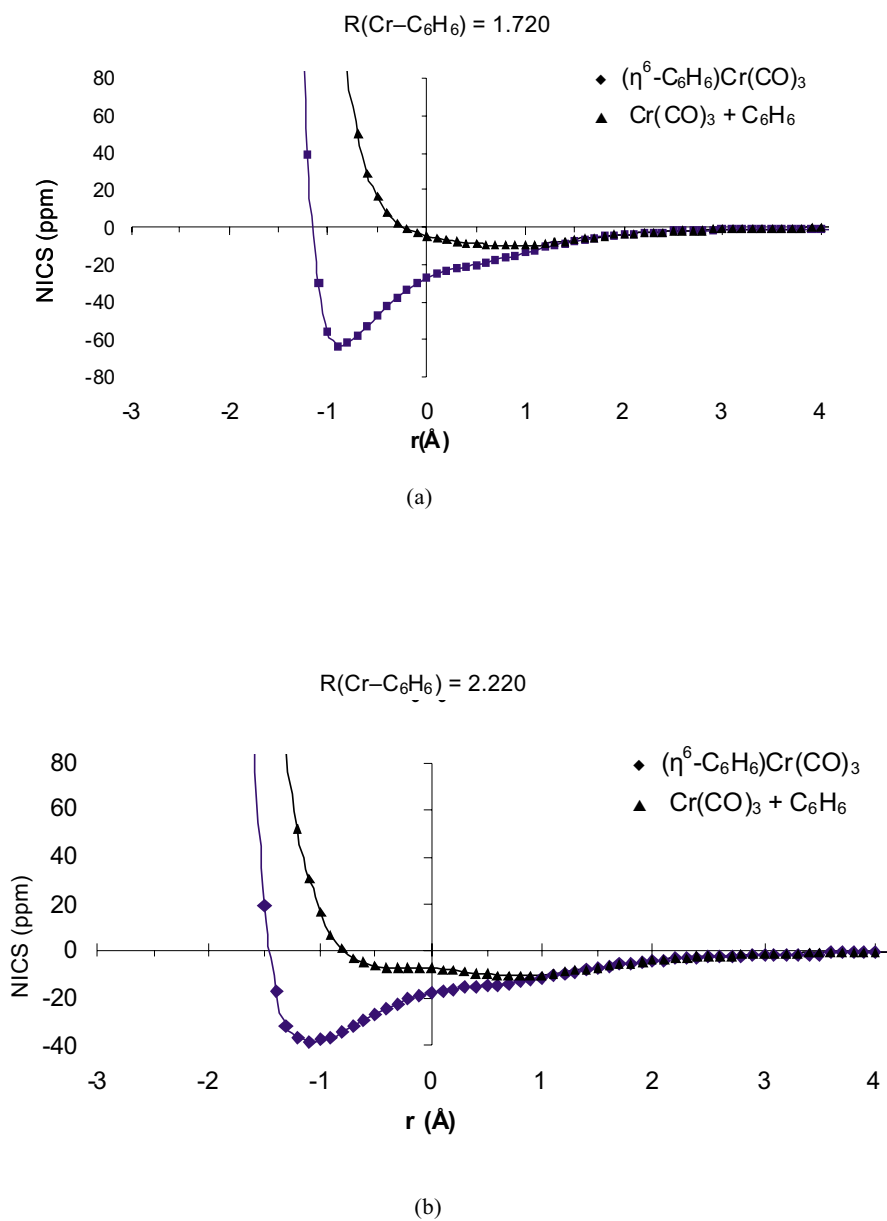


Figure 3. Comparison between the B3LYP/6-31G(d,p) NICS profiles (in ppm) of the $(\eta^6\text{-C}_6\text{H}_6)\text{Cr}(\text{CO})_3$ complex and the sum of the NICS profiles of the isolated and optimized benzene and $\text{Cr}(\text{CO})_3$ complex for different $\text{Cr}-\text{C}_6\text{H}_6$ distances (in Å). Positive (negative) r values correspond to points located in the C_3 axis at a distance r from the ring centre away from (towards) the $\text{Cr}(\text{CO})_3$ complex.

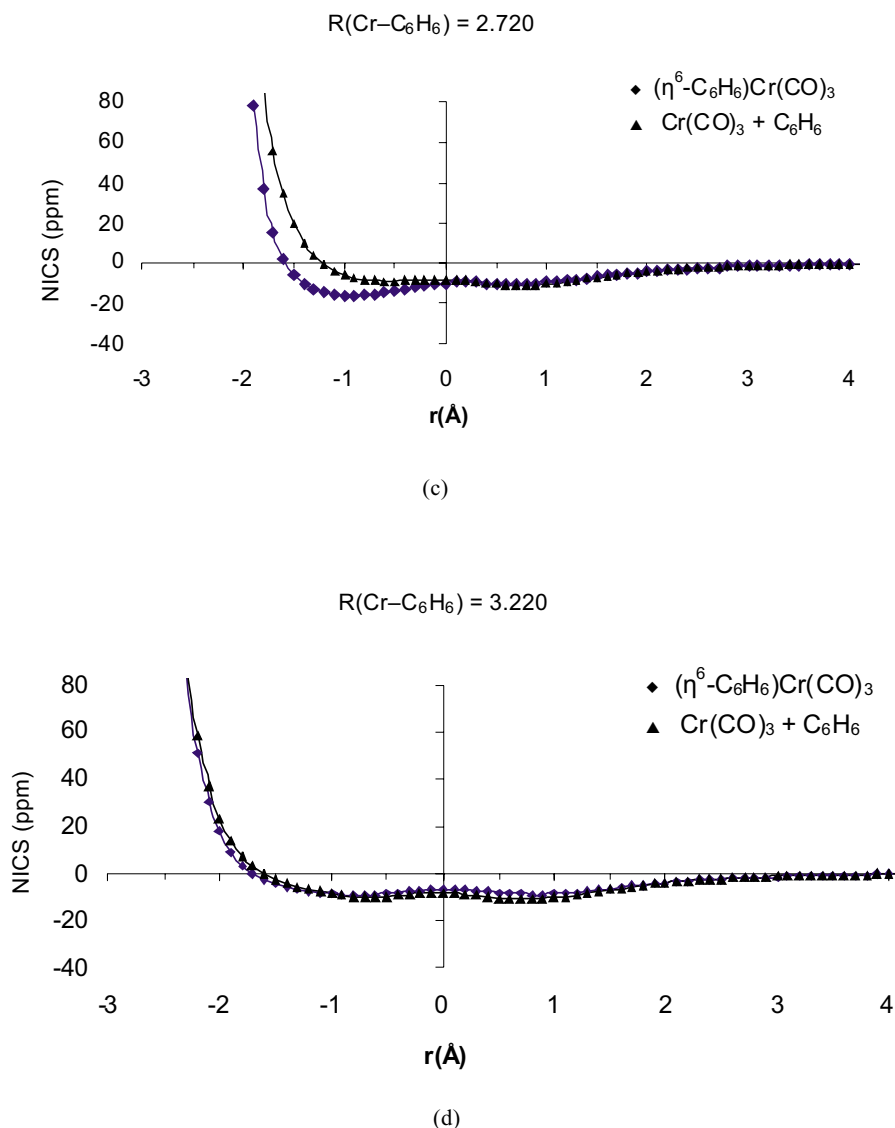


Figure 3. Continuation

Finally, we have represented in Figure 4, the NICS surface obtained by changing both the $R(\text{Cr}-\text{C}_6\text{H}_6)$ distance and the distance r from the center of the ring to a given point located at the C_3 axis of the $(\eta^6-\text{C}_6\text{H}_6)\text{Cr}(\text{CO})_3$ complex, using for benzene and $\text{Cr}(\text{CO})_3$ the same geometries as those of the equilibrium structure of the complex. The horizontal lines shown in Figure 4 generate NICS(0), NICS(1), and NICS(-1) profiles for different $R(\text{Cr}-\text{C}_6\text{H}_6)$ distances. As can be seen in Figure 4, both NICS(0) and NICS(-1) decrease steadily when going from long to short $R(\text{Cr}-\text{C}_6\text{H}_6)$ distances starting from *ca.* 4 Å, thus indicating an increased aromaticity character of the ring

which, as shown before, is not real but due to bond formation. The vertical dashed line provides a NICS profile, as those depicted in Figure 3, for a given $R(\text{Cr}-\text{C}_6\text{H}_6)$ distance (in the particular case of Figure 4, $R(\text{Cr}-\text{C}_6\text{H}_6) = 1.720 \text{ \AA}$). It is noteworthy that for $R(\text{Cr}-\text{C}_6\text{H}_6)$ distances of about 3 \AA (small vertical solid line in Figure 4) or larger, one gets NICS profiles with a clear double-well profile similar to that found for the isolated benzene molecule (see Figure 2a) with a local maximum of NICS at the ring center and minima located slightly above and below 1 \AA from the ring center in the direction perpendicular to the molecular plane. For large $R(\text{Cr}-\text{C}_6\text{H}_6)$

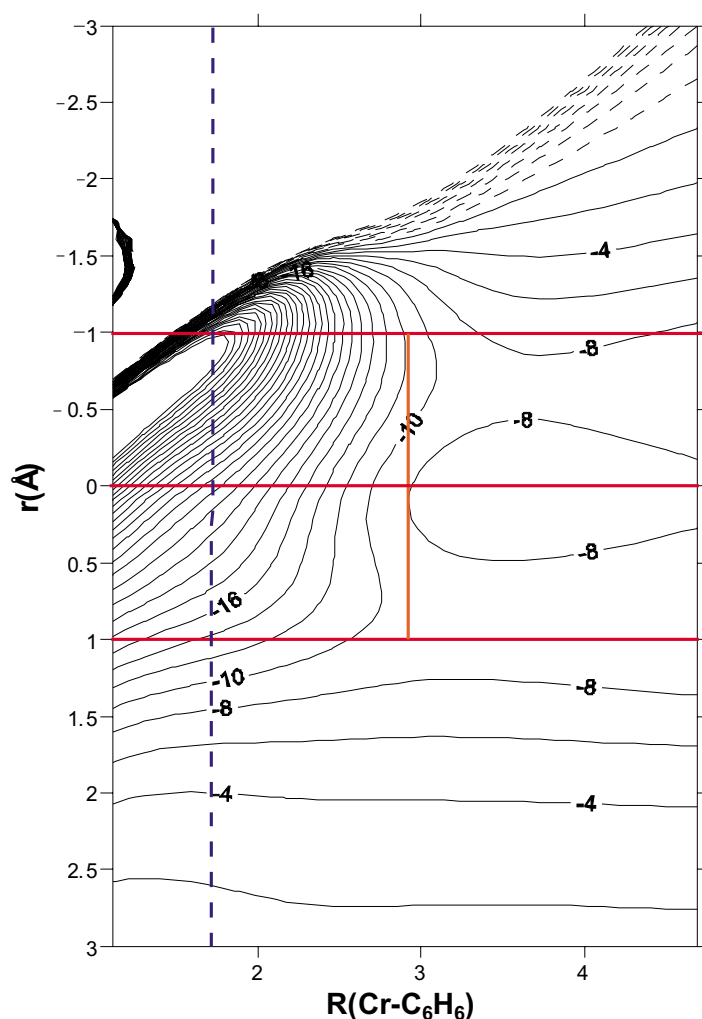


Figure 4. B3LYP/6-31G(d,p) NICS surface (in ppm) of the $(\eta^6\text{-C}_6\text{H}_6)\text{Cr}(\text{CO})_3$ complex. Positive (negative) r values correspond to points located in the C_3 axis at a distance r from the ring centre away from (towards) the $\text{Cr}(\text{CO})_3$ complex. The geometry of the $(\eta^6\text{-C}_6\text{H}_6)\text{Cr}(\text{CO})_3$ complex is kept unchanged and only the $\text{Cr}-\text{C}_6\text{H}_6$ distances are varied from approximately 1 to 5 \AA .

distances, the bond between benzene and the $\text{Cr}(\text{CO})_3$ group is not formed and thus the NICS profiles of the $(\eta^6\text{-C}_6\text{H}_6)\text{Cr}(\text{CO})_3$ complex keep almost invariant.

CONCLUSIONS

In this work, we have analyzed the controversial aromaticity of the benzene ring coordinated to the $\text{Cr}(\text{CO})_3$ complex. We have shown that a geometric descriptor like HOMA, a magnetic index like NICS_{zz} , and several electronic measures of aromaticity such as PDI, FLU, and SCI, indicate that there is a clear reduction of aromaticity of the benzene ring upon complexation as expected from the bonding mechanism. In our opinion, the result obtained with these five indexes is clear and should end the debate about the aromaticity of the benzene ring in the $(\eta^6\text{-C}_6\text{H}_6)\text{Cr}(\text{CO})_3$ complex. Somewhat surprisingly, the NICS index erroneously denotes a larger aromaticity of the benzene ring in the $(\eta^6\text{-C}_6\text{H}_6)\text{Cr}(\text{CO})_3$ complex than in benzene itself. We have analyzed the reason for this failure of the NICS index and we have concluded that the extra delocalization gained by the electron pairs that contribute the most to the chemical bond explains the reduction of the NICS value. Therefore, the NICS reduction is not the result of a larger aromaticity but the result of increased ring currents due to bond formation. This result suggests exercising caution in the use of single-point NICS or NICS scans as a quantitative measure of aromaticity for aromatic rings in transition metal complexes. Finally, it is worth noting that NICS_{zz} is a more reliable index of aromaticity for this particular system.

Acknowledgments

Financial help has been furnished by the Spanish Ministerio de Educación y Ciencia (MEC) project No. CTQ2005-08797-C02-01/BQU and by the Catalan Departament d'Universitats, Recerca i Societat de la Informació (DURSI) of the Generalitat de Catalunya project No. 2005SGR-00238. F.F. and E.M. thank the MEC for the doctoral fellowships no. AP2005-2997 and AP2002-0581, respectively. JOCJH thanks the DURSI for financial support through the grant 2005FI/00451. J.P. also acknowledges the European Union for a Marie Curie fellowship. We also thank the Centre de Supercomputació de Catalunya (CESCA) for partial funding of computer time.

Dedication

This work is dedicated to Prof. Tadeusz Marek Krygowski as a proof of our admiration for his brilliant contributions to chemistry.

REFERENCES

1. Mann B.E., *Chem. Soc. Rev.*, **15**, 167 (1986).
2. Dötz K.H. and Stendel J., Jr., *Modern Arene Chemistry*, Astruc D. (ed), Wiley-VCH, Weinheim, p. 250 (2002).
3. Dötz K.H., Szesni N., Nieger M. and Nattinen K., *J. Organomet. Chem.*, **672**, 58 (2003).
4. Dötz K.H. and Jahr H.C., *Chem. Rec.*, **4**, 61 (2004).
5. Dötz K.H., Wenzel B. and Jahr H.C., *Top. Curr. Chem.*, **248**, 63 (2004).
6. Jahr H.C., Nieger M. and Dötz K.H., *Chem. Eur. J.*, **11**, 5333 (2005).
7. Künding E.P., Desobry V., Grivet C., Rudolph B. and Spichiger S., *Organometallics*, **6**, 1173 (1987).
8. Dötz K.H., Stinner C. and Nieger M., *J. Chem. Soc., Chem. Commun.*, 2535 (1995).

9. Oprunenko Y.F., Akhmedov N.G., Laikov D.N., Malyugina S.G., Mstislavsky V.I., Roznyatovsky V.A., Ustynyuk Y.A. and Ustynyuk N.A., *J. Organomet. Chem.*, **583**, 136 (1999).
10. Jahr H.C., Nieger M. and Dötz K.H., *Chem. Commun.*, 2866 (2003).
11. Pan J., Kampf J.W. and Ashe III A.J., *Organometallics*, **25**, 197 (2006).
12. Akhmedov N.G., Malyugina S.G., Mstislavsky V.I., Oprunenko Y.F., Roznyatovsky V.A., Batsanov A.S. and Ustynyuk N.A., *Organometallics*, **17**, 4607 (1998).
13. Merlic C.A., Walsh J.C., Tantillo D.J. and Houk K.N., *J. Am. Chem. Soc.*, **121**, 3596 (1999).
14. Oprunenko Y., Gloriosov I., Lyssenko K., Malyugina S., Mityuk D., Mstislavsky V., Günter H., von Firks G. and Ebener M., *J. Organomet. Chem.*, **656**, 27 (2002).
15. Dötz K.H., Stendel J., Jr., Müller S., Nieger M., Ketrat S. and Dolg M., *Organometallics*, **24**, 3219 (2005).
16. Stoddart M.W., Brownie J.H., Baird M.C. and Schmider H.L., *J. Organomet. Chem.*, **690**, 3440 (2005).
17. Pan J., Wang J., Banaszak Holl M.M., Kampf J.W. and Ashe III A.J., *Organometallics*, **25**, 3463 (2006).
18. Nambu M. and Siegel J.S., *J. Am. Chem. Soc.*, **110**, 3675 (1988).
19. Low A.A. and Hall M.B., *Int. J. Quantum Chem.*, **77**, 152 (2000).
20. Baldridge K.K. and Siegel J.S., *J. Phys. Chem.*, **100**, 6111 (1996).
21. Elaiss A., Mahieu J., Brocard J., Surpateanu G. and Vergoten G., *J. Mol. Struct. (Theochem)*, **475**, 261 (1999).
22. Arrais A., Diana E., Gervasio G., Gobetto R., Marabello D. and Stanghellini P.L., *Eur. J. Inorg. Chem.*, 1505 (2004).
23. Own Z.Y., Wang S.M., Chung J.F., Miller D.W. and Fu P.P., *Inorg. Chem.*, **32**, 152 (1993).
24. Güell M., Poater J., Luis J.M., Mó O., Yáñez M. and Solà M., *ChemPhysChem*, **6**, 2552 (2005).
25. Hubig S.M., Lindeman S.V. and Kochi J.K., *Coord. Chem. Rev.*, **200–202**, 831 (2006).
26. Merlic C.A., Zechman A.L. and Miller M.M., *J. Am. Chem. Soc.*, **123**, 11101 (2001).
27. Suresh C.H., Koga N. and Gadre S.R., *Organometallics*, **19**, 3008 (2000).
28. Mitchell R.H., Zhou P., Venugopalan S. and Dingle T.W., *J. Am. Chem. Soc.*, **112**, 7812 (1990).
29. Mitchell R.H., Chen Y., Khalifa N. and Zhou P., *J. Am. Chem. Soc.*, **120**, 1785 (1998).
30. Mitchell R.H., *Chem. Rev.*, **101**, 1301 (2001).
31. Mitchell R.H., Brkic Z., Berg D.J. and Barclay T.M., *J. Am. Chem. Soc.*, **124**, 11983 (2002).
32. Schleyer P.v.R., Kiran B., Simion D.V. and Sorensen T.S., *J. Am. Chem. Soc.*, **122**, 510 (2000).
33. Simion D.V. and Sorensen T.S., *J. Am. Chem. Soc.*, **118**, 7345 (1996).
34. Price J.T. and Sorensen T.S., *Can. J. Chem.*, **46**, 515 (1968).
35. Krygowski T.M., Cyrański M.K., Czarnocki Z., Häfelinger G. and Katritzky A.R., *Tetrahedron*, **56**, 1783 (2000).
36. Katritzky A.R., Jug K. and Oniciu D.C., *Chem. Rev.*, **101**, 1421 (2001).
37. Katritzky A.R., Barczynski P., Musumarra G., Pisano D. and Szafran M., *J. Am. Chem. Soc.*, **111**, 7 (1989).
38. Katritzky A.R., Karelson M., Sild S., Krygowski T.M. and Jug K., *J. Org. Chem.*, **63**, 5228 (1998).
39. Krygowski T.M. and Cyrański M.K., *Chem. Rev.*, **101**, 1385 (2001).
40. Cyrański M.K., Krygowski T.M., Katritzky A.R. and Schleyer P.v.R., *J. Org. Chem.*, **67**, 1333 (2002).
41. Kruszewski J. and Krygowski T.M., *Tetrahedron Lett.*, **13**, 3839 (1972).
42. Krygowski T.M., *J. Chem. Inf. Comp. Sci.*, **33**, 70 (1993).
43. Schleyer P.v.R., *Chem. Rev.*, **101**, 1115 (2001).
44. Schleyer P.v.R. and Jiao H., *Pure Appl. Chem.*, **68**, 209 (1996).
45. Schleyer P.v.R., Maerker C., Dransfeld A., Jiao H. and van Eikema Hommes N.J.R., *J. Am. Chem. Soc.*, **118**, 6317 (1996).
46. NICS_π is the NICS obtained using only ring currents from π-electrons. Chen Z., Wannere C.S., Corminboeuf C., Puchta R. and Schleyer P.v.R., *Chem. Rev.*, **105**, 3842 (2005).
47. Poater J., Duran M., Solà M. and Silvi B., *Chem. Rev.*, **105**, 3911 (2005).
48. Poater J., Fradera X., Duran M. and Solà M., *Chem. Eur. J.*, **9**, 400 (2003).
49. Poater J., Fradera X., Duran M. and Solà M., *Chem. Eur. J.*, **9**, 1113 (2003).
50. Fradera X., Austen M.A. and Bader R.F.W., *J. Phys. Chem. A*, **103**, 304 (1999).
51. Fradera X., Poater J., Simon S., Duran M. and Solà M., *Theor. Chem. Acc.*, **108**, 214 (2002).
52. Bader R.F.W., *Atoms in Molecules: A Quantum Theory*. Clarendon, Oxford (1990).
53. Bader R.F.W., *Acc. Chem. Res.*, **18**, 9 (1985).

54. Bader R.F.W., *Chem. Rev.*, **91**, 893 (1991).
55. Portella G., Poater J., Bofill J.M., Alemany P. and Solà M., *J. Org. Chem.*, **70**, 2509 (2005); erratum, *ibid.*, **70**, 4560 (2005).
56. Portella G., Poater J. and Solà M., *J. Phys. Org. Chem.*, **18**, 785 (2005).
57. Matito E., Duran M. and Solà M., *J. Chem. Phys.*, **122**, 014109 (2005); erratum, *ibid.*, **125**, 059901 (2006).
58. Bultinck P., Ponec R. and Van Damme S., *J. Phys. Org. Chem.*, **18**, 706 (2005).
59. Bultinck P., Rafat M., Ponec R., van Gheluwe B., Carbó-Dorca R. and Popelier P., *J. Phys. Chem. A*, **110**, 7642 (2006).
60. Frisch M.J., Trucks G.W., Schlegel H.B., Scuseria G.E., Robb M.A., Cheeseman J.R., Montgomery Jr. J.A., Vreven T., Kudin K.N., Burant J.C., Millam J.M., Iyengar S.S., Tomasi J., Barone V., Mennucci B., Cossi M., Scalmani G., Rega N., Petersson G.A., Nakatsuji H., Hada M., Ehara M., Toyota K., Fukuda R., Hasegawa J., Ishida M., Nakajima T., Honda Y., Kitao O., Nakai H., Klene M., Li X., Knox J.E., Hratchian H.P., Cross J.B., Bakken V., Adamo C., Jaramillo J., Gomperts R., Stratmann R.E., Yazyev O., Austin A.J., Cammi R., Pomelli C., Ochterski J.W., Ayala P.Y., Morokuma K., Voth G.A., Salvador P., Dannenberg J.J., Zakrzewski G., Dapprich S., Daniels A.D., Strain M.C., Farkas O., Malick D.K., Rabuck A.D., Raghavachari K., Foresman J.B., Ortiz J.V., Cui Q., Baboul A.G., Clifford S., Cioslowski J., Stefanov B.B., Liu G., Liashenko A., Piskorz P., Komaromi I., Martin R.L., Fox D.J., Keith T., Al-Laham M.A., Peng C.Y., Nanayakkara A., Challacombe M., Gill P.M.W., Johnson B., Chen W., Wong M.W., Gonzalez C. and Pople J.A., Gaussian 03, Revision C.01. Gaussian, Inc., Pittsburgh, PA (2003).
61. Biegler-König F.W., Bader R.F.W. and Tang T.-H., *J. Comput. Chem.*, **3**, 317 (1982).
62. Becke A.D., *J. Chem. Phys.*, **98**, 5648 (1993).
63. Lee C., Yang W. and Parr R.G., *Phys. Rev. B*, **37**, 785 (1988).
64. Stephens P.J., Devlin F.J., Chabalowski C.F. and Frisch M.J., *J. Phys. Chem.*, **98**, 11623 (1994).
65. Hehre W.J., Ditchfield R. and Pople J.A., *J. Chem. Phys.*, **56**, 2257 (1972).
66. Hariharan P.C. and Pople J.A., *Theor. Chim. Acta*, **28**, 213 (1973).
67. Franci M.M., Pietro W.J., Hehre W.J., Binkley J.S., Gordon M.S., Defrees D.J. and Pople J.A., *J. Chem. Phys.*, **77**, 3654 (1982).
68. Wolinski K., Hilton J.F. and Pulay P., *J. Am. Chem. Soc.*, **112**, 8251 (1990).
69. Matito E., ESI-3D: Electron Sharing Indexes Program for 3D Molecular Space Partitioning. <http://iqc.udg.es/~eduard/ESI>. Girona, IQC (2006).
70. Poater J., Solà M., Duran M. and Fradera X., *Theor. Chem. Acc.*, **107**, 362 (2002).
71. Matito E., Solà M., Salvador P. and Duran M., *Faraday Discuss.*, **135**, 325 (2007).
72. Jeffrey G.A., Ruble J.R., McMullan R.K. and Pople J.A., *Proc. R. Soc. London A*, **414**, 47 (1987).
73. Christiansen O., Stanton J.F. and Gauss J., *J. Chem. Phys.*, **108**, 3987 (1998).
74. Bailey M.F. and Dahl L.F., *Inorg. Chem.*, **4**, 1314 (1965).
75. Rees B. and Coppens P., *Acta Cryst.*, **B29**, 2516 (1973).
76. Furet E. and Weber J., *Theor. Chim. Acta*, **91**, 157 (1995).
77. Mukerjee S.L., Lang R.F., Ju T., Kiss G., Hoff C.D. and Nolan S.P., *Inorg. Chem.*, **31**, 4885 (1992).
78. Albright T.A., Hofmann P., Hoffmann R., Lillya C.P. and Dobosh P.A., *J. Am. Chem. Soc.*, **105**, 3396 (1983).
79. Cases M., Frenking G., Duran M. and Solà M., *Organometallics*, **21**, 4182 (2002).
80. Cioslowski J., *J. Am. Chem. Soc.*, **111**, 8333 (1989).
81. Cyrański M.K. and Krygowski T.M., *Tetrahedron*, **55**, 6205 (1999).
82. Feixas F., Matito E., Poater J. and Solà M., *J. Phys. Chem. A*, submitted for publication (2007).
83. Corminboeuf C., Heine T., Seifert G., Schleyer P.v.R. and Weber J., *Phys. Chem. Chem. Phys.*, **6**, 273 (2004).
84. Fallah-Bagher-Shaidaei H., Wannere C.S., Corminboeuf C., Puchta R. and Schleyer P.v.R., *Org. Lett.*, **8**, 863 (2006).
85. Poater J., Bofill J.M., Alemany P. and Solà M., *J. Org. Chem.*, **71**, 1700 (2006).
86. Osuna S., Poater J., Bofill J.M., Alemany P. and Solà M., *Chem. Phys. Lett.*, **428**, 191 (2006).

6.4 On the Performance of Some Aromaticity Indices: A Critical Assessment Using a Test Set

Feixas, F.; Matito, E.; Poater, J.; Solà, M.; *J. Comput. Chem.* 29, 1543-1554, **2008**

Ferran Feixas, Eduard Matito, Jordi Poater, Miquel Solà. "On the performance of some aromaticity indices: a critical assessment using a test set". *Journal of computational chemistry*. Vol. 29, issue 10 (30 July 2008) : p. 1543-1554

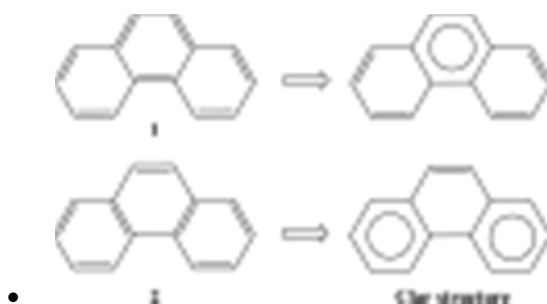
<http://dx.doi.org/10.1002/jcc.20914>

<http://onlinelibrary.wiley.com/doi/10.1002/jcc.20914/abstract>

Article first published online: 12 FEB 2008

Abstract

Aromaticity is a central chemical concept widely used in modern chemistry for the interpretation of molecular structure, stability, reactivity, and magnetic properties of many compounds. As such, its reliable prediction is an important task of computational chemistry. In recent years, many methods to quantify aromaticity based on different physicochemical properties of molecules have been proposed. However, the nonobservable nature of aromaticity makes difficult to assess the performance of the numerous existing indices. In the present work, we introduce a series of fifteen aromaticity tests that can be used to analyze the advantages and drawbacks of a group of aromaticity descriptors. On the basis of the results obtained for a set of ten indicators of aromaticity, we conclude that indices based on the study of electron delocalization in aromatic species are the most accurate among those examined in this work.



6.5 A Test to Evaluate the Performance of Aromaticity Descriptors in All-Metal and Semimetal Clusters. An Appraisal of Electronic and Magnetic Indicators of Aromaticity

Feixas, F.; Jiménez-Halla, J.O.C.; Matito, E.; Poater, J.; Solà M.; *J. Chem. Theory Comput.* 6, 1118-1130, 2010

Ferran Feixas, J. Oscar C. Jiménez-Halla, Eduard Matito, Jordi Poater and Miquel Solà. "A Test to Evaluate the Performance of Aromaticity Descriptors in All-Metal and Semimetal Clusters. An Appraisal of Electronic and Magnetic Indicators of Aromaticity". *Journal of chemical theory and computation*. Vol. 6, issue 4 (13 April 2010) : p. 1118-1130

<http://pubs.acs.org/doi/abs/10.1021/ct100034p>

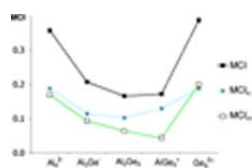
<http://dx.doi.org/10.1021/ct100034p>

Publication Date (Web): March 18, 2010 (Article)

DOI: 10.1021/ct100034p

Abstract

As compared to classical organic aromatic compounds, the evaluation of aromaticity in all-metal and semimetal clusters is much more complex. For a series of these clusters, it is frequently found that different methods used to discuss aromaticity lead to divergent conclusions. For this reason, there is a need to evaluate the reliability of the different descriptors of aromaticity to provide correct trends in all-metal and semimetal aromatic clusters. This work represents the first attempt to assess the performance of aromaticity descriptors in all-metal clusters. To this end, we introduce the series of all-metal and semimetal clusters $[X_nY_{4-n}]^{q\pm}$ (X, Y = Al, Ga, Si, and Ge; $n = 0-4$) and $[X_nY_{5-n}]^{4-n}$ (X = P and Y = S and Se; $n = 0-5$) with predictable aromaticity trends. Aromaticity, in these series, is quantified by means of nucleus-independent chemical shifts (NICS) and electronic multicenter indices (MCI). Results show that the expected trends are generally better reproduced by MCI than by NICS. It is found that NICS(0) _{π} is the kind of NICS that performs better among the different NICS indices analyzed.



Chapter 7

Applications III: Study of electron delocalization in organic/inorganic compounds

7.1 Analysis of Hückel's $[4n+2]$ Rule through Electronic Delocalization Measures

Feixas, F.; Matito, E.; Solà, M.; Poater, J.; *J. Phys. Chem. A* 112 13231-13238, 2008 special issue: Sason Shaik Festschrift.

Ferran Feixas, Eduard Matito, Miquel Solà and Jordi Poater. “Analysis of Hückel’s $[4n + 2]$ rule through electronic delocalization measures”. *Journal of physical chemistry A*. Vol. 112, issue 50 (18 December 2008) : p. 13231-13238

<http://pubs.acs.org/doi/full/10.1021/jp803745f>

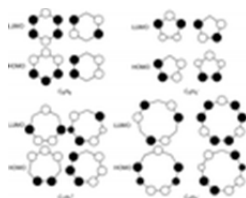
<http://dx.doi.org/10.1021/jp803745f>

Publication Date (Web): October 4, 2008 (Article)

DOI: 10.1021/jp803745f

Abstract

In the present work, we analyze the π -electronic delocalization in a series of annulenes and their dications and dianions by using electron delocalization indices calculated in the framework of the quantum theory of atoms in molecules. The aim of our study is to discuss the Hückel’s $4n + 2$ rule from the viewpoint of π -electronic delocalization. Our results show that there is an important increase of electronic delocalization (of about 1 e) when going from antiaromatic $4n\pi$ systems to aromatic $(4n + 2)\pi$ systems. Less clear is the change in π -electronic delocalization when we move from a $(4n + 2)\pi$ -aromatic to a $4n\pi$ -antiaromatic species by adding or removing a pair of electrons.



7.2 Patterns of π -electron Delocalization in Aromatic and Antiaromatic Organic Compounds in the Light of Hückel's $[4n + 2]$

Feixas, F.; Matito, E.; Solà, M.; Poater, J.; *Phys. Chem. Chem. Phys.* 12, 7126-7137, 2010

Patterns of π -electron delocalization in aromatic and antiaromatic organic compounds in the light of Hückel's $4n + 2$ rule†

Ferran Feixas,^a Eduard Matito,^b Miquel Solà^{*a} and Jordi Poater^{*a}

Received 26th November 2009, Accepted 8th March 2010

First published as an Advance Article on the web 18th May 2010

DOI: 10.1039/b924972a

The total π -electron delocalization of a series of classical aromatic and antiaromatic organic compounds is separated into *ortho* (1,2), *meta* (1,3), *para* (1,4), and successive contributions (the so-called delocalization crossed terms) and the changes that take place in these crossed terms when two electrons are added or removed are analyzed. Our results show that these changes follow a similar alternation pattern in all cases. The patterns found represent a kind of electronic footprints that makes it possible to discern between aromatic and antiaromatic systems.

Introduction

Hückel's $4n + 2$ rule formulated in 1931¹ represents one of the first and most successful approaches to rationalize aromaticity from a theoretical point of view. Using Hückel's molecular orbital (HMO) theory, the aromatic sextet (introduced some years before by Crocker²) was interpreted by Hückel as a closed shell that provides extra stability, similar to the situation found in noble gas elements. Then, according to this rule, a monocyclic system with $(4n + 2)\pi$ -electrons is aromatic, whereas a system with $4n\pi$ -electrons is antiaromatic. The preparation of the cycloheptatrienyl cation, $C_7H_7^+$, by Doering and Knox in 1954³ is considered as the first experimental verification of Hückel's rule.⁴ Very recently, Mayer has given a theoretical derivation for Hückel's rule.⁵ Although the original derivation of Hückel's rule is only strictly valid for monocyclic conjugated systems, this rule was extended to polycyclic aromatic hydrocarbons (PAHs) by Glidewell and Lloyd⁶ as follows: in PAHs, the total π -electron population tends to form the smallest $4n + 2$ groups of π -electrons and to avoid formation of the smallest $4n$ groups. A further development of Hückel's $4n + 2$ rule came when Baird showed, using perturbational molecular orbital theory, that annulenes which are aromatic in their singlet ground state are antiaromatic in their lowest-lying triplet state and *vice versa* for annulenes that are antiaromatic in the ground state.⁷ The identification⁸ of the planar triplet ground states of $C_5H_5^+$ and $C_5Cl_5^+$ as well as a recent photoelectron spectroscopic study⁹ of the first singlet and triplet states of $C_5H_5^+$ provided experimental support for

Baird's extension of Hückel's $4n + 2$ rule. There is also an analogous to Hückel's rule for magnetic susceptibility.¹⁰ More recently, the $2(n + 1)^2$ rule of aromaticity¹¹ for spherical compounds has been considered the spherical analog of the $4n + 2$ rule for the cyclic annulenes. Interestingly, the number of conjugated circuits of $4n + 2$ and $4n$ types has been taken by Randić¹² and Trinajstić¹³ as a measure of aromaticity. Finally, it is worth noting that Hückel's $4n + 2$ rule is applied nowadays in many studies to discuss multifold aromaticity and antiaromaticity in all-metal clusters.¹⁴

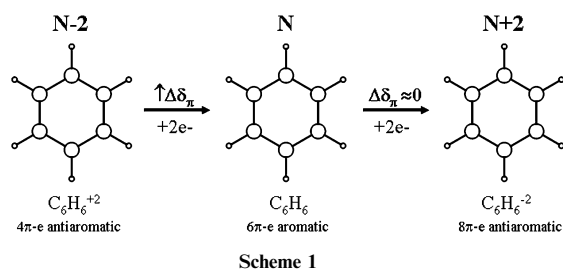
From a theoretical point of view, resonance energy and ring current calculations of annulenes provided preliminary evidence for the reliability of Hückel's $4n + 2$ rule.¹⁵ Later on the validity of Hückel's and Baird's rules was proved through nucleus independent chemical shifts (NICS) and aromatic stabilization energy (ASE) calculations by Schleyer *et al.*¹⁶ as well as from the study of ring currents.¹⁷ Moreover, the study of ring currents in $4n\pi$ -electron monocycles¹⁸ and a recent theoretical work¹⁹ based on the analysis of the bifurcation in the π -contribution to the electron localization function (ELF) for the lowest-lying triplet state of $4n\pi$ -electrons monocycles confirmed the validity of the Baird's rule.

One of the key features of classical aromatic organic molecules is their π -electron delocalization. This electronic delocalization is a byproduct of geometric constraints imposed by σ -electrons and not a driving force by itself since π -electrons are known to favor localized structures.²⁰ However, the properties associated with PAHs²¹ are in most cases linked to the delocalization of π -electrons.²² Given the importance of this phenomenon, we decided to analyze in more detail the π -electron delocalization in aromatic compounds in light of Hückel's $4n + 2$ rule through electronic delocalization measures²³ of the π electrons.

In a first paper,²⁴ we studied the changes in the total π -delocalization index (δ_π) when two electrons have been either added to or removed from a series of aromatic $(4n + 2)\pi$ and antiaromatic $4n\pi$ organic compounds. The aim of the study was to investigate whether the δ_π values are useful for discerning between aromatic and antiaromatic systems. The idea was that when two electrons are added to an aromatic

^a Institut de Química Computacional and Departament de Química, Universitat de Girona, Campus de Montilivi, 17071 Girona, Catalonia, Spain. E-mail: miquel.sola@udg.edu, jordi.poater@udg.edu; Fax: +34-972-418356; Tel: +34-972-418912

^b Institute of Physics, University of Szczecin, 70-451 Szczecin, Poland
† Electronic supplementary information (ESI) available: The supplementary information contains sections S1: effect of geometry and electronic relaxation; S2: effect of planarity restriction; Fig. S3: evolution of $N + 2$ for systems in Fig. 5; S4: monocycles not included in Fig. 5; Tables S5 and S6: evolution of crossed terms and aromaticity criteria at singlet and triplet states of a series of monocycles; S7: aromaticity analysis of the systems under study. See DOI: 10.1039/b924972a



system ($(4n + 2)\pi$ electrons), we reach a $4n\pi$ -electron system, which, according to Hückel's rule, should be antiaromatic. Thus, one could expect that the added electrons in the molecule will be mainly localized, so that the total π -electron delocalization in the system essentially stays the same when going from $4n + 2$ to $4n\pi$ electrons. If the same system loses two electrons, we likewise have a $4n\pi$ -electron system, and therefore loss of electron delocalization is expected (see Scheme 1). For an antiaromatic species, one could anticipate exactly the opposite trend when going from $N - 2$ aromatic to N antiaromatic and from N to $N + 2$ aromatic π -electron system, N being the total number of electrons. In our previous study,²⁴ we found that δ_π perfectly follows the expected trend for aromatic systems, but unexpected trends emerged in antiaromatic systems. So, that analysis did not allow for a clear distinction between aromatic and antiaromatic systems based only on δ_π values.

The present work represents an extension of our previous study.²⁴ Our aim here is to separate the δ_π values into the *ortho* (1,2), *meta* (1,3), *para* (1,4), and successive contributions (crossed terms, see Fig. 1) and to analyze them in order to derive a series of patterns of changes in π -electron delocalization in aromatic and antiaromatic organic compounds when two electrons are added or removed. We will show that these patterns represent a kind of electronic footprints that makes it possible to discern between aromatic and antiaromatic systems. For such purpose, we have taken under study a series of compounds, the aromaticity or antiaromaticity of which is well-known. Our main goal is neither to develop a new aromaticity criterion nor to discuss the aromaticity of the systems studied, but to investigate the changes undergone by the different components of the π -electronic delocalization after adding or removing two electrons. We expect that such analysis will provide us with a deeper understanding of electronic delocalization in aromatic and antiaromatic compounds.

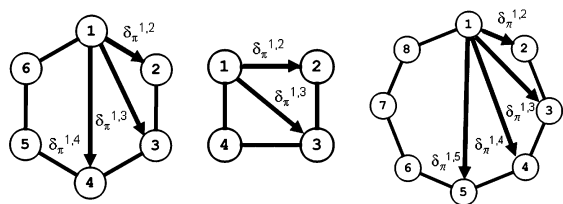


Fig. 1 Decomposition of electron delocalization in crossed-terms $\delta_\pi^{1,x}$ for C_6H_6 , C_4H_4 , and C_8H_8 .

Methodology

In this work we measure the electron delocalization by means of the so-called delocalization indices (DIs), or in a more general nomenclature, the electron sharing indices (ESIs). The ESI value between atoms A and B , $\delta(A, B)$ is obtained by double integration of the exchange–correlation density ($\gamma_{XC}(\vec{r}_1, \vec{r}_2)$) over the molecular space regions corresponding to atoms A and B ,

$$\delta(A, B) = -2 \int_A \int_B \gamma_{XC}(\vec{r}_1, \vec{r}_2) d\vec{r}_1 d\vec{r}_2. \quad (1)$$

For monodeterminantal wave functions one obtains:

$$\delta(A, B) = 2 \sum_{ij}^{\text{occ. MSO}} S_{ij}(A) S_{ij}(B). \quad (2)$$

The summations in eqn (2) run over all occupied molecular spin-orbitals (MSOs). $S_{ij}(A)$ is the overlap between MOs i and j within the molecular space assigned to atom A . $\delta(A, B)$ provides a quantitative idea of the number of electrons delocalized or shared between atoms A and B .

Although several atomic partitions may be used in the ESI definition, the most popular and successful^{25–27} one is that where the partition is carried out in the framework of the quantum theory of atoms-in-molecules (QTAIM) of Bader,²⁸ by which atoms are defined in the condition of zero-flux gradient in the one-electron density, $\rho(\mathbf{r})$. In this study we have preferred this partition over others, such as the fuzzy-atom partition²⁹ or the Mulliken scheme,³⁰ because the QTAIM-ESI produces numbers closer to that which is expected from chemical intuition.^{25,26,31}

In order to study the delocalization effects upon extraction or addition of two electrons, we calculate the total delocalization, which can be exactly split, because of the planarity ($S_{\sigma\pi}(A) = 0$) of all systems taken into study, into the σ and π contributions, this latter being in principle responsible for most of the properties associated to aromaticity:

$$\begin{aligned} \delta_{\text{tot}} &= \sum_{A_i, A_j \neq A_i} \delta(A_i, A_j) \\ &= \sum_{A_i, A_j \neq A_i} \delta^\pi(A_i, A_j) + \sum_{A_i, A_j \neq A_i} \delta^\sigma(A_i, A_j) = \delta_\pi + \delta_\sigma \end{aligned} \quad (3)$$

In addition, δ_π can be split into the different crossed contributions in the ring. For instance, for any six-membered ring (6-MR) and in particular for benzene, we have *ortho* (1,2), *meta* (1,3), and *para* (1,4) terms. In our study we have considered averaged values for the crossed terms (see Fig. 2). For any 6-MR we have:

$$\begin{aligned} \delta_\pi &= 6\delta_\pi^{1,2} + 6\delta_\pi^{1,3} + 3\delta_\pi^{1,4} \\ \delta_\pi^{1,2} &= \frac{\delta(1,2) + \delta(2,3) + \delta(3,4) + \delta(4,5) + \delta(5,6) + \delta(1,6)}{6} \\ \delta_\pi^{1,3} &= \frac{\delta(1,3) + \delta(2,4) + \delta(3,5) + \delta(4,6) + \delta(1,5) + \delta(2,6)}{6} \\ \delta_\pi^{1,4} &= \frac{\delta(1,4) + \delta(2,5) + \delta(3,6)}{3} \end{aligned} \quad (4)$$

Rings with an even number of atoms follow this previous scheme (see Fig. 2), where the number of farthest crossed

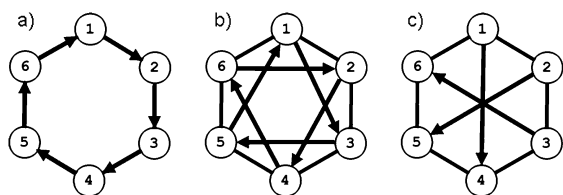


Fig. 2 C_6H_6 crossed contributions $\delta_\pi^{1,x}$ (a) $\delta_\pi^{1,2}$, (b) $\delta_\pi^{1,3}$, and (c) $\delta_\pi^{1,4}$.

terms, *i.e.* $\delta_\pi^{1,3}$ for 4-MRs, $\delta_\pi^{1,4}$ for 6-MRs or $\delta_\pi^{1,5}$ for 8-MRs, that contribute to the average value is half of the members of the ring (*e.g.* C_4H_4 have four $\delta_\pi^{1,2}$ and two $\delta_\pi^{1,3}$). On the other hand, for the rings with an odd number of atoms the number of farthest crossed terms is equal to the number of ring members. For instance, for any 7-MR:

$$\delta_\pi = 7\delta_\pi^{1,2} + 7\delta_\pi^{1,3} + 7\delta_\pi^{1,4}$$

$$\delta_\pi^{1,2} = \frac{\delta(1,2) + \delta(2,3) + \delta(3,4) + \delta(4,5) + \delta(5,6) + \delta(6,7) + \delta(1,7)}{7}$$

$$\delta_\pi^{1,3} = \frac{\delta(1,3) + \delta(2,4) + \delta(3,5) + \delta(4,6) + \delta(5,7) + \delta(1,6) + \delta(2,7)}{7}$$

$$\delta_\pi^{1,4} = \frac{\delta(1,4) + \delta(2,5) + \delta(3,6) + \delta(4,7) + \delta(1,5) + \delta(2,6) + \delta(3,7)}{7}$$
(5)

In our previous work,²⁴ we proved that when analyzing the changes in the total π -electronic delocalization of a series of neutral systems and the corresponding $N \pm 2$ charged species, the effect of geometry and electron relaxation are small enough to be neglected. As total π -electronic delocalization, crossed-terms are hardly affected by geometry and electron relaxation (see section S1 of the supplementary information†). Therefore, for the present series of compounds under analysis, the geometry optimization is only carried out for the N species; then $N - 2$ and $N + 2$ systems keep the geometry and the MOs of the N system, and thus, the wave function of the N species is used throughout the calculations. Moreover, all systems taken into account in this study have been analyzed in their planar conformation. However, in some compounds, *e.g.* cyclooctatetraene, the planar structure is not a minimum. In order to study how the crossed terms are affected by the planarity of the system, we have analyzed the out-of-plane boat-like deformation of benzene and cyclooctatetraene (see section S2 of the supplementary information for complete results†). The crossed-terms slightly change when the out-of-plane deformation angle increases, but more relevantly, the aromaticity trends are not reversed along the out-of-plane distortion. Thus, the fact that geometry and electron relaxation do not affect the electron delocalization makes the study computationally cheaper and, more importantly, we have checked that the trends derived are not altered when using these approximations.

In addition, multiplicity effects have to be taken into account when two electrons are either added or removed from a D_{nh} compound (degenerated HOMO and LUMO orbitals).

Our previous results²⁴ indicated that, for open-shell systems obtained after adding or removing two electrons, the singlet and triplet electronic states yield similar total π -electronic delocalizations. In the first part of the present work, we focus on the systems that follow Hückel's rule of aromaticity and, thus, electronic delocalization in the N , $N - 2$, and $N + 2$ species is computed at their lowest-lying singlet state. Afterwards multiplicity effects and Baird's rule are analyzed by means of crossed π -delocalization measures and then electronic delocalizations are computed for the lowest-lying triplet states of all monocycles up to 8-MRs.

For the aromaticity analysis we have applied the multicenter index (MCI),^{30,32} as it has been recently proven to work correctly for the series of systems under study, especially for the fact that it can be applied to rings of different sizes and with the presence of heteroatoms.³³ MCI is a particular extension of the I_{ring} index.³⁴

$$I_{ring}(\mathcal{A}) = \sum_{i_1, i_2, \dots, i_N} n_{i_1} \dots n_{i_N} S_{i_1 i_2}(A_1) S_{i_2 i_3}(A_2) \dots S_{i_N i_1}(A_N)$$
(6)

n_i being the occupancy of MO i . This expression is used both for closed-shell and open-shell species. In the particular case of a closed-shell monodeterminantal wavefunction we are left with a simpler expression:³⁵

$$I_{ring}(\mathcal{A}) = 2^N \sum_{i_1, i_2, \dots, i_N}^{occ.MO} S_{i_1 i_2}(A_1) S_{i_2 i_3}(A_2) \dots S_{i_N i_1}(A_N)$$
(7)

Summing up all the I_{ring} values resulting from the permutations of indices A_1, A_2, \dots, A_N the mentioned MCI index³⁰ is defined as:

$$MCI(\mathcal{A}) = \frac{1}{2^N} \sum_{P(\mathcal{A})} I_{ring}(\mathcal{A})$$
(8)

where $P(\mathcal{A})$ stands for a permutation operator which interchanges the atomic labels A_1, A_2, \dots, A_N to generate up to the $N!$ permutations of the elements in the string \mathcal{A} .^{32,36} As a tendency, the more positive the MCI values,³⁷ the more aromatic the rings. In the same way as π -electron delocalization, the MCI values are hardly affected by the geometry and electron relaxation (see supplementary information†).

In addition and for comparison purposes, the above MCI aromaticity analysis has been complemented with the calculation of the geometry based harmonic oscillator model of aromaticity (HOMA) index,³⁸ the magnetic based nucleus independent chemical shift (NICS) indicator,³⁹ and the electronic based fluctuation (FLU) index.⁴⁰ HOMA values remain unchanged for $N - 2$ and $N + 2$ species if we use the geometries obtained for the N system. Therefore, to be able to use the HOMA index for the aromaticity analysis, in section D we have used fully optimized geometries with the only restriction that all molecular structures are kept planar. The planarity restriction allows the σ - π separation and the direct comparison with δ_π values. However, as we have already seen for crossed terms, HOMA is hardly affected by the planarity constraint, the HOMA values for fully optimized C_8H_8 and

planar C_8H_8 are -0.25 and -0.20 , respectively. We have considered closed-shell singlet species for all systems analyzed in sections A and B. Moreover, all monocycles up to 8-MRs studied in section A have been computed also in their triplet states.

All calculations have been performed with the Gaussian 03⁴¹ and AIMPAC⁴² packages of programs, at the B3LYP level of theory⁴³ with the 6-311G(d,p) basis set⁴⁴ using Cartesian d and f functions. Calculations of open-shell triplet species have been performed within the unrestricted methodology, while for the singlet molecules we have considered in all cases closed-shell situations and we have used the restricted formalism. We have checked that results obtained considering closed-shell or open-shell singlets do not differ significantly. Calculation of atomic overlap matrices (AOM) and computation of ESIs and MCIs have been performed with the AIMPAC⁴² and ESI-3D⁴⁵ collection of programs. Calculation of these ESIs with the density functional theory (DFT) cannot be performed exactly because the electron-pair density is not available at this level of theory.⁴⁶ As an approximation, we have used the Kohn–Sham orbitals obtained from a DFT calculation to compute Hartree–Fock-like DIs through eqn (2). In particular, this equation does not account for electron correlation effects. In practice the values of the ESIs obtained using this approximation are generally closer to the Hartree–Fock values than correlated ESIs obtained with a configuration interaction method,^{25,46} which means that the inclusion of Coulomb correlation increases the electronic localization, but always qualitatively keeping the same trends. The MCI values have also been obtained from the Kohn–Sham orbitals using eqns (6) and (8). The numerical accuracy of the QTAIM calculations has been assessed using two criteria: (i) the integration of the Laplacian of the electron density ($\nabla^2\rho(r)$) within an atomic basin must be close to zero; and (ii) the number of electrons in a molecule must be equal to the sum of all the electron populations of the molecule, and also equal to the sum of all the localization indices and half of the DIs in the molecule. For all atomic calculations, integrated absolute values of $\nabla^2\rho(r)$ were always less than 0.001 a.u. For all molecules, errors in the calculated number of electrons were always below 0.01 a.u.

Results and discussion

This section is laid out as follows. First, we discuss the crossed δ_π terms in monocyclic aromatic and antiaromatic organic molecules. Second, we study the same contributions in PAHs. Third, we discuss how the change of multiplicity affects these contributions. Finally, we quantify the aromaticity of all studied species by means of different indicators of aromaticity with special emphasis to MCI values.

A δ_π crossed contributions in monocyclic systems

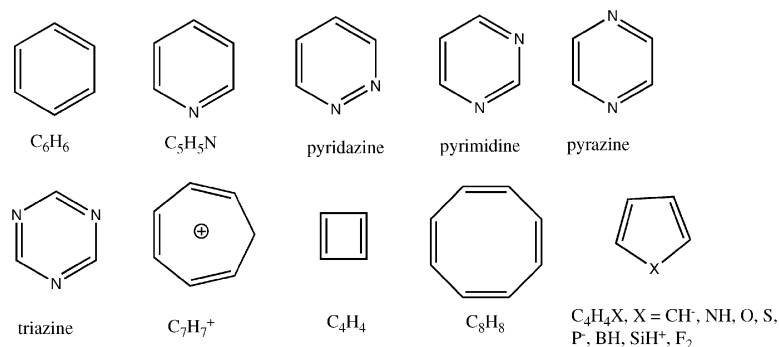
First, we focus on a series of aromatic 6- and 7-MRs, going from benzene to heteroaromatic systems (see Scheme 2). Table 1 encloses the corresponding δ_π values together with its decomposition into the different crossed terms. For benzene, it can be seen that from antiaromatic $N - 2$ to standard aromatic benzene (N), total δ_π increases from 2.614 e to 3.369 e,

whereas from N to $N + 2$, δ_π hardly increases to 3.482 e. These trends are the expected ones for an aromatic system, as already discussed.²⁴ Now, with respect to the crossed terms, the *ortho* $\delta_\pi^{1,2}$ term increases from 0.288 to 0.427 e when two electrons are added to the $N - 2$ species to get N aromatic benzene, the *para* $\delta_\pi^{1,4}$ term also increases from 0.059 to 0.094 e. On the other hand the *meta* $\delta_\pi^{1,3}$ term decreases from 0.087 to 0.037 e. Therefore, the increase in total δ_π when going from antiaromatic $N - 2$ to aromatic N does not imply an increase in all crossed terms. It is important to notice that, for benzene, the higher electronic delocalization in *para* (0.094 e) than in *meta* (0.037 e)^{47,48} was the key factor for the definition of the electronic-based aromaticity criterion named *para*-delocalization index (PDI).⁴⁹ This trend is broken for the corresponding antiaromatic ($C_6H_6^{2+}$) system (0.087 vs. 0.059 e for *meta* and *para*, respectively). If we now focus on the δ_π values from aromatic C_6H_6 to antiaromatic $C_6H_6^{2-}$, the opposite trends are observed: $\delta_\pi^{1,2}$ and $\delta_\pi^{1,4}$ decrease from N to $N + 2$, whereas $\delta_\pi^{1,3}$ increases. In order to simplify this analysis, the difference between these two steps, $\Delta^2 = [2\delta_N - \delta_{N-2} - \delta_{N+2}]$, is calculated (values in Table 1). This measure represents the sum of the changes on the electron delocalization when going from N to $N - 2$ and from N to $N + 2$ species and it is proportional to the numerical second derivative of the corresponding crossed term with respect to the number of electrons. A positive value (convex shape) indicates an overall decrease in the electron delocalization with respect to changes in N , while a negative Δ^2 value (concave shape) represents an overall increase (see Fig. 3).

This trend is also reproduced for heteroaromatic systems when one, two or three nitrogen atoms are incorporated to the benzene ring (see Table 1). For pyridine, pyrimidine, pyrazine, pyridazine, and triazine, $\delta_\pi^{1,2}$ and $\delta_\pi^{1,4}$ increase from $N - 2$ to N systems and $\delta_\pi^{1,3}$ decreases, and the opposite trend is found from N to $N + 2$ systems. Δ^2 also corroborates this alternate pattern, namely, large positive *ortho*-, negative *meta*-, and positive *para*-values.

The same analysis has been applied to rings of a different size. We have started with $C_7H_7^+$, an aromatic system isoelectronic to benzene that has the same crossed terms. Interestingly, for this system the “*meta*” ($\delta_\pi^{1,3}$) and “*para*” ($\delta_\pi^{1,4}$) contributions are equal (0.05 e). As for the previously analyzed 6-MRs, we observe an increase in $\delta_\pi^{1,2}$ and $\delta_\pi^{1,4}$, and a decrease in $\delta_\pi^{1,3}$ when going from $N - 2$ to N . The same trends are also achieved from N to $N + 2$, with the exception of $\delta_\pi^{1,2}$, which shows a slight increase of 0.01 e. Overall, for aromatic 6- and 7-MR systems, we observe alternation among the crossed terms from $N \pm 2$ to N : $\delta_\pi^{1,2}$ increases, $\delta_\pi^{1,3}$ decreases, and $\delta_\pi^{1,4}$ increases.

Next we address antiaromatic systems. We first focus on C_4H_4 (values enclosed in Table 2). In this case, $\delta_\pi^{1,2}$ increases from aromatic $N - 2$ to antiaromatic N systems, from 0.243 to 0.477 e, respectively, whereas $\delta_\pi^{1,3}$ decreases from 0.243 to 0.059 e, respectively. Likewise, from N to $N + 2$, $\delta_\pi^{1,2}$ decreases and $\delta_\pi^{1,3}$ increases. In the same way, for the bigger antiaromatic C_8H_8 system constrained to be planar, $\delta_\pi^{1,2}$ and $\delta_\pi^{1,4}$ increase, whereas $\delta_\pi^{1,3}$ and $\delta_\pi^{1,5}$ decrease from $N \pm 2$ to N . Thus, C_8H_8 behaves like C_4H_4 , with the only difference that the former presents more crossed terms. We have $\delta_\pi^{1,3} < \delta_\pi^{1,4} > \delta_\pi^{1,5}$ when going from $d_{1,3}$ (2.603 Å) to $d_{1,4}$ (3.400 Å)



Scheme 2

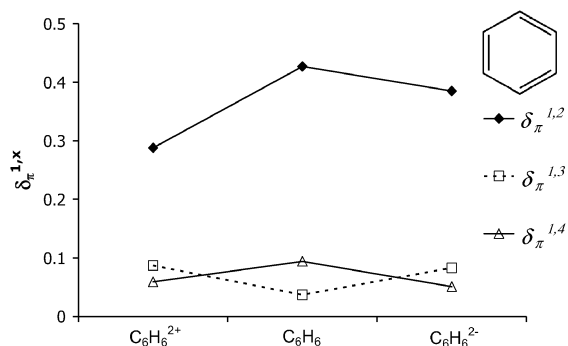


Fig. 3 $\delta_{\pi}^{1,x}$ measures in $C_6H_6^{2+}$, C_6H_6 , and $C_6H_6^{2-}$. Units are electrons.

and to $d_{1,5}$ (3.681 Å) for C_8H_8 , while for both aromatic $C_8H_8^{2+}$ and $C_8H_8^{2-}$ we get the opposite, that is $\delta_{\pi}^{1,3} > \delta_{\pi}^{1,4} < \delta_{\pi}^{1,5}$. It is thus noteworthy that, as already proved for benzene,^{48–50} there is no connection between the C–C distance and the corresponding crossed terms values, *i.e.*, shorter C–C distances does not always imply larger $\delta_{\pi}^{1,x}$ values. Recently, Chesnut also recognized the ESIs for non-bonded carbon-carbon interactions reflect the degree of conjugation between the two atoms in question.⁵¹ Fig. 4 shows the changes on the crossed contributions in C_8H_8 system.

Once the patterns of π -crossed terms delocalization have been discussed in 4-, 6-, 7-, and 8-MRs, we focus now our attention to larger rings. Thus, we have computed the π -electron delocalization for the series: C_4H_4 , C_6H_6 , C_8H_8 , $C_{10}H_{10}$, $C_{12}H_{12}$, $C_{14}H_{14}$, and $C_{16}H_{16}$, and charged $C_{11}H_{11}^+$, $C_{11}H_{11}^-$, $C_{13}H_{13}^+$, $C_{13}H_{13}^-$, and $C_{15}H_{15}^+$. As for C_8H_8 ,

Table 1 Total electronic delocalization (δ_{tot}), total π electronic delocalization (δ_{π}), and the corresponding crossed contributions to the latter ($\delta_{\pi}^{1,x}$) for a series of six- and seven-membered monocyclic compounds. Units are electrons

	$N - 2$	N	$N + 2$	Δ^2		$N - 2$	N	$N + 2$	Δ^2
C_6H_6					Pyridazine				
δ_{tot}	14.863	15.618	15.731		δ_{tot}	12.161	13.095	12.981	
δ_{π}	2.614	3.369	3.482		δ_{π}	2.296	3.230	3.116	
$\delta_{\pi}^{1,2}$	0.288	0.427	0.385	0.181	$\delta_{\pi}^{1,2}$	0.283	0.418	0.369	0.184
$\delta_{\pi}^{1,3}$	0.087	0.037	0.083	-0.096	$\delta_{\pi}^{1,3}$	0.062	0.042	0.085	-0.063
$\delta_{\pi}^{1,4}$	0.059	0.094	0.051	0.078	$\delta_{\pi}^{1,4}$	0.051	0.096	0.044	0.097
C_5H_5N					Triazine				
δ_{tot}	13.518	14.359	14.367		δ_{tot}	11.346	11.87	11.948	
δ_{π}	2.446	3.287	3.296		δ_{π}	2.535	3.059	3.137	
$\delta_{\pi}^{1,2}$	0.284	0.422	0.377	0.183	$\delta_{\pi}^{1,2}$	0.276	0.410	0.369	0.175
$\delta_{\pi}^{1,3}$	0.076	0.040	0.084	-0.080	$\delta_{\pi}^{1,3}$	0.107	0.039	0.091	-0.120
$\delta_{\pi}^{1,4}$	0.056	0.093	0.047	0.083	$\delta_{\pi}^{1,4}$	0.055	0.087	0.055	0.064
Pyridazine					$C_7H_7^+$				
δ_{tot}	12.703	13.418	13.27		δ_{tot}	16.434	17.89	18.155	
δ_{π}	2.533	3.247	3.099		δ_{π}	2.834	3.677	3.942	
$\delta_{\pi}^{1,2}$	0.303	0.423	0.364	0.179	$\delta_{\pi}^{1,2}$	0.244	0.389	0.403	0.131
$\delta_{\pi}^{1,3}$	0.081	0.041	0.080	-0.079	$\delta_{\pi}^{1,3}$	0.103	0.050	0.061	-0.064
$\delta_{\pi}^{1,4}$	0.045	0.094	0.049	0.094	$\delta_{\pi}^{1,4}$	0.041	0.050	0.042	0.017
Pyrimidine									
δ_{tot}	12.307	13.102	13.034						
δ_{π}	2.385	3.180	3.113						
$\delta_{\pi}^{1,2}$	0.291	0.415	0.363	0.176					
$\delta_{\pi}^{1,3}$	0.074	0.041	0.082	-0.074					
$\delta_{\pi}^{1,4}$	0.040	0.091	0.052	0.090					

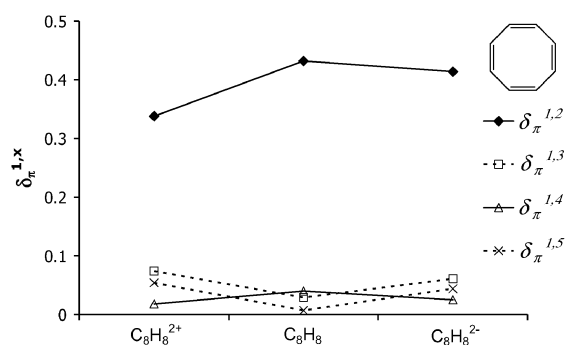


Fig. 4 $\delta_{\pi}^{1,x}$ measures in $C_8H_8^{2+}$, C_8H_8 , and $C_8H_8^{2-}$. Units are electrons.

some systems are not minima because they are forced to be planar. We kept them planar as this way the separation between the σ - and π -electron delocalization is exact. Our analysis is qualitative in the sense that we just want to see whether the alternation pattern for the crossed terms in aromatic and antiaromatic systems is maintained when going to larger rings. To analyze the trends very precise numbers are not necessary and, therefore, instead of tabulating the δ_{π} values, we have depicted the corresponding values for the most representative systems in Fig. 5. In addition, in this set of rings we have concentrated our analysis in the $N - 2$ and N species. In all cases, $N - 2$ and $N + 2$ follow the same trends and, in order to simplify the analysis and make the trends in the plots more visible, $N + 2$ values are not included in Fig. 5 (complete results can be found in Fig. S3 of the supplementary information†). Thus, Fig. 5a shows how for antiaromatic C_4H_4 , $\delta_{\pi}^{1,2}$ increases from $N - 2$ to N , whereas $\delta_{\pi}^{1,3}$ decreases, as above mentioned. For aromatic benzene (see Fig. 5b), $\delta_{\pi}^{1,2}$ increases, $\delta_{\pi}^{1,3}$ decreases and $\delta_{\pi}^{1,4}$ increases, and for the other larger systems the alternation is kept for both aromatic ($C_{14}H_{14}$) and antiaromatic (C_8H_8 and $C_{16}H_{16}$) systems. It must be noticed that the larger the x value in the $\delta_{\pi}^{1,x}$ crossed term, the smaller the alternation. This is especially visible in Fig. 5e for $C_{16}H_{16}$. The same conclusions are extracted from the systems in the series not enclosed in Fig. 5 but included as

Table 2 Total electronic delocalization (δ_{tot}), total π electronic delocalization (δ_{π}), and the corresponding crossed contributions to this latter ($\delta_{\pi}^{1,x}$) for C_4H_4 and C_8H_8 antiaromatic compounds. Units are electrons

	$N - 2$	N	$N + 2$	Δ^2
C_4H_4				
δ_{tot}	9.562	10.26	10.382	
δ_{π}	1.519	2.217	2.339	
$\delta_{\pi}^{1,2}$	0.243	0.477	0.375	0.336
$\delta_{\pi}^{1,3}$	0.243	0.059	0.233	-0.358
C_8H_8				
δ_{tot}	20.344	20.866	21.172	
δ_{π}	3.955	4.477	4.783	
$\delta_{\pi}^{1,2}$	0.338	0.432	0.414	0.112
$\delta_{\pi}^{1,3}$	0.074	0.029	0.061	-0.077
$\delta_{\pi}^{1,4}$	0.018	0.040	0.025	0.037
$\delta_{\pi}^{1,5}$	0.054	0.007	0.044	-0.084

supplementary information (see Fig. S4†). The alternation between even ($\delta_{\pi}^{1,2}$ $\delta_{\pi}^{1,4}$...) and odd ($\delta_{\pi}^{1,3}$ $\delta_{\pi}^{1,5}$...) crossed terms is kept.

The observed trends have been schematically represented in Table 3 for the different rings analyzed (except for 5-MRs) and from antiaromatic N to aromatic $N \pm 2$ and *vice versa*. It is clear that the patterns of changes found help to distinguish between aromatic and antiaromatic rings. Thus, for instance, for an aromatic 6-MR, $\delta_{\pi}^{1,4}$ decreases when adding or removing two electrons, while the opposite is observed in antiaromatic systems. Moreover, the crossed term corresponding to the two farthest atoms in the ring (*i.e.*, $\delta_{\pi}^{1,4}$ in 6-MRs or $\delta_{\pi}^{1,5}$ in 8-MRs) decreases in aromatic species when two electrons are added or removed, whereas the opposite is true for antiaromatic species. These patterns of π -electron delocalization allow for a clear differentiation between aromatic and antiaromatic rings. It is important to mention that by just focusing on the total δ_{π} , we cannot appreciate any difference between C_6H_6 and C_4H_4 , as in the latter δ_{π} increases in 0.70 and 0.12 e from $N - 2$ to N and from N to $N + 2$, respectively, values very close to those of C_6H_6 (0.76 and 0.11 e, respectively).

Let us finally discuss the particular case of heteroaromatic 5-MRs (C_4H_4X) that, depending on the heteroatom X (see Scheme 2) can be either aromatic ($X = CH^-, NH, O, S, P^-$) or antiaromatic ($X = BH, SiH^+, F_2$). The corresponding δ_{π} values for these species are enclosed in Table 4. For aromatic C_4H_4X systems, from antiaromatic $N - 2$ to aromatic N we would expect an increase in $\delta_{\pi}^{1,3}$ since 1 and 3 are the two C atoms furthest separated in the ring. However, the opposite trend is obtained. Thus, $\delta_{\pi}^{1,2}$ increases from 0.337 to 0.436 e from $N - 2$ to N in $C_5H_5^-$ and $\delta_{\pi}^{1,3}$ decreases from 0.104 to 0.085 e. And the same tendency is observed for the rest of the aromatic species ($X = NH, O, S, P^-$). On the other hand, for the antiaromatic species, the expected tendency would be an increase in $\delta_{\pi}^{1,2}$ from aromatic $N - 2$ to antiaromatic N , and a decrease of $\delta_{\pi}^{1,3}$. From the values in Table 4 it is shown that all three antiaromatic C_4H_4X ($X = BH, SiH^+, F_2$) compounds follow this trend. Thus, for aromatic species the 5-MRs do not follow the expected trend. Our hypothesis is that $\delta_{\pi}^{1,3}$ could also be considered $\delta_{\pi}^{1,4}$ (depending whether one follows clockwise or anticlockwise directions in the ring when going from one atom to the farthest one in the ring), which means that this particular crossed term can be considered between the equivalent *meta* and *para* in benzene. For this reason, big differences are not generally observed in $\delta_{\pi}^{1,3}$ for 5-MRs when going from $N - 2$ to N and from N to $N + 2$, and the main change takes place on $\delta_{\pi}^{1,2}$. This makes the series of 5-MRs a particular case for which the patterns of changes in crossed term delocalizations do not allow for a clear separation between aromatic and antiaromatic species. Notwithstanding, it is worth mentioning that the smallest unsigned Δ^2 values for the $\delta_{\pi}^{1,3}$ crossed term when going from N to $N \pm 2$ are found for aromatic species, whereas the largest ones correspond to antiaromatic ones. In addition, the aforementioned alternation pattern is retained in higher crossed terms of larger rings with odd number of members. Thus, for $C_7H_7^+$, even though it follows the expected alternation, the *para* Δ^2 value is only 0.017 as compared to 0.078 or -0.084 in C_6H_6 or C_8H_8 , respectively, while the rest

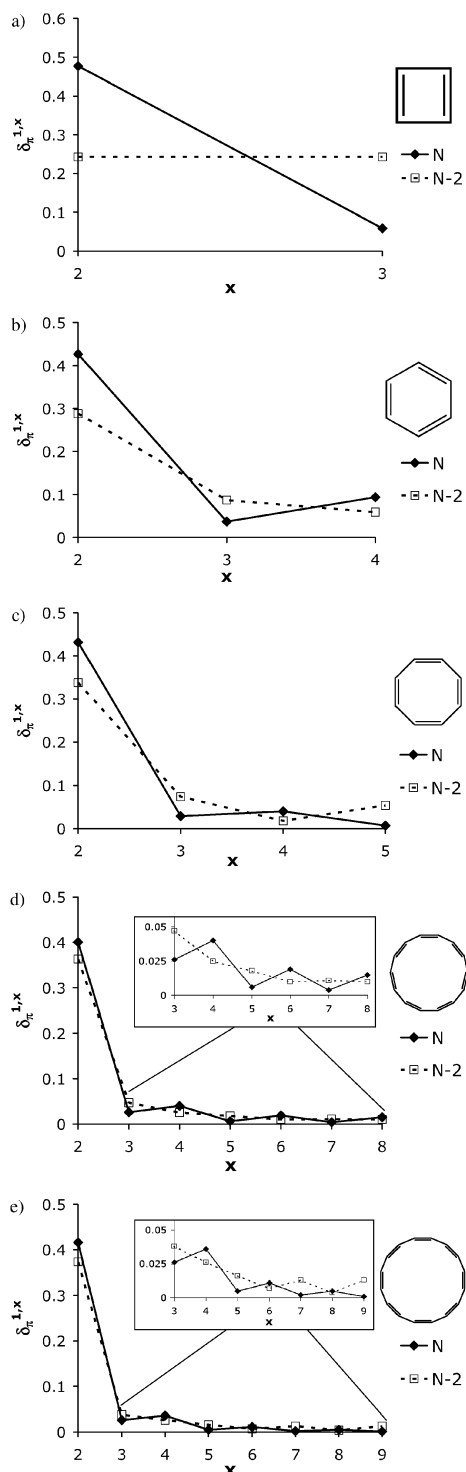


Fig. 5 Evolution of $\delta_{\pi}^{1,x}$ (in electrons) in N and $N - 2$ species for (a) C_4H_4 , (b) C_6H_6 , (c) C_8H_8 , (d) $C_{14}H_{14}$, and (e) $C_{16}H_{16}$.

of Δ^2 values are relatively similar for either even or odd membered rings. And the same behavior is observed when comparing $C_9H_9^-$ to $C_{10}H_{10}$.

Table 3 Schematic representation of the behavior of the crossed contributions to the total π -electronic delocalization in antiaromatic and aromatic compounds of different ring sizes. \uparrow and \downarrow refer to increase and decrease, respectively

	Antiaromatic $N \rightarrow N \pm 2$			Aromatic $N \rightarrow N \pm 2$		
	4-MR	6-,7-MR	8-,9-MR	4-MR	6-,7-MR	8-,9-MR
$\delta_{\pi}^{1,2}$	\downarrow	\uparrow	\downarrow	\uparrow	\downarrow	\uparrow
$\delta_{\pi}^{1,3}$	\uparrow	\downarrow	\uparrow	\downarrow	\uparrow	\downarrow
$\delta_{\pi}^{1,4}$		\uparrow	\downarrow		\downarrow	\uparrow
$\delta_{\pi}^{1,5}$			\uparrow			\downarrow

B δ_{π} crossed contributions in polycyclic aromatic hydrocarbons

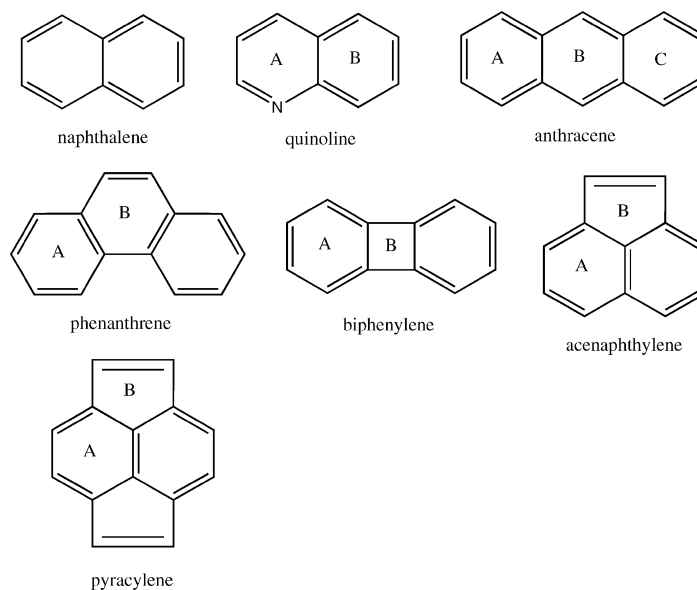
The above analysis has been performed on monocyclic systems for which Hückel's rule holds. The next step is to see if the above patterns of π -electron delocalization are kept for PAHs. For this purpose, we analyze in this section the following series of PAHs: naphthalene, quinoline, anthracene, phenanthrene, biphenylene, acenaphthylene, and pyracylene (see Scheme 3). Table 5 encloses the δ_{π} values for this series and the corresponding crossed terms (in the calculation of the crossed terms C atoms from different rings can be involved). For naphthalene, the trends observed for benzene are kept. By comparison of the values, from benzene (see Table 1) to naphthalene, it is observed how all differences in δ_{π} from $N - 2$ to N decrease. For benzene, the differences in δ_{π} are 0.14, -0.05 , and 0.11 for $\delta_{\pi}^{1,2}$, $\delta_{\pi}^{1,3}$ and $\delta_{\pi}^{1,4}$, respectively, whereas for naphthalene they are 0.07, -0.01 , and 0.03, respectively, thus showing the decrease in electron delocalization changes in the rings when going from benzene to the 6-MRs of naphthalene, which have a lower aromaticity, as previously observed.⁵² This trend is even more pronounced for the external ring of anthracene, even though for both rings the expected pattern of electron delocalization for an aromatic ring is observed. This conclusion can be extrapolated to the rest of the systems in this series. The 4-MR in biphenylene also behaves like C_4H_4 , but also with much lower differences between the values for the $N - 2$ and N species. 5-MRs in acenaphthylene and pyracylene also present the expected trend for antiaromatic 5-MRs. Analogous conclusions might be drawn by checking the $N + 2$ to N crossed terms, and therefore, by Δ^2 values.

C Multiplicity

In this section, the patterns of crossed π -delocalization measures are studied for the lowest-lying triplet states of all monocycles analyzed in Tables 1, 2, and 4. In a previous work, we showed that in dicationic or dianionic D_{nh} annulenes, the lowest-lying singlet and triplet states present similar *total* π -electronic delocalization values. Consequently, total δ_{π} cannot discern between singlet and triplet states. However, as we can see in Fig. 6 and 7, the crossed terms can clearly reproduce the multiplicity effects and show opposite trends according to Hückel's and Baird's rules. While the lowest-lying triplet state of C_6H_6 is antiaromatic, $C_6H_6^{2+}$ and $C_6H_6^{2-}$ are aromatic. Thus, for the antiaromatic C_6H_6 triplet state, lower $\delta_{\pi}^{1,2}$ and $\delta_{\pi}^{1,4}$ and higher $\delta_{\pi}^{1,3}$ are observed in comparison to the aromatic lowest-lying singlet state (see Fig. 6). In the antiaromatic C_6H_6 triplet state, $\delta_{\pi}^{1,2}$ and $\delta_{\pi}^{1,4}$ decrease from aromatic

Table 4 Total electronic delocalization (δ_{tot}), total π electronic delocalization (δ_{π}), and the corresponding crossed contributions to this latter ($\delta_{\pi}^{1,2}$, $\delta_{\pi}^{1,3}$) for a series of five-membered monocyclic compounds. Units are electrons

	$N - 2$	N	$N + 2$	Δ^2		$N - 2$	N	$N + 2$	Δ^2
C_5H_5^-					$\text{C}_4\text{H}_4\text{P}^-$				
δ_{tot}	12.634	13.177	13.056		δ_{tot}	11.308	11.908	11.676	
$\delta_{\pi}^{1,2}$	2.430	2.973	2.852		$\delta_{\pi}^{1,2}$	2.330	2.930	2.698	
$\delta_{\pi}^{1,3}$	0.337	0.436	0.338	0.197	$\delta_{\pi}^{1,2}$	0.341	0.440	0.361	0.178
	0.104	0.085	0.091	-0.025	$\delta_{\pi}^{1,3}$	0.083	0.088	0.092	0.001
$\text{C}_4\text{H}_4\text{NH}$					$\text{C}_4\text{H}_4\text{BH}$				
δ_{tot}	11.688	12.383	12.186		δ_{tot}	10.972	11.702	12.39	
$\delta_{\pi}^{1,2}$	2.074	2.769	2.572		$\delta_{\pi}^{1,2}$	1.550	2.281	2.969	
$\delta_{\pi}^{1,3}$	0.281	0.417	0.329	0.224	$\delta_{\pi}^{1,2}$	0.158	0.361	0.404	0.160
	0.106	0.086	0.091	-0.025	$\delta_{\pi}^{1,3}$	0.135	0.053	0.093	-0.122
$\text{C}_4\text{H}_4\text{O}$					$\text{C}_4\text{H}_4\text{SiH}^+$				
δ_{tot}	10.572	11.278	11.117		δ_{tot}	10.915	11.632	12.369	
$\delta_{\pi}^{1,2}$	1.931	2.638	2.477		$\delta_{\pi}^{1,2}$	1.577	2.294	3.031	
$\delta_{\pi}^{1,3}$	0.256	0.407	0.322	0.236	$\delta_{\pi}^{1,2}$	0.157	0.359	0.440	0.121
	0.112	0.081	0.095	-0.045	$\delta_{\pi}^{1,3}$	0.144	0.065	0.085	-0.099
$\text{C}_4\text{H}_4\text{S}$					$\text{C}_4\text{H}_4\text{F}_2$				
δ_{tot}	11.244	11.889	11.665		δ_{tot}	12.619	13.282	13.472	
$\delta_{\pi}^{1,2}$	2.059	2.704	2.480		$\delta_{\pi}^{1,2}$	2.447	3.129	3.363	
$\delta_{\pi}^{1,3}$	0.269	0.417	0.335	0.230	$\delta_{\pi}^{1,2}$	0.167	0.358	0.316	0.233
	0.123	0.082	0.087	-0.046	$\delta_{\pi}^{1,3}$	0.113	0.043	0.090	-0.117

**Scheme 3**

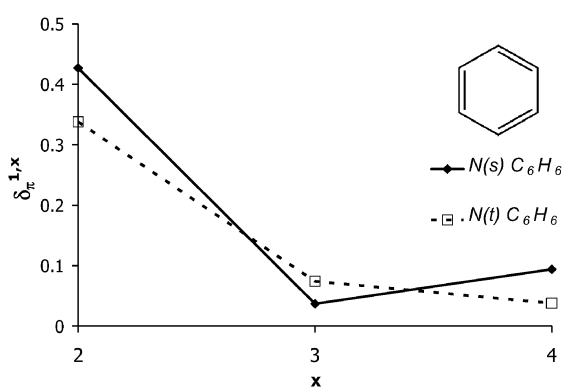
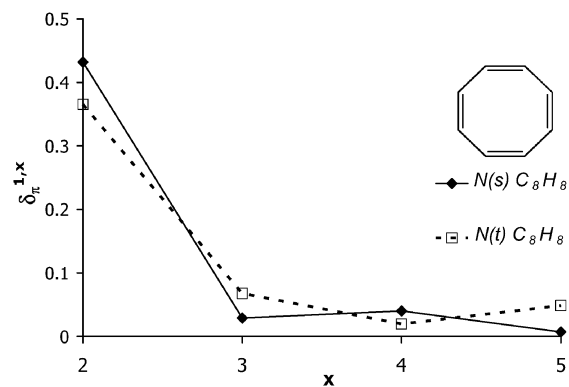
$N - 2(t)$ to antiaromatic $N(t)$, whereas $\delta_{\pi}^{1,3}$ increases (see Table 6). The opposite trend has been already shown for the singlet ground state. The Δ^2 measures contained in Table 6 show opposite patterns for the lowest-lying singlet and triplet states in line with Baird's rule.

For the C_8H_8 species, the aromatic lowest-lying triplet, $N(t)$, presents higher $\delta_{\pi}^{1,3}$ and $\delta_{\pi}^{1,5}$ and lower $\delta_{\pi}^{1,2}$ and $\delta_{\pi}^{1,4}$ than the antiaromatic lowest-lying singlet, $N(s)$. Thus, alternation of the crossed terms between antiaromatic $N(s)$ and aromatic $N(t)$ is confirmed (see Fig. 7) showing opposite patterns according to Baird's rule. As we previously showed, it is especially interesting to analyze the relationship between distance and electron delocalization. In the constrained planar optimized C_8H_8 molecule, the distance between the farthest

positions (*i.e.* $d_{1,5}$) is practically the same for the singlet and triplet states (3.680 vs. 3.665 Å). However, the behavior of the electron delocalization is completely different, because in antiaromatic $N(s)$, $\delta_{\pi}^{1,5}$ is only 0.007 e, while it increases to 0.049 e in aromatic $N(t)$. Moreover, the rest of the monocycles from Tables 1, 2, and 4 have been analyzed by means of electron delocalization patterns for $N(s)$ and $N(t)$ species (see Tables S5 and S6 of the supplementary information†). All systems studied follow the expected trends and the alternation between $N(s)$ and $N(t)$ crossed terms is observed. Again, the aromatic 5-MRs represent the only exception, in this particular case, $\delta_{\pi}^{1,2}$ decreases while $\delta_{\pi}^{1,3}$ is hardly affected and the alternation is not observed when going from aromatic $N(s)$ to antiaromatic $N(t)$.

Table 5 Total electronic delocalization (δ_{tot}), total π electronic delocalization (δ_{π}), and the corresponding crossed contributions to this latter ($\delta_{\pi}^{1,x}$) for a series of planar polycyclic aromatic hydrocarbons. Units are electrons. *A* and *B* refer to the different rings in the PAH (see Scheme 3)

	<i>N</i> - 2	<i>N</i>	<i>N</i> + 2	Δ^2		<i>N</i> - 2	<i>N</i>	<i>N</i> + 2	Δ^2
Naphthalene					Biphenylene				
δ_{tot}	24.554	25.079	25.318		δ_{tot}	28.755	29.249	29.554	
δ_{π}	5.113	5.639	5.877		$\delta_{\pi}^{1,2A}$	6.281	6.774	7.079	
$\delta_{\pi}^{1,2}$	0.308	0.376	0.356	0.088	$\delta_{\pi}^{1,3A}$	0.328	0.409	0.369	0.121
$\delta_{\pi}^{1,3}$	0.039	0.029	0.038	-0.019	$\delta_{\pi}^{1,4A}$	0.049	0.033	0.039	-0.022
$\delta_{\pi}^{1,4}$	0.039	0.066	0.038	0.055	$\delta_{\pi}^{1,2B}$	0.171	0.201	0.229	0.001
Quinoline					Acenaphthylene				
δ_{tot}	23.309	23.826	23.999		δ_{tot}	29.112	29.632	29.848	
$\delta_{\pi}^{1,2A}$	0.343	0.373	0.338	0.065	$\delta_{\pi}^{1,2A}$	6.148	6.668	6.884	
$\delta_{\pi}^{1,3A}$	0.037	0.031	0.042	-0.017	$\delta_{\pi}^{1,3A}$	0.313	0.365	0.347	0.070
$\delta_{\pi}^{1,4A}$	0.052	0.065	0.031	0.047	$\delta_{\pi}^{1,3B}$	0.029	0.025	0.032	-0.011
$\delta_{\pi}^{1,2B}$	0.268	0.372	0.366	0.110	$\delta_{\pi}^{1,4A}$	0.034	0.063	0.040	0.052
$\delta_{\pi}^{1,3B}$	0.048	0.029	0.036	-0.026	$\delta_{\pi}^{1,2B}$	0.197	0.309	0.332	0.089
$\delta_{\pi}^{1,4B}$	0.034	0.065	0.046	0.050	$\delta_{\pi}^{1,3B}$	0.065	0.026	0.050	-0.063
Anthracene					Pyracylene				
δ_{tot}	34.626	35.086	35.348		δ_{tot}	33.017	33.466	33.773	
δ_{π}	7.357	7.816	8.078		$\delta_{\pi}^{1,2A}$	7.464	7.914	8.221	
$\delta_{\pi}^{1,2A}$	0.335	0.363	0.364	0.027	$\delta_{\pi}^{1,3A}$	0.319	0.358	0.344	0.053
$\delta_{\pi}^{1,3A}$	0.030	0.024	0.030	-0.012	$\delta_{\pi}^{1,4A}$	0.031	0.027	0.031	-0.008
$\delta_{\pi}^{1,4A}$	0.048	0.058	0.049	0.019	$\delta_{\pi}^{1,2B}$	0.026	0.058	0.039	0.051
$\delta_{\pi}^{1,2B}$	0.272	0.333	0.309	0.085	$\delta_{\pi}^{1,3B}$	0.236	0.301	0.326	0.040
$\delta_{\pi}^{1,3B}$	0.022	0.022	0.023	-0.001	$\delta_{\pi}^{1,4B}$	0.033	0.029	0.045	-0.020
$\delta_{\pi}^{1,4B}$	0.021	0.058	0.021	0.074					
Phenanthrene									
δ_{tot}	34.078	34.56	34.843						
δ_{π}	7.427	7.910	8.192						
$\delta_{\pi}^{1,2A}$	0.336	0.386	0.369	0.067					
$\delta_{\pi}^{1,3A}$	0.038	0.031	0.035	-0.011					
$\delta_{\pi}^{1,4A}$	0.042	0.072	0.044	0.058					
$\delta_{\pi}^{1,2B}$	0.265	0.321	0.306	0.071					
$\delta_{\pi}^{1,3B}$	0.034	0.022	0.033	-0.023					
$\delta_{\pi}^{1,4B}$	0.024	0.038	0.022	0.030					

**Fig. 6** $\delta_{\pi}^{1,x}$ measures in aromatic C_6H_6 (s) and antiaromatic C_6H_6 (t). Units are electrons.**Fig. 7** $\delta_{\pi}^{1,x}$ measures in antiaromatic C_8H_8 (s) and aromatic C_8H_8 (t). Units are electrons.

D Aromaticity analysis

In this last subsection we quantify the aromaticity of the rings studied to corroborate their aromatic or antiaromatic character. For this purpose the electronic aromaticity criterion called multicenter index (MCI) has been applied, as we have recently demonstrated it performs very well for different aromatic series of compounds³³ and, in addition, it can be

applied to any ring. Despite the good performance of MCI, for the aim of comparison, HOMA, NICS(0), NICS(0)_{zzz}, NICS(1) and NICS(1)_{zzz}, and FLU aromaticity criteria have been also calculated. All aromaticity indices reported in this section have been calculated at the fully relaxed geometries of all species (*N*, *N* - 2, and *N* + 2) with the only constrain that all molecular structures are kept planar, at variance with the above analysis (values enclosed in the supplementary information). It is worth

Table 6 Crossed terms measures in C₆H₆ and C₈H₈ for *N* − 2, *N*, and *N* + 2 triplet states. Units are electrons

	<i>N</i> − 2(<i>t</i>)	<i>N</i> (<i>t</i>)	<i>N</i> + 2(<i>t</i>)	Δ ² (triplet)	Δ ² (singlet) ^a
C ₆ H ₆					
δ _π ^{1,2}	0.275	0.338	0.405	−0.004	0.181
δ _π ^{1,3}	0.070	0.074	0.057	0.021	−0.096
δ _π ^{1,4}	0.103	0.038	0.068	−0.095	0.078
C ₈ H ₈					
δ _π ^{1,2}	0.316	0.365	0.417	−0.002	0.112
δ _π ^{1,3}	0.061	0.068	0.046	0.029	−0.077
δ _π ^{1,4}	0.041	0.020	0.036	−0.038	0.037
δ _π ^{1,5}	0.015	0.049	0.026	0.056	−0.084

^a Results from Table 1.

noting that the geometry-based HOMA indicator of aromaticity does not denote changes of aromaticity if the same geometry is used for the *N*, *N* − 2, and *N* + 2 species.

The MCI values for the whole series of compounds analyzed are enclosed in Table 7. First, for 6-MR systems, in all cases the *N* ring appears to be the most aromatic, with the corresponding increase in aromaticity from *N* − 2 to *N* and the decrease from *N* to *N* + 2 as expected from the above δ_π^{1,4} values, that increases in *para* positions from antiaromatic *N* − 2 to aromatic *N*, and decreases from *N* to antiaromatic *N* + 2. The same behavior is observed for C₇H₇⁺, and completely opposite for both antiaromatic C₄H₄ and C₈H₈, in which *N* − 2 and *N* + 2 present higher aromaticities than *N*, again in line with δ_π trends.

For the series of five-membered rings (C₄H₄X), it is important to notice that while the crossed contributions to δ_π do not give the expected trends for the aromatic systems, the aromaticity analysis clearly confirms the higher aromaticity of *N* vs *N* − 2 and *N* + 2 for the aromatic X = CH[−], NH, O, S, and P[−], whereas the *N* ring is the least aromatic for X = BH, SiH⁺, and F₂. The aromaticity analysis carried out for the PAHs also shows the expected trends derived from the δ_π values. It is important to notice the decrease of MCI of these polycyclic systems as compared to benzene, as well as the smaller differences between antiaromatic *N* − 2 and aromatic *N* systems. Moreover, when the effects of multiplicity are taken into account, the MCI values show opposite trends between lowest-lying singlet and triplet states according to Baird's rule.

Finally, Table S7 (see supplementary information†) encloses the values corresponding to HOMA, FLU, and NICS aromaticity criteria. There is a very good correspondence of these indices with MCI, thus corroborating the trends obtained with this electronic indicator of aromaticity. The only exceptions have been found for the *N* − 2 species of C₄H₄, C₄H₄BH, C₄H₄SiH⁺ and C₄H₄F₂, where NICS(0) and NICS(0)_{zz} predict antiaromatic behavior whereas the opposite trend is found for the rest of the indices. In particular and in contrast to NICS(0), NICS(1) and NICS(1)_{zz} show aromatic character for these *N* − 2 species and predict the correct trends for all the systems analyzed. For aromatic organic compounds, NICS(1) is considered to better reflect the π-electron effects than NICS(0).⁵³ Moreover, MCI, HOMA, FLU and NICS indices agree with the Baird's rule and predict a reduction of aromaticity for the lowest-lying triplet state when the lowest-lying

Table 7 MCI measures of the series of compounds. *A* and *B* refer to the different rings in the PAH (see Scheme 3). Units are electrons

	<i>N</i> − 2	<i>N</i>	<i>N</i> + 2
C ₆ H ₆	−0.020	0.073	0.002
C ₅ H ₅ N	−0.010	0.069	0.004
Pyridazine	0.000	0.070	0.002
Pyrimidine	0.001	0.066	0.002
Pyrazine	0.006	0.066	0.003
Triazine	−0.016	0.064	0.002
C ₇ H ₇ ⁺	−0.005	0.058	−0.017
C ₄ H ₄	0.183	0.009	0.064
C ₈ H ₈	0.040	−0.001	0.014
C ₅ H ₅ [−]	−0.028	0.072	0.010
C ₄ H ₄ NH	−0.014	0.050	0.011
C ₄ H ₄ O	−0.010	0.029	0.013
C ₄ H ₄ S	−0.021	0.041	0.014
C ₄ H ₄ P [−]	−0.019	0.068	0.014
C ₄ H ₄ BH	0.022	−0.003	0.040
C ₄ H ₄ SiH ⁺	0.037	−0.006	0.057
C ₄ H ₄ F ₂	0.017	−0.005	0.023
Naphthalene	0.020	0.039	0.018
Quinoline ^A	0.021	0.037	0.016
Quinoline ^B	0.008	0.038	0.020
Anthracene ^A	0.028	0.029	0.025
Anthracene ^B	0.013	0.027	0.012
Phenanthrene ^A	0.019	0.047	0.020
Phenanthrene ^B	0.010	0.018	0.008
Biphenylene ^A	0.008	0.056	0.010
Biphenylene ^B	0.054	0.021	0.016
Acenaphthylene ^A	0.014	0.038	0.019
Acenaphthylene ^B	0.005	0.011	0.034
Pyracylene ^A	0.015	0.032	0.019
Pyracylene ^B	0.017	0.012	0.030
C ₆ H ₆ (<i>t</i>)	0.079	−0.002	0.036
C ₈ H ₈ (<i>t</i>)	−0.002	0.028	0.007

singlet state is aromatic and *viceversa*. Just to conclude, even though we have calculated NICS for all systems (see Table S7 of the supplementary information†), it should be mentioned that the manner in which we compute the open-shell NICS values is somewhat lacking in rigour.⁵⁴

Conclusions

In the present work, we have analyzed the changes in the crossed contributions to the total π electronic delocalization (δ_π) when two electrons are added or removed for a given species and we have shown that the patterns derived can be used to distinguish between aromatic and antiaromatic systems. Remarkably, all crossed terms contribute to the description of the aromaticity and antiaromaticity of the system. For aromatic benzene, *ortho* (δ_π^{1,2}) and *para* (δ_π^{1,4}) contributions increase and *meta* (δ_π^{1,3}) decrease from antiaromatic C₆H₆²⁺ or C₆H₆^{2−} to aromatic C₆H₆. Likewise, for the antiaromatic cyclobutadiene, from aromatic C₄H₄²⁺ to antiaromatic C₄H₄ δ_π^{1,2} increases and δ_π^{1,3} decreases. Both of the alternation patterns are kept for larger aromatic and antiaromatic rings. Aromatic 5-MR systems are the only exception to the general behavior found and this may be attributed to the fact that for such small ring size, δ_π^{1,3} could also be considered δ_π^{1,4} depending whether one follows clockwise or anticlockwise directions in the ring when going from one atom to the farthest one in the ring. It has been proven that the expected alternation pattern is kept for large annulenes like C₁₆H₁₆, although

becomes smaller when the separation between the atoms involved increases. The rules presented are also perfectly valid for planar polycyclic aromatic hydrocarbons. In addition, crossed terms show opposite trends between lowest-lying singlet and triplet states in line with the Baird's rule. Finally, the aromaticity of the rings has been corroborated by means of the MCI, HOMA, NICS, and FLU indices of aromaticity.

As a whole, the present analysis based on crossed terms of the delocalization index represents a step forward towards a better comprehension of the electronic delocalization behavior of aromatic or antiaromatic systems. We consider that this analysis can be extended to the analysis of aromaticity/antiaromaticity in pure metal and semi-metal aromatic clusters or to evaluate the strength of the conjugation and hyperconjugation effects in conjugated systems. More research is underway in our laboratory concerning these particular issues.

Acknowledgements

Financial help has been granted by the Spanish MEC Project No. CTQ2008-03077/BQU and by the Catalan DIUE through project No. 2009SGR637. F. F. and J. P. thank the MEC for the doctoral fellowship No. AP2005-2997 and the Ramón y Cajal contract, respectively. E. M. acknowledges financial support from the Lundbeck Foundation Center and from the Marie Curie IntraEuropean Fellowship, Seventh Framework Programme (FP7/2007-2013), under grant agreement No. PIEF-GA-2008-221734, and from the Polish Ministry of Science and Higher Education (Project No. N N204 215634). M.S. is indebted to the Catalan DIVE for financial support through the ICREA Academia Prize 2009. We thank the Centre de Supercomputació de Catalunya (CESCA) for partial funding of computer time.

References

- 1 P. Hückel, *Z. Phys.*, 1931, **70**, 204; P. Hückel, *Z. Phys.*, 1932, **76**, 628.
- 2 E. C. Crocker, *J. Am. Chem. Soc.*, 1922, **44**, 1618.
- 3 W. v. E. Doering and L. H. Knox, *J. Am. Chem. Soc.*, 1954, **76**, 3203.
- 4 S. Kikuchi, *J. Chem. Educ.*, 1997, **74**, 194.
- 5 I. Mayer, *Theor. Chem. Acc.*, 2010, **125**, 203.
- 6 C. Glidewell and D. Lloyd, *Tetrahedron*, 1984, **40**, 4455.
- 7 N. C. Baird, *J. Am. Chem. Soc.*, 1972, **94**, 4941.
- 8 R. Breslow, H. W. Chang, R. Hill and E. Wasserman, *J. Am. Chem. Soc.*, 1967, **89**, 1112; M. Saunders, R. Berger, A. Jaffe, J. M. McBride, J. O'Neill, R. Breslow, J. M. Hoffmann Jr., C. Perchonock, E. Wasserman, R. S. Hutton and V. J. Huck, *J. Am. Chem. Soc.*, 1973, **95**, 3017.
- 9 H. J. Wörner and F. Merkt, *Angew. Chem., Int. Ed.*, 2006, **45**, 293.
- 10 N. Mizoguchi, *Chem. Phys. Lett.*, 1984, **106**, 451.
- 11 A. Hirsch, Z. Chen and H. Jiao, *Angew. Chem., Int. Ed.*, 2000, **39**, 3915; Z. H. Chen, H. J. Jiao, A. Hirsch and W. Thiel, *Mol. Model.*, 2001, **7**, 161; Z. F. Chen, A. Hirsch, S. Nagase, W. Thiel and P. v. R. Schleyer, *J. Am. Chem. Soc.*, 2003, **125**, 15507.
- 12 M. Randić, *Chem. Rev.*, 2003, **103**, 3449.
- 13 D. Plavšić, S. Nikolic and N. Trinajstić, *J. Math. Chem.*, 1991, **8**, 113.
- 14 A. I. Boldyrev and L. S. Wang, *Chem. Rev.*, 2005, **105**, 3716; C. A. Tsipis, *Coord. Chem. Rev.*, 2005, **249**, 2740; H.-J. Zhai, A. E. Kuznetsov, A. Boldyrev and L.-S. Wang, *ChemPhysChem*, 2004, **5**, 1885; F. De Proft, P. W. Fowler, R. W. A. Havenith, P. v. R. Schleyer, G. Van Lier and P. Geerlings, *Chem.-Eur. J.*, 2004, **10**, 940; A. N. Alexandrova, A. I. Boldyrev, H.-J. Zhai and L.-S. Wang, *J. Phys. Chem. A*, 2004, **108**, 3509; Y. Jung, T. Heine, P. v. R. Schleyer and M. Head-Gordon, *J. Am. Chem. Soc.*, 2004, **126**, 3132.
- 15 R. C. Haddon, *J. Am. Chem. Soc.*, 1979, **101**, 1722; I. Gutman, M. Milun and N. Trinajstić, *J. Am. Chem. Soc.*, 1977, **99**, 1692.
- 16 H. J. Jiao, P. v. R. Schleyer, Y. Mo, M. A. McAllister and T. T. Tidwell, *J. Am. Chem. Soc.*, 1997, **119**, 7075.
- 17 E. Steiner and P. W. Fowler, *Chem. Commun.*, 2001, 2220; E. Steiner and P. W. Fowler, *J. Phys. Chem. A*, 2001, **105**, 9553; A. Soncini, P. W. Fowler and F. Zerbetto, *Chem. Phys. Lett.*, 2005, **405**, 136.
- 18 P. W. Fowler, E. Steiner and L. W. Jenneskens, *Chem. Phys. Lett.*, 2003, **371**, 719.
- 19 S. Villaume, H. A. Fogarty and H. Ottosson, *ChemPhysChem*, 2008, **9**, 257.
- 20 P. C. Hiberty, D. Danovich, A. Shurki and S. Shaik, *J. Am. Chem. Soc.*, 1995, **117**, 7760; P. C. Hiberty and S. Shaik, *Theor. Chem. Acc.*, 2005, **114**, 169; P. C. Hiberty and S. S. Shaik, *Phys. Chem. Chem. Phys.*, 2004, **6**, 224; S. Shaik, S. Zilberg and Y. Haas, *Acc. Chem. Res.*, 1996, **29**, 211; S. S. Shaik and P. C. Hiberty, *J. Am. Chem. Soc.*, 1985, **107**, 3089; S. S. Shaik, P. C. Hiberty, J.-M. Le Four and G. Ohanessian, *J. Am. Chem. Soc.*, 1987, **109**, 363; S. S. Shaik, A. Shurki, D. Danovich and P. C. Hiberty, *Chem. Rev.*, 2001, **101**, 1501; S. C. A. H. Pierrefixe and F. M. Bickelhaupt, *Chem.-Eur. J.*, 2007, **13**, 6321; A. Gobbi, Y. Yamaguchi, G. Frenking and H. F. Schaefer III, *Chem. Phys. Lett.*, 1995, **244**, 27; A. Rehaman, A. Datta, S. S. Mallajosyula and S. K. Pati, *J. Chem. Theory Comput.*, 2006, **2**, 30; K. Jug and A. M. Koster, *J. Am. Chem. Soc.*, 1990, **112**, 6772; N. D. Epitotis, *Pure Appl. Chem.*, 1983, **55**, 229.
- 21 R. Dabestani and I. N. Ivanov, *Photochem. & Photobiol.*, 1999, **70**, 10.
- 22 N. Sadlej-Sosnowska, *J. Org. Chem.*, 2001, **66**, 8737.
- 23 J. Poater, M. Duran, M. Solà and B. Silvi, *Chem. Rev.*, 2005, **105**, 3911; G. Merino, A. Vela and T. Heine, *Chem. Rev.*, 2005, **105**, 3812.
- 24 F. Feixas, E. Matito, M. Solà and J. Poater, *J. Phys. Chem. A*, 2008, **112**, 13231.
- 25 E. Matito, M. Solà, P. Salvador and M. Duran, *Faraday Discuss.*, 2007, **135**, 325.
- 26 E. Matito, J. Poater, M. Solà, M. Duran and P. Salvador, *J. Phys. Chem. A*, 2005, **109**, 9904.
- 27 P. Bultinck, D. L. Cooper and R. Ponec, *J. Phys. Chem. A*, 2010, DOI: 10.1021/jp101707w.
- 28 R. F. W. Bader, *Acc. Chem. Res.*, 1985, **18**, 9; R. F. W. Bader, *Atoms in Molecules: A Quantum Theory*, Clarendon, Oxford, 1990; R. F. W. Bader, *Chem. Rev.*, 1991, **91**, 893.
- 29 I. Mayer and P. Salvador, *Chem. Phys. Lett.*, 2004, **383**, 368.
- 30 P. Bultinck, M. Rafat, R. Ponec, B. van Ghele, R. Carbó-Dorca and P. Popelier, *J. Phys. Chem. A*, 2006, **110**, 7642.
- 31 E. Matito, P. Salvador, M. Duran and M. Solà, *J. Phys. Chem. A*, 2006, **110**, 5108.
- 32 P. Bultinck, R. Ponec and S. Van Damme, *J. Phys. Org. Chem.*, 2005, **18**, 706.
- 33 F. Feixas, E. Matito, J. Poater and M. Solà, *J. Comput. Chem.*, 2008, **29**, 1543.
- 34 M. Giambiagi, M. S. de Giambiagi, C. D. dos Santos and A. P. de Figueiredo, *Phys. Chem. Chem. Phys.*, 2000, **2**, 3381.
- 35 L. Lain, A. Torre, R. C. Boicchio and R. Ponec, *Chem. Phys. Lett.*, 2001, **346**, 283.
- 36 J. Cioslowski, E. Matito and M. Solà, *J. Phys. Chem. A*, 2007, **111**, 6521.
- 37 P. Bultinck, R. Ponec, A. Gallegos, S. Fias, S. Van Damme and R. Carbó-Dorca, *Croat. Chem. Acta*, 2006, **79**, 363; M. Mandado, M. J. González-Moa and R. A. Mosquera, *J. Comput. Chem.*, 2007, **28**, 127; M. Mandado, M. J. González-Moa and R. A. Mosquera, *J. Comput. Chem.*, 2007, **28**, 1625.
- 38 J. Kruszewski and T. M. Krygowski, *Tetrahedron Lett.*, 1972, **13**, 3839; T. M. Krygowski and M. K. Cyranski, *Chem. Rev.*, 2001, **101**, 1385.
- 39 P. v. R. Schleyer, C. Maerker, A. Dransfeld, H. Jiao and N. J. R. van Eikema Hommes, *J. Am. Chem. Soc.*, 1996, **118**, 6317; Z. F. Chen, C. S. Wannere, C. Corminboeuf, R. Puchta and P. v. R. Schleyer, *Chem. Rev.*, 2005, **105**, 3842.

- 40 E. Matito, M. Duran and M. Solà, *J. Chem. Phys.*, 2005, **122**, 014109; Erratum: E. Matito, M. Duran and M. Solà, *J. Chem. Phys.*, 2006, **125**, 059901.
- 41 M. J. Frisch, G. W. Trucks, H. B. Schlegel, G. E. Scuseria, M. A. Robb, J. R. Cheeseman, J. A. Montgomery Jr., T. Vreven, K. N. Kudin, J. C. Burant, J. M. Millam, S. S. Iyengar, J. Tomasi, V. Barone, B. Mennucci, M. Cossi, G. Scalmani, N. Rega, G. A. Petersson, H. Nakatsuji, M. Hada, M. Ehara, K. Toyota, R. Fukuda, J. Hasegawa, M. Ishida, T. Nakajima, Y. Honda, O. Kitao, H. Nakai, M. Klene, X. Li, J. E. Knox, H. P. Hratchian, J. B. Cross, V. Bakken, C. Adamo, J. Jaramillo, R. Gomperts, R. E. Stratmann, O. Yazyev, A. J. Austin, R. Cammi, C. Pomelli, J. W. Ochterski, P. Y. Ayala, K. Morokuma, G. A. Voth, P. Salvador, J. J. Dannenberg, G. Zakrzewski, S. Dapprich, A. D. Daniels, M. C. Strain, O. Farkas, D. K. Malick, A. D. Rabuck, K. Raghavachari, J. B. Foresman, J. V. Ortiz, Q. Cui, A. G. Baboul, S. Clifford, J. Cioslowski, B. B. Stefanov, G. Liu, A. Liashenko, P. Piskorz, I. Komaromi, R. L. Martin, D. J. Fox, T. Keith, M. A. Al-Laham, C. Y. Peng, A. Nanayakkara, M. Challacombe, P. M. W. Gill, B. Johnson, W. Chen, M. W. Wong, C. Gonzalez and J. A. Pople, *GAUSSIAN 03*, Revision C.01 edn, Gaussian Inc., Pittsburgh, PA, 2003.
- 42 F. W. Biegler-König, R. F. W. Bader and T.-H. Tang, *J. Comput. Chem.*, 1982, **3**, 317.
- 43 A. D. Becke, *J. Chem. Phys.*, 1993, **98**, 5648; C. Lee, W. Yang and R. G. Parr, *Phys. Rev. B: Condens. Matter*, 1988, **37**, 785; P. J. Stephens, F. J. Devlin, C. F. Chabalowski and M. J. Frisch, *J. Phys. Chem.*, 1994, **98**, 11623.
- 44 R. Krishnan, J. S. Binkley, R. Seeger and J. A. Pople, *J. Chem. Phys.*, 1980, **72**, 650; M. J. Frisch, J. A. Pople and J. S. Binkley, *J. Chem. Phys.*, 1984, **80**, 3265.
- 45 E. Matito, *ESI-3D: Electron Sharing Indices Program for 3D Molecular Space Partitioning* (<http://iqc.udg.edu/~eduard/ESI>), Institute of Computational Chemistry, Girona, 2006.
- 46 J. Poater, M. Solà, M. Duran and X. Fradera, *Theor. Chem. Acc.*, 2002, **107**, 362.
- 47 R. L. Fulton, *J. Phys. Chem.*, 1993, **97**, 7516.
- 48 R. F. W. Bader, A. Streitwieser, A. Neuhaus, K. E. Laidig and P. Speers, *J. Am. Chem. Soc.*, 1996, **118**, 4959.
- 49 J. Poater, X. Fradera, M. Duran and M. Solà, *Chem.–Eur. J.*, 2003, **9**, 400.
- 50 R. L. Fulton and S. T. Mixon, *J. Phys. Chem.*, 1993, **97**, 7530.
- 51 D. B. Chesnut, *Chem. Phys.*, 2009, **358**, 75.
- 52 G. Portella, J. Poater, J. M. Bofill, P. Alemany and M. Solà, *J. Org. Chem.*, 2005, **70**, 2509; Erratum: G. Portella, J. Poater, J. M. Bofill, P. Alemany and M. Solà, *J. Org. Chem.*, 2005, **70**, 4560.
- 53 C. Corminboeuf, T. Heine, G. Seifert, P. v. R. Schleyer and J. Weber, *Phys. Chem. Chem. Phys.*, 2004, **6**, 273; P. v. R. Schleyer, M. Manoharan, H. J. Jiao and F. Stahl, *Org. Lett.*, 2001, **3**, 3643.
- 54 V. Gogonea, P. v. R. Schleyer and P. R. Schreiner, *Angew. Chem., Int. Ed.*, 1998, **37**, 1945; E. D. Becker, C. L. Fisk and C. L. Khetrapal, in *Encyclopedia of Nuclear Magnetic Resonance*, ed. D. M. Grant and R. K. Harris, Wiley, Chichester, 1996, vol. 1, p. 41.

7.3 Aromaticity and electronic delocalization in all-metal clusters with single, double, and triple aromatic character

Feixas, F.; Matito, E.; Duran, M.; Poater, J.; Solà, M.; *Theor. Chem. Acc.* Accepted for publication, **2010**

Aromaticity and electronic delocalization in all-metal clusters with single, double, and triple aromatic character

Ferran Feixas · Eduard Matito · Miquel Duran ·
Jordi Poater · Miquel Solà

Received: 4 July 2010 / Accepted: 23 August 2010
© Springer-Verlag 2010

Abstract A series of monocyclic planar inorganic compounds with single, double, and triple (anti)aromatic character has been studied. The electron delocalization and aromaticity of these compounds have been assessed by means of two-center and multicenter electronic delocalization indices and their σ -, π -, and δ -components. Results show that these indices are excellent predictors of the σ -, π -, and δ -aromatic character of all-metal and semimetal clusters.

Keywords Electronic multicenter delocalization indices · Inorganic rings · Aromaticity · DFT calculations

1 Introduction

There is hardly a need to stress the important role played by the concept of aromaticity in chemistry. Since the discovery in 1825 of benzene by Michael Faraday [1] and after almost two centuries of intense developments, aromaticity

remains a major research motivation in chemistry. In fact, the last decade has witnessed exciting advances in aromaticity. Among them, we can refer to the introduction of electronic indices [2, 3] as reliable measures of local aromaticity and the definition of more refined magnetic-based indicators [4], although undoubtedly the most important recent breakthrough in the field of aromaticity took place in 2001 when Boldyrev, Wang et al., observed for the first time aromaticity in Al_4^{2-} , an all-metal compound [5]. The rapid synthesis and characterization of new all-metal and semimetal clusters exhibiting aromaticity further fueled the interest in these systems [6–8]. At variance with the classical aromatic organic molecules that possess only π -electron delocalization, these clusters can have σ -, π -, and δ - (involving d orbitals) [9–11] or even ϕ - (involving f orbitals) [12] electron delocalization, exhibiting characteristics of what has been called multifold aromaticity [6–8, 13–16].

The presence of multifold aromaticity and the lack of all-metal and semimetal aromatic clusters that can serve as inorganic reference systems (like benzene does in classical aromatic organic molecules) make the measure of aromaticity in these new systems much more complicated. Indeed, most of the current available methods to quantify aromaticity have been designed to measure the aromaticity of organic molecules and take benzene or other aromatic organic molecules as a reference in their definitions. This is the case of, for instance, the structural-based harmonic oscillator model of aromaticity (HOMA) [17, 18] or the electronic-based descriptors such as the aromatic fluctuation (FLU) index [19], the bond order index of aromaticity (BOIA) [20], or the aromaticity descriptor θ proposed by Matta and Hernández-Trujillo [21, 22]. Likewise, energetic-based indicators such as resonance energies (RE) or aromatic stabilization energies (ASE) [23] are difficult to

Published as part of the special issue celebrating theoretical and computational chemistry in Spain.

Electronic supplementary material The online version of this article (doi:10.1007/s00214-010-0805-8) contains supplementary material, which is available to authorized users.

F. Feixas · M. Duran · J. Poater · M. Solà (✉)
Institut de Química Computacional and Departament de
Química, Universitat de Girona, Campus de Montilivi,
17071 Girona, Catalonia, Spain
e-mail: miquel.sola@udg.edu

E. Matito
Institute of Physics, University of Szczecin,
70-451 Szczecin, Poland

Published online: 16 September 2010

 Springer

compute accurately in all-metal clusters because of the lack of appropriate reference systems [13, 24]. Although indices relying on reference systems are not adequate for the study of chemical reactivity [25], these methods are quite popular in the organic aromaticity realm. However, they cannot be applied directly to inorganic clusters without further refinements. For the moment, the most widely used methods to discuss aromaticity in inorganic clusters are the basic electron counting based on the $4n + 2$ Hückel's rule [26–29] and the magnetic-based indicators of aromaticity, in particular, the nucleus-independent chemical shifts (NICS) [30]. A great advantage of NICS, apart from being very accessible and easy to compute, is that it does not use reference values, so it can be easily applied to any molecule.

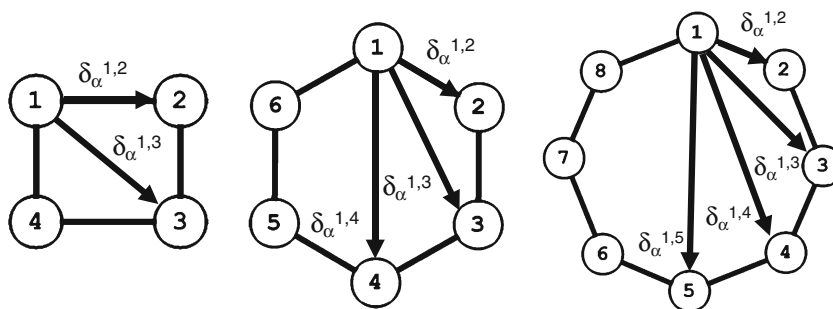
Less common is the use of electronic multicenter indices (MCI) [20, 31–34] to study multifold aromaticity in inorganic species [35–37]. As for NICS, the MCI definition is general and free from reference values. In recent work [38, 39], we have shown that MCI does an excellent work in inorganic aromatic clusters providing aromaticity trends that are superior to those furnished by NICS. An interesting property of the MCI index is that for planar systems with only σ - and π -occupied orbitals the total MCI value can be exactly decomposed into their σ - and π -components. For planar species with additional occupied orbitals of δ -type, the separation into the different components is not exact because of some σ - and δ -orbital mixing within a given atomic domain. However, the errors introduced by assuming exact separability in these systems turn out to be in general negligible (vide infra). The first aim of the present manuscript is to examine whether the separation of the MCI values into the σ -, π -, and δ -components for a series of well-studied all-metal (anti)aromatic clusters can provide valuable information about the different σ -, π -, and δ -contributions to the total aromatic character of the molecules.

We have also recently shown that changes in the so-called crossed contributions (for instance, the ortho-, meta-, and para-components in six-membered rings, 6-MRs) to the total π -electronic delocalization (δ_π) when two

electrons are added or removed for a given species can be used to distinguish between aromatic and antiaromatic systems [40, 41]. Thus, we have found that for benzene, ortho ($\delta_\pi^{1,2}$) and para ($\delta_\pi^{1,4}$) contributions increase and meta ($\delta_\pi^{1,3}$) decreases from antiaromatic $C_6H_6^{2+}$ or $C_6H_6^{2-}$ to aromatic C_6H_6 . Likewise, for the antiaromatic cyclobutadiene, from aromatic $C_4H_4^{2+}$ to antiaromatic C_4H_4 the $\delta_\pi^{1,2}$ contribution increases and $\delta_\pi^{1,3}$ decreases. Moreover, we found that the crossed term corresponding to the two farthest atoms in the ring (i.e., $\delta_\pi^{1,3}$ in 4-MRs, $\delta_\pi^{1,4}$ in 6-MRs or $\delta_\pi^{1,5}$ in 8-MRs, see Fig. 1) decreases in aromatic species when two electrons are added or removed, whereas the opposite is true for antiaromatic species [41]. It was reported that this crossed term is higher for the most aromatic molecule in a series of same-membered rings [41]. As a second main objective of this work, we want to investigate whether such alternation patterns are also present in the all-metal inorganic cluster Al_4^{2-} , not only for total π -electronic delocalization but also for the total σ -component of the electronic delocalization. In addition, we aim to know whether the crossed term corresponding to the two farthest atoms in the ring can be a good descriptor of aromaticity in all-metal and semimetal clusters.

To reach these goals, we have chosen a series of all-metal clusters with well-established aromatic character. In particular, we will discuss electron delocalization and aromaticity in some 4-MRs having, first, double σ - and π -aromaticity (Al_4^{2-} [5, 13, 24, 35, 36, 42–51], MAl_4^- ($M = Li, Na, Cu$) [35, 49, 52, 53], Al_3Ge^- [54], Al_2Ge_2 [16, 55], $AlGe_3^+$ [56], and Ge_4^{2+} [56]), and, second, σ -aromaticity and π -antiaromaticity (the Al_4^{4-} unit attached to Li^+ cations, $Li_xAl_4^{q\pm}$ [49–51, 57, 58]). Then, we have selected a series of transition-metal 3-MRs with single σ -aromaticity (Cu_3^+) [59], conflicting σ -aromaticity (Cu_3H_3) [60], double σ - and π -aromaticity (Y_3^- and La_3^-) [61], double π - and δ -aromaticity ($Ta_3O_3^-$) [10], and finally, triple σ -, π -, and δ -aromaticity (Hf_3) [11, 62]. In addition, the aromaticity of two open-shell species, $^5Ta_3^-$ [62] and 3Hf_3 [11], will be analyzed in detail. We shall reach the conclusion, which we anticipate here, that both MCI and the analysis of crossed contributions to the total

Fig. 1 Decomposition of electron delocalization in crossed-terms $\delta_\alpha^{1,x}$ ($\alpha = \sigma, \pi, \delta \dots$) for four-, six-, and eight-membered rings



σ -, π -, and δ -electronic delocalization are excellent indicators of σ -, π -, and δ -aromaticity in inorganic clusters.

2 Computational details

All calculations reported in this work were performed by means of the Gaussian03 [63] computational package. The gas-phase optimized geometries reported here were calculated in the framework of density-functional theory (DFT) using the B3LYP functional [64] which combines the three-parameter Becke's exchange non-local functional [65] and the Lee–Yang–Parr's correlation non-local functional [66]. The 6–311+G(d) basis set [67, 68] was used for all calculations, except for the study of the Cu_3^+ , Cu_3H_3 , Y_3^- , La_3^- , Ta_3O_3^- , Hf_3 , $^5\text{Ta}_3^-$, and $^3\text{Hf}_3$ species for which we have used the Stuttgart 14-valence-electron pseudopotentials and the valence basis sets augmented with two f-type polarization functions [69, 70] in order to take into account relativistic effects. In Cu_3H_3 and Ta_3O_3^- , the aug-cc-pVTZ basis set [71, 72] was used for the H and O atoms. To ensure that a minimum on the potential energy surface (PES) was obtained, we carried out vibrational frequency calculations at the same level, either B3LYP/6–311+G(d) or B3LYP/X/Stuttgart+2f (X = Cu, Y, La, Ta, and Hf).

We report here results for an unstable dianion such as Al_4^{2-} . In a recent work, Lambrecht et al. [73] have shown that Al_4^{2-} is unstable when compared to $\text{Al}_4^- + \text{free } e^-$ and, consequently, its properties change significantly when increasing the number of diffuse functions in the basis set. Indeed, after inclusion of certain number of diffuse functions, the Al_4^{2-} evolves to $\text{Al}_4^- + \text{free } e^-$. In this sense, Lambrecht et al. [73] warned about the validity of calculations carried out for such unstable dianions. In a recent comment [74] (see also the rebuttal in Ref. [75]) on the work by Lambrecht et al. [73], Zubarev and Boldyrev argued against this point of view and considered that the bound state of the individual Al_4^{2-} is an adequate model of Al_4^{2-} in a stabilizing environment such as in LiAl_4^- or Li_2Al_4 . They also considered that calculations for isolated Al_4^{2-} species using a 6–311+G(d) basis provide an accurate model for the Al_4^{2-} unit embedded in a stabilizing environment. Following the Zubarev and Boldyrev arguments [74], we will discuss the properties of the bound state of Al_4^{2-} by employing the 6–311+G(d) basis set. The same hypothesis has been assumed in the calculations of the isolated Al_4^{4-} and $\text{Li}_2\text{Al}_4^{2-}$ species.

In this work, we measure the electron delocalization by means of the so-called delocalization indices (DIs), or in a more general nomenclature, the electron sharing indices (ESIs) [76–78]. The ESI value between atoms A and B , $\delta(A,B)$ is obtained by double integration of the exchange–

correlation density ($\gamma_{XC}(\vec{r}_1, \vec{r}_2)$) [79] over the molecular space regions corresponding to atoms A and B ,

$$\delta(A,B) = -2 \int_A \int_B \gamma_{XC}(\vec{r}_1, \vec{r}_2) d\vec{r}_1 d\vec{r}_2 \quad (1)$$

For monodeterminantal wave functions, one obtains:

$$\delta(A,B) = 2 \sum_{ij}^{occ.MSO} S_{ij}(A)S_{ij}(B) \quad (2)$$

The summations in Eq. (2) run over all occupied molecular spin-orbitals (MSOs). $S_{ij}(A)$ is the overlap between MOs i and j within the molecular space assigned to atom A . $\delta(A,B)$ provides a quantitative idea of the number of electrons delocalized or shared between atoms A and B .

To study the delocalization effects upon extraction or addition of two electrons, we calculate the total delocalization, which for planar systems with only σ - and π -occupied orbitals can be exactly split ($S_{\sigma\pi}(A) = 0$) into the σ - and π -contributions.

$$\begin{aligned} \delta_{tot} &= \sum_{A_i, A_i \neq A_j} \delta(A_i, A_j) = \sum_{A_i, A_i \neq A_j} \delta_\pi(A_i, A_j) \\ &+ \sum_{A_i, A_i \neq A_j} \delta_\sigma(A_i, A_j) = \delta_\pi + \delta_\sigma \end{aligned} \quad (3)$$

In the case of species with occupied orbitals of δ -symmetry, we have also computed the δ_δ component (see Supporting Information), although in this case the separation in δ_σ , δ_π , and δ_δ is not strictly exact.

In addition, δ_α ($\alpha = \sigma, \pi$, and δ) can be split into the different crossed contributions in the ring. For instance, for a given four-membered ring (4-MR) we have ortho- (1,2) and meta- (1,3) terms (see Fig. 1). In our study, we have considered averaged values for the crossed terms, so in a 4-MR we have:

$$\begin{aligned} \delta_\alpha &= 4\delta_\alpha^{1,2} + 2\delta_\alpha^{1,3} \\ \delta_\alpha^{1,2} &= \frac{\delta_\alpha(1,2) + \delta_\alpha(2,3) + \delta_\alpha(3,4) + \delta_\alpha(1,4)}{4} \\ \delta_\alpha^{1,3} &= \frac{\delta_\alpha(1,3) + \delta_\alpha(2,4)}{2} \end{aligned} \quad (4)$$

For the aromaticity analysis, we have also applied the multicenter index (MCI) [20, 32]. MCI is a particular extension of the I_{ring} index [31].

$$I_{\text{ring}}(\mathcal{A}) = \sum_{i_1, i_2, \dots, i_N} n_{i_1} \dots n_{i_N} S_{i_1 i_2}(A_1) S_{i_2 i_3}(A_2) \dots S_{i_N i_1}(A_N) \quad (5)$$

n_i being the occupancy of MO i and $\mathcal{A} = \{A_1, A_2, \dots, A_N\}$ a string containing the set of N atoms forming the ring structure. Summing up all I_{ring} values resulting from the

permutations of indices A_1, A_2, \dots, A_N , the mentioned MCI index [32] is defined as:

$$\text{MCI}(\mathcal{A}) = \frac{1}{2N} \sum_{P(\mathcal{A})} I_{\text{ring}}(\mathcal{A}) \quad (6)$$

where $P(\mathcal{A})$ stands for a permutation operator that interchanges the atomic labels A_1, A_2, \dots, A_N to generate the $N!$ permutations of the elements in the string \mathcal{A} [20, 34]. MCI and I_{ring} give an idea of the electron sharing between all atoms in the ring. The more positive the MCI values [32, 33, 80], the more aromatic the rings. For planar species with only σ - and π -occupied orbitals, the MCIs like the DIs can be exactly split into the σ - and π -contributions:

$$\text{MCI}(\mathcal{A}) = \text{MCI}_\sigma(\mathcal{A}) + \text{MCI}_\pi(\mathcal{A}) \quad (7)$$

In planar systems with σ - and δ -occupied orbitals, the exact separation between the σ - and δ -components is not possible. In addition, in non-planar systems MCI cannot be exactly separated into σ -, π -, and δ -components. In these cases, we have partitioned MCI into the different contributions in two different ways. First through Eqs. (8–10) by adding the orbital contributions of those orbitals that belong to (or are assumed to belong to) a given symmetry α ($\alpha = \sigma, \pi$, and δ):

$$\text{MCI}(\mathcal{A}) = \sum_{\alpha=\sigma,\pi,\delta,\dots} \text{MCI}_\alpha^{\text{orb}}(\mathcal{A}) \quad (8)$$

$$\text{MCI}_\alpha^{\text{orb}}(\mathcal{A}) = \frac{1}{2N} \sum_{P(\mathcal{A})} I_{\text{ring},\alpha}^{\text{orb}}(\mathcal{A}) \quad (9)$$

$$I_{\text{ring},\alpha}^{\text{orb}}(\mathcal{A}) = \sum_{i_1 \in \alpha, i_2 \in \alpha, \dots, i_N \in \alpha} n_{i_1} \dots n_{i_N} S_{i_1 i_2}(A_1) S_{i_2 i_3}(A_2) \dots S_{i_N i_1}(A_N) \quad (10)$$

In this way, the sum of all $\text{MCI}_\alpha^{\text{orb}}$ yields the exact MCI, but in each $\text{MCI}_\alpha^{\text{orb}}$ some mixing from MOs of different symmetry than α is possible. This was the method used in a previous work to separate DIs into their molecular orbital contributions [81]. An alternative is to substitute Eq. (10) by (11) that assumes $S_{\alpha\beta}(A) = 0$ ($\alpha, \beta = \sigma, \pi$, and δ) for $\alpha \neq \beta$:

$$I_{\text{ring},\alpha}^{\text{ovl}}(\mathcal{A}) = \sum_{i_1 \in \alpha, i_2 \in \alpha, \dots, i_N \in \alpha} n_{i_1} \dots n_{i_N} S_{i_1 i_2}(A_1) S_{i_2 i_3}(A_2) \dots S_{i_N i_1}(A_N) \quad (11)$$

Then, we have:

$$\text{MCI}_\alpha^{\text{ovl}}(\mathcal{A}) = \frac{1}{2N} \sum_{P(\mathcal{A})} I_{\text{ring},\alpha}^{\text{ovl}}(\mathcal{A}) \quad (12)$$

and

$$\text{MCI}(\mathcal{A}) \approx \text{MCI}^{\text{ovl}}(\mathcal{A}) = \sum_{\alpha=\sigma,\pi,\delta,\dots} \text{MCI}_\alpha^{\text{ovl}}(\mathcal{A}) \quad (13)$$

MCI is equal to MCI^{ovl} when the partition between the different components is exact. Otherwise MCI and MCI^{ovl} can differ, and the difference is a measure of the error made in the separation. MCI^{ovl} could be higher or lower than the exact MCI depending on the positive or negative contributions of the overlap products containing $S_{\alpha\beta}(A)$ terms. Despite not being strictly separable (vide supra), for systems with δ -orbitals we report MCIs values split into σ -, π -, and δ -components in the same way that we have described above. This feature is especially interesting to evaluate multifold aromaticity in all-metal clusters.

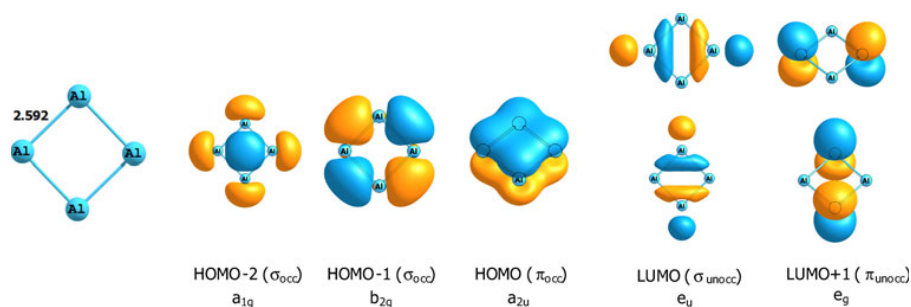
Finally, although several atomic partitions may be used for the calculations of the overlap between MOs i and j within the molecular space assigned to atom A [35, 78, 82, 83] to obtain both the DIs and MCIs, we have chosen in the present work the partition carried out in the framework of the quantum theory of atoms-in-molecules (QTAIM) of Bader [84–86], by which atoms are defined from the condition of zero-flux gradient in the one-electron density, $\rho(\mathbf{r})$. Calculation of overlap matrices and computation of MCI have been performed with the AIMPAC [87] and ESI-3D [88] collection of programs.¹ For molecules containing Ta and Hf, the QTAIM partition failed due to the presence of non-nuclear attractors, regions that cannot be directly associated with a given atomic region. In these cases, we used the “fuzzy atom” partition [89, 90] in which the atomic domains do not have boundaries. Instead, at every point \mathbf{r} of the space a weight factor $w_A(\mathbf{r})$ is defined for each atom, A , to measure to which extent the given point belongs to atom A . These atomic weight factors are chosen to be non-negative and satisfy the following condition when summing over all atoms of the system:

$$\sum_A w_A(\mathbf{r}) = 1 \quad (14)$$

where overlap matrix elements for an atom A are now:

$$S_{ij}(A) = \int \varphi_i^*(\mathbf{r}) w_A(\mathbf{r}) \varphi_j(\mathbf{r}) d\mathbf{r} \quad (15)$$

¹ The numerical accuracy of the QTAIM calculations has been assessed using two criteria: (1) The integration of the Laplacian of the electron density ($\nabla^2 \rho(\mathbf{r})$) within an atomic basin must be close to zero; and (2) The number of electrons in a molecule must be equal to the sum of all the electron populations of the molecule. For all atomic calculations, integrated absolute values of $\nabla^2 \rho(\mathbf{r})$ were always less than 0.001 a.u.. For all molecules, errors in the calculated number of electrons were always below 0.01 a.u.. It is important to mention that the default maximum distance from the nucleus used to integrate the atomic region has to be increased when diffuse functions are employed in the presence of metal atoms. In the AIMPAC program, the default integration maximum distance is 9.0 a.u.. However, we have found that this distance should be increased to 12.0 a.u. for the proper integration of Al and Ge atoms. If this value is not increased, the sum of all electron populations will not be equal to the number of electrons in a molecule. Consequently, these integration distances have to be changed in the input file.

Fig. 2 The low-lying occupied and unoccupied molecular orbitals of Al_4^{2-} 

“Fuzzy atom” DIs and MCIs were calculated with the FUZZY code [89, 91], which implements a Becke’s multi-center integration algorithm with Chebyshev and Lebedev radial and angular quadratures, respectively. A grid of 60 radial by 900 angular points per atom has been used in all cases. We have employed the Becke’s algebraic function with the recommended stiffness parameter $k = 3$. We have used the set of atomic radii determined by Koga [92].

3 Results and discussion

In this section, we first discuss the Al_4^{2-} compound and related species, in particular the $[\text{Al}_n\text{Ge}_{4-n}]^{q\pm}$ ($n = 0-4$) series, in detail. Then, the multifold aromaticity of Cu_3^+ , Cu_3H_3 , Y_3^- , La_3^- , Ta_3O_3^- , Hf_3 , $^5\text{Ta}_3^-$, and $^3\text{Hf}_3$ compounds is analyzed.

Al_4^{2-} is the quintessential all-metal aromatic cluster. The B3LYP/6-311+G(d) molecular structure and the lowest-lying occupied and unoccupied orbitals of Al_4^{2-} are depicted in Fig. 2. Al_4^{2-} contains a pair of delocalized π -electrons and two pairs of σ -electrons that contribute to the overall aromaticity of this species [5, 43, 47]. The two π -electrons obey the $4n + 2$ Hückel rule for monocyclic π -systems [26–29]. Although this is not the case for the σ electrons, it was found that the two pairs of delocalized σ electrons belong to molecular orbitals that follow orthogonal radial and tangential directions, which makes them to be totally independent [48], thus separately following the $4n + 2$ rule. The aromaticity of Al_4^{2-} has been confirmed by four criteria of aromaticity: energetic (resonance energies [13, 24, 48]), structural (planarity with equal bond lengths [5]), magnetic (ring currents [47, 49], induced magnetic field analysis [51], and nucleus-independent chemical shifts (NICS) values [6, 36]) and electronic (electron localization function (ELF) [93] plots [45], hardness and polarizability values [46], and MCI results [35, 36, 38]).

Table 1 lists the MCI and $\delta^{1,3}$ values and their σ - and π -components for Al_4 , Al_4^{2-} , and Al_4^{4-} species. The MCI and MCI_π values obtained for Al_4^{2-} are 0.356 and

Table 1 MCI, MCI_σ , $\delta^{1,3}$, and $\delta_\alpha^{1,3}$ ($\alpha = \sigma$ and π) indices for the Al_4 , Al_4^{2-} , and Al_4^{4-} units at the B3LYP/6-311+G(d) level of theory

	$N - 2_{(2\pi, e^-)}$ $\text{Al}_4 (a_{1g})^a$	$N - 2_{(0\pi, e^-)}$ $\text{Al}_4 (a_{2u})^b$	$N - 2_{(2\pi, e^-)}$ $\text{Al}_4 (b_{2g})^a$	$N_{(2\pi, e^-)}$ Al_4^{2-}	$N + 2_{(4\pi, e^-)}$ $\text{Al}_4^{4-} (e_g)^b$
MCI	0.197	0.182	0.325	0.356	0.222
MCI_σ	0.010	0.182	0.138	0.169	0.210
MCI_π	0.187	0.000	0.187	0.187	0.012
$\delta^{1,3}$	0.437	0.551	0.710	0.817	0.629
$\delta_\sigma^{1,3}$	0.187	0.551	0.460	0.567	0.540
$\delta_\pi^{1,3}$	0.250	0.000	0.250	0.250	0.089
Aromaticity π		σ	$\sigma + \pi$	$\sigma + \pi$	σ

All values in atomic units

^a Orbital from which two electrons have been removed (see Fig. 1)

^b Orbital to which two electrons have been added (see Fig. 1)

0.187 a.u., respectively. The value of the MCI_π (0.1875 a.u. for a monodeterminantal wave function) can be easily obtained from symmetry arguments for any ring X_4 of D_{4h} symmetry with only 2π -electrons occupying the same orbital such as in Al_4^{2-} [38]. Our results indicate that the π delocalization in the Al_4^{2-} species is slightly larger than the σ one (0.187 vs. 0.169 a.u.). This is in line with the previous dissected NICS results [35, 38], showing that $\text{NICS}(0)_\pi$ is somewhat more negative than $\text{NICS}(0)_\sigma$ and also with the result from the ELF indicating higher π - than σ -aromaticity in Al_4^{2-} [45], but in contrast with the fact that the ring current in Al_4^{2-} has a negligible contribution from the two π -electron system [43, 44]. According to the MCI_σ and MCI_π values Al_4^{2-} is σ - and π -aromatic. Adding two electrons to one of the two LUMO+1 orbitals of Al_4^{2-} of e_g symmetry, we reach the singlet Al_4^{4-} species with four π -electrons. The singlet Al_4^{4-} species in this particular electronic state (two electrons in an e_g orbital) is not a true minimum. This is the only species among those reported in this work that it is not a minimum. In spite of that we discuss it here because the analysis of electron delocalization in this system gives interesting insight. As it can be seen in the values of Table 1, addition of these two electrons leads to an antiaromatic 4π -electron system as reflected by the important reduction in the MCI_π value when going from Al_4^{2-} to Al_4^{4-} . There is also some increase in the MCI_σ indicating that the Al_4^{4-} unit has

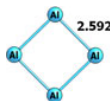
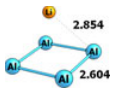
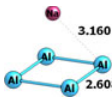
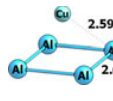
preserved the σ -aromatic character. Removal of two electrons from the Al_4^{2-} species can be performed from different orbitals leading to different states of the Al_4 unit. If one removes two electrons from the b_{2g} orbital, the effect on the MCI values is minor with a slight reduction in the MCI_σ value. On the other hand, if one takes out two electrons from the a_{1g} orbital of Al_4^{2-} , the reduction in the MCI_σ value is huge leading to an Al_4 unit with only π -aromaticity. This result is in agreement with the fact that according to the decomposition of the NICS into their canonical molecular orbital (CMO) components [94], the tangential b_{2g} orbital has a paratropic contribution to NICS ($\text{NICS}(b_{2g}) = +10.8$ ppm), while the radial a_{1g} orbital sustains a diatropic current ($\text{NICS}(a_{1g}) = -3.9$ ppm). Therefore, both the MCI and NICS point out that the contribution to the σ -aromaticity in Al_4^{2-} species of the two electrons in the radial σ -orbital is more important than that from the two electrons in the tangential σ -orbital. Finally, removal of the two electrons from the a_{2u} of π -symmetry results in a system with a significant MCI_σ value and σ -aromatic character.

MCI gives valuable information about the type of aromaticity (σ , π , or δ) present in all-metal clusters. In addition, it correctly orders a series of clusters according to their aromaticity [41]. It has, however, the problem that it does not provide information about antiaromaticity since in both non- and antiaromatic species electrons are localized and the MCI value is close to zero for the two cases [34]. Discrimination between non- and antiaromatic species can be achieved by analyzing the crossed term corresponding

to the two farthest atoms in the ring (i.e., $\delta_x^{1,3}$ in 4-MRs). This term decreases in aromatic species when two electrons are added or removed, whereas the opposite is true for antiaromatic species [41]. For non-aromatic species, this term suffers only minor changes upon addition or extraction of two electrons. Results in Table 1 confirm this trend for Al_4^{2-} . Thus, addition of two electrons to the e_g LUMO+1 orbital of Al_4^{2-} transforms a σ - and π -aromatic Al_4^{2-} into a σ -aromatic and π -antiaromatic Al_4^{4-} system and the $\delta_\pi^{1,3}$ decreases as expected, while the $\delta_\sigma^{1,3}$ remains more or less the same. The same situation is found when the two electrons are removed from the a_{2u} orbital. On the other hand, if the electrons are removed from the a_{1g} σ -orbital $\delta_\pi^{1,3}$ does not change and $\delta_\sigma^{1,3}$ decreases. A decrease is also seen for the withdrawal of two electrons from the tangential σ b_{2g} orbital, although the reduction of the $\delta_\sigma^{1,3}$ is minor in this case, again indicating that the radial contribution to the σ -aromaticity is larger than that of the tangential orbital. As for organic aromatic molecules [41], the change of $\delta_x^{1,3}$ ($x = \sigma, \pi, \text{ and } \delta$) in 4-MRs when adding or removing two electrons is a good indicator of α -(anti)aromaticity. It has the additional advantage with respect to MCI of being a computationally much cheaper descriptor.

Tables 2 and 3 gather the values of MCI and $\delta^{1,3}$ values and their σ - and π -contributions for Al_4^{2-} and Al_4^{4-} species coordinated to Li^+ , Na^+ , and Cu^+ cations to form pyramidal C_{4v} complexes, which are more stable than the planar C_{2v} isomers [53]. The MCI and $\delta^{1,3}$ values of Table 2 indicate a reduction in aromaticity in the order

Table 2 MCI, MCI_x , $\delta^{1,3}$, and $\delta_x^{1,3}$ ($x = \sigma$ and π) indices for the Al_4 unit in Al_4^{2-} , LiAl_4^- , NaAl_4^- , and CuAl_4^- at the B3LYP/6-311+G(d) level of theory

	$N(2\pi e^-)$ Al_4^{2-}	$N(2\pi e^-)$ LiAl_4^-	$N(2\pi e^-)$ NaAl_4^-	$N(2\pi e^-)$ CuAl_4^-
				
MCI	0.356	0.288	0.234	0.129
$\text{MCI}_\sigma^{\text{orb}}$	0.169	0.156	0.157	0.111
$\text{MCI}_\pi^{\text{orb}}$	0.187	0.132	0.077	0.018
MCI^{ov1}	0.356	0.287	0.234	0.106
$\text{MCI}_\sigma^{\text{ov1}}$	0.169	0.153	0.157	0.084
$\text{MCI}_\pi^{\text{ov1}}$	0.187	0.134	0.077	0.022
Error (%) ^a	0	0.33	0	17.84
$\delta^{1,3}$	0.817	0.761	0.708	0.539
$\delta_\sigma^{1,3}$	0.567	0.547	0.549	0.450
$\delta_\pi^{1,3}$	0.250	0.214	0.159	0.089

All distances in Å and all delocalization values in atomic units

^a Calculated as $\left| \frac{\text{MCI} - \text{MCI}^{\text{ov1}}}{\text{MCI}} \right| \times 100$

Table 3 MCI, MCI_σ, δ^{1,3}, and δ_z^{1,3} (α = σ and π) indices for the Al₄ unit in Al₄²⁻, LiAl₄⁻, Li₂Al₄²⁻, Li₃Al₄⁻, and Li₄Al₄ at the B3LYP/6-311+G(d) level of theory

	D _{4h} (2π e ⁻) Al ₄ ²⁻	N(2π e ⁻) LiAl ₄ ⁻	N(2π e ⁻) Li ₂ Al ₄ ²⁻	N(4π e ⁻) Li ₃ Al ₄ ⁻	N(4π e ⁻) Li ₄ Al ₄
MCI	0.356	0.288	0.282	0.214	0.157
MCI _σ ^{orb}	0.169	0.156	0.155	0.155	0.135
MCI _π ^{orb}	0.187	0.132	0.127	0.059	0.021
MCI _σ ^{ovl}	0.356	0.287	0.287	0.240	0.158
MCI _π ^{ovl}	0.169	0.153	0.146	0.159	0.141
MCI _π ^{ovl}	0.187	0.134	0.141	0.081	0.017
Error (%) ^a	0	0.33	2.38	12.41	6.61
δ ^{1,3}	0.817	0.761	0.738	0.627	0.598
δ _σ ^{1,3}	0.567	0.547	0.520	0.500	0.502
δ _π ^{1,3}	0.250	0.214	0.218	0.128	0.095

All distances in Å and all delocalization values in atomic units

^a Calculated as $\left| \frac{MCI - MCI^{ovl}}{MCI} \right| \times 100$ 

$\text{Al}_4^{2-} > \text{LiAl}_4^- > \text{NaAl}_4^- > \text{CuAl}_4^-$. Similar MCI values were reported by Mandado et al. [35] and Roy et al. [36]. The reason for the differences found in the MCI of Al_4^{2-} reported by Mandado et al. [35] and ours has been discussed in a previous paper [38] (see also footnote 1). It is worth to mention that because of the loss of symmetry in some compounds, as MAl_4^- ($\text{M} = \text{Li}^+, \text{Na}^+, \text{and Cu}^+$) or the systems from Table 3, one should talk about pseudo- π instead of π orbitals in these species. However, the overlap between σ and π occupied molecular orbitals is almost zero for Li and Na compounds. We have calculated the relative error between the MCI and MCI^{ovl} values and in both cases is lower than 1%. The only exception is the CuAl_4^- where the error is larger and close to 18% [35]. The reduction in the MCI and $\delta^{1,3}$ values due to metal cation coordination is more important for the π - than for the σ -component, and it is due to the partial transfer of the 2π -electrons from Al_4^{2-} to the cation. Indeed, the electronic charge of the Al_4 unit obtained by Mandado et al. using QTAIM and Hirshfeld populations shows a decrease from LiAl_4^- to CuAl_4^- species [35]. This decrease in electronic delocalization when going from Al_4^{2-} to MAl_4^- ($\text{M} = \text{Li}, \text{Na}, \text{or Cu}$) is similar to that found in Mg_3^{2-} when coordinated to alkali-metal cations [37]. The reduction in aromaticity of Al_4^{2-} due to Li^+ and Cu^+ C_{4v} coordination was also indicated by Sundholm et al. [42] from the calculation of nuclear magnetic shieldings and by Roy et al. [36] from NICS values.

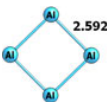
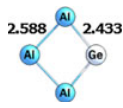
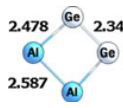
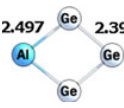
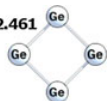
The results of Table 3 show that going from the C_{4v} LiAl_4^- to the highly fluxional [51] C_s Li_2Al_4 species aromaticity slightly decreases. Roy et al. reached the same conclusions based on NICS and MCI results [36]. The values of $\text{MCI}_\alpha^{\text{ovl}}$ and $\delta_\alpha^{1,3}$ are indicative of larger reduction of the σ - than the π -aromatic character (in fact, there is an insignificant gain of π -aromaticity) while $\text{MCI}_\alpha^{\text{orb}}$ values show a slight decrease in both σ and π contributions. This is due to the fact that the second Li^+ interacts more strongly with the σ -orbitals, in particular with the tangential b_{2g} orbital. Taking the values of Al_4^{4-} in Table 1 as reference, we observed that when going from Al_4^{4-} to C_s $\text{Li}_2\text{Al}_4^{2-}$ there is an important decrease of the antiaromatic π -character of the Al_4 unit, which is due to partial transfer of π -electrons from Al_4 unit to the Li^+ cations. Indeed the QTAIM electronic charge of the Al_4 unit changes from -4.000 au in Al_4^{4-} to -2.500 au in $\text{Li}_2\text{Al}_4^{2-}$. The transfer of σ -electrons from Al_4 unit to the Li^+ cation, which is the farthest away from the center of the ring, produces a clear reduction in the σ -aromaticity as can be seen in the MCI_σ and $\delta_\sigma^{1,3}$ values. MCI and $\delta^{1,3}$ results of Table 3 indicate a reduction in aromaticity in the order $\text{Li}_2\text{Al}_4^{2-} > \text{Li}_3\text{Al}_4^- \approx \text{Li}_4\text{Al}_4$. The reduction in the MCI and $\delta^{1,3}$ values when going from C_s $\text{Li}_2\text{Al}_4^{2-}$ to C_s Li_3Al_4^- is more

important for the π - than for the σ -component. On the other hand, differences in electron delocalization and aromaticity between C_s Li_3Al_4^- and C_{2v} Li_4Al_4 are minor. This result is in contradiction to the NICS(0) values of about -4.8 ppm and -11.4 ppm obtained for C_s Li_3Al_4^- and C_{2v} Li_4Al_4 that point out an increase in aromaticity by adding a Li^+ to Li_3Al_4^- [58]. Similarly, Roy et al. reported NICS(0) values of -5.7 , -5.4 and -11.1 ppm for Al_4^{4-} , Li_3Al_4^- , and Li_4Al_4 and MCI values of 0.091, 0.073, and 0.076 for Al_4^{4-} , Li_3Al_4^- , and Li_4Al_4 [36].

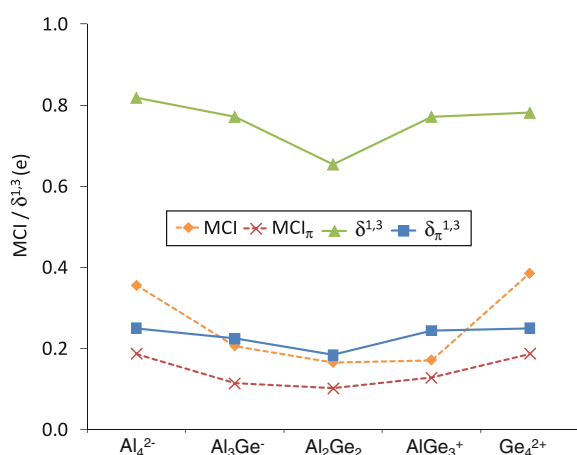
Table 4 collects the values of the MCI and $\delta^{1,3}$ indices, while Fig. 3 depicts the trends for the MCI and $\delta^{1,3}$ indices along the series Al_4^{2-} to Ge_4^{2+} . For this series, one can predict a steep decrease in aromaticity when going from Al_4^{2-} to, for instance, GeAl_3^- due to the reduction in symmetry and the substitution of one Al atom by a more electronegative Ge atom. A smooth reduction in aromaticity when going from Al_3Ge^- to Al_2Ge_2 is also likely, although more questionable. And the same should occur from Ge_4^{2+} to Al_2Ge_2 . Therefore, the expected order of aromaticity is $\text{Al}_4^{2-} > \text{Al}_3\text{Ge}^- \geq \text{Al}_2\text{Ge}_2 \leq \text{AlGe}_3^+ < \text{Ge}_4^{2+}$. Interestingly, both total MCI and MCI_π curves have a clear concave \cup shape providing the expected order of aromaticity. For symmetry reasons, the MCI_π values of D_{4h} Al_4^{2-} and Ge_4^{2+} clusters with 2π -electrons are exactly the same, 0.187 a.u.. It has to be mentioned that MCI_σ values (not shown in Fig. 3) fail by assigning a larger aromaticity to Al_2Ge_2 than to AlGe_3^+ . The correct shape is also provided by the $\delta^{1,3}$ and $\delta_\pi^{1,3}$ components ($\delta_\sigma^{1,3}$ also gives the correct trend, see Table 4) of the total electronic delocalization. As found in organic molecules [41], for inorganic species the crossed term corresponding to the two farthest atoms in the ring (i.e., $\delta_\alpha^{1,3}$ in 4-MRs) is larger for the most aromatic member of a given series.

Since the study of the Ta_3O_3^- , Hf_3 , $^5\text{Ta}_3^-$, and $^3\text{Hf}_3$ species requires the inclusion of relativistic effects, we have employed pseudopotentials for the calculations. As a side effect, the use of pseudopotentials leads to spurious densities close to nuclei that result in the appearance of non-nuclear attractors in the QTAIM partition. This makes the calculation of the $\text{S}_{ij}(\text{A})$ terms cumbersome. For this reason, the overlap between MOs i and j within the molecular space assigned to atom A has been calculated for these molecules using the fuzzy atom partition. Table 5 compares the B3LYP/6-311+G(d) results of the MCI, MCI_α , $\delta^{1,3}$, and $\delta_\alpha^{1,3}$ ($\alpha = \sigma$ and π) indices for Al_4^{2-} and Al_3Ge^- computed with the QTAIM and fuzzy atomic partitions of the molecular space. For Al_4^{2-} , the results obtained with the QTAIM and fuzzy partition differ by few hundredths of an electron. This is not surprising, since it is well known that for species involving only homonuclear bonds the different atomic partitions lead to very similar

Table 4 MCI, MCI_σ, δ^{1,3}, and δ_α^{1,3} (α = σ and π) indices for the [Al_nGe_{4-n}]^{q±} (n = 0–4) series at the B3LYP/6–311+G(d) level of theory

	Al ₄ ²⁻	Al ₃ Ge ⁻	Al ₂ Ge ₂	AlGe ₃ ⁺	Ge ₄ ²⁺
					
Symmetry	D _{4h}	C _{2v}	C _{2v}	C _{2v}	D _{4h}
MCI	0.356	0.206	0.165	0.171	0.386
MCI _σ	0.169	0.092	0.063	0.043	0.199
MCI _π	0.187	0.114	0.102	0.128	0.187
δ ^{1,3}	0.818	0.771	0.654	0.771	0.781
δ _σ ^{1,3}	0.568	0.546	0.469	0.527	0.531
δ _π ^{1,3}	0.250	0.224	0.184	0.244	0.250

All distances in Å and all delocalization values in atomic units

**Fig. 3** Variation of MCI, MCI_σ, MCI_π, δ^{1,3}, and δ_π^{1,3} (in electrons) along the series Al₄²⁻, Al₃Ge⁻, Al₂Ge₂, AlGe₃⁺, and Ge₄²⁺

atomic charges and multicenter ESI values [82, 95, 96]. The differences between QTAIM and fuzzy partitions are more noticeable in the case of the Al₃Ge⁻ species, but the qualitative trends are the same. Thus, the different QTAIM and fuzzy MCI and δ_α^{1,3} (α = σ and π) values indicate a reduction in aromaticity when going from Al₄²⁻ to Al₃Ge⁻, although more evident in the case of the QTAIM partition. As found in a previous study [96], here we also observe that ESI values between non-bonded atoms (δ_α^{1,3} (α = σ and π) in our case) tend to be larger when using fuzzy atoms. Since for Ta₃O₃⁻, Ta₃⁻, and Hf₃ species, we analyze the aromaticity of the rings containing only homonuclear bonds (Ta–Ta or Hf–Hf), we expect that the fuzzy partition will produce results quite similar to those yielded by the QTAIM partition. In order to compare the aromaticity of transition-metal rings, the results of Tables 6

Table 5 Comparison of the MCI, MCI_σ, δ^{1,3}, and δ_α^{1,3} (α = σ and π) indices for Al₄²⁻ and Al₃Ge⁻ computed with the QTAIM and fuzzy atomic partitions of the molecular space at the B3LYP/6–311+G(d) level of theory

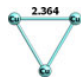



	QTAIM Al ₄ ²⁻	FUZZY Al ₄ ²⁻	QTAIM Al ₃ Ge ⁻	FUZZY Al ₃ Ge ⁻
MCI	0.356	0.364	0.206	0.314
MCI _σ	0.169	0.177	0.092	0.147
MCI _π	0.187	0.187	0.114	0.167
δ ^{1,3}	0.817	0.874	0.771	0.799
δ _σ ^{1,3}	0.567	0.622	0.547	0.561
δ _π ^{1,3}	0.250	0.252	0.224	0.238

All values in atomic units

and 7 have been obtained using the fuzzy partition for all the 3-MR species.



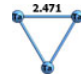

In the next section, we will focus on the analysis of transition-metal rings with single, double, and triple aromatic character. Table 6 assembles the MCI values of the Cu₃⁺, Cu₃H₃, Y₃⁻, and La₃⁻ species. Yong et al. showed that the Cu₃⁺ unit is a single σ-aromatic system with only s-atomic orbitals (AO) involved in chemical bonding [59]. These observations were supported by MO analysis and NICS(0) and NICS(1) values of –28.22 and –12.31 ppm, respectively. Interestingly, the MCI values confirm the σ-aromaticity in Cu₃⁺ giving a large MCI_σ contribution (0.188 a.u.) while MCI_π is almost zero (0.001 a.u.). In 2003, Tsipis and Tsipis investigated the aromaticity of Cu_nH_n (n = 3–6) cyclic species [60]. They concluded that these compounds are σ-aromatic due to the equivalence of Cu–Cu and Cu–H bonds. Moreover, Tsipis et al. performed NICS calculations, which also support the cyclic electron delocalization in these systems. However, in 2006, Lin et al. showed that Cu₄H₄ did not sustain any strong magnetically

Table 6 MCI, MCI_π, and MCI_σ indices for Cu₃⁺, Cu₃H₃, Y₃⁻ and La₃⁻ at the B3LYP/X/Stuttgart+2f (X = Cu, Y, and La) level of theory computed with the fuzzy partition

	Cu ₃ ⁺	Cu ₃ H ₃	Y ₃ ⁻	La ₃ ⁻
				
MCI	0.189	0.013	0.754	0.750
MCI _σ	0.188	0.013	0.458	0.454
MCI _π	0.001	0.000	0.296	0.296
MCI _δ	0.000	0.000	0.000	0.000
Aromaticity	σ	–	σ + π	σ + π

All distances in Å and all delocalization values in atomic units

Table 7 MCI, MCI_σ, MCI_π, and MCI_δ indices for the Ta₃ unit in Ta₃O₃⁻, Hf₃, ⁵Ta₃⁻, and ³Hf₃ at the B3LYP/X/Stuttgart+2f (X = Ta and Hf) level of theory computed with the fuzzy partition

	Ta ₃ O ₃ ⁻	Hf ₃	⁵ Ta ₃ ⁻	³ Hf ₃
				
MCI	0.584	1.037	0.776	0.653
MCI _σ ^{orb}	0.111	0.445	0.362	0.453
MCI _π ^{orb}	0.272	0.296	0.178	0.200
MCI _δ ^{orb}	0.201	0.295	0.235	0.000
MCI ^{ov1}	0.624	1.038	0.878	0.653
MCI _σ ^{ov1}	0.085	0.445	0.403	0.453
MCI _π ^{ov1}	0.272	0.296	0.178	0.200
MCI _δ ^{ov1}	0.267	0.296	0.296	0.000
Error (%) ^a	6.90	0.16	13.5	0
Aromaticity	π + δ	σ + π + δ	σ + π + δ	σ + π

^a Calculated as $\left| \frac{MCI - MCI^{ov1}}{MCI} \right| \times 100$

All distances in Å and all delocalization values in atomic units

induced ring current, and, then, this molecule should not be considered as aromatic [97]. In order to assess the aromaticity of Cu_nH_n species, we have analyzed the behavior of the electron delocalization in the Cu₃H₃ molecule. As shown in Table 6, the MCI value of Cu₃H₃ is practically zero in comparison with Cu₃⁺ unit. In addition, MCI values of 0.005, 0.001, and 0.000 a.u. have been found for Cu₄H₄, Cu₅H₅, and Cu₆H₆, respectively. Consequently, according to these electron delocalization measures, Cu_nH_n (n = 3–6) cyclic species cannot be considered as aromatic. In 2007, Chi and Liu found that D_{3h} structures for Sc₃⁻, Y₃⁻, and La₃⁻ are d-orbital σ- and π-aromatic systems with large negative NICS values [61]. These species were the first reported transition-metal systems with double σ- and π-aromaticity. Their large MCI_σ and MCI_π values confirm the double aromatic character of Y₃⁻ and La₃⁻.

Finally, we have analyzed the multifold aromaticity of a series of species with δ-aromatic character. As said in the introduction, Ta₃O₃⁻ has double π- and δ-aromaticity [10]. This is supported by the small MCI_σ, in comparison with Y₃⁻, La₃⁻, and Hf₃, and the relatively large MCI_π and MCI_δ values of Table 7. Interestingly, the large MCI_σ (α = σ, π, and δ) for Hf₃ concurs with the σ-, π-, and δ-aromaticity found in this inorganic cluster [11]. According to our results, the π- and δ-aromatic character in Hf₃ is similar and smaller than the σ-aromatic character. In addition, we have studied how the electronic delocalization measures describe the aromaticity in open-shell systems with multiple aromaticity. To this end, two D_{3h} species have been selected. First, quintet ⁵Ta₃⁻ which is the ground state for Ta₃⁻ anion [62] and, then, ³Hf₃ which is the lowest triplet state for Hf₃ [11]. In 2008, Wang et al. [62]

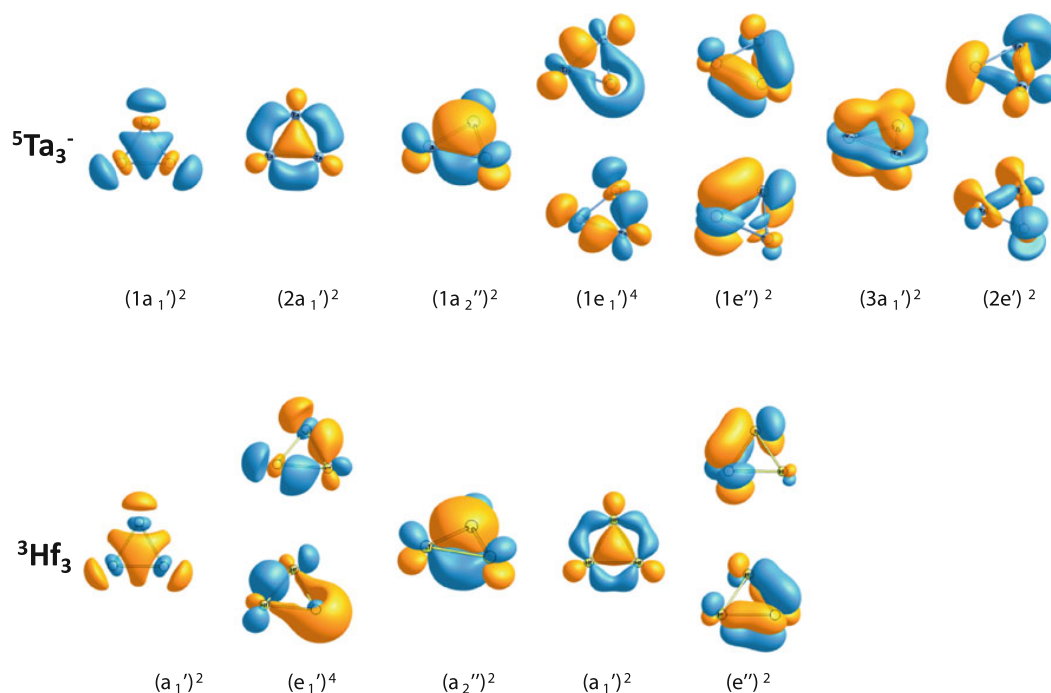


Fig. 4 The low-lying occupied molecular orbitals of ${}^5\text{Ta}_3^-$ and ${}^3\text{Hf}_3$

studied the chemical bonding and aromaticity of lowest-lying states of Ta_3^- and they concluded by means of molecular orbital analysis that ${}^5\text{Ta}_3^-$ possesses partial σ -, partial π -, and δ -aromatic character. Our results confirm these trends, MCI values show a lower σ - and π -aromaticity than σ -, π -, and δ -aromatic Hf_3 or σ - and π -aromatic Y_3^- and La_3^- compounds while δ -aromaticity is practically the same in ${}^5\text{Ta}_3^-$ as in Hf_3 . As shown in Table 7, the relative error for ${}^5\text{Ta}_3^-$ is 13.5%, this is because the strong overlap between σ $2e'$ and δ $3a_1'$ orbitals (see Fig. 4), which prevents a better σ/δ orbital separation. In comparison with Ta_3O_3^- , ${}^5\text{Ta}_3^-$ is more aromatic because the high σ -electron delocalization. Finally, ${}^3\text{Hf}_3$ was presented by Averkiev et al. as the lowest triplet state of Hf_3 with σ - and π -aromaticity [11]. MCI values also reproduce these observations. In comparison with ${}^1\text{Hf}_3$, MCI_σ contribution to the aromaticity of ${}^3\text{Hf}_3$ is more or less the same than the lowest lying singlet state while the π -contribution is reduced 0.1 a.u. due to the single occupation of e'' orbitals in ${}^3\text{Hf}_3$ (see Fig. 4). Consequently, ${}^1\text{Hf}_3$ is more aromatic than ${}^3\text{Hf}_3$ because the first presents δ -aromaticity and its π -aromaticity is somewhat larger. It is worth to mention that ${}^5\text{Ta}_3^-$ and ${}^3\text{Hf}_3$ have four π -electrons that follow the Baird's rule stating that the lowest lying triplet states with $4n$ π -electrons are π -aromatic [98].

In summary, our results show that the σ -, π -, and δ -components of the multicenter indices are excellent

indicators of σ -, π -, and δ -aromaticity in inorganic clusters. We consider that these indices can be very helpful in the non-trivial task of assigning the aromatic character of all-metal and semimetal clusters. The σ -, π -, and δ -crossed contributions to the total electronic delocalization corresponding to the two farthest atoms in the ring (i.e., $\delta_\alpha^{1,3}$ in 4-MRs) are also good descriptors of aromaticity.

4 Conclusions

The quantitative evaluation of aromaticity in inorganic clusters is cumbersome due to the lack of aromatic inorganic systems that can be used as a reference. Basically, the aromaticity of these species can only be assessed by the use of the simple Hückel's $4n+2$ rule and the calculation of the NICS and MCI descriptors. Simple total electronic count is a vague criterion that depends on the number of valence orbitals that one considers delocalized and may lead sometimes to incorrect results [8, 49, 99, 100]. In addition, electron counting does not provide a quantitative value, so comparisons of aromaticity from different compounds are not possible. Moreover, in previous works [38, 101], we have reported that the behavior of MCI is superior to that of the NICS magnetic-based index. In this work, we show that MCI of planar (or pseudo-planar) species can be separated into the σ -, π -, and δ -components.

These MCI_α ($\alpha = \sigma, \pi,$ and δ) indices provide quantitative valuable information about the type of aromaticity that a certain aromatic inorganic cluster has. The MCI_α results reported for all systems studied in the present work were in line with previous classifications of the species according to their aromatic character. The results obtained are invariant with respect to unitary transformation of the molecular orbitals and the errors associated with the partition are measurable and are, in general, minor. Therefore, the use of MCI and its components is recommended in the analysis of aromaticity of all-metal and semimetal clusters. Finally, our results show that the crossed term corresponding to the two farthest atoms in the ring (i.e., $\delta_\pi^{1,3}$ in 4-MRs) decreases also in aromatic inorganic species when two electrons are added or removed and that this crossed term is higher for the most aromatic molecule in a series of same-membered rings. Consequently, this crossed term, which is less computationally demanding than MCI, is also a good descriptor of aromaticity in all-metal and semimetal clusters.

Acknowledgments Financial help has been furnished by the Spanish MICINN project no. CTQ2008-03077/BQU and by the Catalan DIUE through project no. 2009SGR637. F.F. and J.P. thank the MICINN for the doctoral fellowship no. AP2005-2997 and the Ramón y Cajal contract, respectively. E.M. acknowledges financial support from the Lundbeck Foundation Center and from Marie Curie IntraEuropean Fellowship, Seventh Framework Programme (FP7/2007-2013), under grant agreement no. PIEF-GA-2008-221734 and from the Polish Ministry of Science and Higher Education (Project no. N N204 215634). Support for the research of M.S. was received through the ICREA Academia 2009 prize for excellence in research funded by the DIUE of the Generalitat de Catalunya. We thank the Centre de Supercomputació de Catalunya (CESCA) for partial funding of computer time.

References

- Faraday M (1825) *Philos Trans R Soc London* 115:440
- Poater J, Duran M, Solà M, Silvi B (2005) *Chem Rev* 105:3911
- Merino G, Vela A, Heine T (2005) *Chem Rev* 105:3812
- Chen Z, Wannere CS, Corminboeuf C, Puchta R, Schleyer PvR (2005) *Chem Rev* 105:3842
- Li X, Kuznetsov AE, Zhang H-F, Boldyrev A, Wang L-S (2001) *Science* 291:859
- Boldyrev AI, Wang L-S (2005) *Chem Rev* 105:3716
- Tsipis CA (2005) *Coord Chem Rev* 249:2740
- Zubarev DY, Averkiev BB, Zhai H-J, Wang L-S, Boldyrev AI (2008) *Phys Chem Chem Phys* 10:257
- Huang X, Zhai H-J, Kiran B, Wang L-S (2005) *Angew Chem Int Ed* 44:7251
- Zhai H-J, Averkiev BB, Zubarev DY, Wang L-S, Boldyrev AI (2007) *Angew Chem Int Ed* 46:4277
- Averkiev BB, Boldyrev AI (2007) *J Phys Chem A* 111:12864
- Tsipis AC, Kefalidis CE, Tsipis CA (2008) *J Am Chem Soc* 130:9144
- Zhan C-G, Zheng F, Dixon DA (2002) *J Am Chem Soc* 124:14795
- Zhai H-J, Kuznetsov AE, Boldyrev A, Wang L-S (2004) *ChemPhysChem* 5:1885
- Liu Z-Z, Tian W-Q, Feng J-K, Zhang G, Li W-Q (2005) *J Phys Chem A* 109:5645
- Chi XX, Chen XJ, Yuan ZS (2005) *J Mol Struct (Theochem)* 732:149
- Kruszewski J, Krygowski TM (1972) *Tetrahedron Lett* 13:3839
- Krygowski TM (1993) *J Chem Inf Comp Sci* 33:70
- Matito E, Duran M, Solà M (2005) *J Chem Phys* 122:014109
- Bultinck P, Ponec R, Van Damme S (2005) *J Phys Org Chem* 18:706
- Matta CF (2003) *J Comput Chem* 24:453
- Matta CF, Hernández-Trujillo J (2003) *J Phys Chem A* 107:7496
- Cyranowski MK (2005) *Chem Rev* 105:3773
- Boldyrev AI, Kuznetsov AE (2002) *Inorg Chem* 41:532
- Matito E, Poater J, Duran M, Solà M (2005) *J Mol Struct (Theochem)* 727:165
- Hückel E (1931) *Z Physik* 70:104
- Hückel E (1931) *Z Physik* 72:310
- Hückel E (1932) *Z Physik* 76:628
- Hückel E (1937) *Z Elektrochemie* 43:752
- Schleyer PvR, Maerker C, Dransfeld A, Jiao H, van Eikema Hommes NJR (1996) *J Am Chem Soc* 118:6317
- Giambiagi M, de Giambiagi MS, dos Santos CD, de Figueiredo AP (2000) *Phys Chem Chem Phys* 2:3381
- Bultinck P, Rafat M, Ponec R, van Gheluwe B, Carbó-Dorca R, Popelier P (2006) *J Phys Chem A* 110:7642
- Mandado M, González-Moa MJ, Mosquera RA (2007) *J Comput Chem* 28:127
- Cioslowski J, Matito E, Solà M (2007) *J Phys Chem A* 111:6521
- Mandado M, Krishtal A, Van Alsenoy C, Bultinck P, Hermida-Ramón JM (2007) *J Phys Chem A* 111:11885
- Roy DR, Bultinck P, Subramanian V, Chattaraj PK (2008) *J Mol Struct Theochem* 854:35
- Jiménez-Halla JOC, Matito E, Blancafort L, Robles J, Solà M (2009) *J Comput Chem* 30:2764
- Feixas F, Jiménez-Halla JOC, Matito E, Poater J, Solà M (2010) *J Chem Theory Comput* 6:1118
- Solà M, Feixas F, Jiménez-Halla JOC, Matito E, Poater J (2010) *Symmetry* 2:1156
- Feixas F, Matito E, Solà M, Poater J (2008) *J Phys Chem A* 112:13231
- Feixas F, Matito E, Solà M, Poater J (2010) *Phys Chem Chem Phys* 12:7126
- Jusélius J, Straka M, Sundholm D (2001) *J Phys Chem A* 105:9939
- Fowler PW, Havenith RWA, Steiner E (2001) *Chem Phys Lett* 342:85
- Fowler PW, Havenith RWA, Steiner E (2002) *Chem Phys Lett* 359:530
- Santos JC, Tiznado W, Contreras R, Fuentealba P (2004) *J Chem Phys* 120:1670
- Chattaraj PK, Roy DR, Elango M, Subramanian V (2005) *J Phys Chem A* 109:9590
- Lin YC, Jusélius J, Sundholm D, Gauss J (2005) *J Chem Phys* 122:214308
- Havenith RWA, van Lenthe JH (2004) *Chem Phys Lett* 385:198
- Havenith RWA, Fowler PW, Steiner E, Shetty S, Kanhere D, Pal S (2004) *Phys Chem Chem Phys* 6:285
- Datta A, Patti SK (2005) *J Chem Theory Comput* 1:824
- Islas R, Heine T, Merino G (2007) *J Chem Theory Comput* 3:775
- Mang C, Liu C, Wu K (2010) *Int J Quantum Chem* 110:1127
- Mang C, Liu C, Zhou J, Li Z, Wu K (2010) *Chem Phys Lett* 438:20
- Li X, Zhang H-F, Wang L-S, Kuznetsov AE, Cannon NA, Boldyrev AI (2001) *Angew Chem Int Ed* 40:1867

55. Seal P (2009) *J Mol Struct Theochem* 893:31
56. Nigam S, Majumder C, Kulshreshtha SK (2005) *J Mol Struct Theochem* 755:187
57. Kuznetsov AE, Birch KA, Boldyrev AI, Zhai H-J, Wang L-S (2003) *Science* 300:622
58. Chen Z, Corminboeuf C, Heine T, Bohmann J, Schleyer PvR (2003) *J Am Chem Soc* 125:13930
59. Yong L, Wu SD, Chi XX (2007) *Int J Quantum Chem* 107:722
60. Tsepis AC, Tsepis CA (2003) *J Am Chem Soc* 125:1136
61. Chi XX, Liu Y (2007) *Int J Quantum Chem* 107:1886
62. Wang B, Zhai H-J, Huang X, Wang L-S (2008) *J Phys Chem A* 112:10962
63. Frisch MJ, Trucks GW, Schlegel HB, Scuseria GE, Robb MA, Cheeseman JR, Montgomery JA Jr, Vreven T, Kudin KN, Burant JC, Millam JM, Iyengar SS, Tomasi J, Barone V, Mennucci B, Cossi M, Scalmani G, Rega N, Petersson GA, Nakatsuji H, Hada M, Ehara M, Toyota K, Fukuda R, Hasegawa J, Ishida M, Nakajima T, Honda Y, Kitao O, Nakai H, Klene M, Li X, Knox JE, Hratchian HP, Cross JB, Bakken V, Adamo C, Jaramillo J, Gomperts R, Stratmann RE, Yazyev O, Austin AJ, Cammi R, Pomelli C, Ochterski JW, Ayala PY, Morokuma K, Voth GA, Salvador P, Dannenberg JJ, Zakrzewski G, Dapprich S, Daniels AD, Strain MC, Farkas O, Malick DK, Rabuck AD, Raghavachari K, Foresman JB, Ortiz JV, Cui Q, Baboul AG, Clifford S, Cioslowski J, Stefanov BB, Liu G, Liashenko A, Piskorz P, Komaromi I, Martin RL, Fox DJ, Keith T, Al-Laham MA, Peng CY, Nanayakkara A, Challacombe M, Gill PMW, Johnson B, Chen W, Wong MW, Gonzalez C, Pople JA (2003) *Gaussian 03*. Gaussian, Inc, Pittsburgh, PA
64. Stephens PJ, Devlin FJ, Chabalowski CF, Frisch MJ (1994) *J Phys Chem* 98:11623
65. Becke AD (1993) *J Chem Phys* 98:5648
66. Lee C, Yang W, Parr RG (1988) *Phys Rev B* 37:785
67. Frisch MJ, Pople JA, Binkley JS (1984) *J Chem Phys* 80:3265
68. Krishnan R, Binkley JS, Seeger R, Pople JA (1980) *J Chem Phys* 72:650
69. Andrae D, Haussermann U, Dolg M, Stoll H, Preuss H (1990) *Theor Chim Acta* 77:123
70. Küchle W, Dolg M, Stoll H, Preuss H (1994) *J Chem Phys* 100:7535
71. Dunning TH Jr (1989) *J Chem Phys* 90:1007
72. Kendall RA, Dunning TH Jr, Harrison RJ (1992) *J Chem Phys* 96:6796
73. Lambrecht DS, Fleig T, Sommerfeld T (2008) *J Phys Chem A* 112:2855
74. Zubarev DY, Boldyrev AI (2008) *J Phys Chem A* 112:7984
75. Lambrecht DS, Fleig T, Sommerfeld T (2008) *J Phys Chem A* 112:7986
76. Fradera X, Austen MA, Bader RFW (1999) *J Phys Chem A* 103:304
77. Fradera X, Poater J, Simon S, Duran M, Solà M (2002) *Theor Chem Acc* 108:214
78. Matito E, Solà M, Salvador P, Duran M (2007) *Faraday Discuss* 135:325
79. Ruedenberg K (1962) *Rev Mod Phys* 34:326
80. Mandado M, González-Moa MJ, Mosquera RA (2007) *Chem-PhysChem* 8:696
81. Güell M, Matito E, Luis JM, Poater J, Solà M (2006) *J Phys Chem A* 110:11569
82. Matito E, Poater J, Solà M, Duran M, Salvador P (2005) *J Phys Chem A* 109:9904
83. Ponec R, Cooper D (2005) *J Mol Struct Theochem* 727:133
84. Bader RFW (1985) *Acc Chem Res* 18:9
85. Bader RFW (1990) *Atoms in Molecules: A Quantum Theory*. Clarendon, Oxford
86. Bader RFW (1991) *Chem Rev* 91:893
87. Biegler-König FW, Bader RFW, Tang T-H (1982) *J Comput Chem* 3:317
88. Matito E (2006) ESI-3D: electron sharing indexes program for 3D molecular space partitioning, <http://iqc.udg.es/~eduard/ESI>. Girona, Institute of Computational Chemistry
89. Mayer I, Salvador P (2004) *Chem Phys Lett* 383:368
90. Salvador P, Mayer I (2004) *J Chem Phys* 120:5046
91. Mayer I, Salvador P (2003) Program FUZZY. Girona, Available from <http://occam.chemres.hu/programs>
92. Suresh CH, Koga N (2001) *J Phys Chem A* 105:5940
93. Becke AD, Edgecombe KE (1990) *J Chem Phys* 92:5397
94. Corminboeuf C, Heine T, Weber J (2003) *Phys Chem Chem Phys* 5:246
95. Matito E, Salvador P, Duran M, Solà M (2006) *J Phys Chem A* 110:5108
96. Heyndrickx W, Salvador P, Bultinck P, Solà M, Matito E (2010) *J Comput Chem*. doi:10.1002/jcc.21621
97. Lin YC, Sundholm D, Juselius J, Cui LF, Li X, Zhai HJ, Wang LS (2006) *J Phys Chem A* 110:4244
98. Baird NC (1972) *J Am Chem Soc* 94:4941
99. Jung Y, Heine T, Schleyer PvR, Head-Gordon M (2004) *J Am Chem Soc* 126:3132
100. Aihara J, Kanno H, Ishida T (2005) *J Am Chem Soc* 127:13324
101. Feixas F, Matito E, Poater J, Solà M (2008) *J Comput Chem* 29:1543

Chapter 8

Results and Discussion

In the following chapter, the main achievements of this thesis will be briefly summarized. To simplify the analysis, we have divided the results section into two different blocks: chemical bonding and aromaticity. First, we will focus on the analysis of the nature of the chemical bond from the Electron Localization Function and the Domain-Averaged Fermi Hole points of view (see Chapter 5). Second, we present a critical assessment of the performance of some widely used aromaticity indices taking into account both organic and inorganic species (see Chapter 6). Third, taking advantage of the information gathered in the previous part, the aromaticity of a large series of compounds is evaluated in detail by means of electron sharing indices (see Chapter 7).

8.1 Applications I: The nature of the Chemical Bond from the Electron Localization Function and Domain-Averaged Fermi Holes

The following section summarize the results obtained in sections 5.1, 5.2, and 5.3 from Chapter 5.

8.1.1 Electron Localization Function

The ELF represents one of the most powerful approaches to studying the electron (de)localization. From its definition in 1990, ELF has been successfully applied to study the peculiarities of chemical bonding in a broad range of molecular systems. Among the potential applications of the ELF, one can find the analysis of metal-

metal bonding in organometallic complexes,⁶⁶ electronic structure changes along the IRC,^{200,201} or the mechanism analysis of complex electrocyclic reactions.^{92,202}

Electron Localization Function at the Correlated Level: A Natural Orbital Formulation

Originally, Becke and Edgecombe formulated the ELF for single determinant wave functions,⁶ i.e. HF or DFT within the Kohn-Sham formalism. Later on, the correlated version of the ELF in terms of two-particle densities (2-PD) was described.⁹² However, the calculation of the *exact* 2-PD is the bottleneck of the process and, thus, the investigations of the ELF at the correlated level are sparse and limited to small systems. Over the last years, many approximated expressions of the 2-PD in terms of 1-RDM or natural orbitals have been explored in the literature.^{203–207} Since the inclusion of electron correlation is essential to describe a large list of chemical phenomena, the first aim of this thesis is to investigate the ability of some of the 2-PD approximations described in the literature to calculate reliable values of the ELF at correlated level.

As previously mentioned, the pair density can be expressed in terms of exchange-correlation density as $\gamma^{(2)}(\vec{r}_1, \vec{r}_2) = \gamma^{(1)}(\vec{r}_1)\gamma^{(1)}(\vec{r}_2) + \gamma_{XC}(\vec{r}_1, \vec{r}_2)$. In practice, in order to reduce the computational cost associated with the *exact* 2-PD, we have to approximate the exchange correlation density (XCD). The ELF analysis is divided into three steps. First, the ELF function is calculated for a grid of points. Second, from these points, the basin boundaries are defined through the gradient of the ELF function. Third, the population analysis over the ELF basins is performed.

As we said in Chapter 1, the 2-PD can be decomposed into its spin terms, i.e. $\gamma^{(2)}(\vec{r}_1, \vec{r}_2) = \gamma^{(2)\alpha\alpha}(\vec{r}_1, \vec{r}_2) + \gamma^{(2)\alpha\beta}(\vec{r}_1, \vec{r}_2) + \gamma^{(2)\beta\alpha}(\vec{r}_1, \vec{r}_2) + \gamma^{(2)\beta\beta}(\vec{r}_1, \vec{r}_2)$. From Eq. 2.52, one can see that the calculation of the ELF and the posterior definition of the basin boundaries need the same spin pair functions, $\gamma^{(2)\sigma\sigma}(\vec{r}_1, \vec{r}_2)$. In addition, the Pauli principle, which states that $\gamma^{(2)\sigma\sigma}(\vec{r}_1, \vec{r}_1) = 0$, and the electron-electron cusp condition,²⁰⁸ $\nabla_{r_2}\gamma^{(2)\sigma\sigma}(\vec{r}_1, \vec{r}_1)|_{\vec{r}_2=\vec{r}_1} = \vec{0}$, must be fulfilled. Then, the only approximation of the XCD that accomplishes both requirements is the HF like approximation of the exchange correlation density (HF-XCD), i.e. $\gamma^{(2)\sigma\sigma}(\vec{r}_1, \vec{r}_2) = \gamma^{(1)\sigma}(\vec{r}_1)\gamma^{(1)\sigma}(\vec{r}_2) - \gamma^{(1)\sigma}(\vec{r}_1|\vec{r}_2)\gamma^{(1)\sigma}(\vec{r}_2|\vec{r}_1)$. Thus, the HF-XCD is the approximation chosen for the calculation of the ELF.

To analyze the performance of the HF like approach, we have calculated the profile of

the electron localization function along the internuclear axis of the carbon monoxide molecule. To this end, we have computed the ELF for two internuclear distances. First, the equilibrium distance, then at 2.0 Å. In addition to that, we have assessed how the HF-XCD works in the ELF using a plethora of methods: HF, B3LYP, MP2, CISD, CCSD, and CASSCF. In the cases of CISD and CASSCF, we have calculated the *exact* 2-PD in order to compare it with the approximated values. As can be seen in Figure 8.1, at the equilibrium all distances yield results in very good agreement. However, at a larger distance, 2.0 Å, where the effects of electron correlation are more evident, the differences are more important. To put it in a nutshell, in the bonding region we expect to find two maxima associated with the bond splitting. This trend is only reproduced by CASSCF, CASSCF-HF, B3LYP, and CCSD-HF. Remarkably, the CASSCF-HF curve mimics the *exact* CASSCF one. Contrarily, HF does not show the second maxima, and CISD, CISD-HF, and MP2-HF, exhibit a small minima. To sum up, the performance of the HF-XCD approximation is extremely good in comparison with the *exact* methods.

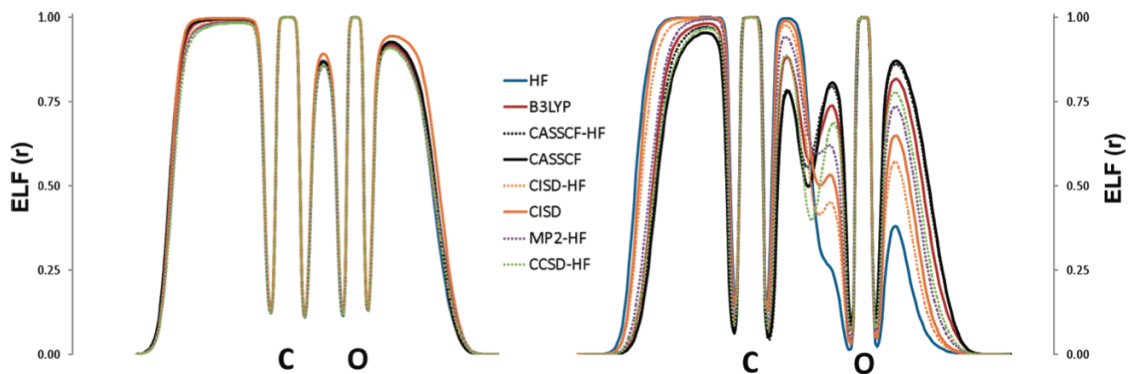


Figure 8.1: Profile of the electron localization function along the internuclear axis of the carbon monoxide molecule (left: $R = 1.123$ Å; right: $R = 2.0$ Å) for the different methods studied.

In contrast to the first two steps, the population analysis of the ELF also needs the cross-spin terms, $\gamma^{(2)\sigma\sigma'}(\vec{r}_1, \vec{r}_2)$, to obtain the pair population, the variance, and the covariance. In this case, the approximated 2-PD must fulfill the sum rule. Among the approximations of the XCD, we have chosen Müller's formula in terms of natural orbitals, $\gamma_{XC}(\vec{r}_1, \vec{r}_2) = \sum_{ij} \eta_i^{1/2} \eta_j^{1/2} \varphi_i(\vec{r}_1) \varphi_j(\vec{r}_2)$,²⁰³ which is also called the Buijse and Baerend's (BB) approximation.^{205,206}

In order to assess the performance of BB approach, we have selected a set of molecules that has been divided into three groups. First, species with small correlation effects, NH_3 , H_2O , and CO_2 ; second, molecules with moderated electron correlation, CO , NO^+ , CN^- , and N_2 ; and third, molecules showing larger correlation effects, H_2O_2 and F_2 . The basin populations, which are only affected by the HF-XCD approach, and the variance of the electron population, which is based on BB approximation, have been analyzed for all the systems. In conclusion, the larger differences in the populations with respect to CASSCF have been found for HF, CISD, CISD-BB, and MP2-BB. Thus, the HF-XCD performs very well with respect to the basin populations. On the other hand, the BB is evaluated by comparing the values of the variance of the electron population, σ^2 . In this case, the values of the σ^2 are sensibly smaller for the methods that use the approximated 2-PD. These values are also affected by the HF-XCD approximation, used to calculate the basin boundaries and, thus, further differences than in the case of electron populations have been found.

Finally, the dissociation of the N_2 molecule has been analyzed. Figures 8.2 and 8.3 show the change in the bonding basins population and its variance, respectively, along the reaction path. In general, HF splits the bond too late, MP2-BB too early, while the rest of the methods give similar results. Thus, the HF-XCD and BB approaches describe very well the dissociation of N_2 .

To sum up, with this new methodology, one can calculate the ELF at the correlated level with a reasonable computational cost. Interestingly, B3LYP exhibits a performance close enough to the approximated CASSCF, thus it can be used to inexpensively introduce the correlation effects in the ELF. However, for those systems where DFT is an inappropriate choice, the above described methodology must be used. We are currently studying by means of the ELF analysis the mechanism of several cycloaddition reactions that can only be elucidated from multireference calculations.

8.1.2 Domain-Averaged Fermi Holes

The Domain-Averaged Fermi Hole analysis, introduced by Robert Ponec in 1997, performs remarkably well to discern the picture of the bonding in nontrivial molecules

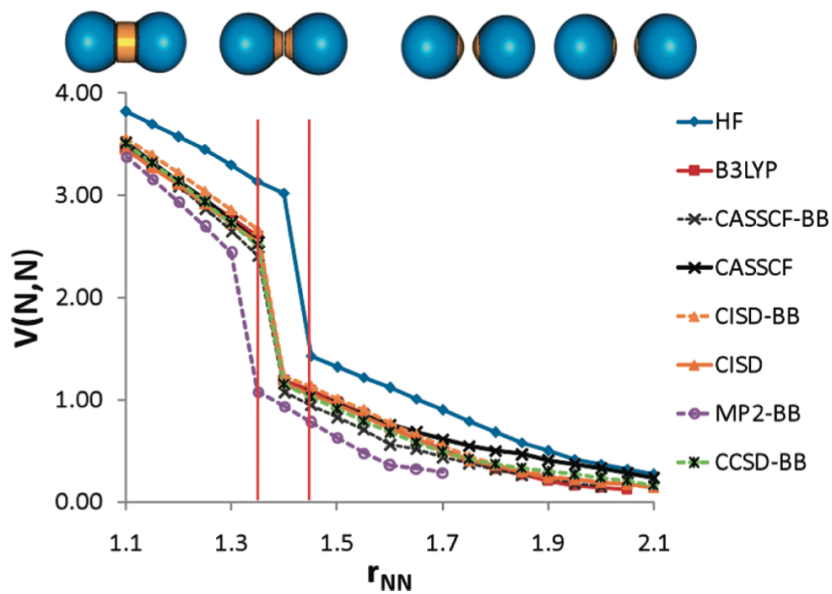


Figure 8.2: The population of the bonding basin of N_2 along the dissociation curve. When the basin splits into two, only the population of one of them is represented.

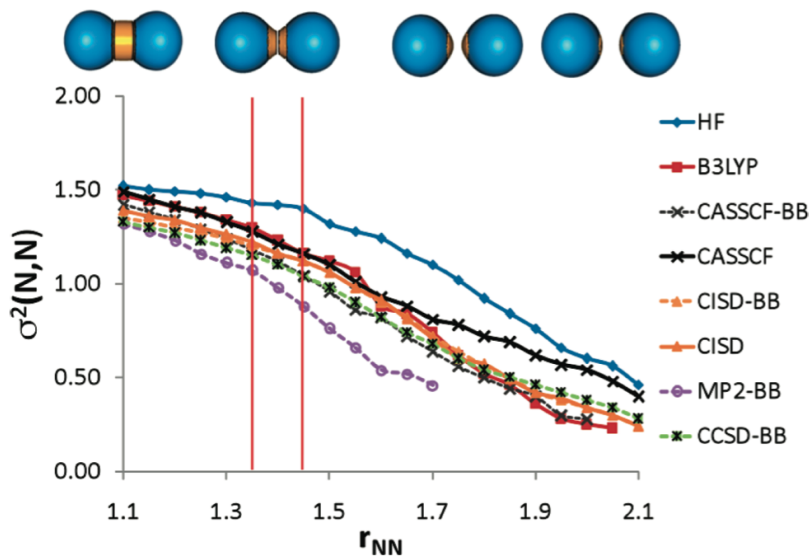


Figure 8.3: The variance of the population of the bonding basin along the dissociation curve. As the molecule stretches the lone-pair basin absorbs the bonding basin.

at the restricted Hartree Fock (RHF) level.^{7,8} In 2007, this analysis was extended in terms of 2-RDM to correlated wave functions by means of modern valence bond calculations.⁷⁶ From 1997, the DAFH has been applied to study numerous systems with intricate bonding such as multicenter bonding,^{82,209,210} hypervalence,⁷² or metal-metal bonding.^{74,78} Notwithstanding, until now, the DAFH analysis has been restricted to closed-shell systems. Thus, the DAFH section is organized as follows. First, the DAFH analysis is generalized to open-shell systems; second, we take advantage of the previous generalization to study the triplet state of $[C_2O_4]^{2+}$; third, we examine the peculiarities of multiple Cr-Cr bonding.

Domain-Averaged Fermi Hole Analysis for open-shell systems

The first aim of this section is the extension of the DAFH methodology to the analysis and visualization of bonding interactions in open-shell systems. Thus, we reformulate the original approach from Eq. 2.39, $g_A(\vec{r}_1) = N_A h_A(\vec{r}_1)$, within the framework of unrestricted Hartree-Fock (UHF) and Kohn-Sham formalisms. The formula in terms of 1-RDM is given by

$$g_A(\vec{r}_1) = g_A^\alpha(\vec{r}_1) + g_A^\beta(\vec{r}_1) = N_A^\alpha h_A^\alpha(\vec{r}_1) + N_A^\beta h_A^\beta(\vec{r}_1)$$

$$g_A^\alpha(\vec{r}_1) = \int_A \gamma^{(1)\alpha\alpha}(\vec{r}_1|\vec{r}_2)\gamma^{(1)\alpha\alpha}(\vec{r}_2|\vec{r}_1)d\vec{r}_2 = \sum_i^{occ} \sum_j^{occ} S_{ij}(A)\phi_i(\vec{r}_1)\phi_j(\vec{r}_1)$$

$$g_A^\beta(\vec{r}_1) = \int_A \gamma^{(1)\beta\beta}(\vec{r}_1|\vec{r}_2)\gamma^{(1)\beta\beta}(\vec{r}_2|\vec{r}_1)d\vec{r}_2 = \sum_i^{occ} \sum_j^{occ} S_{ij}(A)\varphi_i(\vec{r}_1)\varphi_j(\vec{r}_1) \quad (8.1)$$

where ϕ and φ denote the (occupied) molecular orbitals for α and β spins, respectively, and $S_{ij}(A)$ is the overlap integral of the molecular orbitals ϕ_i and ϕ_j over the domain A . Once the spin-resolved DAFHs are introduced, the subsequent analysis is exactly the same as in the case of closed-shell species described in Chapter 2. Thus, we separately diagonalize the matrices that represent the α and β holes, obtaining the corresponding α and β eigenvectors and eigenvalues. In order to assess the performance of the new methodology, the doublet state of the NH_3^+ radical cation and the triplet ${}^3\Sigma_g^-$ ground state of the O_2 are analyzed. The DAFH eigenvectors of NH_3^+ and its eigenvalues for the NH fragment have been summarized in Figure 8.6. The most striking feature of this figure is that, besides the unpaired electron, all of

the remaining DAFH eigenvectors present remarkable resemblance for the electrons of both α and β . Hence, the unpaired electron can be easily localized to a region of the space in visual terms.

The results obtained from DAFH for the doublet state of NH_3^+ and the triplet state of O_2 are in agreement with other methodologies such as delocalization indices.²¹¹ But in contrast to these approaches that rely only on numerical values, the DAFH analysis provides an explanation in both numerical and visual fashion closer to classical chemical thinking. Thus, the DAFH analysis allows for the transition from the complex world of real numbers characteristic of quantum mechanics to the whole numbers more related to classical chemical thinking. This new analysis could be applied to discern the bonding patterns of more complicated chemical systems such as the $[C_2O_4]^{2+}$ which will be the key system of the next work.

Bonding Analysis of the $[C_2O_4]^{2+}$ Intermediate Formed in the Reaction of CO_2^{2+} with Neutral CO_2

From the very beginning, the electron-transfer reactions between gaseous dications and neutral molecules have fascinated the physical chemists. In such processes, one electron is transferred from the neutral to the dication to obtain two monocations. In general, it is assumed that, in electron transfer processes, the energy released upon the formation of two monocations is statistically partitioned between the resulting products, let us say in a "symmetric" fashion. However, Roithová and coworkers have recently found indications of "asymmetric" deposition of the energy between the pair of monocations.²¹² In particular, they have studied the reaction of triplet CO_2^{2+} dication with neutral CO_2 , obtaining $2CO_2^+$.²¹³ Thus, the monocation originated from the dication, formed upon electron capture, dissociates substantially more than the one that comes from the neutral counterpart. This "asymmetry" has been attributed to the fact that the triplet ground state of the dication can access to predissociative quartet states upon electron capture, which are not accessible by a single electron removal from the singlet ground state of neutral CO_2 .²¹⁴ Position-sensitive coincidence (PSCO) experiments have shown the involvement of a long-lived intermediate $C_2O_4^{2+}$ (see Figure 8.5), which could help us to give an explanation for the asymmetry of this charge transfer process.²¹⁴ Thus, we think that a more detailed understanding of the chemical bonding patterns of the triplet $C_2O_4^{2+}$ may shed light on the energy distribution of this fundamental reaction. Taking advantage of the previous generalization (Eq. 8.1), we have used the DAFH analysis to study the picture of the electron distribution of the triplet ground state



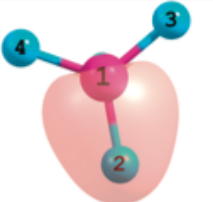
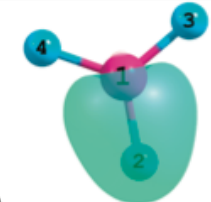


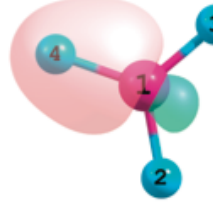
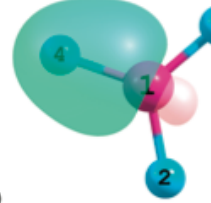
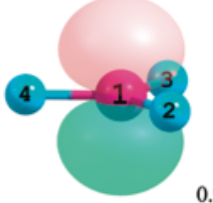
DAFH eigenvectors	
α spin	β spin
 a) 1.000 (0.999)	 b) 1.000 (0.999)
 c) 0.997 (0.991)	 d) 0.997 (0.991)
 e) 0.779 (0.671)	 f) 0.759 (0.645)
 g) 0.779 (0.671)	 h) 0.759 (0.645)
 i) 0.988 (1.000)	

Figure 8.4: Eigenvalues and eigenvectors resulting from the DAFH analysis over the fragment NH of the radical cation NH_3^+ . The numbers indicate the eigenvalues of the corresponding hole for the “exact” AIM form of the analysis, and the values in parentheses correspond to the “approximate” Mulliken-like approach

of the transient complex $[C_2O_4]^{2+}$.

Since the intermediate is formed from the ground states of both triplet CO_2^{2+}

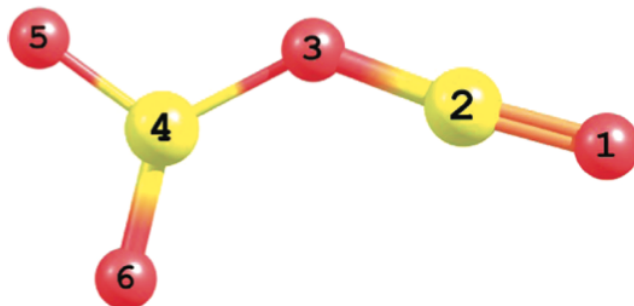


Figure 8.5: B3LYP/6-311G* optimized structure of the $[C_2O_4]^{2+}$ intermediate with notation of the six atoms involved, where $O(1)C(2)O(3)$ stems from the neutral CO_2 molecule and $O(5)C(4)O(6)$ stems from the dicationic reactant CO_2^{2+}

and singlet CO_2 , the DAFH analysis has been performed for two fragments: first, the $O(5)C(4)O(6)$ fragment that comes from the triplet CO_2^{2+} dication, and second the $O(1)C(2)O(3)$ fragment corresponding to the neutral CO_2 (see Figure 8.5 for the notation used). For the $O(5)C(4)O(6)$ fragment, we have found 12 non-zero eigenvalues for the electrons of α -spin and 10 non-zero eigenvalues for the electrons of β -spin. Interestingly, the unpaired electrons remain totally localized in this fragment. Both α - and β -holes averaged over the $O(5)C(4)O(6)$ fragment are summarized in Figures 8.6 and 8.7. The eigenfunctions summarized in Figure 8.6 show that the form of these localized functions is very similar for electrons of both α - and β -spin. Moreover, the eigenvalues associated to these eigenvectors are close to the unity and are clearly associated with electron pairs, i.e. chemical bonds, core electrons, or lone pairs, located in this region of the molecule. The localized functions represented in Figures 8.6-e and 8.6-j are more relevant. In this case, the eigenvalues deviate significantly from the unity due to the fact that this electron pair corresponds to the *broken valence* of the bond $C(4)O(3)$ (remember that $O(3)$ is not included in the fragment). When the electron pair is equally shared between the two fragments, i.e. apolar bond, the corresponding eigenvalue would be associated with values close to 0.5 for each α and β functions. In our case we have a polar bond where the carbon contributes with 0.4 electrons ($\alpha + \beta$ eigenvalues) while the oxygen with 1.6.

On the other hand, Figure 8.7 displays the DAFH eigenvectors associated with

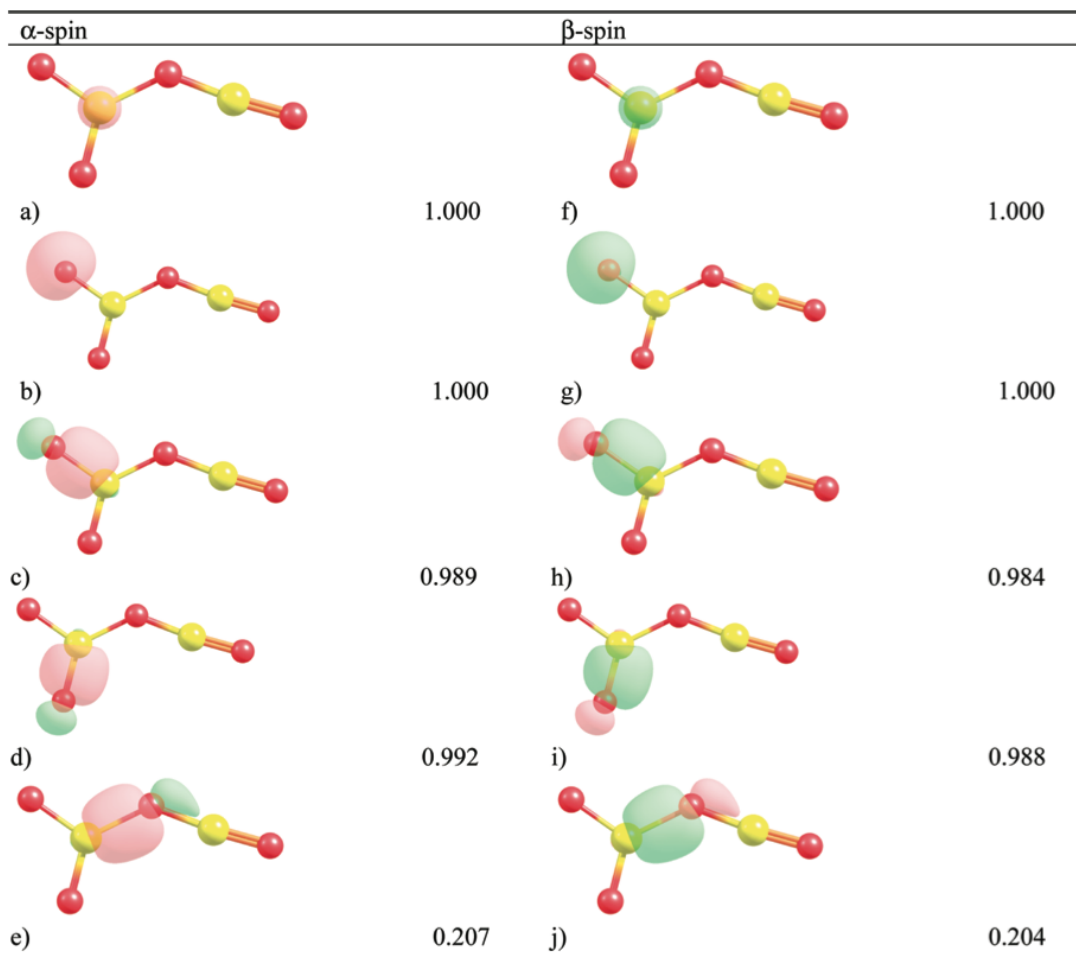


Figure 8.6: Selected eigenvectors of the DAFH corresponding to completely paired α - and β -spin electrons in the fragment $O(5)C(4)O(6)$ of the triplet state of the transient complex $[C_2O_4]^{2+}$

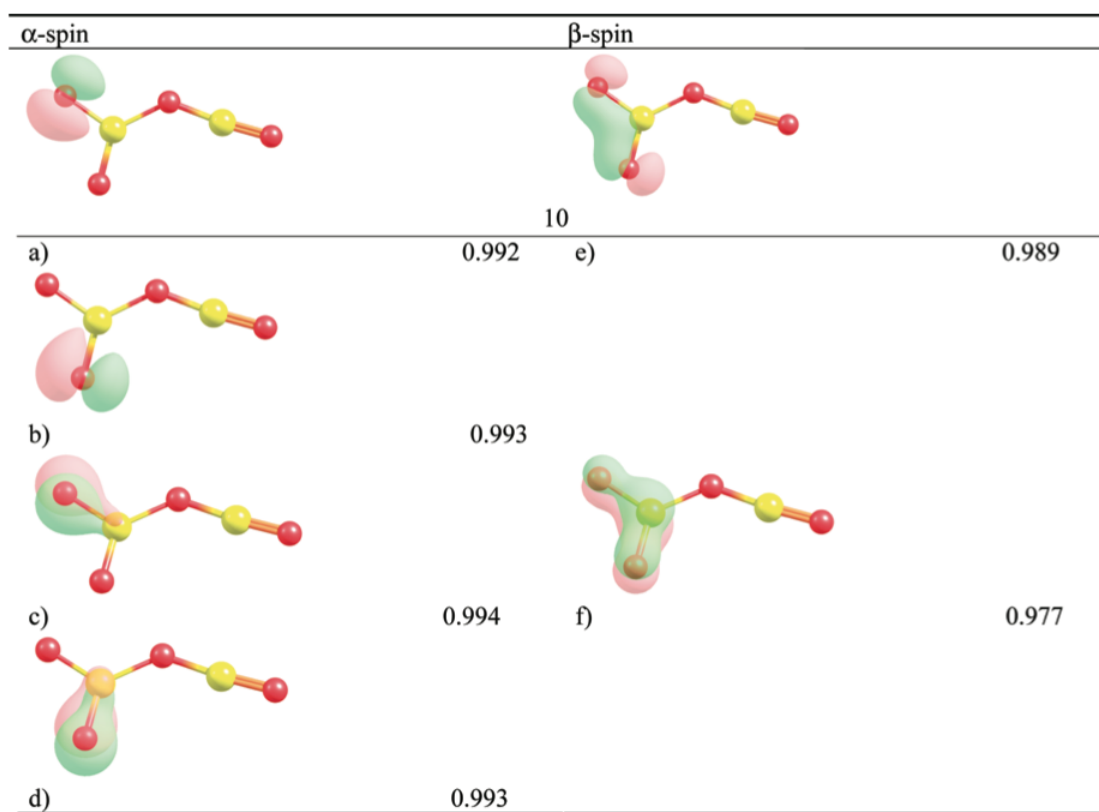


Figure 8.7: Selected eigenvectors of the DAFH responsible for the open-shell character in the fragment $O(5)C(4)O(6)$ of the triplet state of the transient complex $[C_2O_4]^{2+}$

the unpaired electrons. At first glance, one can see the different shape of α and β localized functions. As the number of α - and β -eigenvectors is different, the α - and β -DAFH eigenvectors cannot be paired. The α -eigenvectors are mainly localized, whereas the β electrons are delocalized through the three centers forming a 3c-2e bond. These differences are associated with the open-shell character of the fragment $O(5)C(4)O(6)$. Interestingly, the localized functions of Figure 8.7 can be split into two groups, one of which is localized in the molecular plane (a, b and e), and the other is perpendicular to it (c, d and f). Thus, one unpaired α electron resides in the molecular plane while the other is delocalized over the π system. The DAFH analysis of the $O(1)C(2)O(3)$ fragment clearly implies that no unpaired electrons are found in this region. This fragment is bound to the $O(5)C(4)O(6)$ fragment by a polar σ_{CO} bond.

Hence, from the DAFH analysis we have found a “local triple state” localized in the $O(5)C(4)O(6)$ fragment. In addition, when the polar bond σ_{CO} between $O(3)$ and $C(4)$ is split, we observe the formation of singly charged $O(1)C(2)O(3)^+$ that leads to the formation of doublet CO_2^+ in the ground electronic state. On the other hand, the remaining singly charged ion $O(5)C(4)O(6)^+$ bears three unpaired electrons and corresponds therefore to a quartet state. CCSD calculations confirm that this quartet state correlates with the $CO^+ + O$ dissociation limit and, thus, it explains this fragmentation preferentially observed for the monocation formed by electron capture of the dication. Notoriously, the structural asymmetry of the $C_2O_4^{2+}$ intermediate is also associated with an electronic asymmetry because the unpaired density stays strictly localized at the $O(5)C(4)O(6)$ fragment.

Peculiarities of Multiple Cr-Cr bonding. Insights from the Analysis of Domain-Averaged Fermi Holes

The exciting properties of metal-metal bonding has captivated the interest of both theoretical and experimental chemists from the very beginning. One of the most striking features is the existence of unusual bond multiplicities that can exceed the usual limits known from organic chemistry. As the experimental chemists were synthesizing new compounds with progressively shorter metal-metal bonds, the theoretical chemists were developing new methodologies to elucidate the nature of these fundamental bonding interactions. The first successful approaches were based on elementary molecular orbital (MO) analysis which allowed the multiple metal-metal bond in terms of σ , π , or δ components to be described.²¹⁵

Recently, the first stable molecules with a presumable quintuple Cr-Cr bond have been synthesized.^{216–219} Although the qualitative description based on MO analysis and the ultrashort interatomic distances seem to be consistent with the presence of quintuple multiplicity in Cr-Cr bond, sophisticated theoretical calculations suggest that the number of effective electron pairs involved in the multiple bond is lower than five.^{220,221} Thus, the nature of the bonding interactions in the realm of metal-metal bonding can be much more complicated. In order to contribute to the clarification of the bonding interactions in the Cr-Cr bond, we perform the analysis of DAFH for a recently reported complex with an ultrashort Cr-Cr bond.²¹⁷

The structure of the complex and the more relevant results of the DAFH analysis are summarized in Figure 8.8. The fragments analyzed by means of DAFH are the Cr-Cr bond and the domain involving one Cr atom. First, we will focus on the complex obtained by Kreisel et al. with the experimental bond length 1.8 Å. From the MOs analysis it is difficult to predict the multiplicity of the bond. Although there are five bonding electron pairs involved in metal-metal bond, only four are predominantly localized between metal atoms, and the remaining MO is delocalized toward the neighboring N ligands. In addition, the reported effective bond order is 4.28.²¹⁷ Therefore, the authors preferred to classify the bond as a quadruple rather than a quintuple bond. The analysis of DAFHs for the Cr-Cr fragment yields 27 non-zero eigenvalues. Among them, only five are associated with the Cr-Cr bonding interactions (see Figure 8.8), that is, the same number of electron pairs available for the Cr-Cr bond. *A priori*, the analysis of the shape of the eigenvectors seems compatible with the anticipated quintuple bond (one σ , two π , and two δ). However, after exploring the eigenvalues associated to the DAFH eigenvectors, only four localized functions present eigenvalues close to two (Figures 8.8-a, 8.8-b, 8.8-c, and 8.8-d) and, thus, solely four electron pairs can be assigned to the metal-metal bonding. The situation of the remaining eigenvector (δ -8.8-e) is more complex. Since its eigenvalue is close to 1, its association with the fifth bonding pair is evidently questionable. According to DAFH analysis, there is a partial depletion of the electron density from one of the electron pair participating in the Cr-Cr bonding. In contrast to the MOs analysis, the DAFH provides a more detailed quantitative estimate of the extent of depletion that can be linked to the dramatic decrease of the bond order. Thus, we also prefer to characterize the Cr-Cr bond of this complex as an effectively quadruple bond.

The discrepancy between the number of electron pairs involved and the effective

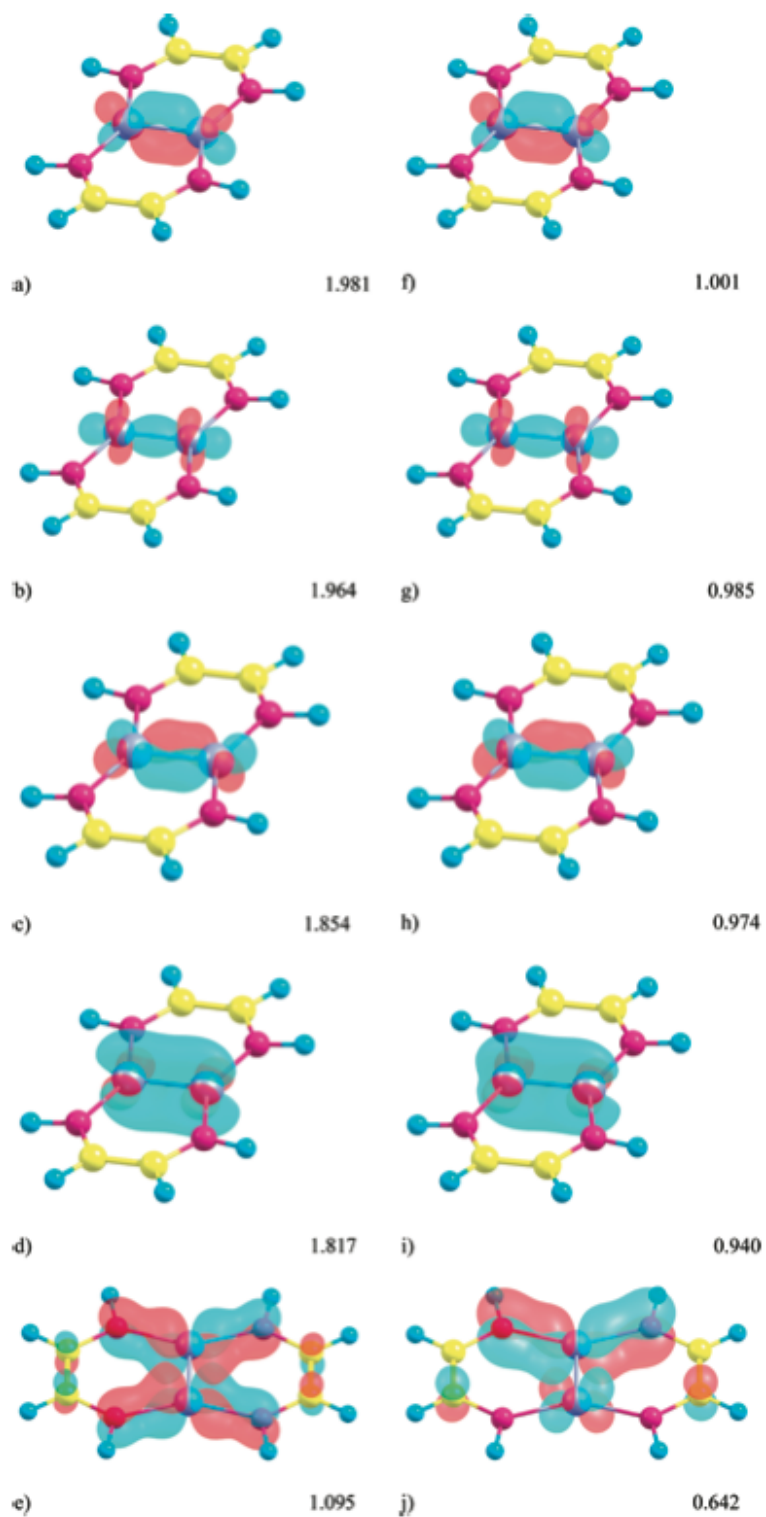


Figure 8.8: Results of the DAFH analysis for complex I. Selected eigenvectors of the Fermi holes corresponding to electron pairs and broken valances of the Cr-Cr bond for the holes averaged over the fragment Cr-Cr (left column) and the domain involving one Cr atom (right column), respectively.

multiplicity of the bond is quite frequently observed in the realm of metal-metal bonding. But what makes the Cr-Cr bond unusual is the mechanism of the reduction of the bond order. Previous theoretical studies²¹⁹ pointed out that the reduction of the overlap of the delocalized δ orbital is a favorable situation for the switch of the bonding interactions from ordinary sharing to antiferromagnetic coupling.²²² To this end, we have performed the DAFH analysis over only one of the Cr atoms in order to study the consequences of the formal splitting associated with the isolation of one Cr atom from the rest of the molecule. As can be seen from the right column of Figure 8.8, there are four eigenvectors with eigenvalues close to 1 that can be directly related to the *broken valences* of bonding electron pairs. The shape of these eigenvectors is exactly the same as the previously observed for the Cr-Cr fragment, that is, the electron density is delocalized through the two Cr atoms. Remarkably, the shape of the remaining eigenvector (Figure 8.8-j) is sensibly different from the one obtained for the Cr-Cr fragment (Figure 8.8-e). In contrast to the delocalized nature of the four bonding electron pairs, the eigenvector 8.8-j displays an increased localization toward one of the metal atoms which clearly confirms that one of the δ components of the Cr-Cr bond is indeed different from the remaining four. The weakness of this particular component due to its localization over one Cr atom could be attributed to the operation of antiferromagnetic coupling of the metals similar to that recently reported in the Cr_2 cluster.

To sum up, the new interesting insights provided by the DAFH analysis have allowed us to reveal the origin of the observed discrepancy between the number of available electron pairs and the calculated bond orders. Moreover, the dominant contribution to Cr-Cr bonding is due to four shared electron pairs, while the fifth is related to antiferromagnetic coupling.

8.2 Applications II: Critical assessment on the performance of a set of aromaticity indices

The following section gathers the results of sections 6.1, 6.2, 6.3, 6.4, and 6.5 from Chapter 6.

The concept of aromaticity is one of the cornerstones of past and current chemistry. However, at the same time, it is also considered a *chemical unicorn* because aromaticity is not a directly measurable property, that is, it cannot be defined

unambiguously.⁵ As the number of new aromatic molecules grows, the quest for the quantification of aromaticity has become one of the challenges for theoretical chemists.

The evaluation of aromaticity is not unique since a plethora of different measures based on structural-,[?] magnetic-,¹¹⁸ energetic-,¹⁶³ and electronic-based¹⁸² indices can be used to quantify the aromaticity of a given set of compounds. In many cases, results obtained from different indicators of aromaticity may reveal contradictory trends. In addition, principal component analysis suggests that aromaticity has a multidimensional character.¹⁴¹ Consequently, aromatic compounds cannot normally be well-characterized by using a unique index. In recent years, some authors pointed out that the multidimensional character of aromaticity is sometimes an excuse to hide the drawbacks of aromaticity descriptors.³² To overcome the controversies generated by bad correlations between aromaticity indices, we propose a new methodology to evaluate the performance of such descriptors.

Despite the large list of aromaticity descriptors, each one presents their advantages and drawbacks according to the nature of the system that is analyzed. The main aim of this part of the thesis is to study the ability of some of the most widely used aromaticity indices to give the expected answer from a series of tests that share widely accepted and well-understood aromatic trends. First, we study the nature of electronic indices at the HMO level. Second, we analyze the most common benzene distortions. Third, we focus on the intricate case of $(\eta^6 - C_6H_6)Cr(CO)_3$. Then, we define a series of 15 tests that could be useful to evaluate the performance of current and future aromaticity indices. Finally, we extend the previous test set to the recently discovered realm of all-metal clusters.

8.2.1 Electronic Aromaticity indices at HMO level

Electron Delocalization and Aromaticity Measures within the Hückel Molecular Orbital Method

In this work we study the behavior of the most common electronic aromaticity measures, i.e. FLU,¹⁸¹ PDI,⁵⁰ I_{ring} ,⁶⁰ and MCI,⁶¹ in the framework of the Hückel molecular orbital (HMO) theory.^{112,113} Exploring the nature of these indices at the HMO level is relevant not only for its own sake but as a way to go into the real meaning and behavior of these descriptors. Despite taking into account drastic approximations, the π electron ring current, which is the essence of organic aromaticity,

remains for the HMO wave function. In addition, the reduced computational cost associated with the HMO theory allows us to assess the aromaticity of large carbon skeleton molecules which would be unimaginable with *ab initio* calculations.

First, we have obtained the formulas for Coulson bond orders (CBO)²²³ for $4N$ - and $(4N + 2)\pi$ -electrons annulenes within the framework of HMO. The molecular space is partitioned into non-penetrating domains which are defined by the D_{nh} symmetry of the system. However, the electronic structure according to the CBO does not predict antiaromatic compounds as such, because the symmetry of the system is constrained to be D_{nh} . Obviously, this limitation is overcome by current *ab initio* calculations. Next, we have derived the expressions for the electron sharing indices at HMO level. One of the most significant features is that the bond orders between pairs separated by one atom is zero. Thus, there is no electron delocalization between non-contiguous atoms for cyclobutadiene, as one would expect for an antiaromatic system. What is more, Fulton²²⁴ and Bader²²⁵ noticed by means of *ab initio* calculations that the electron sharing between para-related carbons of benzene is more important than between meta-related carbons. Interestingly, this feature is retained at the HMO level because the ESI value for meta-related atoms is also zero.

Then, from the bond order expressions, one can produce the analytical functions for some of the aromaticity measures. First, we have studied the evolution of aromaticity when going from the outer to the inner ring of polyacenes up to 23 rings. For anthracene, FLU predicts the inner ring as the most aromatic, whereas PDI, I_{ring} and MCI give the opposite trend. However, the aromaticity of rings in anthracene must be considered quite similar. On the contrary, for polyacenes of more than three rings, all aromaticity descriptors predict the aromaticity to increase from the inner to the outer ring, with the exception of PDI which gives the opposite trend. Finally, we have analyzed large carbon macrocycles with an increasing number of benzenoid rings up to 11 crowns to emulate the situation of a graphite layer. In consonance with *ab initio* calculations, all the indices calculated at the HMO level show a qualitative agreement of the limit where inner rings are surrounded by enough benzenoid rings to show convergence in aromaticity measures (see Figure 8.9). In addition, unlike MCI and I_{ring} , PDI and especially FLU perform surprisingly well identifying the Clar sextets as the most aromatic rings in the macrocycle.

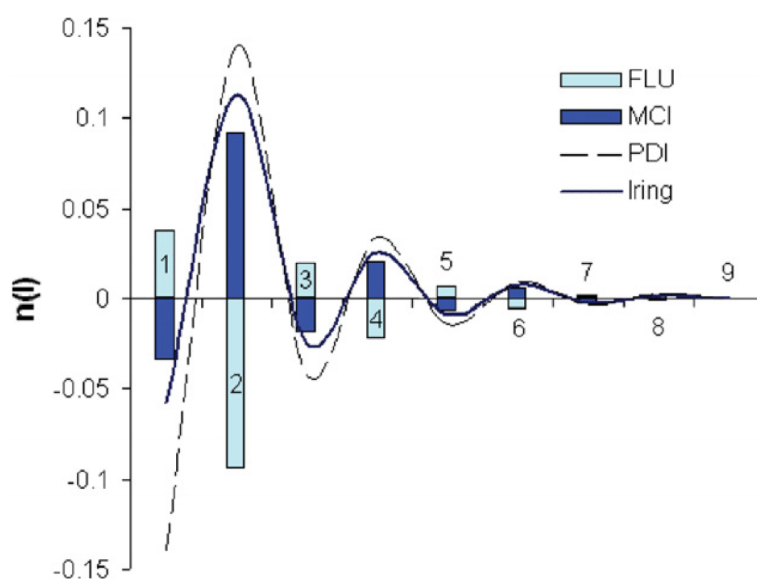


Figure 8.9: Aromaticity in central benzenoid macrocycle as a function of the number of crowns. Each aromaticity index is normalized with respect to its limit value to fit the graphic ($n(I) = (I_i - I_{11})/I_{11}$), with I being an aromaticity index).

8.2.2 A Critical Assessment on the Performance of Aromaticity Criteria in Organic Systems

When a new index of aromaticity is defined, usually the results obtained by this new index in a set of chosen aromatic compounds are correlated with some previously defined descriptors of aromaticity. If correlations are acceptable, it is reported that the new index is a good indicator of aromaticity. If not, frequently it is simply said that the result obtained is a manifestation of the multidimensional character of aromaticity. The problem with this approach is obvious: how can one differentiate methods that provide essentially spurious results from those that simply do not correlate because of the multidimensional character of aromaticity? Moreover, some aromaticity descriptors fail to give the expected answer from most elementary chemical problems. For this reason, the performance of aromaticity indices and their adequacy for each chemical situation must be a prime aim for the researchers in this field.

The key point of this section is the definition of 15 tests of aromaticity that can be used to evaluate the performance of the most widely used descriptors and to

define new indices that correlate better with the chemical intuition (see Figure 8.10 and Table 8.1). Before starting with the analysis of the test set, we briefly summarize two previous works that have led us to the proposal of this test set of aromaticity.

Aromaticity of Distorted Benzene Rings: Exploring the Validity of Different Indicators of Aromaticity

The changes on the aromaticity have been studied for some of the most common deformations of the benzene molecule. First, we have analyzed three in-plane distortions: bond length alternation (BLA), bond length elongation (BLE) and clamping conformations. Then, the study is completed with three-out-of-plane deformations: boatlike, chairlike, and hydrogen pyramidalization. Since benzene at its equilibrium geometry is the point of departure of each distortion, a loss of aromaticity is expected when the deformation is applied. Nine widely used descriptors of aromaticity based on structural (HOMA¹⁴⁷), magnetic (NICS(0), NICS(1), and NICS(1)_{zz}),¹¹⁸ reactivity (hardness¹⁵¹) and electronic (PDI, FLU, I_{ring} , and MCI) properties are used to quantify the changes on aromaticity along the deformation. The main results are summarized in Table 8.1. Surprisingly, FLU is the only index which is able to account for the loss of aromaticity in the six distortions that have been analyzed. However, the evolution of aromaticity along BLE is at least arguable since this deformation preserves the D_{6h} symmetry. For this reason, we have not included this distortion as a possible test of aromaticity (see Figure 8.10). If we do not take into account the BLE deformation, NICS(1), NICS(1)_{zz}, MCI, I_{ring} , and the above mentioned FLU reproduce the expected trends for the remaining series of benzene distortions analyzed. Remarkably, PDI remains almost unaffected by five distortions (BLE, clamping, boatlike, chairlike, and pyramidalization) while HOMA tends to overestimate the loss of aromaticity. Finally, the hardness fails to account for the loss of aromaticity associated with the BLA deformation. Thus, chemists wishing to use indicators of aromaticity to study the aromaticity of benzene rings should be aware of the advantages and drawbacks of each index.

Is the Aromaticity of the Benzene Ring in the $(\eta^6-C_6H_6)Cr(CO)_3$ Complex Larger than that of the Isolated Benzene Molecule?

We have decided to analyze $(\eta^6-C_6H_6)Cr(CO)_3$ system because we were puzzled by the claims of Mitchell and co-workers that the benzene ring in tricarbonylchromium-complexed benzene is ca. 30-40% more aromatic than benzene itself based on NICS results.²²⁶ It is widely accepted that the structure, reactivity, and aromaticity of

the benzene ring are altered significantly upon complexation with the chromium tricarbonyl complex. Thus, after coordination, the ring expands, loses its planarity (the hydrogen atoms of the benzene ring slightly bent towards the $Cr(CO)_3$ fragment), and shows an increased difference between alternated short and long C-C bonds. These changes can be rationalized taking into account the charge transfer from the highest occupied π -orbitals of the arene to the lowest unoccupied $2e$ and $2a_1$ orbitals of $Cr(CO)_3$, that partially breaks the C-C bonds, thus explaining the observed expansion of the aromatic ring and the increase in bond length alternation in the benzene ring of $(\eta^6 - C_6H_6)Cr(CO)_3$. Because of the loss of π electron density in the ring, one should expect a partial disruption of aromaticity in the benzene ring of $(\eta^6 - C_6H_6)Cr(CO)_3$ in comparison to free benzene, as discussed by Hubig et al.²²⁷ and not the increase of aromaticity observed by Mitchell and co-workers. Indeed, all indices used by us, except NICS(0) and NICS(1), show that there is a clear reduction of the aromaticity of benzene upon coordination to the $Cr(CO)_3$ complex. We have analyzed the particular behavior of the NICS index and we conclude that the reduction of the NICS value in the benzene ring of the $(\eta^6 - C_6H_6)Cr(CO)_3$ complex is not a manifestation of an increased aromaticity of the 6-MR but is due to the ring currents generated by the electron pairs that take part in the benzene- $Cr(CO)_3$ bonding. The coupling of the induced magnetic field generated by these electron pairs and that of the aromatic ring leads to an artificial reduction of the NICS(0) and NICS(1) values pointing to a non-existent increase of aromaticity. However, it has to be said that NICS(1)_{zz} index indicates the correct reduction of aromaticity of the benzene ring upon complexation.

On the Performance of Some Aromaticity indices: A Critical Assessment Using a Test Set

From the information gathered in the previous works, we have decided to extend the list of aromaticity tests to 15 systems (see Figure 8.10) that can be used to analyze the advantages and drawbacks of a group of aromaticity descriptors. The chosen tests must fulfill two requirements: first, the size of the systems involved must be relatively small to facilitate a fast application and, second, controversial cases must be avoided. Fortunately, the accumulated chemical experience provides several examples for which most chemists would agree about the expected aromaticity trends in a given series of compounds. As an example of a controversial case, we can mention the aromaticity of the anthracene rings, where half of the indices predict higher aromaticity for the inner-ring while the other half predict the opposite. Briefly, the test set contains: the five benzene deformations that have been previously analyzed,

two tests that study the effect of substitution and complexation of the benzene ring, a couple of tests that evaluate the ring and atom size dependence, then the effect of heteroatom is studied by means of two series of heteroaromatic systems with different size, two more containing a series of so-called Clar's and fulvenes systems, and finally, a couple of tests that assess the aromaticity in chemical reactions, i.e. Diels-Alder and $[2 + 2 + 2]$ trimerization of acetylene.

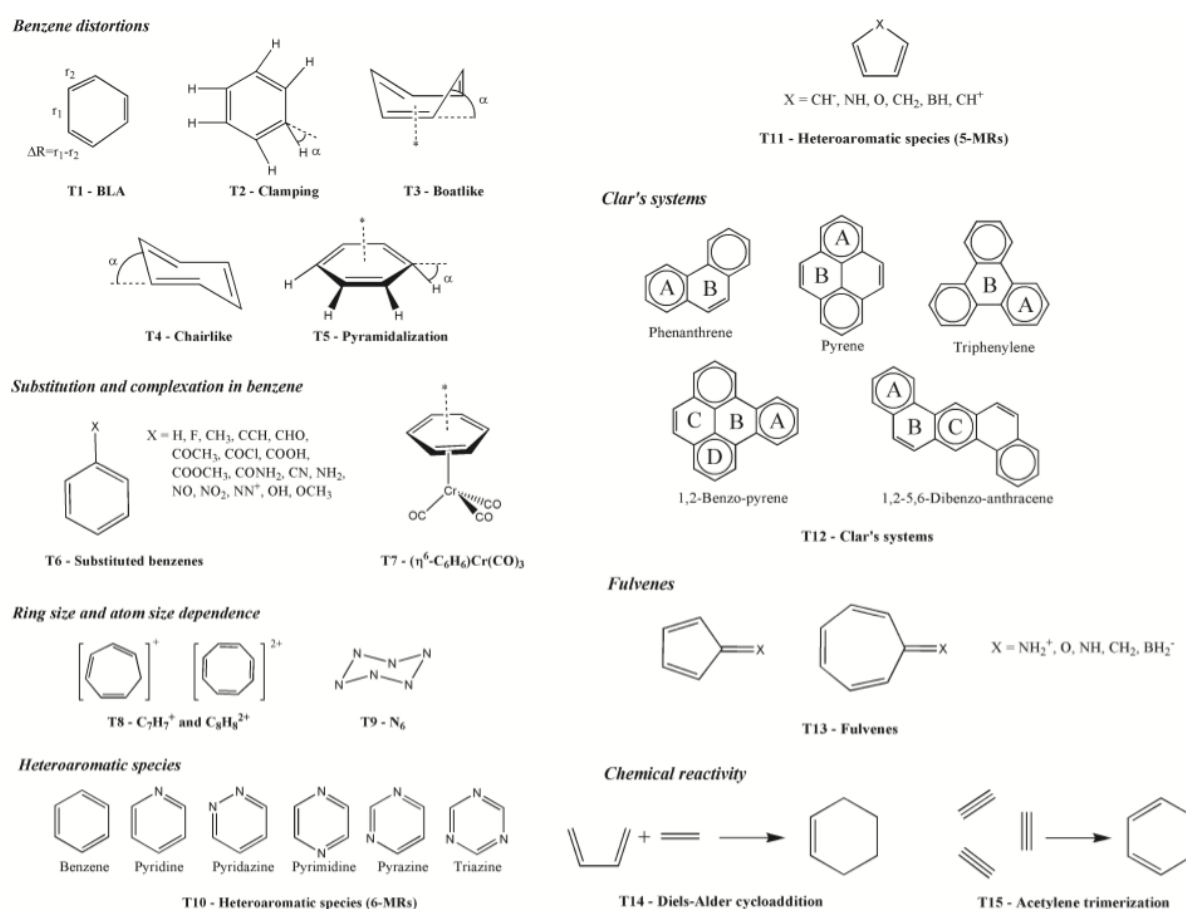


Figure 8.10: Schematic representation of the fifteen proposed tests. The sign “*” indicates the position where NICS (1) has been calculated.

Table 8.1: Summary of the fifteen tests applied at the B3LYP/6-311++G(d,p) level for the ten descriptors of aromaticity analyzed.

Test	PDI	FLU ^{1/2}	MCI	I _{NB}	I _{ring}	I _{NG}	HOMA	NICS(0)	NICS(1)	NICS(1) _{zz}
T1	yes	yes	yes	yes	yes	yes	unclear ^a	yes	yes	yes
T2	unclear ^b	yes	yes	yes	yes	yes	unclear ^a	unclear ^c	yes	yes
T3	unclear ^b	yes	yes	yes	yes	yes	yes	yes	yes	yes
T4	unclear ^b	yes	yes	yes	yes	yes	yes	yes	yes	yes
T5	unclear ^b	yes	yes	yes	yes	yes	yes	yes	yes	yes
T6	yes	yes	yes	yes	yes	yes	unclear ^d	no	no	yes
T7	yes	yes	yes	yes	yes	yes	yes	no	no	yes
T8	N/A	yes	yes	yes	yes	yes	yes	no	yes	yes
T9	no	yes	yes	yes	yes	yes	yes	yes	no	no
T10	no	unclear ^e	unclear ^f	unclear ^f	unclear ^f	unclear ^f	no	no	no	no
T11	N/A	unclear ^e	yes	yes	yes	unclear ^e	unclear ^e	yes	yes	yes
T12	yes	yes	yes	yes	yes	yes	unclear ^a	yes	yes	yes
T13	N/A	no	yes	yes	unclear ^e	unclear ^e	unclear ^e	yes	yes	yes
T14	yes	no	yes	yes	yes	yes	no	unclear ^g	unclear ^g	yes
T15	yes	no	yes	yes	yes	yes	no	unclear ^g	unclear ^g	unclear ^g

^a Loss of aromaticity is overemphasized. ^b The aromaticity remains almost unchanged with the distortion. ^c The trend in aromaticity remains almost unchanged with some oscillations. ^d The aromaticity is higher than that of benzene only for a small number of molecules. ^e Fails only in ordering one molecule. ^f Fails only in ordering one molecule. ^g The aromaticity of the TS is higher than that of benzene.

Exploring the successes and breakdowns of the different aromaticity indices is relevant not only for analyzing the performance of current descriptors but as a way to get ideas of how to improve present indicators of aromaticity and define new indices that correlate better with chemical intuition for most of the well-established cases. For this reason, it is very important, in our opinion, to devise methodologies that allow us to quantify the performance of the existing and new defined indices of local aromaticity. To this end, we consider that the use of a set of simple tests that include systems having widely-accepted aromaticity behaviors can be helpful to discuss aromaticity in organic species.

In order to analyze the performance of aromaticity indices in a series of 15 tests, we made a selection of different descriptors of aromaticity based on structural (HOMA), magnetic (NICS(0), NICS(1) and NICS(1)_{zz}) and electronic (PDI, FLU, MCI, I_{NB} , I_{ring} , and I_{NG}) manifestations of aromaticity. Table 8.1 summarizes the results obtained in all tests. We write "yes" when certain indices follow the expected trend in aromaticity for a given test, "no" otherwise, and "unclear" when the failure of the index is minor.

Finally, we outline the major conclusions and recommendations. First, our results indicated that the best indices are the electronic multicenter indices, especially MCI that fails only in test T10. The problem with MCI is its high computational cost that limits its application to rings with less than ten members, as well as their dependence on the level of calculation. $FLU^{1/2}$ indicator of aromaticity represents a cheaper alternative. However, like HOMA, FLU clearly fails to predict the evolution of aromaticity in chemical reactions. PDI, which has a similar computational cost as FLU, provides quite good results for the chemical reactions, but is unsuccessful when describing the loss of aromaticity in benzene distortions. In general, HOMA performs notably well despite its low computational cost. On the other hand, NICS(1)_{zz} is the form of NICS that performs the best among the different NICS indices analyzed, while NICS(0) presents several problems associated to substituted and complexed benzene, and also strong ring-size dependence. These results are in line with a previous study where a set of NICS indices were assessed and compared with aromatic stabilization energies (ASE) of 75 five-membered rings.¹⁷¹ Recently, we have analyzed the performance of NICS(0) _{π_{zz}} which has shown a similar behavior to NICS(1)_{zz}.²²⁸

At this point, a question arises, could the information gathered for organic species

be useful to study the multifold aromaticity characteristic of all-metal clusters?

8.2.3 A Critical Assessment on the Performance of Aromaticity Criteria in All-Metal Clusters

The properties of clusters make them potentially useful for technical applications such as specific and very efficient catalysts, drugs, and other novel materials with as yet unimagined features. Recently discovered, all-metal and semimetal aromatic clusters represent one of the new boundaries of material science.^{229,230} The unusual stability of all these clusters comes from their aromatic character. Indeed, the aromaticity is a key property of these compounds since it explains their molecular and electronic structure, stability, and reactivity. Unfortunately, in the case of inorganic clusters only few indices can provide reliable measures of aromaticity. Thus, in the spirit of the previous work, we propose a test to evaluate the performance of current aromaticity indices in the realm of all-metal clusters.

A Test to Evaluate the Performance of Aromaticity Descriptors in All-Metal and Semimetal Clusters. An Appraisal of Electronic and Magnetic Indicators of Aromaticity

The presence of multifold aromaticity and the lack of all-metal and semimetal aromatic clusters that can serve as inorganic reference systems (like benzene does in classical aromatic organic molecules) make the measure of aromaticity in these new systems much more complicated. Indeed, most of the currently available methods to quantify aromaticity have been designed to measure the aromaticity of organic molecules and take benzene or other aromatic organic molecules as a reference in their definitions. For the moment, the most widely used methods to discuss aromaticity in inorganic clusters are the qualitative analysis of MOs, the basic electron counting based on the $4n + 2$ Hückel's rule,²³¹ and the magnetic-based indicators of aromaticity, in particular, NICS; while less common is the use of electronic multicenter indices (MCI). As we have seen for organic species, it is frequently found for all-metal clusters that the aromaticity indices lead to divergent conclusions. Therefore, there is a need to assess the performance of aromaticity descriptors for these recently discovered species. To this end, we propose a series of all metal and semimetal clusters $[X_nY_{4-n}]^{q\pm}$ (X, Y = Al, Ga, Si, and Ge; $n = 0 - 4$) and $[X_nY_{5-n}]^{4-n}$ (X = P and Y = S and Se; $n = 0 - 5$) with predictable aromaticity trends. Since the series of $[X_nY_{4-n}]^{q\pm}$ species present double aromaticity, i.e. σ and π , the NICS and MCI indices are decomposed into their σ and π counterparts.

These series present an expected aromaticity trend because one can predict a sudden decrease in aromaticity when going from Al_4^{2-} to, for instance, Al_3Ge^- due to the reduction of symmetry and the substitution of one Al atom by a more electronegative Ge atom. A smooth reduction of aromaticity when going from Al_3Ge^- to Al_2Ge_2 is also likely, although more arguable. And the same should occur from Ge^{2+} to Al_2Ge_2 . Therefore, for instance, the expected order of aromaticity in the series $[Al_nGe_{4-n}]^{n-2}$ ($n = 0$ to 4) is $Al_4^{2-} > Al_3Ge^- \geq Al_2Ge_2 \leq AlGe_3^+ < Ge_4^{2+}$. A similar behavior is likely to be present in a series where X and Y come from different groups of the Periodic Table. As shown in Figure 8.11, MCI and MCI $_{\pi}$ curves exhibit a clear concave \cup shape. In general, electron multicenter indices perform very satisfactory for these species (see Table 8.2).

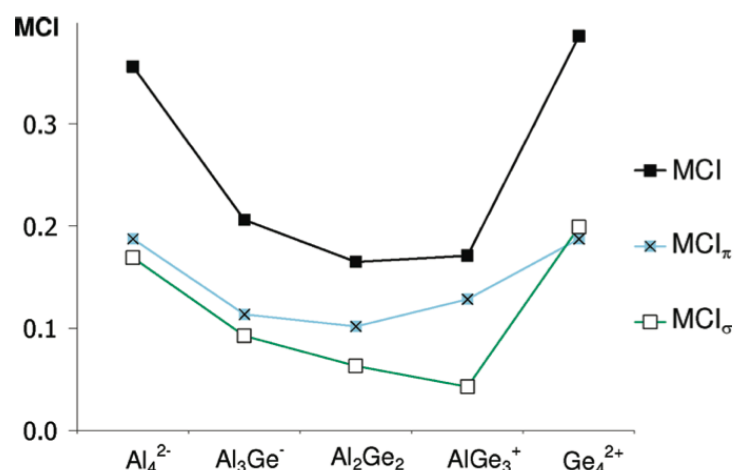


Figure 8.11: Variation of MCI, MCI $_{\pi}$, and MCI $_{\sigma}$ along the series Al_4^{2-} , Al_3Ge^- , Al_2Ge_2 , $AlGe_3^+$, and Ge_4^{2+} .

On the other hand, we have found that NICS values in inorganic systems strongly depend on the point where they are calculated. When they are computed at the geometrical center, NICS(0) predicts a progressive increase of the aromaticity from Al_4^{2-} to Ge_4^{2+} (see Figures 8.12 and 8.13), while when it is calculated at the ring critical point the curve shows the expected concave shape. Interestingly, NICS(0) $_{zz}$ and NICS(1) $_{zz}$ are less affected by this phenomena. Therefore, our first conclu-

Table 8.2: Summary of the results obtained at the B3LYP/6-311+g(d) level for the six series studied with seven descriptors of aromaticity analyzed.

series	MCI	MCI _π	NICS(0) ^{r_{cp}}	NICS(1) ^{r_{cp}}	NICS(0) _{zz} ^{r_{cp}}	NICS(1) _{zz} ^{r_{cp}}	NICS(0) _π ^{r_{cp}}
Al/Ge	yes	yes	yes	yes	unclear ^a	yes	yes
Al/Si	unclear ^a	yes	unclear ^a	yes	yes	yes	yes
Ga/Si	yes	yes	unclear ^a	unclear ^a	yes	yes	yes
Ga/Ge	yes	yes	yes	yes	yes	yes	yes
P/S	yes	yes	no	no	no	no	yes
P/Se	yes	yes	no	no	no	no	unclear ^a

^a Fails in ordering one molecule.

sion is that in the case of all-metal clusters, the NICS values must be calculated at the ring critical point. In addition to that, we have found a superior behavior of NICS(0)_π and NICS(0)_{zz} as compared to NICS(0). In a recent study, we have also evaluated the performance of NICS(0)_{πzz}, obtaining the same results as NICS(0)_π.²²⁸

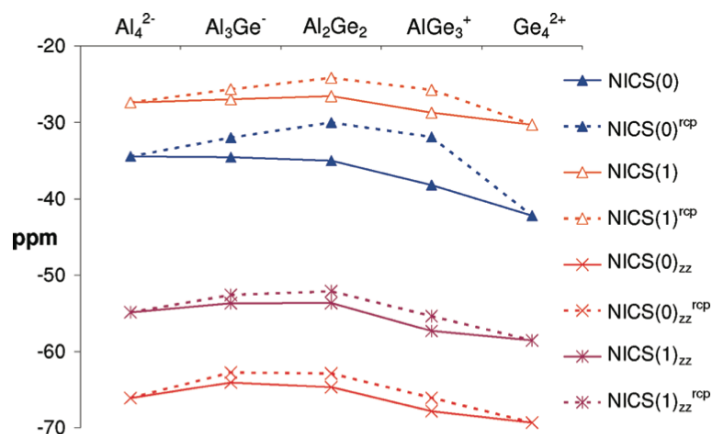


Figure 8.12: Comparison between NICS (ppm) indices calculated at the ring center and at the ring critical point (dotted line) along the series Al_4^{2-} , Al_3Ge^- , Al_2Ge_2 , $AlGe_3^+$, and Ge_4^{2+} .

To sum up, MCI and NICS are perfectly valid indicators of aromaticity for all metal clusters. However, if one wants to order a series of inorganic compounds according

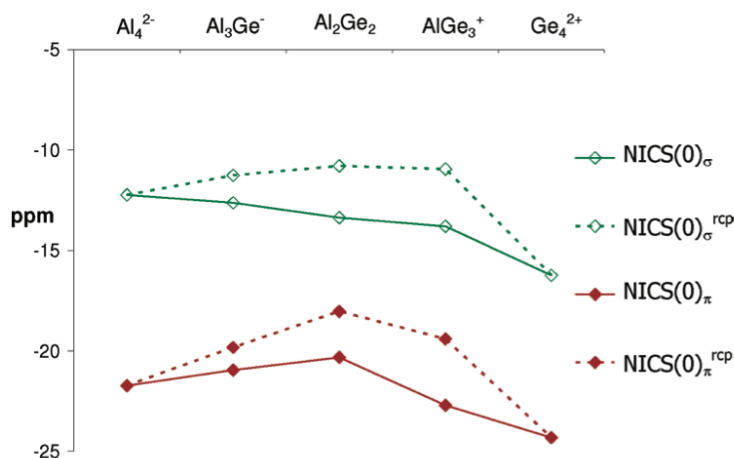


Figure 8.13: Comparison between dissected NICS (ppm) indices calculated at the ring center and at the ring critical point (dotted line) along the series Al_4^{2-} , Al_3Ge^- , Al_2Ge_2 , $AlGe_3^+$, and Ge_4^{2+} .

to their aromaticity, it is recommendable to use multicentric electronic indices or $NICS(0)_{\pi zz}$ values. For this purpose, neither $NICS(0)$ nor $NICS(1)$ are reliable, as we have seen for $(\eta^6 - C_6H_6)Cr(CO)_3$ molecule. On the other hand, if one wants to discuss whether a given all-metal cluster is aromatic or not, then both MCI and NICS do a good job. Finally, the performance of NICS and MCI has been validated for light atoms of the Periodic Table, but still remains to be assessed for more complicated transition metals having δ - or ϕ -aromaticity. The latter will be the aim of the last study of this thesis.

8.3 Applications III: Understanding electron delocalization in organic and inorganic compounds

Up to now, we have seen that, in general, electron delocalization measures provide very satisfactory results for both organic and inorganic aromatic species. This is not a surprise since the concept of aromaticity is tightly connected with electron delocalization. In fact, Schleyer's definition of aromaticity begins as follows: "Aromaticity is a manifestation of electron delocalization in closed circuits".¹¹⁸ Most of the electronic indices of aromaticity come from the XCD and the concept of ESI. Among the electronic based indices, multicenter indices, and specially MCI, perform remarkably well. Notwithstanding, MCI has been associated with high computa-

tional cost and relative dependence on the level of calculation.¹⁹¹ These facts limit its use to rings up to ten members. On the other hand, PDI descriptor can be only applied to 6-MR while FLU index strongly depends on reference values which prevent the use of FLU for inorganic species. Therefore, there is still a long way to go in the field of electronic delocalization descriptors. To this end, the aim of this section is to study in detail the electron delocalization of aromatic and antiaromatic compounds of both organic and inorganic, large and small systems. We consider that this analysis would represent a step forward towards a better comprehension of the electronic delocalization behavior of aromatic and antiaromatic systems that could help us to define a new aromaticity index in the near future.

8.3.1 Electron Delocalization in Organic Systems

Analysis of Hückel's $[4n + 2]$ Rule through Electronic Delocalization Measures

The $(4n + 2)\pi$ -electron rule has played a key role in the concept of aromaticity from the very beginning. According to this rule, a monocycle ring with $(4n + 2)\pi$ -electrons is aromatic, while a system with $4n\pi$ -electrons is antiaromatic. In the last decades, experimental evidences that have proven the validity of this rule have been found.²³² In addition, the original definition, which was limited to monocycles, was extended to take into account polycyclic aromatic hydrocarbons. A further development came when Baird showed that annulenes which are aromatic in their singlet ground state are antiaromatic in their lowest-lying triplet state, and vice versa. Several theoretical calculations have proven the validity of both Hückel and Baird rules.²³³⁻²³⁶

In order to explore the nature of the electron delocalization in aromatic compounds, we have analyzed the changes on π -electron delocalization when we add or subtract two electrons to a series of annulenes. To this end, we have calculated the total π -electron delocalization (δ_π) which is obtained from the sum of all the delocalization indices (DI) between pairs of atoms in the molecule:

$$\delta_{tot} = \sum_{A_i, A_j \neq A_i} \delta(A_i, A_j) = \sum_{A_i, A_j \neq A_i} \delta_\pi(A_i, A_j) + \sum_{A_i, A_j \neq A_i} \delta_\sigma(A_i, A_j) = \delta_\pi + \delta_\sigma \quad (8.2)$$

We expect that the trends followed by the δ_π when adding or removing two π electrons should allow us to discern between aromatic and antiaromatic systems. Our hypothesis is based on the premise that in aromatic systems the electrons are mainly

delocalized whereas in antiaromatic systems the electrons are mainly localized. If an aromatic $(4n + 2)\pi$ system incorporates two π -electrons then we reach an antiaromatic $4n\pi$ -electron systems. Thus, one expects that the two added electrons will be mainly localized, this is to say that the total π -electron delocalization stays the same when going from $(4n + 2)\pi$ to $4n\pi$ system. On the contrary, when we add two electrons to an antiaromatic $4n\pi$ we obtain an aromatic $(4n + 2)\pi$ system, and hence, these electrons are mainly delocalized throughout the molecule. Previous studies on the electron delocalization of H_2 and H_2^- molecules showed that the change in total δ may be positive and around 1 electron when this pair of electrons is completely delocalized.²¹¹ Figure 8.14 summarizes our hypothesis with respect to an aromatic system (C_6H_6) and an antiaromatic one (C_8H_8) when going from $N - 2$ to N and from N to $N + 2$ systems, where N is the number of π electrons.

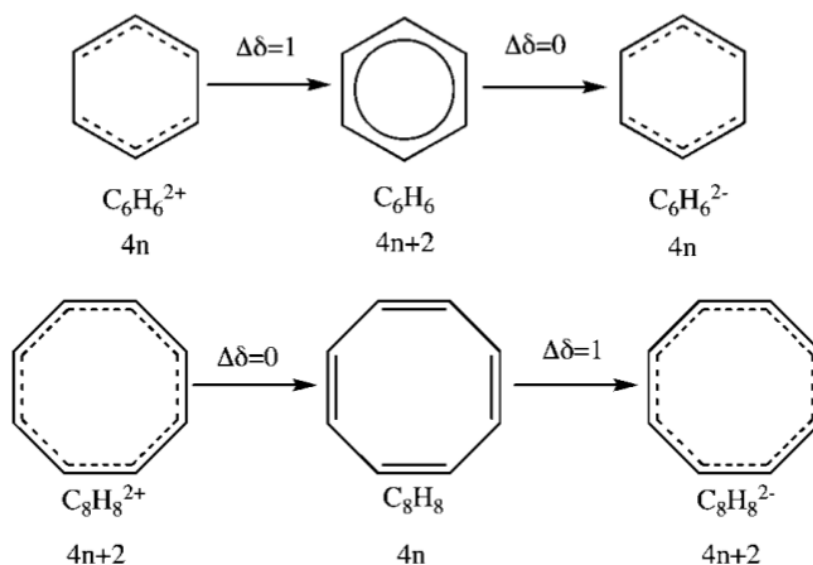


Figure 8.14: Expected behavior of δ_π when two electron are added or removed from C_6H_6 and C_8H_8 .

First, we have found that the effects of geometry and electron relaxation on δ_π are small enough to be neglected. Then, our results show how δ_π perfectly follows the expected trend for aromatic compounds but unexpected trends emerge in antiaromatic systems. Thus, we cannot establish a clear frontier between aromatic and

antiaromatic compounds from the analysis of δ_π . In addition, the total δ_π is practically the same for singlet and triplet species. Therefore, from δ_π one cannot prove the validity of the Baird's rule.¹²⁶ The nature of these drawbacks will be addressed in the following section.

Patterns of π -electron Delocalization in Aromatic and Antiaromatic Organic Compounds in the Light of Hückel's $[4n + 2]$ rule

This work represents an extension of the previous section. Following the idea of PDI descriptor of aromaticity, which is based on the electron delocalization between *para*-related carbons, we have decomposed the δ_π into its counterparts, that is, the *ortho* (1,2), *meta* (1,3), *para* (1,4), and successive contributions, the so-called crossed terms (see Figures 8.15 and 8.16). For instance, for any 6-MR we have:

$$\delta_\pi = 6\delta_\pi^{1,2} + 6\delta_\pi^{1,3} + 3\delta_\pi^{1,4} \quad (8.3)$$

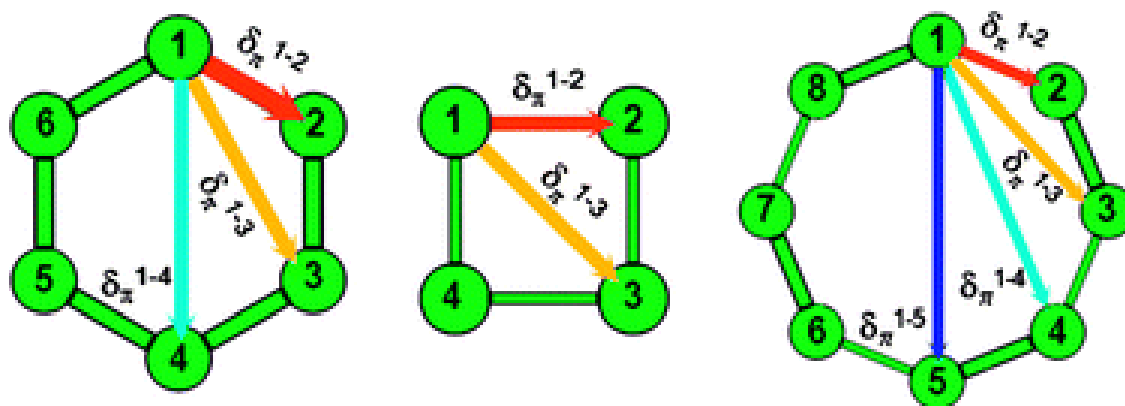


Figure 8.15: Decomposition of electron delocalization in crossed-terms $\delta_\pi^{1,x}$ for C_6H_6 , C_4H_4 , and C_8H_8 .

Our aim is to investigate how the crossed-terms change when two electrons are added or removed from aromatic or antiaromatic systems. For such a purpose, we have undertaken a study of a series of aromatic and antiaromatic systems with well-known trends of aromaticity. In order to simplify the analysis, we will assess the changes on the crossed terms for the aromatic C_6H_6 and for the antiaromatic C_8H_8 (see Figures 8.16 and 8.17). In the case of benzene, when we go from antiaromatic $C_6H_6^{2+}$ to aromatic C_6H_6 , the *ortho*, $\delta_\pi^{1,2}$, and the *para*, $\delta_\pi^{1,4}$, terms increase, while

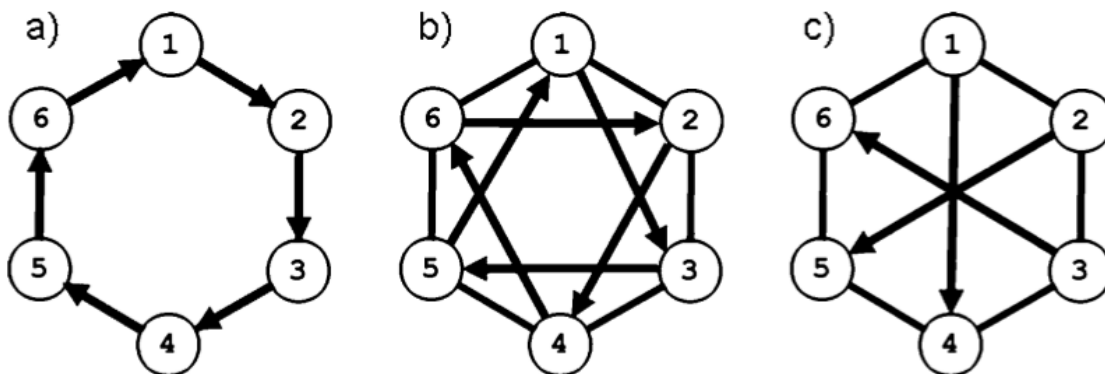


Figure 8.16: C_6H_6 crossed contributions $\delta_\pi^{1,x}$: (a) $\delta_\pi^{1,2}$ (b) $\delta_\pi^{1,3}$, and (c) $\delta_\pi^{1,4}$.

surprisingly, the *meta* term decreases. Remarkably, the increase on total δ_π when going from antiaromatic $N - 2$ to aromatic N species does not imply an increase in all crossed terms. On the other hand, when two electrons are added to aromatic C_6H_6 in order to obtain antiaromatic $C_6H_6^{2-}$, the opposite trends are observed, i.e. $\delta_\pi^{1,2}$ and $\delta_\pi^{1,4}$ decrease while $\delta_\pi^{1,3}$ increases. At first glance, large values of $\delta_\pi^{1,2}$ and $\delta_\pi^{1,4}$ could be related to aromaticity, the latter is the basis of PDI, whereas large $\delta_\pi^{1,3}$, or low $\delta_\pi^{1,2}$ and $\delta_\pi^{1,4}$, values could be associated with antiaromaticity in 6-MR.

In contrast to C_6H_6 , planar C_8H_8 is antiaromatic. As Figure 8.18 shows, when going from antiaromatic C_8H_8 to aromatic $C_8H_8^{2+}$ or $C_8H_8^{2-}$, $\delta_\pi^{1,2}$ and $\delta_\pi^{1,4}$ decrease, while $\delta_\pi^{1,3}$ and $\delta_\pi^{1,5}$ increase. Thus, we observe a clear alternation between crossed terms separated by even and odd number of atoms. This alternation, which has been proven with rings of up to 16 members, is driven by the the crossed-term corresponding to the two farthest atoms in the ring, i.e. $\delta_\pi^{1,4}$ in 6-MRs or $\delta_\pi^{1,5}$ in 8-MRs, which is always larger for aromatic compounds. Interestingly, there is no connection between the C-C distance and the corresponding crossed term values, that is, shorter C-C distances do not always imply larger $\delta_\pi^{1,x}$ values. In conclusion, the crossed-term corresponding to the two farthest atoms in the ring decreases in aromatic species when two electrons are added or removed, whereas the opposite is true for antiaromatic rings. As shown in Table 8.3, the remaining crossed terms follow an alternation pattern in function of the behavior of the crossed term associated with the two farthest atoms. At variance with total δ_π , these patterns of π -electron

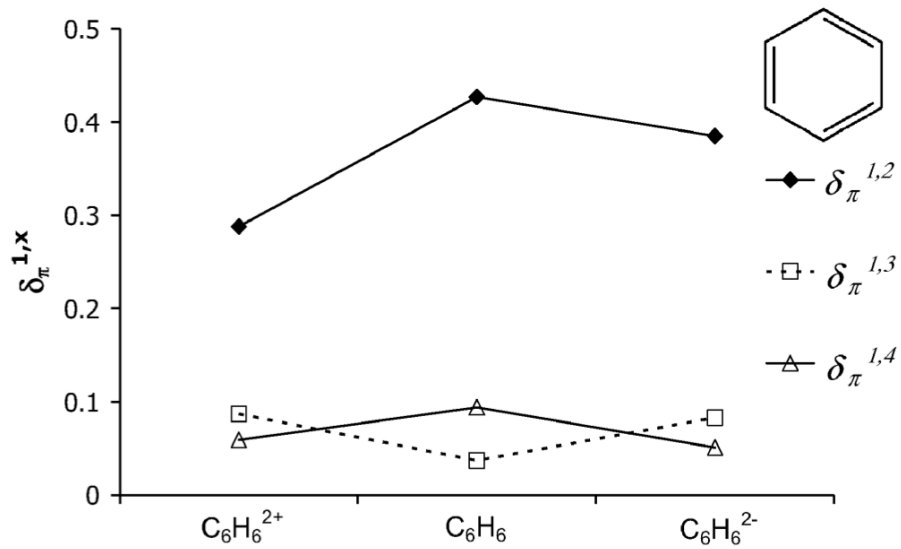


Figure 8.17: $\delta_{\pi}^{1,x}$ measures in $C_6H_6^{2+}$, C_6H_6 , and $C_6H_6^{2-}$. Units are in electrons.

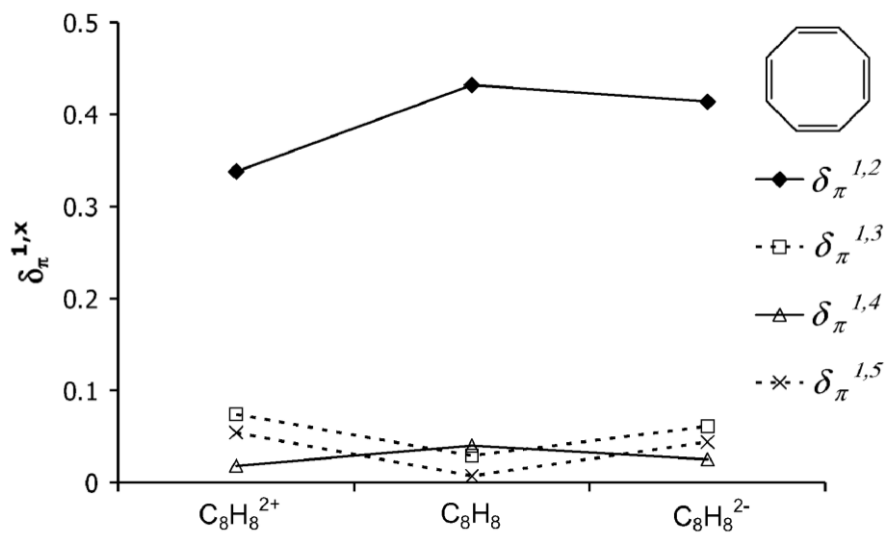


Figure 8.18: $\delta_{\pi}^{1,x}$ measures in $C_8H_8^{2+}$, C_8H_8 , and $C_8H_8^{2-}$. Units are in electrons.

Table 8.3: Schematic representation of the behavior of the crossed contributions to the total π -electronic delocalization in antiaromatic and aromatic compounds of different ring sizes. \uparrow and \downarrow refer to increase and decrease, respectively.

	Antiaromatic $N \rightarrow N \pm 2$			Aromatic $N \rightarrow N \pm 2$		
	4-MR	6-,7-MR	8-,9-MR	4-MR	6-,7-MR	8-,9-MR
$\delta_{\pi}^{1,2}$	\downarrow	\uparrow	\downarrow	\uparrow	\downarrow	\uparrow
$\delta_{\pi}^{1,3}$	\uparrow	\downarrow	\uparrow	\downarrow	\uparrow	\downarrow
$\delta_{\pi}^{1,4}$		\uparrow	\downarrow		\downarrow	\uparrow
$\delta_{\pi}^{1,5}$			\uparrow			\uparrow

delocalization represent a kind of electronic footprints that makes it possible to discern between aromatic and antiaromatic systems. However, we have found some discrepancies in the case of 5-MR systems that prevent the use of crossed terms analysis for such rings. This opposite behavior of 5-MR may be attributed to the fact that for such small ring size, $\delta_{\pi}^{1,3}$ could also be considered $\delta_{\pi}^{1,4}$ depending on whether one follows clockwise or anti-clockwise directions in the ring when going from one atom to the farthest one in the ring.

Another drawback of δ_{π} was its inability to discern between the aromaticity of singlet and triplet states in the framework of Baird's rule. As can be seen from Figures 8.19 and 8.20, this disadvantage is overcome by the analysis of crossed terms which also show alternation patterns between the aromatic singlet state of C_6H_6 and its antiaromatic lowest-lying triplet state. Exactly the opposite trends are observed between the antiaromatic singlet state of C_8H_8 and its aromatic triplet state.

To sum up, the PDI descriptor of aromaticity measures the electron delocalization between two carbons in *para* position, i.e. $\delta_{\pi}^{1,4}$, and thus, is limited to 6-MR. Interestingly, we have found that not only the $\delta_{\pi}^{1,4}$ but all the crossed terms are relevant for describing the aromaticity of the system, hence this analysis can be extended to rings of different size. In addition, these crossed terms follow alternation patterns of π -electron delocalization that can be used to discern between aromatic and antiaromatic organic compounds. This analysis will be extended to inorganic species in the following section.

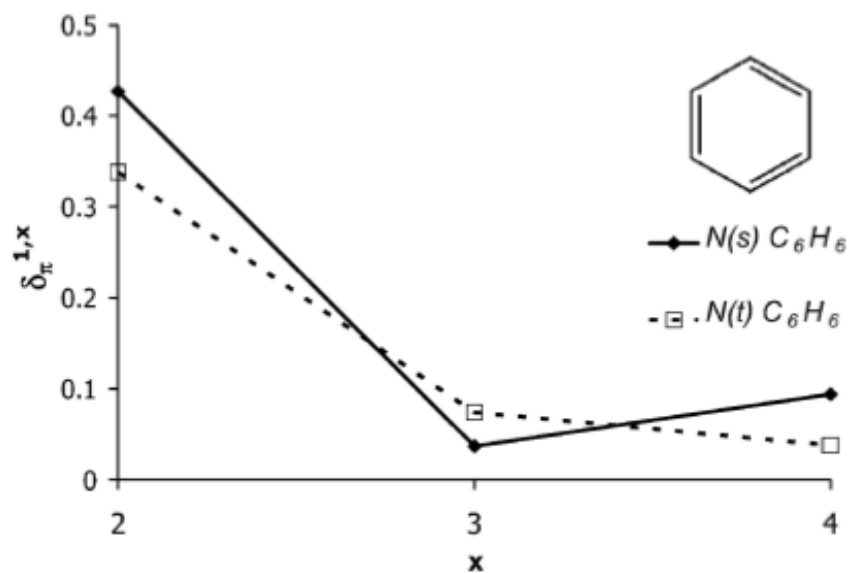


Figure 8.19: $\delta_{\pi}^{1,x}$ measures in aromatic singlet C_6H_6 (s), and antiaromatic triplet C_6H_6 (t). Units are in electrons.

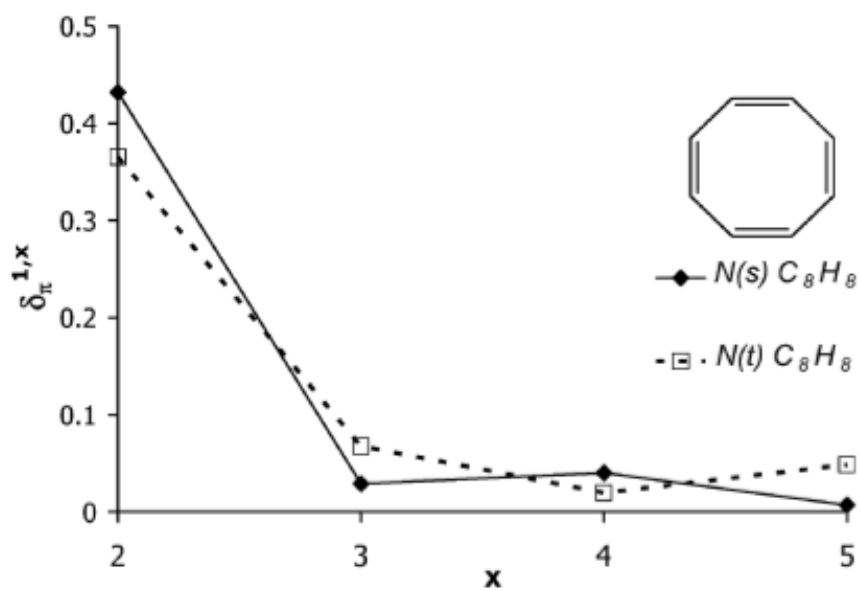


Figure 8.20: $\delta_{\pi}^{1,x}$ measures in antiaromatic singlet C_8H_8 (s), and aromatic triplet C_8H_8 (t). Units are in electrons.

The information gathered in current studies could help the researchers in this field to define more successful and universal descriptors of aromaticity that could be applied without any restriction. For instance, in the last decade, the synthesis of large porphyrinic systems with Hückel and Möbius aromaticity has been one of the main focus of interest in the field of novel aromatic compounds.²³⁷ However, very few indices can be applied to study the aromaticity of such large systems. In the future, our aim will be to find an electronic based approach to evaluate the aromaticity of these exciting compounds.

8.3.2 Electron Delocalization in All-Metal Clusters

At the end of this thesis, some questions have remained unanswered. First, whether the electronic indices can account for δ -aromaticity, which is characteristic of all-metal clusters, with the same good performance as they have previously shown with σ - and π -aromaticity. Second, if the above mentioned alternation patterns are also present in inorganic species with multiple aromaticity. Both questions are faced in the next section.

Aromaticity and Electronic Delocalization in All-metal Clusters with Single, Double, and Triple Aromatic Character

In 2001, Boldyrev and Wang discovered the first all-metal aromatic clusters.⁴ This finding, which is considered one of the major breakthroughs in the field of aromaticity, provoked immense repercussions on the fundamentals of aromaticity. In addition, six years later, the same authors proposed the first compound with δ -aromaticity, $Ta_3O_3^-$.¹³⁴ Later on, they proposed the first compounds with triple aromaticity, Hf_3 ²³⁸ and $^5Ta_3^-$.²³⁹ Since the previous authors only assessed the aromaticity by using simple Hückel's ($4n + 2$) rule, we propose the use of electronic delocalization measures to quantify the aromaticity of these recently discovered compounds.

Previously, we have investigated the ability of MCI to order a series of double σ - and π -aromatic clusters according to their degree of aromaticity. Now, a series of all-metal clusters with single, double, and triple (anti)aromatic character is studied. The aromaticity has been evaluated through two-center and multicenter electronic delocalization indices and their σ -, π , and δ components. To this end, we have selected a series of compounds that are classified as follows: first, 4-MR

having double σ - and π -aromaticity (Al_4^{2-} , MAl_4^- (M = Li, Na, Cu),⁴ Al_3Ge^- ,²⁴⁰ Al_2Ge_2 ,²⁴¹ $AlGe_3^+$,²⁴² and Ge_4^{2+} ²⁴²), and second, σ -aromaticity and π antiaromaticity (the Al_4^{4-} unit attached to Li^+ cations, $Li_xAl_4^{q\pm}$ ^{243,244}). Then we have selected a series of transition-metal 3-MRs with single σ -aromaticity (Cu_3^+ ²⁴⁵), conflicting σ -aromaticity (Cu_3H_3 ¹³³), double σ - and π -aromaticity (Y_3^- and La_3^- ²⁴⁶), double π - and δ -aromaticity ($Ta_3O_3^-$ ¹³⁴), and finally, triple σ -, π -, and δ -aromaticity (Hf_3 ²³⁸). Moreover, the aromaticity of two open-shell species, $^5Ta_3^-$ ²³⁹ and 3Hf_3 ,²³⁸ has been analyzed. Since the study of complexes with Ta and Hf requires the inclusion of relativistic effects, we have employed pseudopotentials for the calculations. As a side effect, the use of pseudopotentials leads to the appearance of the above mentioned non-nuclear attractors (NNA)¹⁹ within the QTAIM partition. In order to avoid the problems associated with these NNA, the atomic-overlap matrix has been calculated using the fuzzy atom partition.¹⁸ Our results show that both partitions lead to similar MCI values when the molecule has homonuclear bonds. These observations are in line with previous results reported in the literature.

An interesting property of MCI index is that for planar systems with only σ - and π -occupied orbitals the total MCI value can be exactly decomposed into their σ - and π -components. Thus, MCI shows the σ -aromatic and π -antiaromatic character of the Al_4^{4-} unit. For planar species with additional δ orbitals, the separation is not exact due to some σ - and δ mixing within a given atomic domain. However, these errors associated with the partition can be calculated and are, in general, negligible. In all cases, MCI calculations not only reproduces the previously reported behavior but offers the possibility to quantify the multiple aromaticity of each component, i.e. σ -, π -, and δ .

Finally, we have carried out the crossed-terms analysis for the 4-MRs of the above mentioned compounds. Our results show that the crossed-term corresponding to the two farthest atoms in the ring, i.e. $\delta^{1,3}$, reproduces the trends described by MCI. What is more, we have analyzed the performance of $\delta^{1,3}$ and $\delta_\pi^{1,3}$ along the above mentioned series of $Al_4^{2-} > Al_3Ge^- \geq Al_2Ge_2 \leq AlGe_3^+ < Ge_4^{2+}$. As Figure 8.21 shows, the $\delta^{1,3}$ and $\delta_\pi^{1,3}$ curves mimic the shape of the MCI one. Since the calculation of $\delta^{1,3}$ is less computationally demanding than MCI, this approach represents a good alternative to the use of multicenter indices in all-metal clusters.

In summary, our results show that the σ -, π -, and δ -components of MCI are excellent indicators of σ -, π -, and δ -aromaticity.

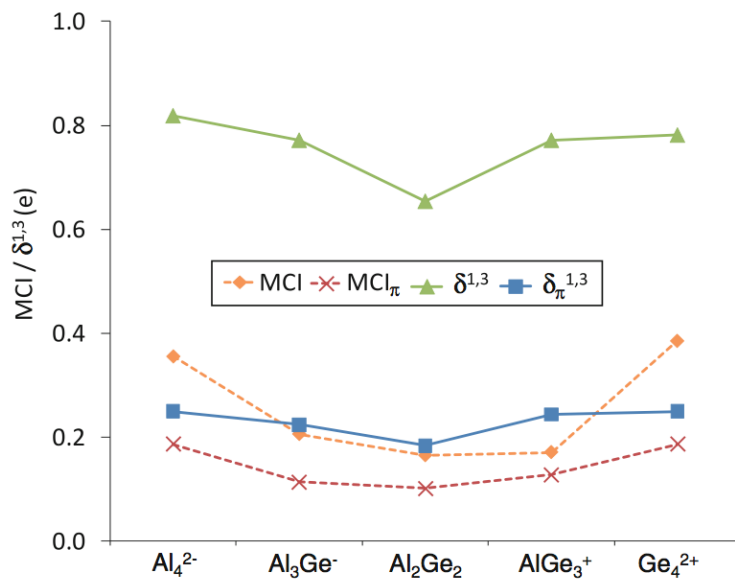


Figure 8.21: Variation of MCI, MCI_π , $\delta^{1,3}$, and $\delta_\pi^{1,3}$ along the series Al_4^{2-} , Al_3Ge^- , Al_2Ge_2 , $AlGe_3^+$, and Ge_4^{2+} .

Chapter 9

Conclusions

We present the conclusions of this thesis organized in three groups of applications:

Applications I: The nature of the Chemical Bond from Electron Localization Function and Domain-Averaged Fermi Holes

First:

We have presented a 2-fold approximation for the calculation of the ELF which avoids the use of the expensive two-particle density (2-PD). Since the 2-PD is approximated in terms of natural orbitals, the natural orbitals and their occupancies are only needed. The first approximation is based on the single determinant approach for the calculation of the 2-PD (HF-XCD) and it is used for the calculation of the ELF itself and for the definition of the basin boundaries. The HF-XCD performs remarkably well as shown in a number of examples. The second approximation relies on the expression proposed by Müller and popularized by Baerends and Buijse (BB), and it is used for the calculation of the pair densities integrated in the ELF basins. The performance of BB is also very convincing, especially for CASSCF calculations. Interestingly, B3LYP exhibits a good behavior except for those molecules where B3LYP is an inappropriate choice for the description of the system. This approximation represents a step forward towards the calculation of the ELF for medium sized-molecules with correlated methods.

Second:

The formalism of DAFH has been extended to open shell systems. In order to test the applicability of the proposed generalization, the doublet state of NH_3^+ and the ground triplet state of O_2 molecules have been analyzed in detail. The picture of the bonding resulting from the DAFH analysis is completely consistent with the con-

clusions of previous theoretical approaches. In contrast to these approaches which are based only on numerical values, the DAFH analysis of open shell systems also provides simple qualitative insights, that can be used to rationalize the electronic structure in a visual way close to classical chemical thinking. These analyses could be applied to elucidate the nature of chemical bonding in open-shell molecules with non-trivial bonding, such as $[C_2O_4]^{2+}$.

Third:

The bonding patterns of $[C_2O_4]^{2+}$ have been analyzed by means of DAFH analysis. The reaction between the triplet state of CO_2^{2+} and the singlet ground state of CO_2 leads to the formation of $[C_2O_4]^{2+}$ intermediate with two unpaired electrons. The DAFH analysis of $[C_2O_4]^{2+}$ shows that the two CO_2 entities are bound via a polar σ -bond between an oxygen atom of the originally neutral CO_2 and the carbon atom of CO_2^{2+} dication. In addition, the DAFH picture reveals an electron asymmetry of the $[C_2O_4]^{2+}$, that is, the two unpaired electrons are strictly localized at the OCO fragment originated from the CO_2^{2+} reactant. This asymmetry leads to the formation of two monocations CO_2^+ after electron transfer: first, the doublet ground state originated from the neutral CO_2 fragment, and second, the excited quartet state that has arisen from the triplet CO_2^{2+} fragment. Finally, the quartet state is correlated with the $CO^+ + O$ dissociation limit and, thus, explains the previously observed asymmetry in the energy distribution.

Fourth:

We have analyzed the nature of the intricate bonding interactions in an ultrashort presumably quintuple Cr-Cr bond by means of the DAFH analysis. The new interesting insights provided by this analysis have allowed us to reveal the origin of the observed discrepancy between the number of available electron pairs and the calculated bond order. Our results show that Cr-Cr bond must be characterized as an effectively quadruple bond where the dominant contribution to Cr-Cr is due to four shared electron pairs, while the fifth available pair is involved via the contribution of antiferromagnetic coupling of metals.

Applications II: Critical assessment on the performance of a set of aromaticity indices

Fifth:

Some electronically based aromaticity indices have been reviewed at the Hückel molecular orbital (HMO) method. The analysis has been restricted to aromatic

compounds because antiaromatic molecules are not recognized as such from the electron distribution picture which arises from HMO calculations. In general, the values of electronic indices at HMO level are in agreement with *ab initio* calculations available in the literature. First, we have analyzed a series of polyacenes up to 23 rings. FLU, MCI, and I_{ring} predict an increase of aromaticity from the inner to the outer ring, while PDI points out the opposite trend. Second, due to their reduced computational cost, we have been able to study the patterns of aromaticity in large carbon macrocycles, with an increasing number of benzenoid rings to emulate the situation of a graphite layer. All indices give a qualitative agreement of the limit where inner rings are surrounded by enough benzenoid rings to show convergence in aromaticity measures. Moreover, PDI and FLU perform reasonably well identifying the Clar structures.

Sixth:

We have introduced a series of fifteen aromaticity tests that can be used to analyze the advantages and drawbacks of a group of aromaticity descriptors in organic species. On the basis of the results obtained for a set of ten indicators of aromaticity, we conclude that the indices based on the study of electron delocalization are the most accurate among those examined in this work. The chosen tests must fulfill two requirements: first, the size of the systems involved must be relatively small to facilitate a fast application and, second, controversial cases must be avoided. Briefly, the test set contains: five benzene deformations, two tests that study the effect of substitution and complexation of the benzene ring, a couple of tests that evaluate the ring and atom size dependence, the effect of heteroatom is studied by means of two series of heteroaromatic systems with different size, two tests more containing a series of so-called Clar's and fulvenes systems, and, finally, a couple of tests that assess the aromaticity in chemical reactions, i.e. Diels-Alder and $[2 + 2 + 2]$ trimerization of acetylene. In many cases, results obtained from different indicators of aromaticity may reveal contradictory trends. Moreover, some aromaticity descriptors fail on giving the expected answer from most elementary chemical problems. For instance, NICS(0) and NICS(1) predict that the benzene ring in $(\eta^6-C_6H_6)Cr(CO)_3$ benzene is more aromatic than benzene itself whereas the remaining indices point out the opposite behavior.

To sum up, the results obtained have allowed us to describe a list of recommendations. The best indices that can be used in practically each situation are the multicenter indices, especially MCI. PDI is unsuccessful for describing the loss of

aromaticity in benzene distortions while FLU and HOMA are unable to distinguish the aromatic transition state of chemical reactions. NICS(1)_{zz} and NICS(0)_{πzz} perform the best among all NICS indices analyzed. Finally, this new methodology could be used to assess the performance of new aromaticity indices.

Seventh:

Compared to classical organic aromaticity compounds, the evaluation of aromaticity in all-metal clusters is much more complex. In the spirit of the previous work, we have introduced a series of all-metal and semimetal clusters with predictable aromaticity trends. This work represents the first attempt to assess the performance of aromaticity descriptors in all-metal clusters. Results show that the expected trends are generally better reproduced by MCI than NICS. NICS(0)_π and NICS(0)_{πzz} are the kind of NICS that performs the best among the different NICS indices analyzed. In addition, we have found that NICS values in inorganic species strongly depend on the point where they are calculated. To this end, NICS values must be calculated at the ring critical point of the all-metal cluster.

Applications III: Study of electron delocalization in organic and inorganic compounds

Eight:

In order to understand the nature of the electron delocalization in organic aromatic and antiaromatic systems, we have discussed the $(4n + 2)\pi$ rule from the point of view of π -electron delocalization. First, we have analyzed the changes on the *total* π -electron delocalization (δ_π) when two electrons are added or removed from an aromatic or antiaromatic compound. Our hypothesis was that when going from an aromatic to an antiaromatic systems the electrons will be mainly localized while when moving from antiaromatic to aromatic species these electrons will be delocalized throughout the molecule. Our results show that there is an important increase of δ_π (of about 1e) when going from antiaromatic $4n\pi$ systems to aromatic $(4n + 2)\pi$ systems and, thus, confirming the expected trend. But less clear is the change in δ_π when we move from a $(4n + 2)\pi$ -aromatic system to a $4n\pi$ -antiaromatic species. From the analysis of δ_π we cannot establish a frontier between aromatic and antiaromatic compounds. In addition, the total δ_π is practically the same for the lowest-lying singlet and triplet states. Therefore, from δ_π one cannot prove the validity of Baird's rule.

The drawbacks that δ_π presents can be overcome by the analysis of the so-called

crossed terms ($\delta_{\pi}^{1,x}$) which are obtained from the values of the delocalization indices. To obtain $\delta_{\pi}^{1,x}$, the total π -electron delocalization is decomposed into its crossed terms, that is, *ortho* $\delta_{\pi}^{1,2}$, *meta* $\delta_{\pi}^{1,3}$, *para* $\delta_{\pi}^{1,4}$, and successive contributions. Then, we have analyzed the changes on the crossed contributions when two electrons are added or removed. Our results show that these changes follow similar patterns in all cases. We have observed that the crossed terms show an alternation pattern led by the crossed term corresponding to the two farthest positions of the ring. The patterns found represent a kind of electronic footprints that make it possible to discern between aromatic and antiaromatic systems. In contrast to δ_{π} , crossed terms show opposite trends between lowest-lying singlet and triplet states in line with Baird's rule. Interestingly, we have found that not only the $\delta_{\pi}^{1,4}$ but all the crossed terms are relevant for describing the aromaticity of the system, hence this analysis can be extended to rings of different size without any restriction. This analysis represents a step forward towards a better comprehension of the electronic delocalization behavior of aromatic and antiaromatic systems. Moreover, these electron delocalization patterns have been also found in 4-MR all-metal clusters.

Ninth

The quantitative evaluation of σ -, π -, and δ -aromaticity in inorganic clusters is rather cumbersome due to the lack of inorganic systems that can be used as a reference, and because the multifold aromaticity characteristic of all-metal clusters complicates the evaluation of aromaticity in such systems. To solve this problem, we have proposed the separation of MCI into the σ -, π -, and δ -components. These MCI_{α} (where $\alpha = \sigma, \pi, \text{ and } \delta$) indices provide quantitative information about the type of aromaticity that a certain all-metal cluster exhibits. The MCI_{α} results reported for all systems studied are in line with previous classifications of the species according to their aromatic character. Therefore, the use of MCI and its components is recommended in the analysis of aromaticity in all-metal and semimetal clusters.

Bibliography

- [1] Fahrenkamp-Uppenbrink, J.; Szuromi, P.; Yeston, J.; Coontz, R. *Science* **2008**, *321*, 783.
- [2] Lewis, G. *J. Am. Chem. Soc.* **1916**, *38*, 762–785.
- [3] Faraday, M. *Phil. Trans. R. Soc. Lon.* **1825**, *115*, 440–466.
- [4] Li, X.; Kuznetsov, A.; Zhang, H.; Boldyrev, A.; Wang, L. *Science* **2001**, *291*, 859.
- [5] Frenking, G.; Krapp, A. *J. Comp. Chem.* **2007**, *28*, 15–24.
- [6] Becke, A.; Edgecombe, K. *J. Chem. Phys.* **1990**, *92*, 5397.
- [7] Ponec, R. *J. Math. Chem.* **1997**, *21*, 323–333.
- [8] Ponec, R. *J. Math. Chem.* **1998**, *23*, 85–103.
- [9] Cioslowski, J. *Many-electron densities and reduced density matrices*; Springer Us, 2000.
- [10] Mazziotti, D. *Reduced-density-matrix mechanics: with applications to many-electron atoms and molecules*; Wiley-Interscience, 2007.
- [11] Ruedenberg, K. *Rev. Mod. Phys.* **1962**, *34*, 326–376.
- [12] Kutzelnigg, W.; Mukherjee, D. *J. Chem. Phys.* **1999**, *110*, 2800.
- [13] McWeeny, R. *Rev. Mod. Phys.* **1960**, *32*, 335–369.
- [14] Mulliken, R. *J. Chem. Phys.* **1955**, *23*.
- [15] Voronoi, G.; Reine, Z. *Angew. Math.* **1908**, *134*, 198.

- [16] Daudel, R.; Bader, R.; Stephens, M.; Borrett, D. *Can. J. Chem.* **1974**, *52*, 1310–1320.
- [17] Bader, R. *Atoms in Molecules—A Quantum Theory*, International Series of Monographs on Chemistry, No. 22. 1990.
- [18] Mayer, I.; Salvador, P. *Chem. Phys. Lett.* **2004**, *383*, 368–375.
- [19] Gatti, C.; Fantucci, P.; Pacchioni, G. *Theor. Chem. Acc.* **1987**, *72*, 433–458.
- [20] Gatti, C.; MacDougall, P.; Bader, R. *J. Chem. Phys.* **1988**, *88*, 3792.
- [21] Pendás, A.; Blanco, M.; Costales, A.; Sánchez, P.; Luaña, V. *Phys. Rev. Lett.* **1999**, *83*, 1930–1933.
- [22] Bader, R. *J. Phys. Chem. A* **1998**, *102*, 7314–7323.
- [23] Grimme, S.; Mück-Lichtenfeld, C.; Erker, G.; Kehr, G.; Wang, H.; Beckers, H.; Willner, H. *Angew. Chem. Int. Ed.* **2009**, *48*, 2592–2595.
- [24] Cerpa, E.; Krapp, A.; Vela, A.; Merino, G. *Chem. Eur. J.* **2008**, *14*, 10232–10234.
- [25] Cerpa, E.; Krapp, A.; Flores-Moreno, R.; Donald, K.; Merino, G. *Chem. Eur. J.* **2009**, *15*, 1985–1990.
- [26] Poater, J.; Solà, M.; Bickelhaupt, F. *Chem. Eur. J.* **2006**, *12*, 2889–2895.
- [27] Bader, R. *Chem. Eur. J.* **2006**, *12*, 2896–2901.
- [28] Pendás, A.; Francisco, E.; Blanco, M.; Gatti, C. *Chem. Eur. J.* **2007**, *13*, 9362–9371.
- [29] Bader, R. *J. Phys. Chem. A* **2009**, *113*, 10391–10396.
- [30] Wang, S.; Qiu, Y.; Schwarz, W. *Chem. Eur. J.* **2009**, *15*, 6032–6040.
- [31] Hirshfeld, F. *Theor. Chem. Acc.* **1977**, *44*, 129–138.
- [32] Bultinck, P. *Faraday Discuss.* **2007**, *135*, 347–365.
- [33] Bultinck, P.; Cooper, D.; Neck, D. *Phys. Chem. Chem. Phys.* **2009**, *11*, 3424–3429.

- [34] Becke, A. *J. Chem. Phys.* **1988**, *88*, 2547.
- [35] Suresh, C.; Koga, N. *J. Phys. Chem. A* **2001**, *105*, 5940–5944.
- [36] Slater, J. *J. Chem. Phys.* **1964**, *39*, 3199.
- [37] Matito, E.; Poater, J.; Solà, M.; Duran, M.; Salvador, P. *J. Phys. Chem. A* **2005**, *109*, 9904–9910.
- [38] Matito, E.; Salvador, P.; Duran, M.; Solà, M. *J. Phys. Chem. A* **2006**, *110*, 5108–5113.
- [39] Matito, E.; Solà, M.; Salvador, P.; Duran, M. *Faraday Discuss.* **2007**, *135*, 325–345.
- [40] Fonseca-Guerra, C.; Handgraaf, J.; Baerends, E.; Bickelhaupt, F. *J. Comp. Chem.* **2004**, *25*, 189–210.
- [41] Heyndrickx, W.; Salvador, P.; Bultinck, P.; Solà, M.; Matito, E. *J. Comp. Chem.* *accepted for publication*
- [42] Coulson, C. *Proceedings of the Royal Society of London* **1938**, *164*, 383–396.
- [43] Fulton, R.; Mixon, S. *J. Phys. Chem.* **1993**, *97*, 7530–7534.
- [44] Mayer, I. *Chem. Phys. Lett.* **1983**, *97*, 270–274.
- [45] Mayer, I. *Int. J. Quantum Chem.* **1984**, *26*, 151–154.
- [46] Mayer, I. *Int. J. Quantum Chem.* **1986**, *29*, 73–84.
- [47] Mayer, I. *Int. J. Quantum Chem.* **1986**, *29*, 477–483.
- [48] Wiberg, K. *Tetrahedron* **1968**, *24*, 1083–1096.
- [49] Fradera, X.; Austen, M.; Bader, R. *J. Phys. Chem. A* **1999**, *103*, 304–314.
- [50] Poater, J.; Fradera, X.; Duran, M.; Solà, M. *Chem. Eur. J.* **2003**, *9*, 1113.
- [51] Ponec, R.; Mayer, I. *J. Phys. Chem. A* **1997**, *101*, 1738–1741.
- [52] Bochicchio, R.; Ponec, R.; Torre, A.; Lain, L. *Theor. Chem. Acc.* **2001**, *105*, 292–298.
- [53] Bader, R.; Stephens, M. *J. Am. Chem. Soc.* **1975**, *97*, 7391–7399.

- [54] Cioslowski, J.; Mixon, S. *J. Am. Chem. Soc.* **1991**, *113*, 4142–4145.
- [55] Cioslowski, J. *Int. J. Quantum Chem.* **1990**, *38*, 015–028.
- [56] Cioslowski, J. *J. Math. Chem.* **1991**, *8*, 169–178.
- [57] Angyan, J.; Loos, M.; Mayer, I. *J. Phys. Chem.* **1994**, *98*, 5244–5248.
- [58] Ponec, R.; Uhlik, F. *J. Mol. Struct. (THEOCHEM)* **1997**, *391*, 159–168.
- [59] Giambiagi, M.; Giambiagi, M. S. d.; Mundimt, K. C. *Struct. Chem.* **1990**, *1*, 423.
- [60] Giambiagi, M.; Giambiagi, M. S. d.; dos Santos Silva, C. D.; da Figueredo, A. P. *Phys. Chem. Chem. Phys.* **2000**, *2*, 3381.
- [61] Bultinck, P.; Ponec, R.; Van Damme, S. *J. Phys. Org. Chem.* **2005**, *18*, 706.
- [62] Francisco, E.; Pendás, A.; Blanco, M. *J. Chem. Phys.* **2007**, *126*, 094102.
- [63] Feixas, F.; Matito, E.; Swart, M.; Poater, J.; Solà, M. *AIP Conference Proceedings of the International Conference on Computational Methods in Science and Engineering, ICCMSE 2009, T. E. Simos and G. Maroulis, Eds., AIP* **2010**, Accepted for publication.
- [64] Feixas, F.; Matito, E.; Maseras, F.; Poater, J.; Solà, M. In preparation.
- [65] Poater, J.; Duran, M.; Solà, M.; Silvi, B. *Chem. Rev* **2005**, *105*, 3911–3947.
- [66] Matito, E.; Solà, M. *Coord. Chem. Rev.* **2009**, *253*, 647–665.
- [67] Ponec, R.; Cooper, D. *J. Mol. Struct. (THEOCHEM)* **2005**, *727*, 133–138.
- [68] Bultinck, P.; Cooper, D.; Ponec, R. *J. Phys. Chem. A* **2010**, 534.
- [69] Matito, E.; Ramos-Cordoba, E.; Salvador, P. **2010**, In preparation.
- [70] Dewar, M. *Bull. Soc. Chim. Fr. (Paris)* **1951**, *18*, C71–79.
- [71] Chatt, J.; Duncanson, L. *J. Chem. Soc* **1953**, *2939*, 88.
- [72] Ponec, R.; Roithová, J. *Theor. Chem. Acc.* **2001**, *105*, 383–392.
- [73] Ponec, R.; Roithová, J.; Girones, X.; Jug, K. *J. Mol. Struct. (THEOCHEM)* **2001**, *545*, 255–264.

- [74] Ponec, R.; Gironés, X. *J. Phys. Chem. A* **2002**, *106*, 9506–9511.
- [75] Ponec, R.; Yuzhakov, G.; Gironés, X.; Frenking, G. *Organometallics* **2004**, *23*, 1790–1796.
- [76] Ponec, R.; Cooper, D. *Faraday Discuss.* **2007**, *135*, 31–42.
- [77] Ponec, R.; Cooper, D. *J. Phys. Chem. A* **2007**, *111*, 11294–11301.
- [78] Ponec, R.; Lendvay, G.; Chaves, J. *J. Comp. Chem.* **2008**, *29*, 1387–1398.
- [79] Cooper, D.; Ponec, R. *Phys. Chem. Chem. Phys.* **2008**, *10*, 1319–1329.
- [80] Ponec, R.; Gatti, C. *Inorg. Chem.* **2009**, *48*, 11024–11031.
- [81] Wigner, E. *Phys. Rev.* **1934**, *46*, 1002–1011.
- [82] Ponec, R.; Cooper, D.; Savin, A. *Chem. Eur. J.* **2008**, *14*, 3338–3345.
- [83] Francisco, E.; Pendás, A.; Blanco, M. *J. Chem. Phys.* **2009**, *131*, 124125.
- [84] Savin, A.; Becke, A.; Flad, J.; Nesper, R.; Preuss, H.; Von Schnering, H. *Angew. Chem. Int. Ed.* **1991**, *30*, 409–412.
- [85] Silvi, B. *J. Phys. Chem. A* **2003**, *107*, 3081–3085.
- [86] Kohout, M. *Int. J. Quantum Chem.* **2004**, *97*, 651–658.
- [87] Kohout, M.; Pernal, K.; Wagner, F.; Grin, Y. *Theor. Chem. Acc.* **2004**, *112*, 453–459.
- [88] Dobson, J. *J. Chem. Phys.* **1991**, *94*, 4328.
- [89] Becke, A. *Int. J. Quantum Chem.* **1983**, *23*, 1915–1922.
- [90] Silvi, B.; Savin, A. *Nature* **1994**, *371*, 683–686.
- [91] Savin, A.; Silvi, B.; Coionna, F. *Can. J. Chem.* **1996**, *74*, 1088–1096.
- [92] Matito, E.; Poater, J.; Duran, M.; Solà, M. *Chem. Phys. Chem.* **2006**, *7*, 111–113.
- [93] Tiana, D.; Francisco, E.; Blanco, M.; Macchi, P.; Sironi, A.; Martšn PendGs, A. *J. Chem. Theory Comput.* **2010**, *6*, 1064–1074.

- [94] Matito, E.; Poater, J.; Bickelhaupt, F.; Solà, M. *J. Phys. Chem. B* **2006**, *110*, 7189–7198.
- [95] Wannier, G. *Physical Review* **1937**, *52*, 191–197.
- [96] Hughbanks, T.; Hoffmann, R. *J. Am. Chem. Soc.* **1983**, *105*, 3528–3537.
- [97] Gatti, C. *Zeitschrift für Kristallographie* **2005**, *220*, 399–457.
- [98] Savin, A.; Jepsen, O.; Flad, J.; Andersen, O.; Preuss, H.; von Schnering, H. *Angew. Chem. Int. Ed.* **1992**, *31*, 187–188.
- [99] Savin, A.; Nesper, R.; Wengert, S.; Fässler, T. *Angew. Chem. Int. Ed.* **1997**, *36*, 1808–1832.
- [100] Conteras, J. *PhD thesis: Chemical Bonding in Crystalline Solids*; University of Oviedo, 2008.
- [101] La Penna, G.; Furlan, S.; Solà, M. *submitted for publication* **2010**,
- [102] Baranov, A.; Kohout, M. *Girona Seminar 2010 Electron Density, Density Matrices, and Density Functional Theory: poster presentation* **2010**,
- [103] Schleyer, P. *Chem. Rev* **2001**, *101*, 1115–1118.
- [104] Schleyer, P. *Chem. Rev* **2005**, *105*, 3433–3435.
- [105] Heilbronner, E. *Tetrahedron Lett.* **1964**, *5*, 1923–1928.
- [106] Rzepa, H. *Chem. Rev* **2005**, *105*, 3697–3715.
- [107] Bühl, M.; Hirsch, A. *Chem. Rev* **2001**, *101*, 1153–1184.
- [108] Chen, Z.; King, R. *Chem. Rev* **2005**, *105*, 3613–3642.
- [109] Masui, H. *Coord. Chem. Rev.* **2001**, *219*, 957–992.
- [110] Dewar, M.; McKee, M. *Pure Appl. Chem.* **1980**, *6*, 1431–1441.
- [111] Dewar, M. *J. Am. Chem. Soc.* **1984**, *106*, 669–682.
- [112] Hückel, E. *Z. Phys.* **1931**, *70*, 204.
- [113] Hückel, E. *Z. Phys.* **1932**, *76*, 628.

- [114] Beck, L. *A manual of chemistry*; Webster and Skinners, 1831.
- [115] Mitscherlich, E. *Annalen der Physik* **1834**, *108*, 225–227.
- [116] Kekulé, A. *Bulletin mensuel de la Société Chimique de Paris* **1865**, *3*, 98.
- [117] Erlenmeyer, E. *Ann.* **1866**, *137*, 327–359.
- [118] Chen, Z.; Wannere, C.; Corminboeuf, C.; Puchta, R.; Schleyer, P. *Chem. Rev* **2005**, *105*, 3842–3888.
- [119] Crocker, E. *J. Am. Chem. Soc.* **1922**, *44*, 1618–1630.
- [120] Evans, M.; Warhurst, E. *Trans. Faraday Soc.* **1938**, *34*, 614–624.
- [121] Calvin, M.; Wilson, K. *J. Am. Chem. Soc.* **1945**, *67*, 2003–2007.
- [122] Winstein, S.; Kosower, E. *J. Am. Chem. Soc.* **1959**, *81*, 4399–4408.
- [123] Breslow, R. *Acc. Chem. Res.* **1973**, *6*, 393–398.
- [124] Osawa, E. *Kagaku (Kyoto)* **1970**, *25*, 854–863.
- [125] Clar, E. *The aromatic sextet*; John Wiley & Sons, 1972.
- [126] Baird, N. *J. Am. Chem. Soc.* **1972**, *94*, 4941–4948.
- [127] Aihara, J. *J. Am. Chem. Soc.* **1978**, *100*, 3339–3342.
- [128] Jemmis, E.; Schleyer, P. *J. Am. Chem. Soc.* **1982**, *104*, 4781–4788.
- [129] Shaik, S.; Hiberty, P. *J. Am. Chem. Soc.* **1985**, *107*, 3089–3095.
- [130] Kroto, H. *Nature* **1985**, *318*, 162.
- [131] et al. , *Nature* **1991**, *354*, 56–58.
- [132] Wannere, C.; Corminboeuf, C.; Wang, Z.; Wodrich, M.; King, R.; Schleyer, P. *J. Am. Chem. Soc* **2005**, *127*, 5701–5705.
- [133] Tsipis, A.; Tsipis, C. *J. Am. Chem. Soc* **2003**, *125*, 1136–1137.
- [134] Zhai, H.; Averkiev, B.; Zubarev, D.; Wang, L.; Boldyrev, A. *Angew. Chem. Int. Ed.* **2007**, *119*, 4355–4358.
- [135] Tsipis, A.; Kefalidis, C.; Tsipis, C. *J. Am. Chem. Soc.* **2008**, *130*, 9144–9155.

- [136] Wörner, H.; Merkt, F. *Angew. Chem. Int. Ed.* **2006**, *45*, 293–296.
- [137] Hirsch, A.; Chen, Z.; Jiao, H. *Angew. Chem. Int. Ed.* **2001**, *40*, 2834–2838.
- [138] Datta, A.; Mallajosyula, S.; Pati, S. *Acc. Chem. Res* **2007**, *40*, 213–221.
- [139] Balaban, A. *Pure Appl. Chem* **1980**, *52*, 1409–1429.
- [140] Lazzeretti, P. *Phys. Chem. Chem. Phys.* **2004**, *6*, 217–223.
- [141] Katritzky, A.; Barczynski, P.; Musumarra, G.; Pisano, D.; Szafran, M. *J. Am. Chem. Soc.* **1989**, *111*, 7–15.
- [142] Pauling, L. *Cornell, Ithaca, NY* **1960**,
- [143] Meyer, L.; Saika, A.; Gutowsky, H. *J. Am. Chem. Soc.* **1953**, *75*, 4567–4573.
- [144] Bernstein, H.; Schneider, W.; Pople, J. *Proceedings of the Royal Society of London* **1956**, *236*, 515–528.
- [145] Schaad, L.; Hess Jr, B. *Chem. Rev* **2001**, *101*, 1465–1476.
- [146] Dauben Jr, H.; Wilson, J.; Laity, J. *J. Am. Chem. Soc.* **1968**, *90*, 811–813.
- [147] Kruszewski, J.; Krygowski, T. *Tetrahedron Lett.* **1972**, *13*, 3839–3842.
- [148] Gomes, J.; Mallion, R. *Chem. Rev* **2001**, *101*, 1349–1384.
- [149] Jug, K. *J. Org. Chem.* **1983**, *48*, 1344–1348.
- [150] Bird, C. *Tetrahedron* **1985**, *41*, 1409–1414.
- [151] Zhou, Z.; Parr, R. *J. Am. Chem. Soc.* **1989**, *111*, 7371–7379.
- [152] Paquette, L.; Bauer, W.; Sivik, M.; Buehl, M.; Feigel, M.; Schleyer, P. *J. Am. Chem. Soc.* **1990**, *112*, 8776–8789.
- [153] Schleyer, P.; Maerker, C.; Dransfeld, A.; Jiao, H.; van Eikema Hommes, N. *J. Am. Chem. Soc* **1996**, *118*, 6317–6318.
- [154] Steiner, E.; Fowler, P. *Int. J. Quantum Chem.* **1996**, *60*, 609–616.
- [155] von Rague Schleyer, P.; Jiao, H.; van Eikema Hommes, N.; Malkin, V.; Malkina, O. *J. Am. Chem. Soc* **1997**, *119*, 12669–12670.

- [156] De Proft, F.; Geerlings, P. *Chem. Rev* **2001**, *101*, 1451–1464.
- [157] Jusélius, J.; Sundholm, D. *Phys. Chem. Chem. Phys.* **1999**, *1*, 3429–3435.
- [158] Heine, T.; Schleyer, P.; Corminboeuf, C.; Seifert, G.; Reviakine, R.; Weber, J. *J. Phys. Chem. A* **2003**, *107*, 6470–6475.
- [159] Merino, G.; Heine, T.; Seifert, G. *Chem. Eur. J.* **2004**, *10*, 4367–4371.
- [160] Jusélius, J.; Sundholm, D.; Gauss, J. *J. Chem. Phys.* **2004**, *121*, 3952.
- [161] Stanger, A. *J. Org. Chem* **2006**, *71*, 883–893.
- [162] Jiménez-Halla, J.; Matito, E.; Robles, J. *J. Organomet. Chem.* **2006**, *691*, 4359–4366.
- [163] Cyrański, M. *Chem. Rev* **2005**, *105*, 3773–3811.
- [164] Krygowski, T.; Cyraski, M. *Tetrahedron* **1996**, *52*, 10255–10264.
- [165] Lazzeretti, P. *Progress in Nuclear Magnetic Resonance Spectroscopy* **2000**, *36*, 1–88.
- [166] Aihara, J. *Chem. Phys. Lett.* **2002**, *365*, 34–39.
- [167] von Ragué Schleyer, P.; Manoharan, M.; Wang, Z.; Kiran, B.; Jiao, H.; Puchta, R.; van Eikema Hommes, N. *Org. Lett* **2001**, *3*, 2465–2468.
- [168] Corminboeuf, C.; Heine, T.; Weber, J. *Phys. Chem. Chem. Phys.* **2003**, *5*, 246–251.
- [169] Glendening, E.; Badenhoop, J.; Reed, A.; Carpenter, J.; Bohmann, J.; Morales, C.; Weinhold, F. *Theoretical Chemistry Institute, University of Wisconsin, Madison, WI* **2001**,
- [170] Corminboeuf, C.; Heine, T.; Seifert, G.; Schleyer, P.; Weber, J. *Phys. Chem. Chem. Phys.* **2004**, *6*, 273–276.
- [171] Fallah-Bagher-Shaidaei, H.; Wannere, C.; Corminboeuf, C.; Puchta, R.; Schleyer, P. *Org. Lett* **2006**, *8*, 863–866.
- [172] Katritzky, A.; Jug, K.; Oniciu, D. *Chem. Rev* **2001**, *101*, 1421–1450.

- [173] Castro, A.; Osorio, E.; JimÓñez-Halla, J.; Matito, E.; Tiznado, W.; Merino, G. *Journal of Chemical Theory and Computation* **139**.
- [174] Matito, E.; Poater, J.; Duran, M.; Solà, M. *J. Mol. Struct. (THEOCHEM)* **2005**, *727*, 165.
- [175] Poater, J.; Solà, M.; Viglione, R.; Zanasi, R. *J. Org. Chem* **2004**, *69*, 7537–7542.
- [176] Poater, J.; Bofill, J.; Alemany, P.; Solà, M. *J. Org. Chem* **2006**, *71*, 1700–1702.
- [177] Osuna, S.; Poater, J.; Bofill, J.; Alemany, P.; Solà, M. *Chem. Phys. Lett.* **2006**, *428*, 191–195.
- [178] Chesnut, D.; Bartolotti, L. *Chem. Phys.* **2000**, *257*, 175–181.
- [179] Silvi, B. *Phys. Chem. Chem. Phys.* **2004**, *6*, 256–260.
- [180] Santos, J.; Tiznado, W.; Contreras, R.; Fuentealba, P. *J. Chem. Phys.* **2004**, *120*, 1670.
- [181] Matito, E.; Duran, M.; Solà, M. *J. Chem. Phys.* **2005**, *122*, 014109.
- [182] Poater, J.; Duran, M.; Solà, M.; Silvi, B. *Chem. Rev.* **2005**, *105*, 3911.
- [183] Portella, G.; Poater, J.; Bofill, J.; Alemany, P.; Solà, M. *J. Org. Chem.* **2005**, *70*, 2509.
- [184] Poater, J.; Bofill, J. M.; Alemany, P.; Solà, M. *J. Phys. Chem. A* **2005**, *109*, 10629.
- [185] Portella, G.; Poater, J.; Bofill, J.; Alemany, P.; Solà, M. *J. Org. Chem.* **2005**, *70*, 4560.
- [186] Güell, M.; Poater, J.; Luis, J.; Mó, O.; Yáñez, M.; Solà, M. *Chem. Phys. Chem.* **2005**, *6*, 2552.
- [187] Huertas, O.; Poater, J.; Fuentes-Cabrera, M.; Orozco, M.; Solà, M.; Luque, F. *J. Phys. Chem. A* **2006**, *110*, 12249–12258.
- [188] Alonso, M.; Poater, J.; Solà, M. *Structural Chemistry* **2007**, *18*, 773–783.
- [189] Poater, J.; Bickelhaupt, F.; Solà, M. *J. Phys. Chem. A* **2007**, *111*, 5063–5070.

- [190] Bollini, C. G.; Giambiagi, M.; Giambiagi, M. S. d.; de Figuereido, A. P. *Struct. Chem.* **2001**, *12*, 113.
- [191] Cioslowski, J.; Matito, E.; Solà, M. *J. Phys. Chem. A* **2007**, *111*, 6521–6525.
- [192] Bultinck, P.; Rafat, M.; Ponec, R.; Gheluwe, B. V.; Carbó-Dorca, R.; Popelier, P. *J. Phys. Chem. A* **2006**, *110*, 7642, and references cited therein.
- [193] Bultinck, P.; Fias, S.; Ponec, R. *Chem. Eur. J.* **2006**, *12*, 8813.
- [194] Mandado, M.; Bultinck, P.; González-Moa, M.; Mosquera, R. *Chem. Phys. Lett* **2006**, *433*, 5–9.
- [195] Bultinck, P.; Ponec, R.; Carbó-Dorca, R. *J. Comput. Chem.* **2007**, *28*, 152.
- [196] Fias, S.; Van Damme, S.; Bultinck, P. *J. Comp. Chem.* **2010**, *31*, 2286–2293.
- [197] Fias, S.; Fowler, P.; Delgado, J.; Hahn, U.; Bultinck, P. *Chem. Eur. J.* **2008**, *14*, 3093–3099.
- [198] Roy, D.; Bultinck, P.; Subramanian, V.; Chattaraj, P. *J. Mol. Struct. (THEOCHEM)* **2008**, *854*, 35–39.
- [199] Bultinck, P.; Mandado, M.; Mosquera, R. *J. Math. Chem.* **2008**, *43*, 111–118.
- [200] Krokidis, X.; Noury, S.; Silvi, B. *J. Phys. Chem. A* **1997**, *101*, 7277–7282.
- [201] Berski, S.; Andrés, J.; Silvi, B.; Domingo, L. *J. Phys. Chem. A* **2003**, *107*, 6014–6024.
- [202] Matito, E.; Solà, M.; Duran, M.; Poater, J. *J. Phys. Chem. B* **2005**, *109*, 7591–7593.
- [203] Müller, A. *Phys. Lett. A* **1984**, *105*, 446–452.
- [204] Goedecker, S.; Umrigar, C. *Phys. Rev. Lett.* **1998**, *81*, 866–869.
- [205] Buijse, M.; Baerends, E. *Mol. Phys.* **2002**, *100*, 401–421.
- [206] Gritsenko, O.; Pernal, K.; Baerends, E. *J. Chem. Phys.* **2005**, *122*, 204102.
- [207] Piris, M. *Int. J. Quantum Chem.* **2006**, *106*, 1093–1104.
- [208] Kato, T. *Comm. Pure Appl. Math.* **1957**, *10*, 151–177.

- [209] Ponec, R.; Roithová, J.; Sannigrahi, A.; Lain, L.; Torre, A.; Boicchio, R. *J. Mol. Struct. (THEOCHEM)* **2000**, *505*, 283–288.
- [210] Ponec, R.; Yuzhakov, G.; Cooper, D. *Theor. Chem. Acc.* **2004**, *112*, 419–430.
- [211] Fradera, X.; Solà, M. *J. Comp. Chem.* **2002**, *23*, 1347–1356.
- [212] Roithová, J.; Schröder, D. *Phys. Chem. Chem. Phys.* **2007**, *9*, 2341–2349.
- [213] Roithová, J.; Ricketts, C.; Schröder, D.; Price, S. *Angew. Chem. Int. Ed.* **2007**, *46*, 9316–9319.
- [214] Ricketts, C.; Schröder, D.; Roithová, J.; Schwarz, H.; Thissen, R.; Dutuit, O.; Žabka, J.; Herman, Z.; Price, S. *Phys. Chem. Chem. Phys.* **2008**, *10*, 5135–5143.
- [215] Cotton, F. *Acc. Chem. Res.* **1978**, *11*, 225–232.
- [216] Nguyen, T.; Sutton, A.; Brynda, M.; Fettinger, J.; Long, G.; Power, P. *Science* **2005**, *310*, 844.
- [217] Kreisel, K.; Yap, G.; Dmitrenko, O.; Landis, C.; Theopold, K. *J. Am. Chem. Soc.* **2007**, *129*, 14162–14163.
- [218] Hsu, C.; Yu, J.; Yen, C.; Lee, G.; Wang, Y.; Tsai, Y. *Angew. Chem. Int. Ed.* **2008**, *47*, 9933.
- [219] Noor, A.; Wagner, F.; Kempe, R. *Angew. Chem. Int. Ed.* **2008**, *47*, 7246–7249.
- [220] Brynda, M.; Gagliardi, L.; Widmark, P.; Power, P.; Roos, B. *Angew. Chem. Int. Ed.* **2006**, *45*, 3804–3807.
- [221] DuPré, D. *J. Phys. Chem. A* **2009**, *113*, 1559–1563.
- [222] Mabbs, F.; Machin, D. *Magnetism and transition metal complexes*; Chapman and Hall London, 1973.
- [223] Coulson, C. A. *Proc. Roy. Soc. A* **1939**, *169*, 413.
- [224] Fulton, R. L. *J. Phys. Chem.* **1993**, *97*, 7516.
- [225] Bader, R. F. W.; Streitwieser, A.; Neuhaus, A.; Laidig, K. E.; Speers, P. *J. Am. Chem. Soc.* **1996**, *118*, 4959.

- [226] Mitchell, R.; Brkic, Z.; Berg, D.; Barclay, T. *J. Am. Chem. Soc.* **2002**, *124*, 11983–11988.
- [227] Hubig, S.; Lindeman, S.; Kochi, J. *Coord. Chem. Rev.* **2000**, *200*, 831–873.
- [228] Solà, M.; Feixas, F.; Jiménez-Halla, J.; Matito, E.; Poater, J. *Symmetry* *2*.
- [229] Boldyrev, A.; Wang, L. *Chem. Rev.* **2005**, *105*, 3716–3757.
- [230] Zubarev, D.; Averkiev, B.; Zhai, H.; Wang, L.; Boldyrev, A. *Phys. Chem. Chem. Phys.* **2008**, *10*, 257–267.
- [231] Hückel, E. *Zeitschrift für Elektrochemie* **1937**, *43*, 752–788.
- [232] Von E. Doering, W.; Knox, L. *J. Am. Chem. Soc.* **1954**, *76*, 3203–3206.
- [233] Jiao, H.; Schleyer, P.; Mo, Y.; McAllister, M.; Tidwell, T. *J. Am. Chem. Soc.* **1997**, *119*, 7075–7083.
- [234] Gogonea, V.; Schleyer, P.; Schreiner, P. *Angew. Chem. Int. Ed.* **1998**, *37*, 1945–1948.
- [235] Steiner, E.; Fowler, P. *Chem. Comm.* **2001**, *2001*, 2220–2221.
- [236] Villaume, S.; Fogarty, H.; Ottosson, H. *Chem. Phys. Chem* **2008**, *9*, 257–264.
- [237] Yoon, Z.; Osuka, A.; Kim, D. *Nature Chem.* **2009**, *1*, 113–122.
- [238] Averkiev, B.; Boldyrev, A. *J. Phys. Chem. A* **2007**, *111*, 12864–12866.
- [239] Wang, B.; Zhai, H.; Huang, X.; Wang, L. *J. Phys. Chem. A* **2008**, *112*, 10962–10967.
- [240] Li, X.; Zhang, H.; Wang, L.; Kuznetsov, A.; Cannon, N.; Boldyrev, A. *Angew. Chem.* **2001**, *113*, 1919–1922.
- [241] Xu, W.; Zhang, R.; Lu, S.; Zhang, Y. *J. Mol. Struct. (THEOCHEM)* **2008**, *859*, 18–21.
- [242] Nigam, S.; Majumder, C.; Kulshreshtha, S. *J. Mol. Struct. (THEOCHEM)* **2005**, *755*, 187–194.
- [243] Kuznetsov, A.; Birch, K.; Boldyrev, A.; Li, X.; Zhai, H.; Wang, L. *Science* **2003**, *300*, 622.

- [244] Chen, Z.; Corminboeuf, C.; Heine, T.; Bohmann, J.; Schleyer, P. *J. Am. Chem. Soc.* **2003**, *125*, 13930–13931.
- [245] Yong, L.; Wu, S.; Chi, X. *Int. J. Quantum Chem.* **2007**, *107*, 722–728.
- [246] Chi, X.; Liu, Y. *Int. J. Quantum Chem.* **2007**, *107*, 1886–1896.